MECHANICAL BEHAVIOUR OF FIBRE REINFORCED UNSATURATED CLAY

S. S. E. SAAD

PhD

UNIVERSITY OF BRADFORD

2016

MECHANICAL BEHAVIOUR OF FIBRE REINFORCED UNSATURATED CLAY

This investigation is to determine the improvement in the mechanical behaviour of unsaturated clayey soil after inclusion of carpet fibre waste

Suleiman S E SAAD

Submitted for the Degree of

Doctor of Philosophy

Faculty of Engineering and Informatics

2016

Abstract

To acquire deeper understanding and insights into the mechanical behaviour of fibre reinforced saturated/unsaturated cohesive soils, a programme of work was designed and included. 1) Conducting standard Consolidation Undrained (CU) tests to investigate mechanical behaviour of non-reinforced fully saturated soil. 2) Studying the strength of fibre reinforced clay though unconfined compression tests. 3) Testing the behaviour of unsaturated reinforced soil in unsaturated triaxial tests. 4) Determining the soil-water characteristic curves (SWCC) on soil sample with different fibre content.

The investigation was undertaken on a clay of low plasticity index. Samples tested with addition of 1, 3 and 5 % fibre content and different values of matric suction of 50, 100 and 200 kPa, one of the challenges that were encountered in this research are how to prepare homogenous samples. A method for prepared compacted fibre reinforced soils with improved fibre distribution and density profile has been proposed and examined.

The test results indicated that waste carpet fibres increase the shear strength of unsaturated clay soils. It was also found that relative increase in strength is also a function of applied suction. An increase in waste carpet fibres was found to reduce the hysteresis of soil.

A data analysis conducted on the results of unsaturated tests as a function of fibre content and matric suction. The behaviour modelled was shown to be a perfect fit with the experimental data.

Keywords: Reinforced soils, unsaturated soil, carpet waste fibre, shear strength, laboratory tests.

Dedicated *to my parents and my sons*

Salem, Islam and Al-Mutasim Billah

Acknowledgements

First, I would like to acknowledge my truthful and gratitude to my supervisor, **Dr Mostafa Mohamed** for his patience guidance, encouragement, constructive criticism and kindness throughout my study by giving a lot of helpful advice and support. I would like to extend my thanks to **Dr Ashraf Ashour** for his advice and assistance.

Very warm and deep thanks go to my family especially my **parents** for sacrifice and support. My deepest gratitude, which cannot be put into words, for the continuous caring and understanding, which I have received over the years from my wife.

Special thanks also to Mehdi Mirzababaei for his encouragement, support, invaluable assistance and knowledge sharing.

I would like to express the help I received from laboratory staff, especially, Mr Lee Thomas for their help in manufacturing and refurbished most of the equipment and the tools that have been used in this research. I would also thank engineering technician Miss Joanna Wood for her help during my study.

Finally, over the past five years, I got to know some very special people. Many thanks to my friends who have made my stay in the UK pleasant and fruitful.

Contents

List of figures

List of Tables

List of Symbols

a	a soil parameter which is primarily a function of the AEV of the soil (kPa)
b	curve-fitting parameter
b_d	parameter, *b*, for drying shear strength prediction
b_w	parameter, *b*, for wetting shear strength prediction
c	cohesion intercept
c'	effective cohesion
CL	low plasticity clay
d	fitting parameter
e	natural number, 2.71828
e_0	initial void ratio
i	hydraulic gradient
m	a soil parameter which is primarily a function of the residual water content
n	a soil parameter which is primarily a function of the rate of water extraction from the soil once the AEV has been exceeded
n_d	fitting parameter, *n*, from Fredlund and Xing (1994) equation for drying SWCC
n_w	fitting parameter, *n*, of Fredlund and Xing (1994) equation for wetting SWCC
t	elapsed time
u_a	pore-air pressure
u_w	pore-water pressure

A	cross-sectional area
AEV	air entry value
L	length of sample
P	atmospheric pressure
PI	plasticity index
R	universal gas constant 8.314 (J/mol K)
R_S	radius of curvature of the meniscus
S	degree of saturation
T_S	surface tension of water
α	initial angle of shear strength with respect to matric suction
β	calculated fitting parameter
γ, λ	fitting parameters
θ	volumetric water content
θ_r	residual volumetric water content
θ_s	saturated volumetric water content
θ_w	volumetric water content
k	fitting parameter
ρ_d	dry density
τ	shear strength of soil
χ	a parameter dependent on the degree of saturation
$\boldsymbol{\psi}$	matric suction of soil
ϕ^b	angle indicating the rate of change in shear strength with respect to matric suction
ϕ'	effective internal friction angle of saturated soil

φ	calculated fitting parameter
π	osmotic suction
ε	axial strain
$\boldsymbol{\Theta}$	normalised volumetric water content
$(\sigma - u_a)$	net normal stress
$(u_a - u_w)$	matric suction
$(u_a - u_w)_b$	air-entry value of soil
P & q	stress path parameters
F_r	fibre content used in the model
S'	suction use in model

CHAPTER 1 INTRODUCTION

1.1 Background

There is growing anxiety regarding the rise in waste generated yearly in the world, as well as the safest and greatest economic way of its treatment and disposal, without harming the environment and public health. The problem causing concern arise from the growing size of plastic waste and other Municipal Solid Waste (MSW), and conventional ways of MSW disposal, i.e. mostly landfill and incineration, with little composting and recycling. Recently, in the UK, the total amount of solid waste generated yearly is about 400 Million tonnes, of which approximately 2 % of its total weight consists of textile and other carpet waste (Miraftab and Lickfold 2008).

In England, the percentage of textile waste was 3.2 of its total weight % of total household waste collected in 2008/09, was shown in the table below. Carpet waste Table 1.1 was represented by a high ratio of waste weight. It had a high volume to weight ratio, which means it occupied a large land volume, compared to other constituents of landfill disposal (Mirzababaei et al., 2009).

Table 1.1 Composition of Household-collected waste (Municipal Waste Management Statistics for England)

Components	Household collected %
Paper and card	22.7
Kitchen waste	22.2
Garden waste	16.4
Glass	8.4
Textile	3.2
Plastics	8.8
Ferrous metals	3.4
Miscellaneous combustible	3.6
Disposable nappies	2.4

From the above finding, it has been vitally important for businesses, householders and local authorities to seek updated methods of recycling unwanted carpet materials. As carpets are made of natural and synthetic fibres, which are valuable even after the carpet is no longer needed or used. The fibres can be extracted and utilised in other applications, including carpet waste*. The recovery and recycling of plastic polymer waste, including polypropylene, polyethylene, polyvinyl chloride and other have been investigated using pyrolysis, gasification and liquefaction to produce gas or liquid hydrocarbon fuels, or chemical feedback (Tang et al., 2007). Many studies investigated a different method for the treatment and reuse of carpet fibre waste to improve the properties of soils, and cement or concrete. Wang et al., (1999) recycled carpet waste fibres by mixing them with concrete to improve its physical properties. Whereas Tang et al., (2007) studies the influence of mixing of carpet waste that consisted of polypropylene polymer (PP) with non-cemented and cemented clayey soils. In the literature, the features of unsaturated soil behaviour such as the volume change, shear strength and soil water characteristic carve (SWCC) have been investigated vastly.

**http://www.carpetrecyclinguk.com/*

Only a few studies have been performed on the influence of soil reinforcement on the mechanical behaviour of unsaturated soil. As a matter of fact, there are hardly any studies that have been carried out on the mechanism of the unsaturated soil behaviour involving carpet waste fibre as an element. An unsaturated soil is commonly defined as having three phases, solids, water and air. However, recent research presents of a fourth phase, namely the air-water interface or contractile skin (Fredlund and Morgenstern., 1977).

The new part has influence on the mechanical behaviour of unsaturated soil (Fredlund and Rahardjo 1993).

The unsaturated soil case in soil has been recently considered the base of soil mechanics rather than the saturated case, because of the complexity of shear strength and volume change in the unsaturated case. The soil mechanism field is concerned with two sections, the unsaturated and saturated soil. The differences between the two types of soil can be seen in the fact that saturated soil voids are normally filled with a fluid such as water. On the other hand, the unsaturated soil voids are filled with a fluid and gas, which can be water and air. These differences between the two types of soil cause a difference in the engineering and natural behaviour as well as the climate that can have an influence on the soil existence and texture. Two forces create the unsaturated soil such an upward and downward fluxes process that can happen due to evaporation and evapotranspiration or any sort of precipitation, that aids in the water removal from the soil and result in an unsaturated soil that can be found

in the semi-dry parts of the world. Other factors that force the soil to be naturally unsaturated are excavating, remoulding and re-compacting.

1.2 Aims and objectives

The aim of this project is to study the mechanical behaviour of unsaturated soil and the effect of carpet waste fibre on unsaturated soil reinforcements. The objectives of the study can be summarised as follows:

- Review current literature on soil, fibre-soil reinforcement, fibre, clayey soil and unsaturated soil, as well as review the mechanical behaviour of clayey under unsaturated conditions with a different value of suction.
- Perform standard triaxial test method to determine the physical properties of fully saturated and unsaturated soils, such as suction, volume change and shear strength.
- Implement soil-water characteristic carve to study the hysteresis of clayey soils under different cycles of drying and wetting processes with carpet waste fibre as (1, 3 and 5 %).
- Perform a series of advanced triaxial test on unsaturated soil samples to study the effect of waste carpet fibres on the shear strength of clayey soil specimens prepared with different percentage of fibre inclusion (0, 1, 3 and 5%)
- To develop constitutive model of the unsaturated shear strength of the fibre reinforced clayey soil, to evaluate the effect of fibre and suction on the obtained strength.

1.3 Thesis Layout

Chapter one the introduction of the study by reviewing the fundamental concepts of unsaturated soil mechanics, such as suction and constitutive models, and by describing volume change, shear strength and soil water characteristics curve of unsaturated soils, including the influence of fibre and suction on the soil behaviour.

Chapter two the review of the literature of the mechanical behaviour of unsaturated soils, such as suction and stresses variables, volume change, shear strength and soil water characteristics curve of unsaturated soils.

Chapter three describes the laboratory equipment used to carry out the experimental methodology for the setting up and the material used, including a standard triaxial test and advanced triaxial apparatus for testing unsaturated soil sample and soil water characteristics curve.

Chapter four in this section the calibration of all tools used for controlling or measuring pressure, volume, displacement, etc. and development sample preparation mothed also presents in this chapter.

Chapter five provides a discussion the results of the experimental tests. The results of unsaturated triaxial tests, soil-water characteristic curve to study the mechanical behaviour of shear strength, volume change and soil properties after inclusion of waste carpet fibre.

Chapter six to studies the performance of the developed model to predict shear strength of unsaturated soils after add carpet waste fibre and compare the experimental data with predicted shear strength of unsaturated soils.

Chapter Seven presents the conclusions and gives recommendations for future work.

CHAPTER 2 LITERATURE REVIEW

Summary

This chapter covers literature reviews of the cases related to soil testing in reinforced conditions. A review of the apparatus used to test the soil under triaxial is presented. Besides, a history of soil fibre reinforcement is covered in this chapter. Mechanical behaviour of unsaturated soil is briefly explained with the laboratory techniques used to determine the shear strength parameters and measuring the volume change of unsaturated soil. Techniques used to determine soil water characteristic curve is also presented.

2.1 Background

Some soil types such as weak and soft soils are unsafe for civil engineering structures due to the weak shear strength and high compressibility that would lead to excessive settlements. Many techniques are used to enhance the performance and the desired properties of such poor soil such as, permeability, shear strength and bearing capacity (Tang et al., 2007). These techniques include soil stabilisation and soil reinforcement. The soil stabilisation is a chemical process and can be carried out using cement (Tang et al., 2007 and Ismail et al., 2002). They improve the performance of the poor soil, but it results

in high stiffness and behaviour. The other effective technique, which is used to improve the mechanical behaviour of weak soil, is the inclusion of nature reinforcement or chemical fibres. For example, plant roots Huat et al., (2005), and carpet waste Tang et al., (2007), Miraftab and Lickfold (2008), Mirzababaei et al., (2009), where the fibres are randomly added and mixed with soil. The reinforcing fibres limit the possible weakness levels (Tang et al., 2007). The inclusion of carpet fibre waste as reinforcement to the weak soil significantly improved soil strength and reduced soil stiffness and increasing soil toughness.

Several studies have been conducted recently to investigate the influence of fibre on the mechanical behaviour of soils. In addition, fibre reinforced soils could be used to enhance some other properties such as permeability, swelling pressure, volume change and stability of slopes and embankment, etc. However, there have been comparatively few research investigations on the use of waste fibres particularly waste carpet fibres to reinforce cohesive soils. Due to the huge amount of carpet waste fibres that are dumped in landfills, studies into reuse and recycling of such waste are needed so as to save the environment and costs.

2.2 Soil

Soil is a group of different separated particles in the form of residue, which widely consisted of mineral structure and sometimes the presence organic materials. It also includes different quantities of water and gases. The mineral structure of the soil is due to nature weathering of the earth's crust (BS EN 1997-2:2007). However, the organic part is a deposition of organic debris resulted from the remains of animal, plant and other life forms. Craig (2004) identified soil as any non-cemented or weakly cemented accumulation of

mineral particles formed by the weathering of rocks, with void space between the particles containing water or air. Soil can be categorised according to soil grain size to gravel, sand, silt and clay. Other classification could be related to moisture content such as saturated and unsaturated soils. The constituent particles of soil vary in size, and are broadly grouped as clay, silt, sand, and gravel. Each size fraction contributes different properties to the soil. The size fraction of soil with particles of less than 0.002 mm is referred to as clay and it retains cohesion and plasticity.

Clay particles form plate-like shapes that having high surface area. Most clay mineral consists of silicon-oxygen tetrahedron and an aluminium-hydroxyl octahedron, given final negative charges (Craig 2004). The plasticity is an important property for soils and controls the soil capability to undertake unrecoverable deformation without cracking. The plastic behaviour has been attributed to the presence of water in the very small space between the clay particles. By capillary tension, water is held at negative pressure, which produces cohesion between clay particles, and allows the soil to be deformed.

2.3 Expansive soil

The definition of expansive soils is that the apparent volume changes due to changes in the water content. Due to high content minerals of expansive soil, deep cracks in drier seasons occur over the years. Expansive soil, also known as shrink-swell soil swell, depending upon absorption of water and shrink, causes the water to evaporate (Chen 1988 and Nelson and Miller 1992), which is a prevalent cause of problems in foundations, depending on the source of moisture in the ground. When expansive soil heaves, it causes the lifting of the structure during periods of high moisture, while during periods of moisture

reduction, expansive soil collapses and might result in building settlement. Pressure on the vertical face of a foundation, or retaining wall in expansive soil also causes lateral movement. A weakness of soil strength, or capacity instability could result in several forms of foundation problems and slope failure. Therefore, it was found by civil engineering structures that these soils are severely damaged. These damages cost the UK an estimated about £150 million, $1 billion in the USA and many billions of pounds worldwide. To rectify the problem with expansive soil many techniques have been developed. One of the most effective solutions is the reinforcement of expansive soils (Loehr et al., 2000).

2.3.1 Clay

The combined clay has one or more clay minerals with traces of metal oxides and organic matter, which is defined as fine-grained soil. The expansive soils considered as high sensitivity to moisture with respect to stress, strength and deformation that due to its property, these soils are subjected to different forms of deformation, such as heaving, loss of shear strength at a certain moisture content, and settlement and shrinkage as the moisture content changes. Most of the problem soils in engineering practice are clayey soil. The nature of clay minerals is as follows:

Kaolin Minerals: the kaolin crystal is made of repeating layers; each layer consists of a silica sheet and an alumina sheet sharing a layer of oxygen atoms between them. Chemical weathering of alumina-silicates produces kaolin and halloysite clays. A low silica-alumina ratio is needed for the development of kaolin-type minerals.

Illite: is composed of alternating alumina and silica sheets. However, some of the aluminium in the octahedral sheets is replaced by iron and magnesium, although silicon in the tetrahedral sheets is partly replaced by aluminuim. Illites are characterised by their greater ability to absorb water, swell and shrink more than kaolinites.

Montmorillonite: these minerals have the same layers as Illite. However, the isomorphous substitution occurs mainly in the alumina sheet, with magnesium or iron substituting the dioctahedral minerals. One of the commonly spread mineral clays that belongs to this group is Bentonite, which is usually created from volcanic ash through weathering, and is well known by its large expansive properties (Smith 2007).

Vermiculite: this has mica structure, and resembles montmorillonite except that absorption of water layers is usually limited by the two water molecule layer thickness, and so water enters between a smaller proportion of layers. There is the substitution of aluminium for silicon in the silica sheet, leaving a high net negative charge. Biotite and Chlorite belong to this group. The dominant exchangeable cation in natural vermiculite is magnesium. Vermiculite is a weathering product of mica, and occurs as an accessory mineral in many clay soils. The typical commercial form of expanded vermiculite used for packing is made by rapidly heating the mineral so that steam forces the layers apart. (Smith 2007).

2.3.1.1 Clay properties

a. Hydration of clay

Particles of clay are always hydrated, and are bounded by layers of water molecules, or adsorbed water. This enables the clay to have a low density, even with higher water content. The force holding water molecules to the clay surface arises from the water and also the clay, this means that water is attracted by the charge on the clay surface. The surface density of negative charge on the clay is too small to completely hold water in this way, which means that the force bonding water to the surface is due to the hydrogen bond.

b. Surface area

The large particle size of the clay flake is reflected in the surface area. The surface area of the soil is expressed as the ratio of surface area per gram of mass; therefore, the surface ratio of clay minerals is enormous.

c. Shrinkage and Swelling

Shrinkage takes place when water is forced out of the clay, due to adsorbed layer compression, or a reduction in moisture content due to suction. On the other hand, swelling will take place when water is forced into the clay, under swelling pressure, and so an increase in volume occurs. Shrinkage can be recognised as a series of polygonal cracks that are formed from the surface downwards. Equilibrium of inter-particle and adsorbed layer forces is achieved under constant ambient pressure and temperature conditions, and as a result, water molecules move into, or out of the adsorbed layer. The moisture content changes due to any variation in ambient conditions.

d. Plasticity and cohesion

The plasticity of clay soil is measurable, and is the most characteristic property of such soils. For this reason, when clay soils are compressed, they maintain their new shape. This property is controlled by several factors, which affect the plastic consistency of clay, namely the size and nature of the clay particles, and the nature of adsorbed layer as well as others.

e. Flocculation and dispersion

These are affected by the forces between two neighbouring particles in an aqueous solution. The attraction between particles is due to Van der Waal forces, or the forces of interdependence, whether secondary and repulsive forces, which are due to the negative electric charge on the surface of the particle and the adsorbed layer. Accordingly, the process of flocculation in the soil occurs when the thickness of the layer intensifies as a result of a base exchange reaction. This is attractive, due to Van der Waals forces, increasing between the particles as they come closer to each other. In contrast, higher repulsion occurs in the soil with a thick layer, given free adsorb, and so it remains in the dispersed phase. Attractive forces dominate when the adsorbed layer is thin, and groups of molecules are in positive to negative connections, causing settlement between the groups in the case of suspension. It is very important to stress the fact that the soil tends to fluctuate displaying high liquid limits (Smith 2007).

2.4 Unsaturated soils

The saturated soil turns unsaturated when the rate of evaporation exceeds the rate of rainfall, at which water table is reduced. Besides, soils under compaction and the once near ground surfaces in an arid area are converted to unsaturated (Fredlund et al., 1993).

It may be the unsaturated soil can either increase or decrease in the total volume when exposed to moisture. If the size increases upon wetting, the soil has a swelling nature and where the volume decreases, the soil has a collapse nature. Due to the moisture, the behaviour of unsaturated could occur and can also be relatively dependent on the applied stress plane and stress history of soil (Gens 1996). In addition, the quantity of water in the soil depends on the magnitude of the molecules and its composition. The previous geotechnical studies have shown that unsaturated soil consists of three parts, including solid, water and air. However, recently the research presented unsaturated soil in four phases. The new proposed phase is called contractile skin and is defined as an interface between water and air. It has significant effects on the mechanical behaviour of unsaturated soil (Fredlund et al., 1993). To understand the behaviour of the soil, first there is a need to consider the basic composition of the soil and its properties, particles, water, air and contractile skin. These four phases are representing the total volume and mass of soil specimen, as it is shown in Figure (2.1).

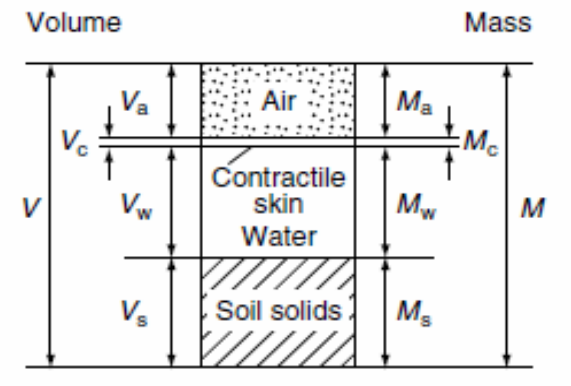

Figure 2.1 Unsaturated soil phases (Fredlund et al 1993)

2.4.1 Nature of unsaturated soil

In saturated soil, voids spaces between particles filled only with water and below ground water table, with positive pore-water pressure. However, in the condition of unsaturated soil, the spaces of voids are filled with water and air. The water in an unsaturated soil takes three forms: the water that is coating the soil particles is called adsorbed water; the bulk water which is flooded in the void spaces; and the meniscus water that surrounds the particle contacts. The negative pore water pressure in an unsaturated soil produces a normal force between the neighbouring particles, which is known as suction and can improve the stability of soil (Kayadelen et al., 2007).

Natural soils in an unsaturated condition in arid or semi-arid areas where the ground water table is very deep with negative-pore water pressure (Murray et al., 2010). Xie et al., (2016) experimentally studied the mechanical behaviour of unsaturated soil by applying an impact load to the soil using drop hammer. The results show that the soil properties had changed and the soil particles were lower water content, smaller void ratio and higher saturation. The density near the by the impact zone was more than the other regions; this change will lead to an effect on the soil suction.

2.4.2 Mechanical behaviour of unsaturated soil

Several important parameters are needed to understand the mechanical behaviour of unsaturated soil, such as stresses, strain, volume change and shear strength.

2.4.2.1 Volume change

Bishop and Blight (1963) have described the volume change behaviour of unsaturated soil by using two stress state variables. The mean net stress and suction. The volume change of unsaturated soil cannot be measured by the flow of water coming in or out of the specimen, because the voids between particles are filled with water and air. Therefore, knowing the volume change of unsaturated soil is based on measuring the volume change of the phases of unsaturated soil. To measure the volume change of unsaturated soil, there are two effective ways, which are internal local strain measurements and the inner cell technique (Cabarkapa and Cuccovillo 2006 and Zhou 2009). The principle of using the inner cell method to determine the volume change of unsaturated soil depends on the measurement of the flow of water coming in or out of the cell. The advantage to use this method is that the value of overall volume change is very precise. On the other hand, using the inner cell technique for measuring the volume change of unsaturated clay is considered very sensitive to any change in pressure and temperature (Sivakumar 1993). The behaviour under isotropic loading was expressed as a path in axes of void ratio *e,* mean net stress (p - u_a) and suction ($u_a - u_w$) as shown in Figure (2.2).

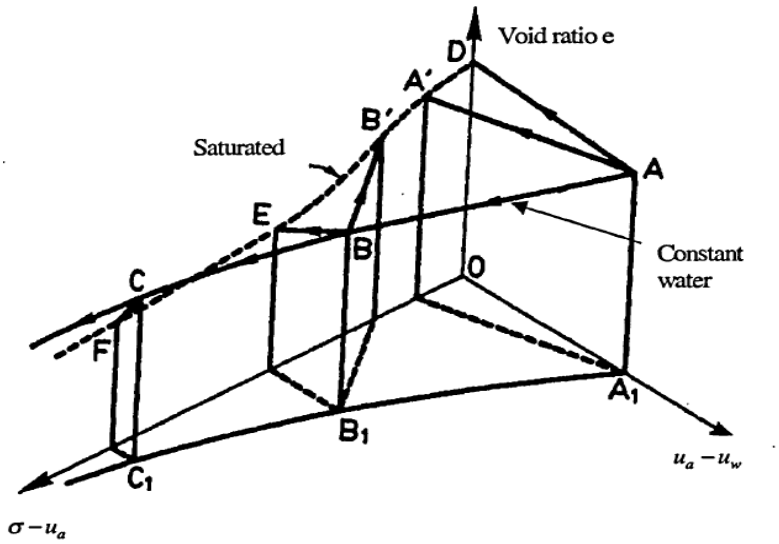

Figure 2.2 Volume change under isotropic loading in paths of void ratio, mean net stress and suction (Bishop and Blight, 1963)

Figure (2.2) presents that at a low value of wetting, the soil (p - u_a)caused swelling (path AD) while soil wetting at a high value of (p - u_a) caused collapse (path BE). Figure (2.2) shows the volume of unsaturated soil decreased, and so did the suction (path ABC) until full saturation was finally achieved. If the sample was saturated at a constant volume, it moves from A to A', but in general, the increase in (p - u_a) during wetting was smaller than the decrease in (p - u_a). Bishop and Blight (1963) mentioned that the two parameters p - u_a and $u_a - u_w$ should be taken into account when describing the volume change in unsaturated soil. Bishop and Donal (1961) triaxial was extended and developed by Wheeler (1988) into a double cell triaxial system to test the soils that have large gas bubbles. The inner cell volume was measured using a water burette. Outside the cell, the vertical axial load was measured by a local proving ring. It was found that in this system, leaking can be a potential obstacle that was fixed by using a rolling diagram between the loading piston and the inner cell. The water volume change measured by burette, is not appropriate for automatic

control and auto matric data acquisition. Wheeler (1988) found out, following some calibration results, that the relationship between volume changes of the inner cell with cell pressure up to 400 kPa was nonlinear.

The issues in the above arrangement were found to be the leaking, even when a rolling diagram was applied due to the differential pressure. The differential pressure can deform the rolling membrane. The differential pressure can also cause the shaft to extend and, consequently, the changes in the volumes and measuring errors in the soil samples. The vertical load on the soil sample could be influenced by the frictional force. The water burette measuring technique is not suitable for computer control and automatic data acquisition.

Yin (2003) developed a double cell triaxial system (DCTS) to continuously measure the volume change of the soil samples. This developed system was based on (Bishop and Donald 1961, Yin 1998 and Wheeler 1988).

Yin (2003) enclosed the inner cell within the outer cell and the de-aired water was used. In addition to this, the inner and outer cell was subject to the same water pressure. This pressure can cause a negligible deformation in the top cap and the inner cell.

2.4.2.2 Shear strength

It is important to understand the shear strength of soil to analyse and solve the geotechnical problems. Bishop (1959) introduced new terms, which are the pore air pressure u_a the pore water pressure u_w and effective stress parameter, χ to modify Terzaghi's (1936) effective stress equation for unsaturated soil as following:

$$\sigma' = (\sigma - u_a) + \chi(u_a - u_w) \quad 2.1$$

where

χ is a parameter that depends on the degree of saturation. Under saturated or dry conditions, the parameter χ takes values from 0 to 1. u_a is the pore air pressure, u_w is the pore water pressure.

Increasing experimental evidence showed that the shear strength of unsaturated soil is higher than saturated soil (e.g. Fredlund et al., 1978). It has been suggested in numerous expressions by researchers for the shear strength difference of unsaturated soils. It is the most widely known, and uses two independent stress variable, as shown in this equation (Fredlund et al., 1978):

$$\tau = c' + (\sigma - u_a)\tan\emptyset' + (u_a - u_w)\tan\emptyset^b \quad 2.2$$

where

c' and $\emptyset^b$ are the cohesion intercept and friction angle respectively at a saturated condition, and $\emptyset^b$ is the friction angle with respect to changes in suction. This equation for the shear strength of an unsaturated soil is an extension of the equation for a saturated soil at the same net stress (Bishop 1959). The part of the equation of $(\sigma - u_a)\tan\emptyset'$ explains the increase in shear strength with increase in matric suction, while the term, $(\sigma - u_a)\tan\emptyset'$ describes the Coulomb failure envelope for unsaturated soil. Moreover, if $\emptyset^b$ is a constant and predicts a linear increase of shear strength with suction. Thereafter, numerous researchers (e.g. Escario and Saez 1986 and Gan et al., 1988) provide experimental proof that shear strength increases in a nonlinear approach with suction.

Khalili and Khabbaz (1998) proposed a two stress state variables with Bishop's stress as the first stress variable, where χ could be calculated from an experimental expression that relates the related current soil suction to the air entry value of the soil. Khalili et al., (2004) tested the validity of the approach and found good agreement between measured and predicted shear strength values. Vanapalli et al., (1996) proposed a model to predict shear strength for unsaturated soils by using the soil-water characteristic curve added to shear strength parameters for saturated conditions. However, Raveendirarj (2009) quizzed the physical reasonable grounds for relating shear strength to the soil-water characteristic curve, arguing that the physical reasons for an increase of shear strength with increasing suction are not completely the same as those for a decrease of degree of saturation with increasing suction.

Goh et al., (2010) tested soil shearing behaviour on the drying and wetting paths by conducting a series of CD Triaxial tests on compacted sand-kaolin samples. The result from the study suggested that the soils on the wetting path had a lower shear strength and showed higher and the stiffness, whereas with the drying path, the shear strength was higher, the stiffness was lower.

2.4.3 Stress state variable

The state of stress in a soil can explain its mechanical behaviour, such as volume change and shear strength. Stress comprises a combination of variables, which are independent of the physical behaviour of the soil (Barnes 2000). The variables used to describe the soil stress state rely on independent soil properties (Fung 1977). The behaviour of saturated soil can be described using the stress state variable, which is basically the effective stress. Therefore, the effective stress does not depend on the soil properties. The effective stress

of saturated soil controls the volume change process and the shear strength. The saturated soil theory can be used for stress analysis of unsaturated soil, since the same principles are used (e.g. Mohr diagrams). Numerous attempts to find the acceptable stress state, and there are two independent stress state variable for unsaturated soil (Fredlund et al., 1993).

2.4.4 Double-wall triaxial cell development

Both the inner and outer cells are pressurised by the same pressure during the test in double-wall system. In theory, null expansion of the inner cell can be achieved. Consequently, the volume change of the inner cell fluid measured during the test will be equal to the volume change of the unsaturated soil specimen tested.

Numerous types of equipment were designed according to the double wall idea. Bishop and Donald (1961) presented the first double wall cell. In this double wall cell, the mercury was used as a cell fluid in the inner container, whereas the outer cell was filled with water and the inner cell was opened. The movement of a stainless steel ball floating in the mercury observed the changes in the level of the mercury surface. In double-wall cell with opened inner cell, the soil volume change can be deduced from the change in the level of the inner cell fluid, which can be monitored by a ball floater Bishop and Donald (1961), a target float Matyas and Radhakrishna (1968), or a thin layer of silicon oil if mercury is replaced by water (Cui and Delage 1996). A differential pressure transducer was used to monitor the change in the level of the inner cell fluid.

Wheeler (1988) developed the double-wall cell, and the two cells were filled with water, (see Figure 2.3). Cui and Delage (1996) presented a cell related to that

presented by Bishop and Donald (1961) and rather than mercury. A coloured water was used in the inner cell.

Yin (1998) proposed almost the same system of Donald and Bishop (1961), but with water to fill the open-top cylindrical container, whereas the outer cell was filled with air. Later, Yin (2003) developed a double-wall triaxial cell using de-aired water to fill the inner and outer cell. Wheeler and SivaKumar (1993) used fluids other than mercury in conjunction with double wall triaxial cell (see Figure 2.4). SivaKumar (1993) increased the stiffness of the cell by reinforcing the cells with fiberglass bands. Sivakumar et al., (2002) presented a double-wall cell with an essential difference and the inner cell was made of the high quality glass, eradicating the absorption of the water by the acrylic walls of the inner cell.

Ng et al., (2002) suggested a double-wall cell with an open-top bottle-shaped inner cell to achieve more accurate reading in the changes of the water surface in the container. The Hong Kong University of Science and Technology have developed a system to further improve the measurement of the total volume of change of the unsaturated soil specimen. GDS has eventually manufactured the system (GDS Instruments 2011).

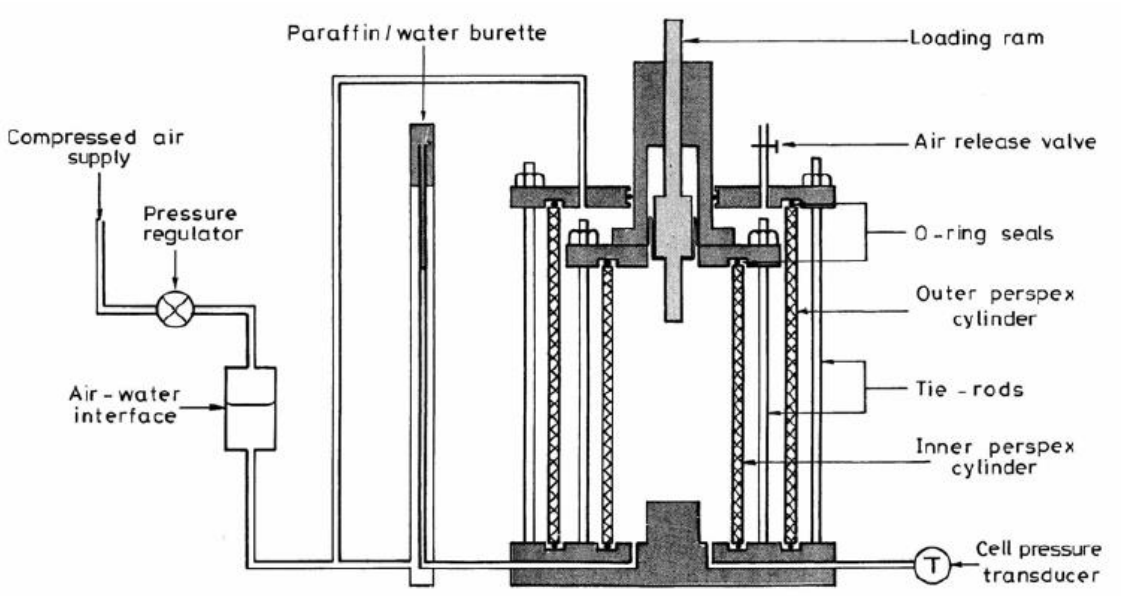

Figure 2.3 Double wall triaxial cell (wheeler 1988)

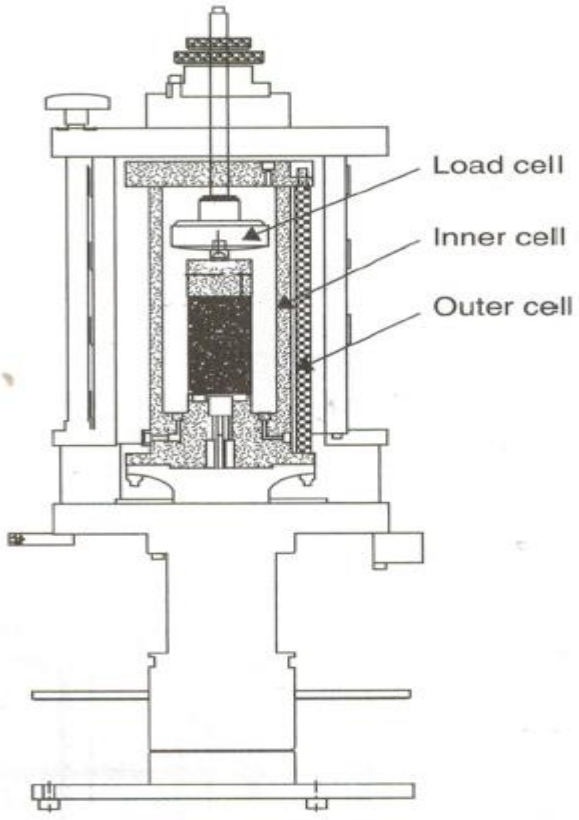

Figure 2.4 Double wall triaxial cell to increase accuracy in volume change measurement (Wheeler and Sivakumar, 1992)

2.5 Suction in unsaturated soil

Porous materials have a basic property of attracting and retaining water. This property is called suction (Bulut et al., 2001). This creates negative stress in the pore water, where the chemo-physical and molecular forces are stronger than the force of gravity, acting at the boundary between water and soil particles. This pulls water into unfilled void spaces, or holds it with no drainage. Soil at any degree of saturation, which has the capacity to absorb water, will pull in additional water at atmospheric pressure. Pour water plays an important role in the mechanics of unsaturated soil (Sivakumar 1993).

2.5.1 Total suction

Soil suction ψ is referred to a free energy state of soil water that can be measured in terms of the vapour pressure, such as total suction is described by Kelvin's equation, as follows;

$$\psi = \frac{RT_k}{M_w} \ln\left[\frac{u_v}{u_{v0}}\right] \qquad 2.3$$

where

ψ = soil suction or total suction in kPa, R is the universal gas constant (8.314 J/mol K), T_k is the absolute temperature (K), M_w is the molecular mass of water vapour (18.016 kg/kmol), are partial pressure of pore water vapour and saturation pressure of water vapour over a flat surface of pore water at the same temperature, kPa respectively. The term $\left[\frac{u_v}{u_{v0}}\right]$ is called relative humidity. Total soil suction is composed of two components: matric and osmotic components. The value of total suction is n addition of components, and depends on the value of osmotic suction (π) and matric suction ($u_a - u_w$).

$$\psi = (u_a - u_w) + \pi \qquad 2.4$$

2.5.2 Osmotic suction

Osmotic suction is produced by the concentration of salt in the water pores, and its pressure is independent, therefore, if the salt content in a soil changes there will be a change in the overall volume and shear strength of soil (Fredlund and Rahardjo 1993). Osmotic suction is very important for knowing soil properties, especially expansive soil, which has a high salt content leading to significant effect on the mechanical behaviour of unsaturated soil (Iwata et al., 1995). However, the effect of osmotic suction is typically neglected, because when the soil solution is dilute enough, the matric suction is not affected by contained solutes (Hillel 1998). Therefore, total suction is considered equal to matric suction Fredlund (1996). The chemical change of the pore fluid (including the salt type and concentration) has an effect on the volumetric behaviour of fine grain soils demonstrated by experimental evidence, particularly for expansive clays, (Alonso 1998).

2.5.3 Matric suction

Matric suction s is well defined as the pore air pressure (u_a) in excess of the pore water pressure (u_w) in unsaturated soils in kn/m^2 and is written as:

$$s = (u_a - u_w) \qquad 2.5$$

It is an important parameter to understand the mechanical behaviour of unsaturated soil, and depends on pore air pressure and water pressure acting at the interface between air and water, which is related to the surface tension

(Fredlund 2000). Accurate measurement and control at matric suction are essential to determine the mechanical behaviour of unsaturated soils. There is a problem for unsaturated soil that the water pressure in the pores is negative in comparison with atmospheric pressure. Obtaining the same condition in the laboratory will cause the cavitation's phenomena, which could be observed by the creation of air bubble in water under negative pressure these bubbles will cause an error on applying and measuring the water pressure. In addition, the measurement of the volume of water will be incorrect due to these bubbles. There are some methods have that been made to improve the suction measurement, such as axis translation technique, osmotic control and relative humidity technique (Sharma 1998 and Estabragh 2002). As follows:

a. **Axis translation technique:**

Hilf (1956) proposed this technique to aid in measuring pore water pressure of unsaturated soil in the laboratory, without the need to change the soil structure and the matric suction. The technique was initially proposed because the water pressure in an unsaturated soil is usually negative and can be difficult to measure. All the pressures from water, air and the total stress are increased by the same amount up to the point pore water pressure reaches above zero.

The suction is created as a result of the difference between air and water pressure. Due to the need to control or measure either of the pressures independently, a fine porous disc (high air entry disc) is used to stop the air from entering the water measuring system. This disc needs to be saturated all of the time and the pressure from the water in the disc is always equal to the pressure in the sample. The air entry value of the disc can control the maximum suction measurement.

Bishop and Donald (1961) provided the experimental indication of the validity of this technique in deformation tests. The hereunder researchers have utilised the technique of the axis translation (Fredlund and Morgenstern 1977, Ho and Fredlund 1982, Sivakumar 1993 and Sharma 1998). This technique has been selected for use in this research.

b. Osmotic control

The idea of osmotic control of matric suction derives from the concept of osmosis. Fredlund (2006) suggested that semi-permeable membranes exist between the sample of the soil and the osmotic solution, such as molecules of polyethylene glycol. The membrane absorbs the water through the pores. On the other hand, the membrane is impermeable towards large ions such as solute molecules.

The best advantage of the osmotic control for matric suction is that the cavitation is allowed to occur as the field condition. The cell pressure increase is not required as it is in the axis translation technique (Delage and Cui 1998).

The disadvantages of this technique is the difficulty in achieving the continuous variation of suction and the drawback in the semi-permeable membrane, which proved to be very weak if it exposed to excessive stress (Delage and Cui 1998).

c. Relative humidity technique

It has been observed that this technique is suitable when the suction is very high. The concept of the technique is to control and monitor the relative humidity of the surrounding air to the specimen (Delage and Cui 1998).

Kelvin's Law explains the relationship between the matric suction and relative humidity p as is written the following equation:

$$u_a - u_w = \frac{R \times T}{M \times g} ln \frac{p}{p_0} \quad 2.6$$

where

R is constant$(8.314\, J/mol\, K)$, M is water molar mass, T is the absolute temperature. The advantage of using this technique is that the values of suction applied are more than $1000\, MPa$. In addition, the difficulty of achieving continuous variation of suction is considered as a disadvantage of using this technique (Sharma 1998).

2.6 Soil Water Characteristic Curve (SWCC)

Soil-Water Characteristic Curve (SWCC) describes the relationship between water content in a soil and the soil suction. The SWCC have an important character in the determination of unsaturated soil property functions (Fredlund et al., 2012). Several researchers e.g. Fredlund and Xing (1994) and Vanapalli et al., (1999) reported that the total suction related to zero water content, and seems essentially the same for all types of soils, and its value is slightly lower than 1000,000 kPa. The SWCC can be expressed in many forms such as volumetric water content, gravimetric water content, or degree of saturation, the normalised water content can also be used in SWCC. These variables are to define the quantity of water in the soils, the mentioned variables are known as follows:

$$w = \frac{M_w}{M_s} \quad 2.7$$

where

w gravimetric water content

M_w is mass of water, and

M_s is mass of soil solid

The gravimetric water is used in geotechnical engineering, and volumetric water content is normally used in agriculture-related controls; it links the amount of water in the soil to the volume of the soil:

$$\theta = \frac{V_w}{V_v + V_s} \qquad 2.8$$

where

θ is volumetric water content, V_w is volume of water, V_v is volume of voids and V_s is volume of solid. The degree of saturation is the volume of water to the volume of voids:

$$S_r = \frac{V_w}{V_v} \qquad 2.9$$

Normalise water content has the quantity of water in the soil normalised between the residual volumetric water content and the initial saturated volumetric water content, the physical soil behaviour between saturated condition and the residual water content condition is isolated by the normalised water content (Ferdlund et al., 2012).

$$\Theta = \frac{\theta - \theta_r}{\theta_s - \theta_r} \qquad 2.10$$

where

θ_r is residual volumetric water content. In addition, a typical soil-water characteristic curve, takes the shape as S-curve when the soil suction is plotted on a logarithmic scale. Some features of the soil characteristic curve are described in Figure (2.5).

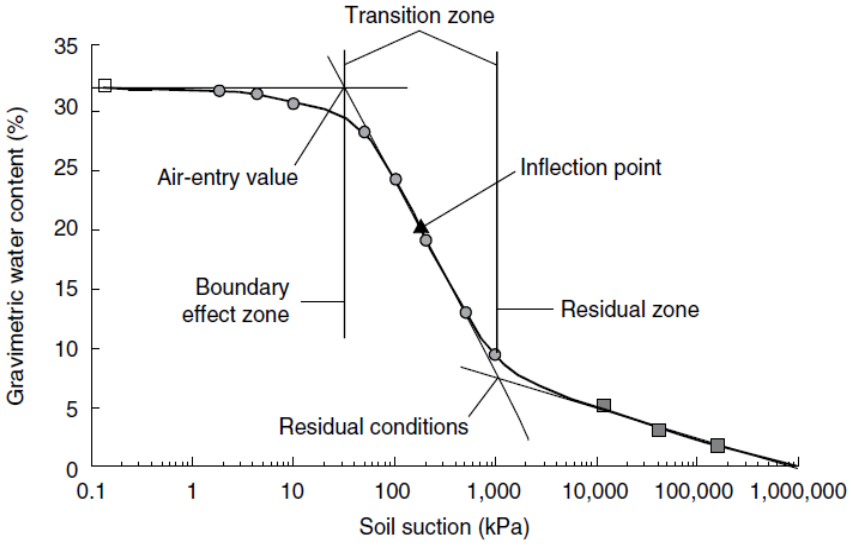

Figure 2.5 Typical soil-water characteristic curve showing different zones (Fredlund et al 2001a).

Based on the SWCC (Figure 2.5), Vanapalli et al., (1994) Identified three zones of desaturation, namely residual zone, transition zone, and boundary effect zone. Boundary effect zone, nearly all the pores are filled with water. In this zone, the flow of water is in a liquid phase. As the applied suction increases, water is released and the soil dries at slow rate until the air entry value (AEV) is reached.

Further increase of the matric suction beyond the air-entry value indicates the beginning of the transition zone. In this zone, the flow of water remains in liquid phase (Vanapalli et al., 1994). However, as the applied suction increases, water is released faster and the soil dries quickly producing reduction in the connectivity of the water within the voids or soil pores. At the end of the transition zone, suction increases largely causing comparatively small changes in soil water content. This is known as residual zone of saturation.

Where the water becomes discontinuous due to the low soil water content, the residual zone of saturation can be considered (Vanapalli et al., 1999). Therefore, in the residual zone, saturation represents humidity, at which it becomes increasingly difficult to remove water from a soil sample even by increasing the suction. The point of residual saturation is not always obviously defined. It should be noted that a graphical procedure is used to define the residual condition of saturation when the entire suction range is used (Vanapalli et al., 1999). Accordingly, the residual point can be obtained on the intersection of the tangent line through the inflection point, on the central straight portion of the SWCC, and the line extending from 1,000,000 kPa tangent to the final portion of the curve.

Different SWCCs are produced during drying and wetting of soil specimen, which is outlined by hysteresis in the relationship. The hysteresis mechanisms can be explained by the difference in the drying and wetting related in the soil-water interaction. The drying curve represents the water desorption of a soil when the matric suction increases while the wetting curve represents the water absorption of a soil when the matric suction decreases. Measurements of the drying curve are easier compared with the wetting curve, which is the time-consuming, (Fredlund 2006). There are some factors that can affect the shape of the SWCC, such as initial water content, soil sample preparation method, grin-size distribution, pore-size, dry density, mineralogy, stress state and etc. (Hillel 1998). It is important to study and understand soil behaviour or using SWCC for unsaturated soil models such as shear strength equation and volume change equation etc.

2.6.1 Air entry value

The air-entry value (AEV) of the soil is defined as the matric suction value that must be exceeded before air gets into the soil pores, (Fredlund and Rahardjo 1993). It represents the differential pressure between the air and water, which is required to cause desaturation of the largest pores (Vanapalli et al., 1999). The corresponding value of suction for that point of intersection is taken as the air entry value of the soil. The Air Entry Value (AEV) is the process of suction where the level of saturation drops under 100 %. When the soil undertakes a small volume changes during the drying path, the degree of saturation, gravimetric water content and volumetric water content will cause a similar value of AEV. When the soil volume change is significant, the AEV is more often less different on the SWCC. In this case, the degree of saturation can determine the AEV and the residual suction (Vanapalli et al., 1999 and Fredlund 2011).

A graphical procedure is used to measure the quantity of the AEV and the residual state when the whole suction range is used (Vanapalli et al., 1999). The procedure consisted of drawing a line tangent to the curve through the inflection point on the straight line liquid of the SWCC. The AEV of the soil is acquired by extending the constant slope portion of the SWCC to interconnect with the line that represents the SWCC in the low suction range (at 100 % saturation).

The water content at the AEV can be determined by the shrinkage curve of soil. Also, the suctions linked to the water contents can result from the suction – water content SWCC. When the drying process is taking place, an originally saturated slurred soil sample can follow the 100 % saturation line until air starts

to enter the largest pores. That is when the shrinkage curve starts to diverge from the 100 % saturation line. The soil carries on drying until the volume of pores remains constant, indicated by the shrinkage limit of the soil.

Fredlund and Rahardjo (1993) considered that the suction related to the shrinkage limit of the clay was the AEV. Before the shrinkage limit proceeds, the soil will significantly saturate. Therefore, the shrinkage limit will be different to the air entry water content. In some cases, the desaturation point can possibly remain close to the plastic limit. Hereafter, the suction related to the plastic limit can be considered the AEV. Fredlund et al., (2011), and Fredlund et al., (2012) proposed that the residual conditions can link to the shrinkage limit of the soil. The AEV is affected by some factors, such as the pore the size and the flow of water.

2.6.2 The capillary phenomena

It is identified as the movement of water in the connected void spaces that results from cohesion, surface tension and forces of adhesion. The capillary action is the difference between air pressure and the water pressure, which act on the interface between water and air (the contractile skin). The surface tension creates the capillary force, air and water keeps the water close to the point of two particles. The capillary phenomena can be seen when a small tube is put in water, the surface tension of the tube will cause the water rise, as shown in Figure (2.6) by (Estabragh., 2002).

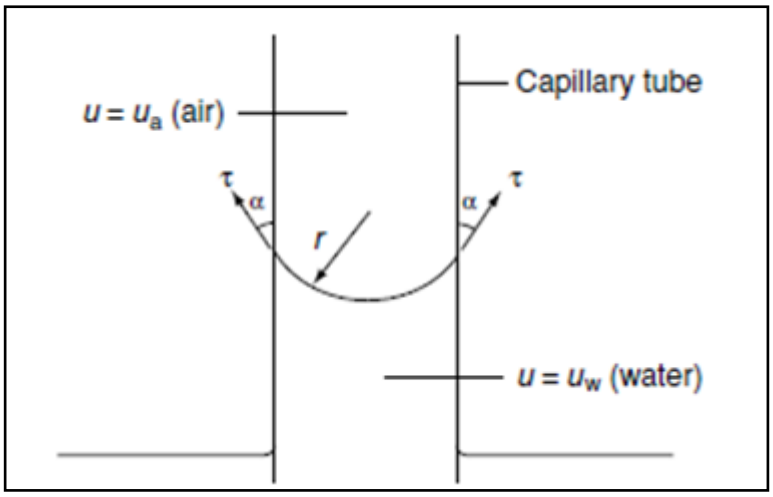

Figure 2.6 Capillary action by (Estabragh 2002)

The elevation of water in the tube $h_c$depends on the radius r, the value of the surface tension T_s and the contact angle α:

At vertical force equilibrium: $2\pi r * T_s * cos\alpha = h_c * \rho_w * g * \pi r^2$

$$h_c = \frac{2 * T_s * cos\alpha}{\rho_w * g * r} \qquad 2.11$$

where

ρ_w is density of water, g is gravitational.

The previous equation can be changed to:

$$h_c = \frac{2 * T_s}{\rho_w * g * R} \qquad 2.12$$

where R is the radius of curvature.

$$R = \frac{r}{cos\alpha} \qquad 2.13$$

2.6.3 Hysteresis

The drying and wetting SWCCs are significantly different. In the drying path of a soil, matric suction increases and the soil desorption of water. During the wetting, the soil adsorbed water while matric suction decreases (Fredlund and Rahardjo 1993). Soil under drying has a higher water content than the soil under wetting, at a given matric suction. The difference is referred to as hysteresis. In addition, the magnitude of the difference is generally dependent on the soil type. The hysteresis phenomenon of unsaturated soils can be explained using capillary theory, or “ink bottle effect”. When an empty capillary tube is placed in a water bath, the water inside the tube will rise above the water table until it reaches an equilibrium level. This corresponds to the wetting process of a soil. When a tube, which is filled with water, is placed in a water bath, the water inside the tube will drain out until it reaches an equilibrium level. This corresponds to the drying process of a soil. During the drying process, the water drainage from the pore is controlled by the neck pore diameter, or open pore diameter. On the other hand, the wetting process is controlled by the body pore diameter (Haines 1930). Therefore, an increase in pressure is required on the water front in order for water to re-enter small pores. This condition generates an imbalance in the pore pressure, which does not allow water to flow into the small pores until the surrounding pores are completely filled. This phenomenon is called the ink-bottle effect (Bear 1979).

The hysteresis can be explained by applying the capillary theory in SWCC of a soil in nature. During the drying and the wetting processes, the water content of soil at a given matric suction can end up being different due to the irregular shapes of pores and their different sizes. Besides all of the above, there are

three particular mechanisms that can cause hysteresis in the SWCC, which are as follows:

Firstly, the soil fabric can change due to the swelling and shrinking of aged soil, structure and pore size distribution, depending on the drying and wetting of a soil history (Hillel and Mottas 1966).

Secondly, the contact angle between air-water and soil solids and the radius of curvature are greater for advancing meniscus during wetting. During drying, the contact angle and the radius of curvature receding meniscus is less (Hillel 1971, Bear, 1979 and Lu and Likos 2004).

Finally, water content of new wetted path of the soil can be decreased, or due to the occurrence on the entrapped air (Hillel 1971 and Fredlund and Rahardjo., 1993a).

2.6.4 Soil-water characteristic curve measurement.

The measurement of the SWCC of a soil is a cost and time-consuming task, especially for clayey soil. Fredlund and Xing (1994) reported that the cost for the unsaturated soil measurements are excessive and could be ten times as much as the cost and time of measuring the saturated soil properties. Consequently, a number of novel technique, equations and models, which include the usage of SWCC and saturated soil properties, can be used to evaluate the unsaturated soil property functions have developed in the past few decades.

Fredlund (2002) found that if the SWCC can be projected from the soil properties such as grain-size distribution curve, the costs for obtaining the unsaturated soil properties can be reduced. Valuation of SWCC functions are termed as Pedo-Transfer Function (PTF). Bouma (1989) defined PTF as a

function that relates to basic soil data such as the grain-size distribution, or porosity and yields a soil property function. There are a number of methods that were introduced for SWCC estimation in the past. SWCC estimation methods can be divided into three broad categories: Functional Parameter Regression Method, Point Regression Method, and Physico-Empirical Method.

2.6.5 Mathematical model of the soil-water characteristic curve

Mckee and Bumb (1987) proposed an empirical equation in the literature to represent the soil-water characteristic curve. An analytical basis for mathematically defining the entire soil-water characteristic is curve provided by (Fredlund and Xing 1994). The equation applies over the entire series of suction from zero to 1.000.000 kPa. This relationship is empirical, but is gained from the pore size distribution, assuming that the soil consists of an interconnected pore that is randomly distributed. Commonly, the equation is written in terms of volumetric content:

$$\theta = C(\boldsymbol{\psi}) \left\{ \frac{\theta_s}{\ln[(e+ \left(\frac{\Psi}{a}\right)^n)]^m} \right\} \qquad 2.14$$

where

θ is volumetric water content

θ_s is saturated volumetric water content

a is a suction related the air-entry value of the soil

n is a soils parameter related to the slope at the inflection point on the soil-water characteristic curve

$\boldsymbol{\psi}$ is soil suction

m is a soil parameter related to the residual water content

θ_r is volumetric water content at residual conditions

e is a natural number, 2.71828 and C($\boldsymbol{\psi}$) is a correction function that of 1000000 kPa and zero water content. The correction factor is clearfield as:

$$C(\boldsymbol{\psi}) = [\,1 - \frac{\ln 1+(\frac{\psi}{c_r})}{\ln(1+\frac{1000000}{c_r})}] \qquad 2.15$$

where

C_r is the suction value corresponding to residual water content. Equation [2.15] can be printed in a regularised form by dividing both sides of the equation by the volumetric water content at saturation.

$$\boldsymbol{\Theta} = \frac{\theta}{\theta_s} \qquad 2.16$$

where

θ is volumetric water content, θ_s is volumetric water content at saturation of 100%. However, the degree of saturation, $S.$ is also equal to the normalised volumetric water content.

To date, many closed formula have been suggested to designate the SWCC. Commonly, these empirical SWCC calculations can be used to best-fit SWCC using a least square regression analysis. All the suggested formulas have one variable that is connected to the AEV of soil, and one variable that is related to the desaturation rate of soil. Fredlund (2006) mentioned that if there is a third variable, it allows the low matric suction range, which is near the AEV, to have a shape that is independent of the high matric suction range which is near the residual matric suction.

Gardner's (1958) equation is one of the earliest equations for best-fitting the SWCC. Formerly, this formula was recommended for modelling the unsaturated coefficient of permeability of soil. However, Sillers et al., (2001) modified this equation for the SWCC of soil. There are two fitting parameters are used in this equation, where parameter "n" is related to the pore size distribution while parameter "a" is related to the inverse of AEV. Gardner (1958) equation is as follows:

$$\theta_w = \theta_r + \frac{\theta_s - \theta_r}{1 + a\psi^n} \qquad 2.17$$

where:

θ_w is volumetric water content

θ_r is residual volumetric water content

θ_s is saturated volumetric water content

$\boldsymbol{\psi}$ is matric suction of soil

Two fitting parameters, a and λ, are used in (Brooks and Corey 1964) equation [2.18]. Brooks and Corey assumed that the water content is constant for the range of matric suction less than AEV. For the range of matric suction higher than AEV, SWCC is proposed to decrease exponentially. Brooks and Corey's (1964) equations are as follows:

$$\theta_w = \theta_s \left(\frac{\psi}{a}\right)^{-\lambda} \qquad 2.18$$

$\theta_w = \theta_s$ when $\boldsymbol{\psi} < a$

where:

a is a fitting parameter which is related to the AEV of the soil.

λ is a fitting parameter which is termed as pore size distribution index.

The more uniform the pore-size distribution of a soil, the greater the value of λ and the steeper the SWCC slope of the soil within the desaturation zone. Equation [2.16] is more recommended to be used for relatively coarse particle soil. However, as no inflection point is included in the equation [2.17], so it is not a continuous function for the entire SWCC. It always results in poor fitting of SWCC over a wide range of matric suction. The sudden alteration in the curve may produce numerical instability when modelling an unsaturated soil behaviour (Sillers, et al., 2001 and Lu and Likos 2004).

The equation [2.19] of van Genuchten (1980) is a continuous SWCC best-fit equation. This equation delivers an extensive range of flexibility in fitting the SWCC information of diversity kinds of soil. Three fitting parameters, *a*, *p* and *q*, which have specific physical connotations are used. The best-fitted fitting parameter values may diverge depending on the convergence procedure, the number of iterations used and the initial values used for iterating the fitting parameters. van Genuchten (1980) equation is given as follows:

$$\theta_w = \theta_s \left[\frac{1}{1+(a\Psi)^p}\right]^q \qquad 2.19$$

where

a is a fitting parameter which is related to the inverse of the AEV.

p is a fitting parameter which is related to the pore-size distribution of the soil.

q is a fitting parameter which is related to the asymmetry of the SWCC curve.

Three fitting parameters with specific physical connotations are used in Fredlund and Xing (1994) equation which has the form in equation [2.19].

Fredlund and Xing (1994) equation has a similar form as (van Genuchten, 1980):

$$\Theta = [C(\psi)] * \left[\frac{1}{\boldsymbol{ln}\left(e + \left(\frac{\psi}{a}\right)^{n}\right)}\right]^{m} \qquad 2.20$$

where

a is a soil parameter which is primarily a function of the AEV of the soil (kPa). n is a soil parameter which is primarily a function of the rate of water extraction from the soil once the AEV has been exceeded.

m is a soil parameter which is primarily a function of the residual water content

e is natural number, 2.71828.

$[C(\psi)]$ = correction function that forces the SWCC through a matric suction of 1 GPa and zero water content.

Correction factor, $C(\psi)$, was presented by Fredlund and Xing (1994) to be used in equation [2.17] to guarantee that the water content is zero at matric suction of 1 GPa. The correction factor, $C(\psi)$, has the following form:

$$C(\psi) = 1 - \frac{ln\left(1+\frac{\psi}{\psi_r}\right)}{ln\left(1+\frac{10^6}{\psi_r}\right)} \qquad 2.21$$

where

ψ_r is suction at which residual water content occurs (kPa).

In equation [2.20] the correction factor, $C(\psi)$, was proposed to be unity by (Leong and Rahardjo., 1997). With $C(\psi)$ = 1, the initial portion of the SWCC, which is relatively important, is not affected by $C(\psi)$ (Leong and Rahardjo.,

1997b). It is appropriate to be used for best-fitting the SWCC of soil at low matric suction range (i.e. less than 1500 kPa). Also, the computational exertion for determining the fitting parameters could be reduced.

Leong and Rahardjo., (1997b) recommended that Fredlund and Xing (1994) equation [2.17] is the best SWCC best-fit equation for an extensive range soils over the entire matric suction range. In contrast with van Genuchten (1980) equation, Fredlund and Xing (1994) equation was created to require less iteration to converge towards the best-fit parameters (Sillers 1997). In addition, the fitting parameters used in Fredlund and Xing (1994) equation have a convinced physical meaning, i.e. *a* is carefully related to AEV, *n* is closely related to pore-size distribution and the slope of the SWCC and *m* is closely related to residual matric suction (Leong and Rahardjo 1997, Yang et al., 2004 and Gallage and Uchimura 2010). As the parameter, *a*, increases, the SWCC curve is lifted to a higher matric suction range without disturbing the overall shape of SWCC. The soil with a more uniform pore-size distribution consumes a greater value of *n* and a sharper slope of SWCC than those with a less uniform pore-size distribution. The parameter, *m*, is lesser in the SWCC with a higher residual water content.

Fredlund and Xing (1994) equation has the same restrictions as van Genuchten (1980), equation, in which the best-fitted fitting parameter values may differ depending on the convergence procedure, number of iterations that are used and the initial values that are used for the fitting parameter

2.7 Fibre reinforcement

The synthetic and natural carpet waste used in this study was obtained from Carpet Recycling UK, and is composed of materials, such as polypropylene,

nylon, cotton, polyester, etc. According to Wang (2006) carpet waste has a high volume to weight ratio, compared to materials that have the same weight as carpet waste volume occupies a large space. The carpets are of interest as they have multiple uses such as conservation of resources. This in its turn causes the reduction of landfills that are needed to store this waste, which subsequently reduces associated tipping fees, and provides low cost raw materials for products. Fibre waste e.g. carpet, can be used in a wide range of applications, such as energy recovery, sport surfaces, insulation and reinforcement. Generally, the fibre produced is categorised into one of three categories, apparel, home furnishing and industrial. Most of the fibre products are short term e.g. disposables, whereas medium term e.g. carpets, can last few years in their service life. Fibrous waste is associated with a number of disadvantages such as tipping cost, environmental concerns e.g. banning landfills from landfill polymers, which are a waste of energy and materials (Mirzababaie 2012).

Logeshwari et al., (2014) studied the stress strain behaviour of clayey sand under unconsolidated undrained triaxial tests, which were conducted for various confining pressures. The specimens were prepared by the slurry consolidation method.

Many studies, along with this one, have investigated carpet waste reinforcement of soils, a large amount of valuable resources that can be used to investigate their role in reinforcing unsaturated soil. Mirzababaei (2012) investigated the carpet waste fibre on clay samples prepared at the same dry unit weight of 17.8 kN/m^3, the result of the investigation shows that, the shear strength parameters increased by 41.4 % compared with non-reinforced same soil at fibre content to 5%. Ayyappan et al., (2010) studied the influence of fibre variables (content and

length) on performance of fibre reinforced soil- fly ash specimens through a series of laboratory unconfined compression strength tests and California bearing ratio tests. It was concluded that the inclusion of fibres had a significant influence on the engineering behaviour of soil-fly ash mixtures. The inclusion of fibres increased the peak compressive strength and ductility of soil-fly ash specimens also showed an increase in fibre length reduced the contribution of fibres to peak compressive strength, while increasing the contribution to energy absorption capacity, or ductility of soil- fly ash specimens. The relative benefit in CBR values due to fibres increases only up-to 1.00 % by dry weight and length up to 12 mm for all soil-fly ash specimens.

Gao et al., (2015) studied the mechanism and effect of basalt fibre reinforced clay soil, through a series of unconfined compressive strength tests conducted on clay soil reinforced with basalt fibre under the condition of maximum dry density and optimum water content. Taking into consideration that the content and the length of basalt fibre are considered in this paper, the strength of basalt fibre reinforced clay soil is influenced by the interfacial force in the form of fibre-soil column and fibre-soil net based on the suggested fibre and soil column-net model and SEM images. The overall strength of soil samples was affected by the large length of fibre through the total stress and distribution configuration of fibre-soil net. The basalt fibre successfully improved the UCS of clay soil. Once the fibre length is constant, the strength increases firstly, then slightly decreases with the length of fibre increasing. The effect of reinforcement reaches the maximum with the length of 12 mm. the basalt fibre reinforced clay soil has the “poststrong” characteristic when compared with the soil without fibre. Also it has a higher breaking strength and a more stable performance.

2.7.1 Fibre-soil reinforcement

Lately, soil reinforcement with fibre is gaining more attention by many investigators around the world. The natural or synthetic fibre have been used to improve the mechanical properties of sand soils. The role of fibre-reinforced soil has a behaves similar to that of composite material, which fibres of comparatively high tensile strength are embedded in a matrix of soil. Shahnazari et al., (2009) study assessed the role of fine sand reinforced with carpet and geotextile strips subjected to dynamic loading by performing two sets of cyclic triaxial test on large and small scale. The experiments results showed that the effect of this type of reinforcement on shear modulus under low confining pressure (less than 100 kPa) are insignificant, whereas in high confining pressure to be significant. In addition, the strain supported the reinforced samples at the failure point, which was much higher than that of plain samples. The results also show that shear strength between soil and strips were increased by enhancing stress level.

Shbib and Okumura (2002) preformed a series of laboratory experiments on discrete fibre/cement very soft clay soil composite (FR-CDM) which was reported to have given a good impression towards using Discrete Randomly Distributed Fibres (DRDF) as a new additional additive to the conventional cement deep mixing of soft ground improvement (CDM) in which the compressive strength of treated soil can be increased dramatically, but with low tensile strength of CDM soils, this causes the failure under compression and tension to be brittle and is associated with increased hazards as the amount of required cement dosage increases. Therefore, it is essential that an optimal concentration is reached, one that would enable the soil to have a high

compressive strength with low brittle and other risks. However, with the addition of fibre this problem was solved, as it significantly enhanced the static response of the composite by increasing the ductility and absorbed strain energy. It is expected that fibre inclusion to cement deep mixing is expected to play a good role as a cost-save factor, which may lead to a new generation of soft ground improvement by cement deep mixing technique.

Chen and Loehy (2008) preformed a series of tests on consolidated-undrained and consolidated-drained type triaxial compression on unreinforced and fibre-reinforced specimens, their experiment looked at the effect of stress-strain pore pressure, as well as effective stress-strain volume change behaviour of fibre-reinforced sands. The results obtained demonstrated that fibres increased the effective stress cohesion intercept and the effective stress friction angle. The reinforcing fibres alter the pore pressure response of the specimen tested under undrained loading condition, and as a result, the volume change response of specimen tested under drained loading condition. The resistance, due to the fibre reinforcement, is mobilised at lower strain in drained tests than in undrained tests, which suggests that volumetric strain plays an important role in mobilisation of fibre resistance. The peak deviator stress in the fibre-reinforced sand specimen were not mobilised until they reached strains of 25 %. It is rare for such large strains to tolerate such stress; therefore, it is important to establish the failure envelope at limiting strains, which helps to evaluate the effects of the fibre inclusion on mobilised resistance at small strains. This helps to implement the fibre-reinforced soil in engineering practice.

Park (2009) carried out a series of unconfined compression tests to examine the effect of fibre reinforcement and distribution on the strength of fibre-

reinforced cemented sand. The experiment consisted of Nakdong River sand, polyvinyl alcohol fibre, cement and water, all of which were mixed and compacted into a cylindrical sample of five equal layers. The polyvinyl alcohol fibre was distributed randomly across the five layers; this resulted in the strength of fibre-reinforced cemented sand to increase as the number of fibre inclusion layers increased. When the fibres were evenly distrusted through the five layers, it was reported that reinforced specimen become twice as strong as a non-fibre reinforced specimen. The experiment went further to investigate the effect of using the same amount of fibre to reinforce two different specimens, one with fibre inclusion, which was 1.5 times stronger than a specimen, with one fibre inclusion layer at the middle of the specimen. This reveals that fibre reinforcement and distribution throughout the entire specimen resulted in an overall significant increase in the strength of fibre-reinforced cemented sand. This shows that the strength of fibre-reinforced cement soil does not only depend on the fibre reinforcement distribution, but also on the amount of fibre used in the specimen.

Malekzade and Bisel (2012) studied the effect of polypropylene fibre on swell and compressibility of expansive soils. Four types of polypropylene fibre dosage (0 %, 0.5 %, 0.75 % and 1 % by dry weight of soil) were implemented in this experimental study. It shows that the swell increased with addition of fibre content from 0.5 % to 0.75 % and reduced with 1 % fibre content. An improvement can be examined on the compressibility of the soil, which has been mixed with 1 % polypropylene fibre. Hydraulic conductivity reduced with addition of fibre content from 0.5 % to 1%. For 0.75 % fibre content, the hydraulic conductivity increased. Some inconsistency of the result was

observed to find the hydraulic conductivity. It happened due to a random distribution of fibre in the soil matrix. As a result, there is a tendency for hydraulic conductivity to increase with the increase of fibre content.

Ramasamy et al., (2013) studied the effect of inclusion of polypropylene fibre content of 0 %, 0.25 %, 0.50 %, 0.75 %, 1.0 % and 1.25 % in clay soil sample on maximum dry density and optimum moisture content. The investigation of the tests concentrated on the unconfined compression test, California bearing ratio test and swelling behaviour of the soil sample.

The test results concluded that the addition of polypropylene fibre does not affect the optimum water content, however maximum dry density has been reduced. The strength of unconfined compressive increased with the addition of polypropylene fibre. The cohesion maximum value was noted with 0.75 % fibre content, which is nearly 1.34 more times of the unreinforced soil. Therefore, the fibre improves the ductile behaviour of soil, reducing shrinkage settlement during drying.

Jiesheng et al., (2014) reported that the sisal fibre was used in the field of soil reinforcement. The fibre content for the soil sample was more or less 0.6 % of the dry unit weight. The test resulted in the strength improvement in the reinforced clay soil. The increase in the fibre content did not influence the strength significantly. It can be argued that the sisal fibre makes cementation links between the soil particles, and fibre promotes the stress distribution on an equal level.

Mukherjee and Mishra (2014) investigated the influence of glass fibre and geo-synthetic clay liner (GCL) on different sand bentonite mixtures. It was noticed that swelling increased with the inclusion of one layer GCL and significantly

deceased with glass fibre. The test result showed that hydraulic conductivity reduced significantly with interaction of GCL, but slightly increased with the addition of glass fibre. It has been also observed that compression index and swelling pressure has been reduced with the addition of glass fibre. Unconfined Compression Strength (UCS) was found to decrease with the addition of one-layer geo-synthetic clay liner, but UCS increased with the inclusion of glass fibre.

A series of consolidated undrained triaxial tests conducted under effective consolidation pressures of 50, 100 and 200 kPa are carried out by Devrim ERDOĞAN and Selim ALTUN (2015) who investigated the undrained response of fibre reinforced sands. It showed that the presence of fibres caused a considerable amount of decrease in excess pore water pressures, while contributing to an increase in deviator stresses of the samples. This would only be possible if sand matrix and the fibre phase both contributed to deviator and hydrostatic stress state of the reinforced samples, which was proved to be absolutely strain level dependent.

Krishna et al., (2015) evaluated the effects of the use of Groundnut Shell Ash and waste fibre material on the shear strength of unsaturated soil by conducting direct shear tests and unconfined compression tests on the soil sample. The results indicated that groundnut shell ash and polypropylene fibre reinforced soil is believed to be an improvement technique on weak soil where it can be used as a substitute to reduce the cost and the energy.

Kumar et al., (2015) investigated the improvement in CBR values of soil reinforced with Jute Fibre. CBR soil value increases with the inclusion of Jute fibre. When the Jute fibre content is increased, the CBR value of soil further

increases and this increase is substantial up to a fibre content of 5 %. It was also found that the preparation of identical soil samples for a CBR test beyond 5 % of fibre content is not possible, and optimum fibre content is expected to be between 4 to 5 % by dry weight of soil. The optimum length of fibre is somewhere between 60 to 80 mm. It is also concluded that there is significant effects of length and diameter of fibre on the CBR value of soil. The CBR soil value increases with the increase in length and diameter of fibre. Further, the addition of Jute fibre makes the soil a composite material whose strength and stiffness is greater than that of unreinforced soil. The strength and stiffness of reinforced soil increases with the increase in fibre content, and it may also due to this reason that the CBR value of reinforced soil was observed to be greater than that of unreinforced soil.

Qu and Sun (2016) studied the shear strength behaviour of Shanghai clayey reinforced with Wheat straw fibres based in a laboratory investigation under different percentages of fibre, the results show that the shear strength generally increases with increasing fibre content, as well as friction angle of the natural soil until an optimum content value is reached. Mathe and Ramesan (2016) investigate and evaluate the effects of polypropylene fibres and coir fibres on various properties of soil. It is approved that when the coir fibre content is mixed, the unconfined compressive strength failed at fibre content more than 1.5 % in case of coir fibre. Therefore, it is concluded that 30 mm fibres at 1.5 % a maximum value of unconfined compressive strength. The best polypropylene fibre content was found 1% by weight of soil. The unconfined compressive strength of reinforced clay was more than 5 times than of unreinforced clay. The coir reinforced clay was more than 4 times that of unreinforced clay. The results

of polypropylene and coir fibres are similar and hence coir fibre can be used as an effective soil reinforcement. As well as, the California Bearing Ratio (CBR) of coir reinforced clay was comparable to PP fibre. The fact that coir fibre is economical and an organic material, makes it an effective reinforcement in soil.

2.7.2 Influence of Fibre on Soil behaviour

The purpose of soil as a construction material has changed the idea of soil reinforcement. Since the 1960s, much of the existing knowledge has been obtained, starting with the pioneering work of (Vidal 1966). For the time being, with the advances in the techniques of using synthetic fabrics and carpet waste, soil reinforcement has progressed in the construction of embankments, foundations, tunnels, slopes, landfill closures, etc. This section describes carpet waste reinforcement, with a focus on laboratory research, such as mixing placement, compaction, and performance of fibre-reinforced soil.

Waldron (1977) gave an important contribution of fibre plant roots to shear strength of soils and slope stability. In this work, direct shear tests were performed on 25 cm diameter root-permeated soil columns, composed of compacted layers of silty-clay loam at 30 cm depth. The results are given in terms of slope safety factor, which showed a remarkable increase due to root reinforcement.

Gray and Ohashi (1983) investigated different synthetic, natural and metallic fibre reinforcement dry sand. A series of small direct shear tests were done, to gauge the effect of parameters such as content, stiffness, fibre orientation and sand density on shear strength. Under laboratory conditions, they presented a force-equilibrium model, which predicted the contribution of fibre to shear

strength of sand. The result showed that the peak shear strength increased, with increase fibre.

Consoli et al., (2003) also showed that the reinforcement of sandy soil with polypropylene fibres improved the behaviour of soil by increasing its strength with the increase in settlement. Palm fibres were shown to improve the ductility of salty sands, which caused the soil to fail at higher axial strains (Marandi et al., 2008). Ayyappan et al., (2010) reported that introducing polypropylene fibres into fly ash soil mixtures increased its unconfined compressive strength significantly. Shukla et al., (2010) studied the influence of fibre on the confining strength of granular soils considering different soil and fibre parameters, such as fibre content, the fibre's modulus of elasticity, the specific gravity and void ratio of soil, as well as initial orientation with respect to shear strength plane.

Freilich et al., (2010) experimented using triaxial tests of both Isotropic Consolidation-Undrained (ICU) and Isotropic Consolidated-Drained (ICD) clays. These two clays had Plasticity Index (*PI*) of 49 and 54. In addition, the fibre used was polypropylene at 5 % by dry weight of clay and was hand mixed into the clays to give 71 mm diameter and 142 mm high specimens. The results showed that given the failure envelopes determined from the ICU test, an increase in the effective shear strength of soil in the fibre's presence was recorded. However, over a long period of time, the drained condition as a proof of the effective of the fibre-reinforced soil may significantly decrease. The effectiveness of fibre on the pore pressure for the period of the CU test will possibly present a higher assessment of effective strength but the decrease in strength was initially attributed to creep along the fibre-soil interface.

A small amount of 2 % by weight of randomly polypropylene fibre has been investigated under compaction with triaxial compression tests on sandy gravel. This investigation showed that the shear strength decreased mostly due to increased porosity, with increasing fibre content. The study concluded that compactive efforts need to be adjusted to reduce porosity (Hoare 1979).

The soil stabilisation method was studied, which involved mixing molecularly oriented net elements in the form of squares, or rectangles with soil, in order to find the important properties of the net and effect of net content on the behaviour of stabilised soil. Testes of triaxial compression (CBR) and model footing test were done by mixing 40 mm square mesh elements with sand. The result showed improved stress resistance and increased ductility (Mercer 1984).

In order to compare the stress-strain response of reinforced sand, experiments using continuous layers of fabric instead of oriented fibre, separately and randomly distributed, were performed. A series of triaxial compression tests were done on dry, uniform sand matrix with two kinds of fibres, high strength, smooth glass fibres, and medium tensile strength, rough, natural reed fibres Gray and Al-refeai (1986). The results revealed that:

1. Both the strength and stiffness increased, due to the presence of fibre reinforcement in the sand.
2. There was a decrease in stiffness at low strains observed fabric inclusion.
3. As fibre inclusion varied, the strength increased linearly up to a fibre content of 2 % by weight.

4. At the same aspect ratio (length over diameter ratio) and weight content, rougher fibres tended to be more effective in increasing strength at low confining stress.

In a related study by Alonso et al., (1987) a limited series of tests were conducted on silicate sand reinforced with randomly distributed wire fibres. The study utilised a new technique, i.e. freezing the sand-fibre composites during the mixing process, in order to limit soil-fibre separation. They found that the inclusion of discrete wire fibre interfered with particle packing, and as a result, a lower sand density for samples with fibre was recorded. However, they concluded that the fibre reinforcement at the same compatible sand density would give higher unconfined compressive strength, and increased axial strength at failure, and reduced post-peak loss of strength in the saturated frozen sand. These findings were reported along with the result of the influence of fibre aspect ratio on frozen compressive strength (Al-Moussawi and Andersland 1988).

Habibagahi and Mostaghel (1974) studied the possibilities of improving the tensile strength of cohesive soil; they investigated the use of gypsum plasters, straw, hemp and cellophane fibres, in several mixtures (by weight) in soil. The outcome presented a two-fold increase in tensile strength with the addition of 5 % gypsum. Furthermore, the addition of hemp or cellophane fibres to the soil increased the tensile strength, provided it was randomly distributed through the sample. Kumar et al., (2006) investigated the compression strength of polyester-reinforced soft clay and polyester-reinforced clayey sand. Even though the compaction degree influenced the process, it was found that the unconfined compressive strength of the clay increased with inclusion of

polyester fibres. This increased further as fibre was mixed with clay sand mixture, and the test showed high repeatability, where fibre to soil ratio was 0.5 %, 1 %, 1.5 %, and 2 % by weight.

For soil stabilisation improvement, different admixtures were used, including mixing soil with randomly placed fibres. Strength tests were conducted by many researchers, using triaxial, unconfined compressive, shear box, CBR, and tensile and flexural strength tests. The random distribution of reinforced fibre is an advantage, as there are no planes of weakness, which can develop parallel to oriented reinforcement. Metal strips, paper, nylon and polyester are widely used as reinforced materials in granular soil.

There are a number of practices to increase the strength and decrease the deformation of soft soils, to overcome their low strength and high compressibility, Estabragh et al., (2011) investigated the clay of low plasticity (CL) reinforced with nylon fibres. In addition, one-dimensional consolidation (Odometer) and Consolidation Undrained (CU) tests were carried out. The result revealed that the mechanical properties changed with increasing fibre content in the reinforced soil during consolidation. The consolidation characteristics of randomly reinforced clay soil have been significant with fibre inclusion.

Failure envelopes determined from CU triaxial tests indicated an increase in the effective shear strength of soil in the presence of fibres. Moreover, the stiffness and shear strength of soil increased with increasing fibre content. The total stresses and effective increased also with increasing fibre content.

Anagnostopoulos et al., (2014) studied the influence of polypropylene fibre reinforced cohesive soils on the shear strength parameters. The researcher used two types of polypropylene fibres with varied percentages of 0.3 % and 1.1 % by the weight of dry soil. A number of tests, such as consolidated drained or undrained direct shear tests, were carried out on the unreinforced and reinforced sandy silt and silty clay samples. The results showed the shear strength increased with the increase of fibre content. The high shear strength is kept due to the micro mechanism involved in the fibre and soil interactions as investigated through the scanning electron micrograph.

Behzad and Sherif (2015) used a resonant column testing, the contents of fibre in clay were identified. The dynamic properties of clay can be improved by using fibre at optimum fibre content at the low shear strains. The test results revealed that both the shear modulus and damping increased. Therefore, the fibre addition in clay can benefit the dynamic response of a site by increasing the stiffness of the site and reducing its vibration.

2.7.3 Fabric of unsaturated soil.

Ground reinforcement is the building or inclusion of elements on the ground, with the main benefit resulting from the structural form of the elements themselves and improvement of the surrounding soil. Ground reinforcement encompasses some techniques, such as biotechnical-soil bioengineering stabilisation, deep mixing, fibre reinforced soil, geo-synthetics, anchors, jet grouting, lime-cement, mechanical stabilisation, micro-mini piles, and soil nailed retaining structures and inclusion of fibre concrete columns and fibre replacements. These techniques were introduced and accepted years ago (Vernon and Schaefer 1997).

The period 1987-1997 saw a dramatic increase in the acceptance and use of jet grouting and other solution. Research is being conducted at several universities to increase the understanding of how these methods perform, and to further develop the design methodologies. Increase in the use of ground anchors, and others in applications is not expected. However, Koerner in the (1996) Tezaghi Lecture suggested new uses for geo-synthetic (Vernon and Schaefer 1987-1997). In this research, the carpet waste fibre reinforced unsaturated soil will be investigated.

According to Toll (1990) the fabric may be less important in saturated soils than in unsaturated soils. In compression test, the fabric will fail due to high stress in saturated soil, but in unsaturated soil, the fabric is supported by suction and may be kept under shear or compressive stress. Croney et al., (1958) pointed out that compacted clays did not exist as a uniform mass of clay particles, but contained aggregations of clay particles, separated by comparatively large air voids.

In unsaturated soil, the fabrication is a more important factor than in saturated soil. The reason for this is that the suction will support the fabric if the unsaturated soil subjected to stress or shear, while the damage will happen immediately in fully saturated soil if subjected to shear force or compression (Toll 1990). In the review of the literature, no issues have been conducted with unsaturated soil reinforced. To the best of the author’s knowledge no studies on the mechanical behaviour of fibre reinforced unsaturated soil have been conducted. Hence, no data are available for the behaviour of fibre reinforced unsaturated soils in the open technical literature.

2.8 Modelling of unsaturated soil

To study particular physical processes, sometimes there is a need to use models. Minshull (1975) states that a model can be a theory, law structured idea, equation, analysis or synthesis of data. To describe a physical process, it is necessary to observe and understand its characteristics and the conditions under which it occurs. In other words, it is possible to use a mathematical model to describe the physical process. Mathematical models are extremely powerful because they usually allow for making predictions about a process; the prediction may provide information for further experimentation or model improvement.

The following advantages and benefits can be derived from a model:

- A model can provide a framework and a consistent way for understanding, discussing and comparing various aspects of unsaturated soil behaviour.
- A model serves to guide future research along different paths and suggests suitable experimental programmes.
- A model may assist in the identification of basic parameters and reference states governing the soil behaviour.

The test in the plan are sufficient to define the soil parameters related to a model for unsaturated soils. The result could be particularly useful for modelling purposes; the modelling will be further validated against results from laboratory tests of unsaturated soil samples.

The shear strength of unsaturated soil equation has been extended by Bishop (1959) for the Terzaghi's (1936) principle of effective stress of saturated soil.

$\tau = [\, c' + (\sigma_n - u_a)\ \tan \emptyset' \,] + [\, \chi\ (u_a - u_w) \tan \emptyset' \,]$ *2.22*

where

τ is shear strength of unsaturated soil

c' is effective cohesion

$\emptyset'$ is angle of frictional resistance

$(\sigma_n - u_a)$ is net normal stress

$(u_a - u_w)$ is matric suction

X is a parameter dependent on the degree of saturation.

Fredlund et al., (1978) proposed a relationship to explain the shear strength of unsaturated soil in terms of two independent stress state variables, the friction angel ($\emptyset'$) associated with net normal stress was assumed to be independent of soil suction, the frication angel ($\emptyset^b$) was also assumed to be independent of net normal stress. The equation was linear in form and was the basis for subsequent nonlinear equation as below:

$\tau = c' + (\sigma_n - u_a) \tan \emptyset' + (u_a - u_w) \tan \emptyset^b$ *2.23*

where

tan $\emptyset^b$ is angle of frictional resistance due to the contribution of matric suction. The investigators have used equation [2.22] or [2.23] for the prediction of the shear strength of unsaturated soil using the Soil-Water Characteristic Curve (SWCC) and the shear strength of saturated soil. The first part of the above equation forms the shear strength of the soil under saturated condition, the

second part of the equations form shear strength contribution due to matric suction.

When the condition of soils is unsaturated and soil suction varies, the shear strength envelope becomes nonlinear and is related to the change of degree of saturation of the soil as soil suction change. The information on the measurement of unsaturated soil shear strength parameter is needed. Many experiential equations have been proposed for estimating the shear strength of unsaturated soils. In most examples, the estimated equations of shear strength based on the saturated shear strength parameters and the SWCC of the soil. Most of the proposed equations of estimated shear strength for an unsaturated soil have been related to SWCC or the classification properties of the soil (Frendlund et al., 2012).

Mohr's circles can be extended from mechanics of saturated soils and used to represent the state of stress at a point using the net vertical and horizontal stresses as the principal stresses, the matric suction pressure as a third dimension. Extended Mohr's circles are used to describe unsaturated soil by using a third axis for matric suction. Figure (2.7) shows a planar failure envelope that intersects the shear stress axis, giving a cohesion intercept c'. The envelope has slope angles of $\emptyset'$ and $\emptyset^b$ with respect to the $(\sigma - u_a)$. Moreover, $(u_a - u_w)$ axes, respectively. Both angles are assumed constants. The cohesion intercept,c'**,** and the slope angles, $\emptyset'$ and $\emptyset^b$**,** are the strength parameters used to relate the shear strength to the stress state variables. The shear strength parameters represent many factors, which have been simulated in the test. The line of intercepts indicates an increase in strength as matric suction increases, which is defined by the angle $\emptyset^b$.

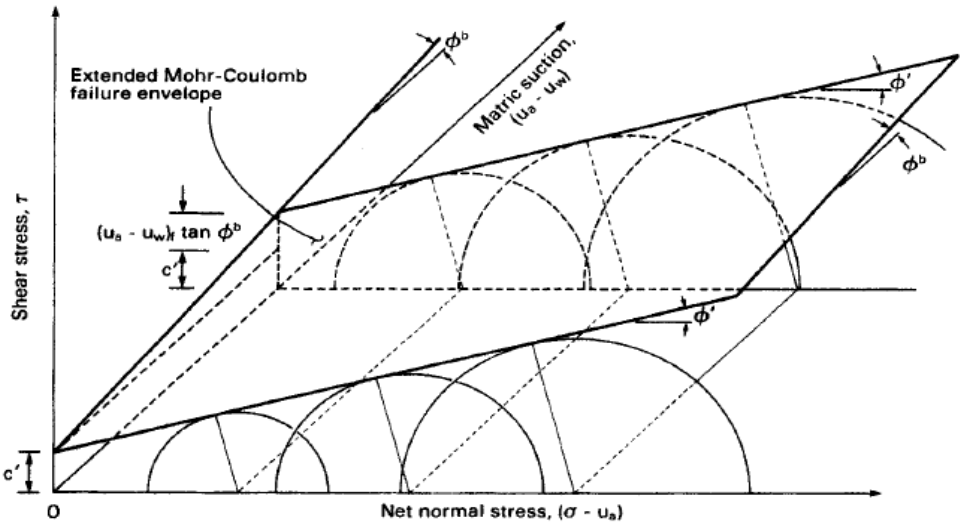

Figure 2.7 Extended Mohr-Coulomb failure envelope for unsaturated soils.

2.8.1 Model of shear strength in unsaturated soils with respect of soil suction

The importance for the shear strength of a soil is required in the bearing capacity of foundations, slopes stability, embankments and pressure against earth retaining structure. Commonly, Moher Coulomb theory is used for predicting the shear strength of saturated soil. Even though unsaturated soils are often encountered in engineering practice, slope stability analyses are usually based on the saturated shear strength parameters. Comparable design approaches have been adopted for pavements, retaining structures, and other earth structures. These approaches are conservative to varying degrees in that the influence of soil suction is ignored. However, Walle and Hachich (1989) states low suction can be responsible for maintaining the stability of slopes. Fredlund and Morgenstern (1977) introduced the theory of stress state variables

to express the behaviour on unsaturated soils. Fredlund et al., (1978) proposed the shear strength of an unsaturated soil, in terms of these stress state variable.

Wheeler and Sivakumar (1995) gives Elastic-plastic, critical state soil mechanics theories with respect to the concept of stress state variables. Although shear strength theories of an unsaturated soil have been found to be consistent with practical experimental behaviour, experimental measurements of shear strength are time intense and require costly laboratory facilities. This has to some degree, limited the application of the shear strength theories for unsaturated soils to research and academic areas. To date, there has been only limited practical application of the unsaturated soils shear strength theory in practice. The success of any theory depends on how readily and successfully it can be applied in engineering practice. It is consequently important to develop a simpler approach for predict the shear strength of unsaturated soil for various engineering applications. This would promote the use of unsaturated shear strength theory in engineering practice.

In many attempts, empirical procedures have been used to predict the shear strength of an unsaturated soil. Experimental data created by Escario and Juca (1989), on different soils have institute that an ellipse with a 2.5°, reproduced the variation of shear strength with respect to suction reasonably well.

Lamborn (1986) proposed an equation to extend the principle of micromechanics model of irreversible thermodynamic to the energy versus volume relationship in a multi-phase material (i.e. solids, fluids and voids). The equation is as follows:

$$\tau = c' + (\sigma - u_a) \tan \emptyset' + (u_a - u_w)\, \theta_w \tan \emptyset' \qquad 2.24$$

where θ_w = volumetric water content which is defined as rhe ration of the volume of water to the total volume of soil.

The volumetric water content, decrease as matric suction increase and it is a non-linear function of matric. However, it should be noted that the friction angel associated with matric suction does not become equal to angle of frictional $\emptyset'$ at saturation unless the volumetric water content is equal to one.

Abramento and Carvalho (1989) used a curve-fitting technique for their experimental data using an exponential function retains the form of the shear strength equation proposed by Fredlund et al., (1978), treating (tan $\emptyset^b$) as a variable with respect to suction. These observed trials may or may not be fit for all soils types. It is required to include a parameter, such as degree of saturation.

$$\tau = c' + (\sigma - u_a) \tan \emptyset' + \alpha\, (u_a - u_w)^{\beta} \qquad 2.25$$

where

α *and* β fitting parameters

Vanaplli et al., (1996a) developed non-linear function for predicting the shear strength of unsaturated soil in terms of suction and a fitting parameter. The approach incorporated the soil-water characteristic curve and saturated shear strength parameter. Fredlund et al., (1996) also proposed the same equation for predicting the shear strength using theoretical formulations:

$$\tau = c' + (\sigma - u_a) \tan \emptyset' + (u_a - u_w)(\Theta^k)(\tan \emptyset') \quad 2.26$$

where

$(\sigma - u_a)$ is the net normal stress on the shear plane at failure, Θ is the normalised volumetric water content = Θ_w/Θ_s , k is a fitting parameter, Θ_w is the volumetric water content at current matric suction and Θ_s is the volumetric water content when S_r = 100 %.

This equation is evaluated using ten data sets of statically compacted soils and provided good comparisons between the measured and predicted values of shear strength for seven soils. Vanaplli et al., (1996) also proposed an equation for the shear strength which removed the need for the fitting parameter. The shear strength equation that involved a normalization of the SWCC between saturated conditions and residual volumetric water content conditions. The relationship took the following form:

$$\tau = c' + (\sigma - u_a) \tan \emptyset' + (u_a - u_w)[(\frac{\theta_w - \theta_r}{\theta_s - \theta_r})] \tan \emptyset' \quad 2.27$$

where

θ_r = volumetric water content at residual suction and

$\frac{\theta - \theta_r}{\theta_s - \theta_r}$ = normalized water content

The normalised water content Θ_n serves as a reduction term for soil suction term. The $\tan \emptyset^b$ term from the linear of Fredlund equation (1978) can be written in a nonlinear form using normalised water content Θ_n

$$\tan \emptyset^b = (\frac{\theta - \theta_r}{\theta_s - \theta_r}) \tan \emptyset' = \Theta_n \tan \emptyset' \quad 2.28$$

The shear strength associated with soil suction. τ_s can be written as

$$\tau_s = (\sigma - u_a)\left(\frac{\theta - \theta_r}{\theta_s - \theta_r}\right) \tan \emptyset' \qquad 2.29$$

Equation [2.29] can also be written directly in terms of degree of saturation:

$$\tau = c' + (\sigma - u_a) \tan \emptyset' + (u_a - u_w)\left[\left(\frac{S - S_r}{100 - S_r}\right)\right] \tan \emptyset' \qquad 2.30$$

where S_r is the residual degree of saturation.

The residual degree of saturation, S_r, or the residual volumetric water content, θ_r, can be determined from the SWCC. Equation [2.26] has been tested of 20 types of soils. The success of the prediction is dependent upon the reliable estimation of the residual degree of saturation. There was a good comparison between the prediction and measured for shear strength of five soils using this equation.

Shen (1996) developed a hyperbolic equation using a fitting parameter *d.* The shear strength envelope is assumed to be hyperbolic in nature in this equation. This assumption facilitates the prediction of the shear strength over large range of suction using limited experimental data.

$$\tau_{us} = \frac{(u_a - u_w)}{1 + d\,.(u_a - u_w)} \tan \emptyset' \qquad 2.31$$

where

τ_{us} shear strength contribution due to suction

Oberg and Sallfours (1997) developed equation of Bishop (1959) except that the χ parameter is replaced by the degree of saturation, *S*. the contribution of

soil suction to shear strength was assumed to be equal to (*S tan ∅′*), the equation provided successful predictions for 2 soils from six soils have been tested, namely sands, silts and non-clayey soils and the equation as:

$$\tau = c' + (\sigma_n - u_a)\ tan\ \emptyset' + (u_a - u_w)[S] tan\ \emptyset' \qquad 2.32$$

Bao et al., (1998) modified Vanapalli's (1996) equation and assumed the soil behaved as saturated soil as long as matric suction less than air-entry value (AEV) of soil:

$$\tau = c' + (\sigma_n - u_a)\ tan\ \emptyset' + (u_a - u_w)[\zeta] tan\ \emptyset' \qquad 2.33$$

The parameter ζ defined as:

$$\zeta = \left[\frac{\log\ (\sigma_a - u_w)_r - \log\ (\sigma_a - u_w)}{\log\ (\sigma_a - u_w)_r - \log\ (\sigma_a - u_w)_b}\right] tan\ \emptyset' \qquad 2.34$$

The influence of soil suction on the shear strength of unsaturated soil was normalised between the (AEV) and residual suction. It was assumed that the shear strength of the soil remained constant beyond residual suction. This equation has been tested on sixteen soils, however, only reliably predicted the shear strength of one soil (CM-ML classified).

Khalili & Khabbaz (1998) re-examined Bishop's (1959) equation and provided a relationship between χ and the suction ratio, which is defined as ratio of the suction over the air entry value:

$$\tau = c' + [(\sigma - u_a) + \chi(u_a - u_w)] tan\emptyset' \qquad 2.35$$

$$\chi = \left[\frac{(\sigma_a - u_w)}{(\sigma_a - u_w)_b}\right]^{-0.55} \qquad 2.36$$

where

$(\sigma_a - u_w)_b$ = the air entry value of soil.

The fitting parameter determined to be (-0.55) in each case for all types of soils which have been tested. This equation was developed for predicting the shear strength of clayey type of soils. Fifteen soils have been tested, only one soil was found to be successful in the prediction of the shear strength.

Rassam and Williams (1999) suggested an equation to incorporates the linear relationship between shear strength and suction up to air entry value (AEV) and a non-linear relationship between suction value greater than (AEV). The fitting parameter (α, *β*, γ and λ) are determined by a computer program to estimate the three-dimensional failure surface based on experimental data.

$$\tau_{us} = (u_a - u_w)\, tan\, \emptyset' \qquad 2.37$$

If $(u_a - u_w) < AEV$ else

$$\tau_{us} = (\gamma + \lambda(u_a - u_w)).[(u_a - u_w) - AEV]^{\beta} + (u_a - u_w)\, tan\, \emptyset' \qquad 2.38$$

Moreover, Rassam and Cook (2002) proposed an equation with four terms to determine the shear strength of unsaturated soils. The soil with negative pore-water pressure behaved as a saturated soil for the first three terms, and the last terms applies a correction factor to account that increase in soil suction are not as effective in increasing shear strength as net normal stress. The equation as below:

$$\tau_{us} = c' + (u_a - u_w)\, tan\, \emptyset' + \varphi((u_a - u_w) - (u_a - u_w)_b)^{\beta} \qquad 2.39$$

where

$(u_a - u_w)_b$ = air entry value, φ and β fitting parameter.

The fitting parameter in the equation incorporates two new variables φ and β defined by the following equations:

$$\varphi = \frac{(u_a - u_w)tan\ \emptyset' - \tau_{us}}{((u_a - u_w) - (u_a - u_w)_b)^{\beta}} \quad 2.40$$

$$\beta = \frac{tan\ \emptyset'((u_a - u_w) - (u_a - u_w)_b)}{(u_a - u_w)tan\ \emptyset' - \tau_{us}} \quad 2.41$$

where

τ_{us} shear strength contribution due to suction

The φ and β terms are part of the correction factor that reduces the shear strength as a result of desaturation of the soil. The term τ_{us} refers to the contribution of matric suction to the shear strength at residual suction condition.

The proposed function used the SWCC and effective angel of shearing resistance of soil. A single value of the air entry value (AEV) from the SWCC of the soil is needed in the model to determine the variation of the suction strength with respect of suction. The logarithmic model offers an easy and convenient method. This suggested model is most suitable for fine-grained soils. It was proposed to predict the shear strength of fine-grained unsaturated soils in low suction range. Four soils have been successful out of sixteen soils examined.

Garven and Vanapalli (2006) summarised six equations from the literature that published shear strength data used for evaluation of the prediction. Comparisons between the measured and prediction value of shear strength data. The types of materials include natural soils, expansive soils, tailings and

residual soils, most of the materials are clay with plasticity index values varying from 0 to 33 and classified as CL. If 50% of the predicted values fall within 15% of measured shear strength values, it is defined as a successful prediction.

Goh et al., (2010) developed Fredlund and Xing (1994) equation which initially only considered drying path of soil sample to include both wetting and drying parameters. Fredlund and Xing (1994) Parameter a, n and m, a is parameter that equates to the air entry value, a = AEV when $\boldsymbol{m}$ is very small, n is parameter that accounts for slope of curve.

$$\tau = C' + [(\sigma - u_a) + (u_a - u_w)_b] \tan \phi' \ [(u_a - u_w)(u_a - u_w)b] \, \mathrm{b}\Theta^k \tan \phi' \qquad 2.42$$

An empirical, analytical model is required to predict the shear strength in terms of suction, use of soil-water characteristic curve (SWCC) and saturated shear strength parameters. Features of typical SWCC define the relationship between the amount of water in the soil and soil suction.

Fibre reinforcement has an effect on the angle of improvement $\emptyset^b$ and thus this effect should lead to an increased suction. Therefore, a prediction model using a parameter to represent the influence of fibre reinforcement on the second part of the shear stress equation can be developed keeping in mind this hyperbolic relationship between secant $\emptyset^b$ and suction.

Sandra (2007) developed an equation that was suggested by Fredlund and Raharjo (1993) which is an unsaturated soil shear strength equation that takes the form of an extended Mohr-Coulomb failure criterion. Therefore, the fitting of secant $\emptyset^b$ shows its relationship to the matric suction is hyperbolic. For fibre

reinforced clay, the parameters a and b could be related to the increase in fibre content (%).

The term of $(u_a - u_w)\tan\phi^b$ was used to account for the increase in shear strength due to suction. The approach used to obtain the secant ϕ^b parameter for a particular value of suction consisted of drawing the Mohr circles in the net normal stress $(\sigma - u_a)$ versus shear strength (τ). The value of ϕ^b is back calculated from total cohesion intercept value.

$$\phi^b = arctan\left[\frac{c - c'}{(u_a - u_w)}\right] \qquad 2.43$$

where

c is total cohesion intercept and ϕ^b secant slope angle. The equation for the prediction of ϕ^b when suction is larger than air entry value (AEV) can be presented as a hyperbola as below

$$\phi^b = \phi' - \left[\frac{\psi^*}{a + b\psi^*}\right] \qquad 2.44$$

where

ψ^* = $(u_a - u_w)$-AEV and the inverse of parameter a is initial slope of the hyperbolic curve when ψ^* = 0

2.9 Conclusion

There is no doubt that naturally the soil could be reinforced by elements such as plant root which have been reported in the literature to have a strengthening effect on the soil. However, other studies have been performed that investigated

the effect of fibre reinforcement. These studies have all reported to have strengthened the weak soil. Interestingly, the effect of fibre adding some flexibility to the soil. Samples without the fibre, did report stiffness, and consequences of being brittle have also been reported. It is established that the fibre does not affect the frictional property of sand, but increases the peak shear strength, limiting post peak reduction in shear resistance. These results are consistent with sandy soil reinforcement with polypropylene fibres. Further to this, clay has been reported to have increased specimen with the addition of fibre.

The need of fibre reinforcement in soil/sand is no doubt beneficial, although naturally the soil is reinforced by matters such as plant routes, but the quantity and the limiting factor of such matter acts as a negative effect of this method, but this is not the case with fibres and other components that are added to the soil to reinforced it.

Most experiments that were performed on sand, clay silt etc., have looked at fibre reinforcement under saturation condition. For example, Mirzababaei (2012) studied the effect of symmetrical amount of waste carpet fibres on shear strength, compression strength and swelling pressure of clay soils. However, up to date no published studies has been performed with unsaturated soil with fibre reinforced. Furthermore, only limited studies have been showed on use of recycled carpet in order to improve the strength properties of unsaturated clayey soil. Therefore, the effect of carpet waste reinforcement to unsaturated soil will shed light on this area of research. Including

Consequently, this study aims to bridge the gap in the literature by undertaking a series of experiments, it has been formed to conduct a thorough investigation

of the mechanical behaviour of fibre-reinforced unsaturated clay soil with waste carpet fibres. The amount of waste carpet fibre on the shear strength, cohesion, and the friction angle has been including.

CHAPTER 3 EXPERIMENTAL TECHIQUES AND MATERIAL

Summary

In this chapter, there are two materials presents, which used in this research including clayey soils and carpet waste fibres. All testing procedures are also covered in this chapter, with a summary of double-wall triaxial device tests, soil water characteristic curve tests, and unconfined compression strength tests, which are carried out to achieve the aims of this study.

3.1 Introduction

In this chapter two sections were presented, the first section is about the materials used in this research, including soils and carpet waste fibre. The other section covers the testing procedures which take place to achieve the objectives of this research.

The mechanical behaviour of unsaturated clay was studied in this research based on the shear strength, and the consolidation, due to the fact that they are two important factors in the soil behaviour.

To investigate the influence of waste carpet fibre on the shear strength, a number of consolidated undrained tests were applied on the non-reinforced and fibre reinforced clay soil samples. Additionally, in the tests carried out, each test went through three stages of equalisation, consolidation and shearing.

In these experiments, the fibre reinforced clay soil samples were prepared fibre contents 0 %, 1 %, 3 % and 5 % of dry soil and varied water content. The outlines of the materials used in this project are highlighted below.

3.2 Fibre

Carpet waste increases annually by 400,000 tonnes in the UK, and is commonly buried in landfill. However, 1.5 % of carpet waste was diverted from the landfill in 2008, and increased to 16.5 % in 2011, where the target was 25 % in 2015, according to Carpet Recycling UK. Figure (3.1) show the carpet consists of both natural and synthetic fibres. In a wide range of applications, the fibre can be used, such as in sports surfaces and insulation roofs. Researchers continue to look for better alternatives for recycling this unwanted material. In this investigation, the aim is to use this type of fibre as a reinforcement for unsaturated soils. The fibres composed of 60 % polypropylene, 20 % styrene butadiene latex rubber (SBR), 15% nylon and 5% wool. Moreover, the diameter of the fibre varied from 0.1 to 1mm and the length between 2 to 20 mm, with specific gravity of 1.30. In terms of physical properties of the carpet waste, absorption of water for polypropylene is 0%, for wool 13 to 15 % and for nylon 4.1 to 4.5. The specific gravity of polypropylene is 0.9, nylon 1.14, and wool 1.32 (Carpet Recycling UK).

Figure 3.1 Carpet waste fibres

3.3 Clay

For the purpose of this research, materials, or clay from a site in the north west of the UK, of which the quantity was 1 ton, was brought from Bolton University as a continuation of a former research student, and was mixed, weighed, and then re-bagged ready for use, in almost 40 plastic bags each weighing 25 kg shown in Figure (3.2). It was a type that can be found in most areas of the UK, and is quite common in England. It was kept in an oven and dried at 105°C for 24 to 48 hours before use.

Figure 3.2 Clay crushing and filled equipment

3.3.1 Classification

Due to the latest development of the practice standards in Europe to Eurocode 7, BSI Group, which has developed standards within the UK and worldwide, has issued the EU7 matched version of BS codes as BS EN 1997-2:2007. Therefore, all the testing procedures and methods mentioned in BS 1377 as still valid. Hence, BS 1377 has been considered as test procedure experiments throughout the research.

Initially, to classify the soil used in the experiment, the moisture content was determined as a percentage of dry soil mass, at temperatures of 105°C to 110°C.

a- Specific Gravity Test

According to BS1377-2:1990 the particle density of soil was found using the Pycnometer Method. This test is suitable for clayey soil, where particles are smaller than 2 mm in diameter. A clean 50 mL density bottle with a stopper was

dried by rinsing it with acetone and blowing warm air through it, and then weighed giving w_1. 10g of oven dried soil sample was added to the density bottle and weighed together with the stopper giving w_2. Boiled air-free distilled water was added to cover the soil in the bottle where the stopper was added to cover the bottle and left for one hour at room temperature; the filled bottle was then weighed giving w_3. The bottle was then cleaned, and air-free water was added, and covered by the stopper, then left for one hour at room temperature, and its weight was recorded as w_4. The test was repeated five times and the average density was taken. The equation for the particle density of the soil particles is as follows:

$$P_s = \frac{(m_2 - m_1)}{(m_4 - m_1) - (m_3 - m_2)} \qquad 3.1$$

where,

m_1= mass of density bottle (g)

m_2= mass of bottle and dry soil (g)

m_3= mass of bottle, soil, and water (g)

m_4= mass of bottle and water (g)

Two methods were used to classify the soil particle size, namely wet sieving and dry sieving by using BS1377-2:1990 standard procedure.

b- Wet Sieve Test

Wet sieving is used in order to separate the fine soil (silt and clay) from the coarse soil (sand and gravel). 250 g of oven dried soil was weighed and transferred to a 63 μm sieve, approximately 500 mL of distilled water was poured through the sieve, and a brush was used, allowing the material to pass

the 63 µm test sieve to be virtually clear, where the passing soil was collected in a receiver that was placed directly below the sieve. The receiver was left for a few hours in order to let the soil settle, and the excess water was discarded. The wet soil was placed in the oven for 24h at 105-110 C^o to be fully dried and ready for the hydrometer test. While the soil retained on sieve 63 µm was collected and placed in the oven for 24 h to be dried and used in the dry sieve test.

c- Dry Sieve Test

The soil was oven dried and a sample of the soil was weighed and placed on a set of different sieve sizes, starting with the largest sieve size (2 mm) on the top to the lowest one (63 µm) on the bottom. A pan was placed below the sieves, and a mechanical shaker was used in order to shake the soil in the sieves for 8 minutes, where the soil retained on each sieve was weighed and recorded.

The soil passing each sieve opening was calculated by the following equation:

Cumulative percentage passing current sieve = (cumulative percentage passing previous sieve) - (percentage retained on current sieve)

The cumulative percentages passing each sieve were plotted against sieve size on a log scale graph.

The median grain diameter (D_{50}) was determined from the graph; it is the particle diameter where 50 % of the particles are smaller in size than this.

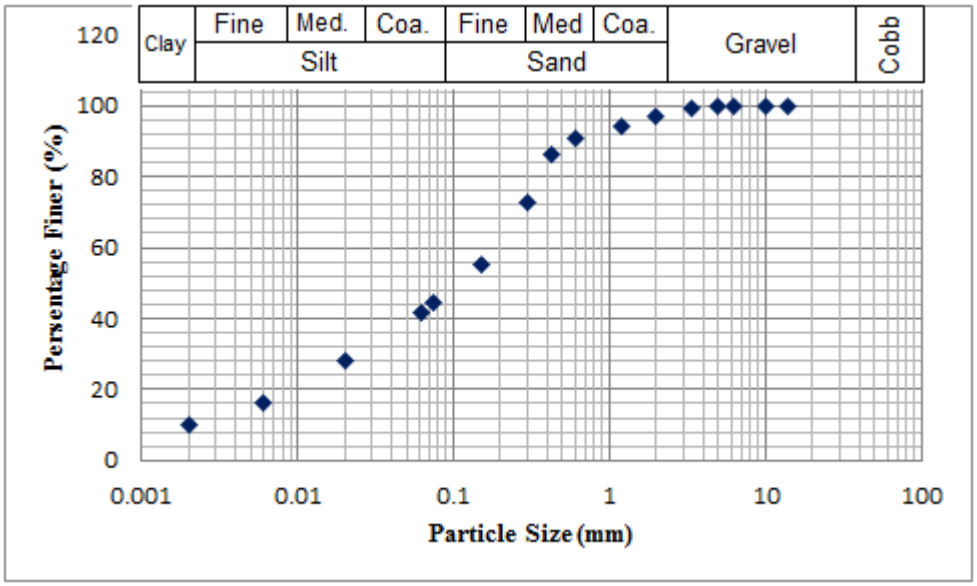

Figure 3.3 Particle size distribution curves

d. Atterburg Limit Test

To prepare a clay soil with plasticity index, the soil was selected based on liquid and plastic limits, the results have provided that the liquid limit (LL) of soil is 21.3 %, the plastic limit (PL) is 10.36 %, and plasticity index (PI) is 10.94 %, low plasticity (CL), according to the Unified Soil Classification System.

The physical properties of soil are shown in Table (3.1), and indeed, it is important to identify the type of soil used. Soil classification and identification were recommended in (BS EN 1997-2:2007); Therefore, soils were classified as low plasticity clayey silt.

Table 3.1 physical properties of soil

Property	Value

Specific Gravity	2.68
Grain Size	
Gravel fraction (%)	1.5
Fine Sand fraction (%) Medium Sand fraction (%) Course Sand fraction (%)	25.3 23 3.5
Silt and Clay fraction (%)	46.66
Atterburg Limits	
Liquid Limit, (%)	21.3
Plastic Limit, (%)	10.36
Plasticity Index, (%)	10.94
Unified Soil Classification System (USCS)	**CL**
Compaction Parameters	
Optimum Moisture Content, (%)	9.35
Maximum Dry Density, (g/cm^3)	2.08
Soil classification	**Clayey silt**

e. Compaction test

According to BS 1377-4:1990 Standard Proctor test was carried out on unreinforced and fibre reinforced soil. The optimum water content and the maximum dry density of unreinforced clays obtained were 9.35 % and 2.08 g/cm^3 respectively. Mirzababaei et al., (2009) reported 11% of optimum water content and 2.01 g/cm^3 of the maximum dry density for the same type of soil. This is close to this research result, and similar to the unified classification of soil (CL).

The Table (3.2) and Figure (3.4) below show results from compaction tests with different percentage of fibre. The results indicate an increase the percentage of

water content with increased percentage of fibre content, while the dry density decreases, due to the amount of fibre, which has permeated between the soils particles.

Table 3.2 compaction tests with different percentage of fibre

Percentage of Fibre %	Water Content %	Dry Density g/cm^3
0	9.35	2.08
1	8.95	2.05
3	10.13	1.98
5	11.4	1.86

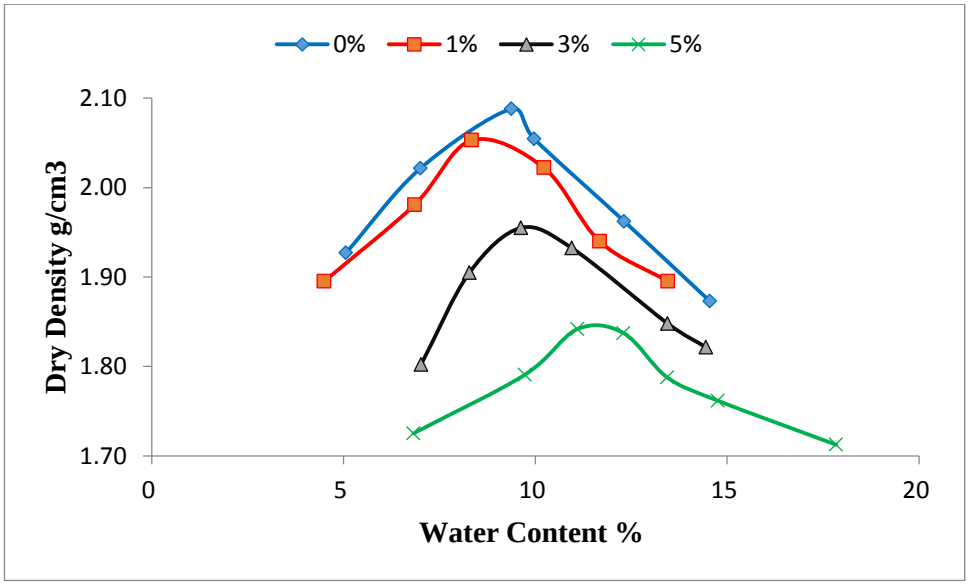

Figure 3.4 Compaction test of different percentage of fibre

3.4 Pressure system

The air pressure and the water pressure system supplied by digital pressure/volume controller units, manufactured by Global Digital Systems Limited UK (GDS) (see Figure 3.5). The characteristics of the pressure/volume controller a microprocessor controlled hydraulic actuator for accurate regulation

and measurement of liquid pressure and liquid volume change. The volumetric capacity is 200 cc and the pressure range is 0-2000 kPa Figure (3.6). The pressure/volume controller unit could be used in computer mode and worked by counting the steps of the stopping motor. It can automate through its own control panel to ramp and cycle pressure and change the volume linearly with respect to the time. The transmission of the information data is in digital form and carried by a single cable linking the computer to the controller. This cable is known as the interface bus cable and plugs directly into the controller. The transmission of digital information backwards and forwards along the interface in accordance with the IEEE-488 standard for a parallel interface. This allows rapid data transfer between a computer and several instruments by Adlink (is the hardware that connect the computer with pressure/volume controllers) at the same time. The data transmission occurs as a result in the computer being transfer to excel file with a set of instructions or software. Also, a volume change gauge or a pore pressure measuring system.

Figure 3.5 The GDS Advanced Digital Controller

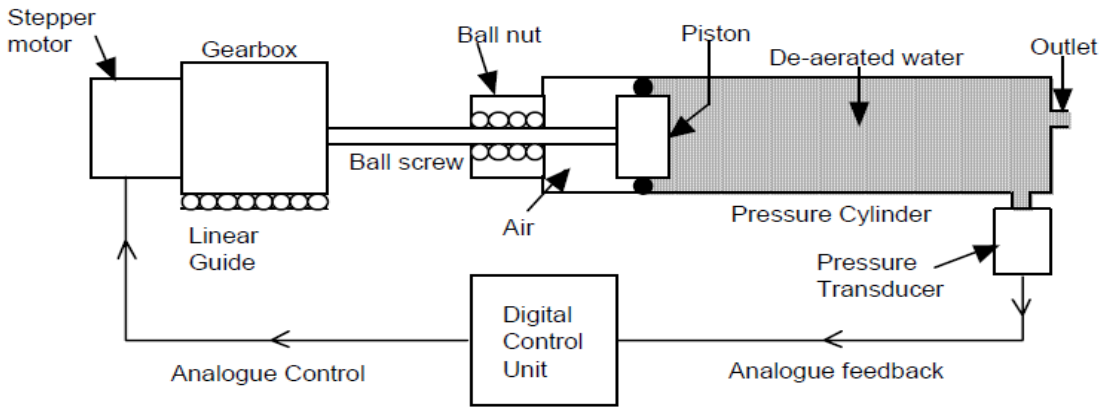

Figure 3.6 Diagram layout of digital controller

3.4.1 Air Pressure

The pore air pressure is normally applied to an unsaturated triaxial sample, using either a compressed air supply, or using an enclosed pore air pressure/volume controller. By using compressed air that case to allow the pore air pressure to be applied more speedily than a pressure/ volume/controller, this is due to the high compressibility of air, and the volume of pore air cannot be recorded with a compressed air supply. In this study, the air pressure was applied by compressor and pressure/volume controller. The air pressure was provided by a compressor through a pressure regulator, which is able to produce a maximum of 500 kPa air pressure. The compressor supplied were connected with pressure/volume controller, in order to control the air pressure at the top face of the soil sample.

3.4.2 Water pressure

A de-aired water pressure must be prepared for applying the pressure to the inner and outer cells, a lower chamber, back pressure and flushing system. The

water pressure to each of these sections was provided from pressure/volume controller. The water pressure in this research as discussed follow.

3.4.2.1 Cell pressure

Both the inner and outer cells were connected separately with two pressure/volume controllers, by a rigid nylon tube, for introducing a predetermined pressure, between the cell and the corresponding pressure/volume controller unit, and there is a tap and a vent that are fitted to remove any of the entrapped air.

3.4.2.2 Back pressure

The pore water pressure was controlled at the base of the soil specimen. The unsaturated soil in field the pore air pressure is zero and the pore water pressure is negative, and it is not easy to produce this condition of soil in the laboratory because of cavitation; the pore water pressure must be increased. The axis translation technique was used to produce a desired suction in the specimen. Consequently, a pressure/volume controller was connected by a nylon tube to the base of pedestal and it was then possible to increase pore water pressure in the specimen. A Digital Pressure Interface (DPI) was used to measure pore water pressure, as shown in Figure (3.7). The device had an IEEE-488 standard parallel computer interface. The LCD was used to show a continually updated display of the current pressure. This water back pressure line was then passed through a connection in the triaxial cell base to the bottom of the soil specimen through air entry value.

Figure 3.7 Digital Pressure Interface (DPI)

3.4.3 Flushing system

The dissolved air may pass through the saturated high air entry disk, depending on the applied suction and it increases with increasing suction. The air bubbles which stock the underneath of the disk should be removed, in order to get accurate result of volume change. This problem was solved by using a flushing system see Figures (3.8) and (3.9). Numerous devices have been proposed to measure the volume of diffused air. Padilla et al., (2006) proposed an automated flushing device that can removes diffused air during unsaturated soil testing. This device has been developed to be used manually in this research. This was then flushed through the spiral groove. This was solved by the means of two pressure/volume controllers that were connected to the pedestal in the pore water pressure line. Both were connected to the centre of the pedestal, and controlled by valves. Flushing was done by sending water from a pressure/volume controller, while the main pressure/volume controller (back pressure) close its valve. the flushing device was connected on the base of

pedestal to the other hole, towards the edge of the pedestal. The bottom of flushing device is attached to transducer indicator on the other side to record the water volume in the water tank, the procedure is as follow:

1. Close the valve (1) and record the current volume V_0 and pressure u_{w0} of pressure/volume controller which is connected to valve (2). As shown in Figure. (3.10).
2. Record the water level in the flushing device through transducer indicator.
3. Set the u_w pressure/volume controller to the volume control.
4. Manually open the valve (2) and set the pressure/volume controller to pomp 200 cm^3 at a rate of 1 cm^3/second. The pressure in this line should not exceed more than 20 kPa.
5. Pump back 210 cm^3 into the pressure/volume controller from the flushing device.
6. Repeat the last two methods at least once.
7. Adjust the water level in the flushing device to the original level.
8. Record the new volume V_f of pressure/volume controller, close valve (2) and open valve (1). Diffused air volume could be calculated as:

Diffused air volume = $V_0 - V_f$

Figure 3.8 Transducer indicator E308 of The flushing apparatus

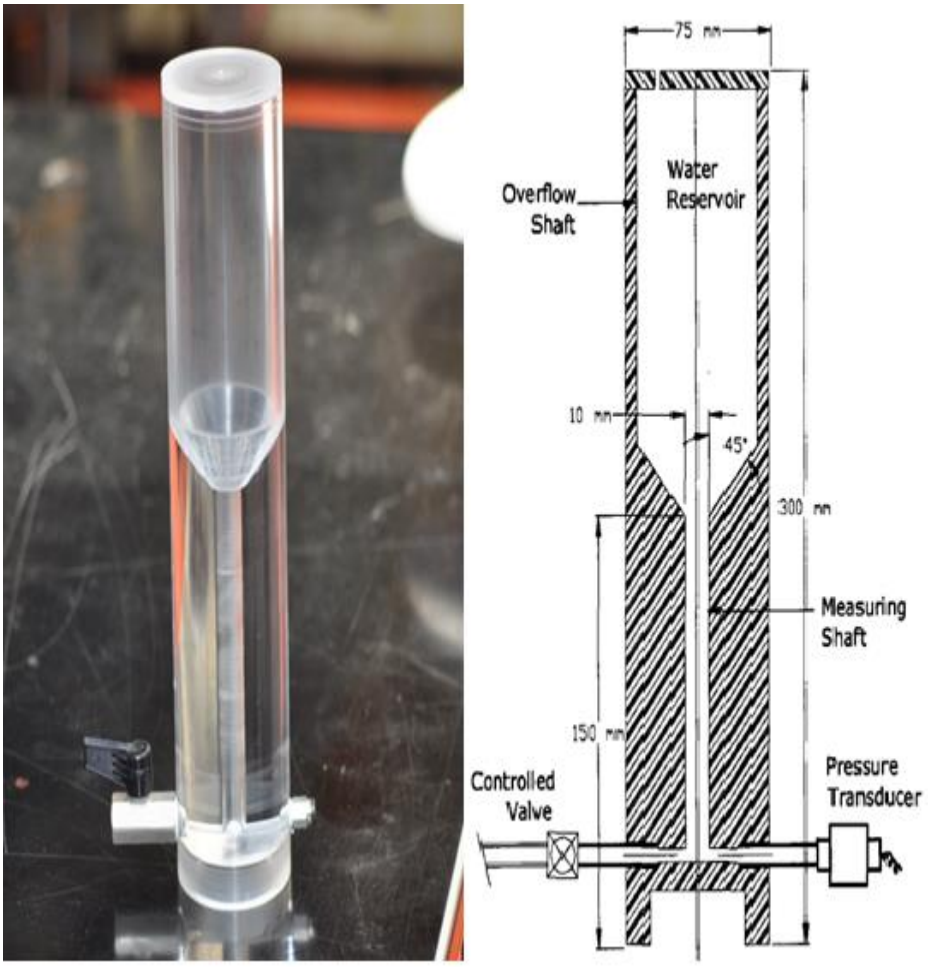

Figure 3.9 flushing apparatus after Fredlund (2)

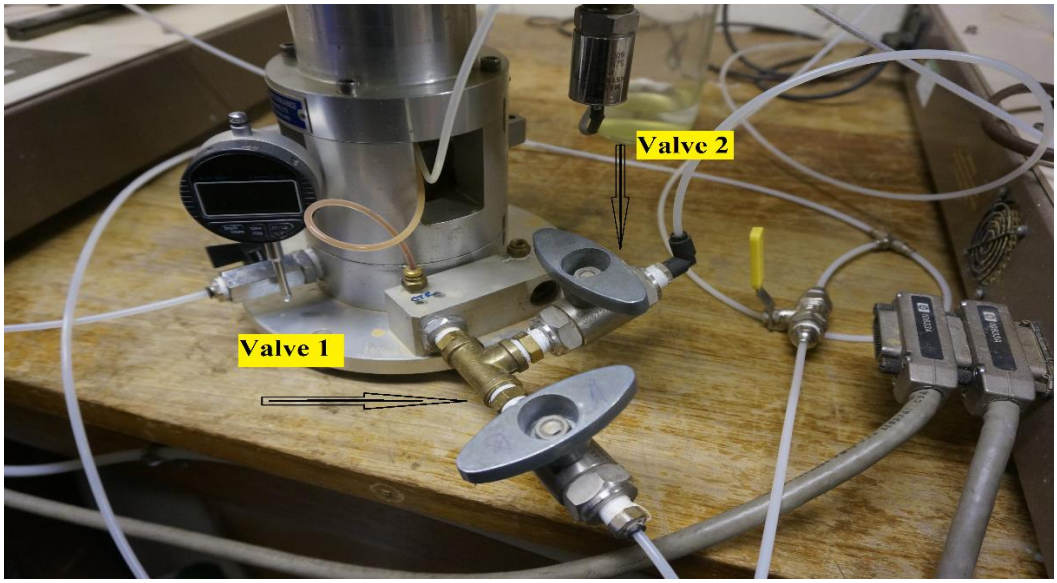

Figure 3.10 The valves 1 and 2 used for flushing

3.4.4 Saturation of Air entry value disk

The high entry value has to be fully saturated before starting the test, to avoid the airflow into the water pressure line through the ceramic disk. Fredlund (1993a) suggested a procedure to ensure the saturation of ceramic disk: First fill the cells with distilled, de-aired water above the disk about 25 mm, and then subject them to an air pressure around 600 kPa. Water is allowed to flow through the disk in 1h. Numerous researchers such as Fredlund and Rahardjo (1993) and Sivakumar (1993) have also proposed procedure to saturation which was selected in this research as follows:

1. The inner and outer cells were filled with distilled water through the connected tube between the cells and the pressure/volume controller.
2. The cells pressure was increased to 600 kPa and held at this pressure for two days by applying a target pressure on the keypad of the GDS, therefore pushing the air out through the disk.

3. The tap of the drainage line was opened and water flowed from the ceramic disk for 24 hours under 600 kPa.
4. The drainage line was closed and the cell was left open for 24 hours at a pressure of 600 kPa, then the drainage line was opened and by selecting, the reset button on the keypad of the pressure/volume controller the cell was left for 24 hours. After each test the ceramic disk was re-saturated by the above procedure.

3.4.5 Lower chamber

The lower chamber of the triaxial cell was also connected to another pressure/volume controller using rigid a nylon tube. This pressure/volume controller was used to drive the loading ram of the cell during a shearing test to carry out strain or stress controlled shearing tests. For instance, if a shear test should be conducted under strain control with a cross-sectional area of Bellofram seal inside the lower chamber equal to 29.4 cm^2, then 29.4 cm^3 of water must be entered into the lower chamber of the triaxial cell to produce 1 cm of position movement. In the pressure/volume controllers' system axial stress in a triaxial test is calculated from Bishop and Wesley's equation [3.2] by using the pressure of the lower chamber and the cell, the area of the Bellofram Rolling Diaphragm (BRD) and the current average area of the test specimen. In order to find the correction of friction, a procedure was performed as mentioned in GDS Instruments manual (2009). The friction correction was found to be less than 5 kPa (Robert et al., 1988). A digital displacement gauge was used to measure the variation of sample height with a maximum travel distance and a precision.

3.4.6 Filling and emptying the system

Distilled de-aired water was used during all the tests. Distilled de-aired water was used in the confining pressure in the two cells, the controllers to supply pressure hydraulically to the lower chamber, back pressure and flushing. As a result, distilled de-aired water was needed to be prepared before start of any test. Distilled de-aired water was collected from the University. This water was then kept in a storage tank, the triaxial cell was filled with water through nylon tubes by cylinder pressure system. To remove any trapped air bubbles from inside the pressure cylinder, each pressure/volume controller was put in a sloping position then its piston was driven to the outlet by pressing the empty button on the keypad. The water flowed from the pressure/volume controller into a container of de-aired water, the piston was then driven backward by pressing the fill button of the keypad and the cylinder was filled with de-aired water. Several times the process was repeated until the pressure/volume controller was properly filled with de-aired water.

3.5 Method for applying suction

In unsaturated soil sample, there are different methods to apply a suction in laboratory, namely, axis translation, osmatic technique and humidity control technique. The osmotic or humidity control techniques are not possible to produce a continuous variation of suction. However, with the axis translation technique it is possible to provide it. Furthermore, some of chemical changes in the pore fluid of the soil sample may be produced by using the osmotic method. It is possible to achieve a particular suction with a particular salt concentration with the humidity control technique and therefore, continuous variation of suction is not easily possible. It was concluded that the axis translation

technique has advantages over the other methods and then was selected as the method of producing suction. The air supply line was connecting with pressure/volume controller to apply a suction. However, during applying suction by the ramped method, it was noted that the motor of pressure/volume controller was moving until the end of its position, which gave the error correction which caused the test to stop automatically, due to compressibility of air. It was decided to apply a suction by keeping the air pressure constant while the pore water pressure changed, either increased or decreased in soil samples in this research work.

3.6 Double-walled triaxial cell

Bishop and Wesley (1975) set out to design a simple and versatile hydraulic triaxial stress path cell, which is called the Bishop and Wesley cell. Figure (3.11) shows the schematic diagram of the triaxial apparatus. By hydraulic pressure inside the lower chamber, the vertical load in the stress path cell could be applied. The lower chamber and the cell chamber (upper) were sealed with bellofram rolling diaphragms that sweep equal volumes of water. The loading ram was placed between these two chambers. Therefore, axial ram is very sample and normally less than 5 kPa of deviator stress (Menzies 1988). By considering equilibrium of the loading ram, the relationship was obtained.

$$\sigma_a = P(a/A) + \sigma_r(1 - a/A) - W/A \qquad 3.2$$

where:

σ_a is the average axial total stress (kPa).

P is stands for the lower chamber pressure (kPa).

σ_r is the radial total stress or cell pressure (kPa).

A Is the cross-sectional area of the soil specimen (mm^2).

a The effective area of Bellofram rolling diaphragm (mm^2).

W The weight of the loading ram (gr).

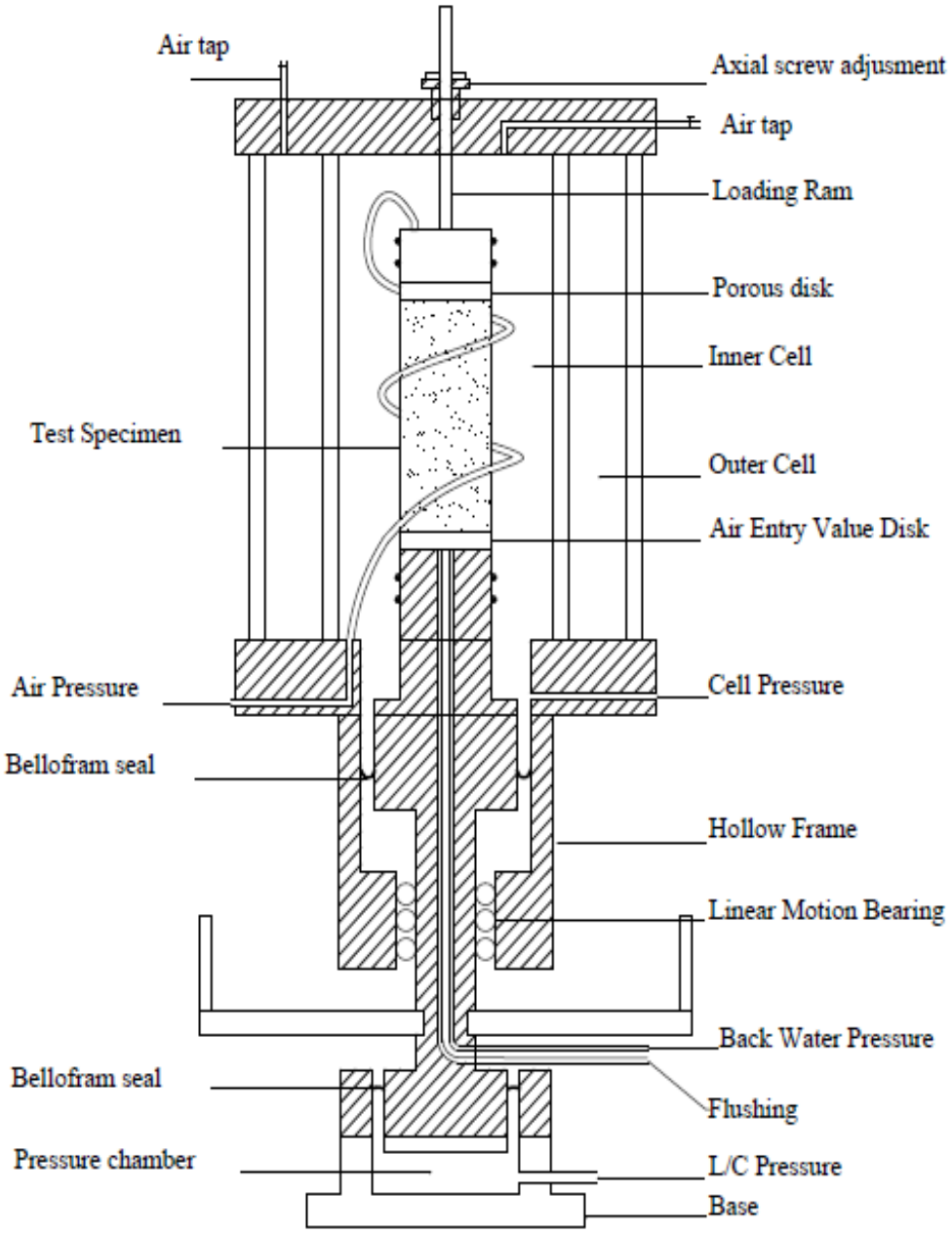

Figure 3.11 Layout of Double-walled triaxial apparatus

According to Fredlund and Rahardjo (1993), and Estabragh (2002), two types of volume change must be taken into account, the whole soil sample volume change and the water volume change in triaxial test of unsaturated soils, Wheeler (1986) in the laboratory modified a double-wall triaxial cell was able to measure the volume change of an unsaturated soil sample. It was the same principle as for the cell developed by Bishop and Wesley (1961), where instead of mercury, they used water as the cell fluid, while the inner cell was sealed from the outer cell. The layout of the modified apparatus is shown in Figure (3.11). The double-walled cell consisting of two Perspex cylinders, one inside and the other outside, the diameter of the inner cell was 132 mm and the distance between the inner and outer cells were 22 mm. The thicknesses of the inner and outer cell walls were 10 and 5 mm, respectively. Each cell is connected to pressure/volume controller, so it was possible to apply the same pressure to both cells at any time and without any minor delay between pressure applications to the both cells, to avoid any error in volume change measurement. The components of the double-walled cell are discussed below:

3.6.1 Plates top and bottom

These plates were made of stainless steel in a circular shape. Two grooves were made in each plate so that the top and bottom ends of the two cell walls were fitted in the grooves. An O-ring in each groove provided sealing of the inner and outer Perspex cells. The top plate rested on top of the cell walls and was fixed to the bottom plate by three bars passing through three holes which were drilled in the plates. A hole was made at the centre of the top plate with an adjustable rod passing through it, and was sealed with O-rings. In order to measure the volume change of a sample in a double walled cell, it is necessary

to prevent air entrapment when the cell is filled with water. Therefore, two other holes were made in the top plate and two taps were fitted in these holes for bleeding the entrapped air from the inner and outer cells. The bottom plate consisted of a circular plate which was clamped to the top plate by three bars. A circular hole was made in the middle of this plate with a diameter equal to the external diameter of the inner cell see Figure (3.11). The wall of the outer cell was fixed by an O-ring in a circular groove which was made in this plate. A hole was horizontally drilled in this plate with a tap fitted to this hole which allowed filling (or emptying) of the water into (or from) the outer cell and applying the desired pressure.

3.6.2 Base plate

The plate was fitted on the triaxial apparatus base. It was used as an extension of the original base of the triaxial apparatus to match the dimensions of the designed double wall cell. The inner and outer cell fixed to this base plate. Two horizontal holes were drilled in this plate and two taps were fitted into these holes. One of the taps was used for filling or emptying of the water in the inner cell, or applying the desired pressure to it. The other one allowed a flexible tube to pass through the plate and connect the air pressure line to the top of it.

3.6.3 Pedestal

The suction is applied by increasing air pressure at the top of a sample and a lower value of pore water pressure at the bottom of the sample. To apply this technique of creating suction, the pedestal and top cap of the triaxial apparatus must be arranged with special filters. The features of the filters in the pedestal and top cap are discussed below:

Bishop (1960) proved a high air entry disk (ceramic disk) to prevent the pore air in an unsaturated sample from entering the pore water pressure control system, and to allow control and measurement of pore water pressure. The pore water pressure in the sample was only measured at the bottom of the pedestal. Porous filter was used on the top of pedestal to apply air pressure at the top of the specimen. The pedestal made from stainless steel to withstand the large loads which could be applied to the sample during shearing.

A ceramic filter with a very uniform pore size is more suitable than one with graded pore sizes as it gives maximum permeability for a given entry value. The diameter of the largest void or channel governs the air entry value. Therefore, the air entry value increases by reducing the pore size of the ceramic filter during manufacturing. As the air entry value of a filter increases, its permeability decreases due to the reduction of pore size. The high air entry disk which was used in this system had an air entry value of 5 bar with 50 mm diameter and 8 mm thickness. It was supplied by Soil Moisture Equipment. Corp. Ltd. Before this disk was sealed into the pedestal, the plane surfaces of the filter were polished to give a smooth surface. It was then glued within the metal annulus of the pedestal. Araldite epoxy resin glue was used for this purpose. The ceramic disc was placed on the top of the 50 mm diameter pedestal on the triaxial apparatus base that was bas plate. (see Figure 3.12).

A spiral groove was made on the top of the pedestal to flush any diffused air from beneath the filter. This spiral groove starts from the pedestal centre and goes to near the edge. Two holes were drilled vertically in the base pedestal to meet the other two holes drilled in the bottom plate for measuring the pore water pressure and flushing. One of these holes is at the centre of the spiral

groove and the other is at the other end. It was made in the workshop of the University of Bradford.

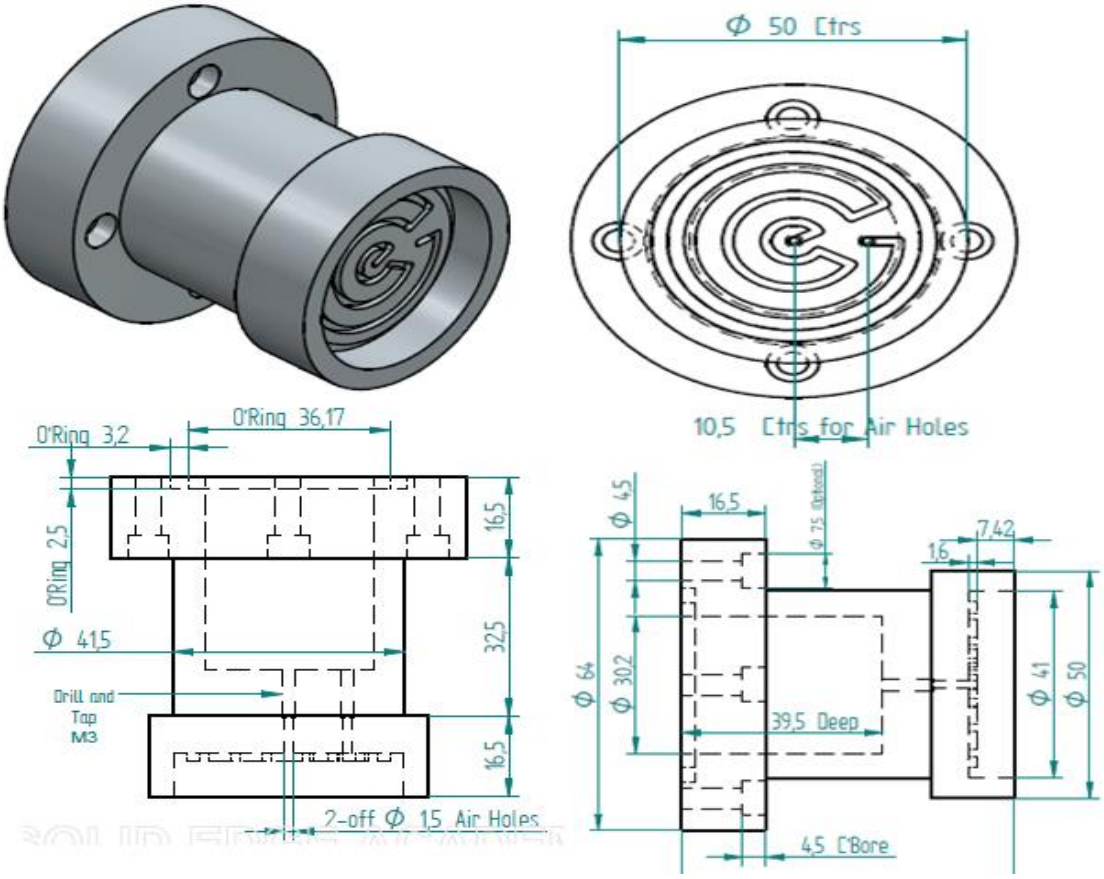

Figure 3.12 Stainless steel Pedestal

3.6.4 Placed soil sample in triaxial cell

Once the sample was removed from the mould, weighted and then its dimensions were measured with a digital calliper, due to the evaporation the water content could be changed during this time. In this case the water content recalculated. The rubber membrane was placed around the sample by using a membrane stretcher, and then soil sample was placed directly on the ceramic disk on the pedestal, and sealed with three O-rings. The top cap filter was placed on the top of sample and the membrane was sealed on it with three O-

rings, any extra of rubber membrane in the top was cut off by a scissor. The negative pore water pressure began to produce quickly in the pedestal drainage path, once the sample was in touch with the ceramic disk. To avoid direct contact between the soil sample and the ceramic disk, two fuse wires, 0.3 mm in diameter and about 3.0mm in length, were placed on the top of the high air entry disk. Direct contact between the soil sample and the ceramic disk before the cell pressure was applied would transfer negative value of pore water pressure to the water in the filter and in the water back pressure line, this could result in cavitation of water within the high entry disk. This technique was first developed at Imperial College and was used successfully by (Sivakumar 1993).

3.6.4.1 Contact between soil sample and pedestal

Sivakumar (1993) used short length of two semi-circular of thin fuse wire with 0.36 mm diameter. He estimated that a cell pressure of about 35 kPa was required to seat the sample on the ceramic disk. Instead of fuse wire it was decided to develop the pedestal itself, that were made, the ceramic disk was placed in the pedestal about 0.5 mm below the service of the pedestal, that were made good contact between soil sample and the ceramic disk.

3.6.5 Cell assembly

After a sample had been placed on the pedestal, a ball bearing was placed in the conical recess within the top cap. The acrylic cells wall (inner and outer) was then placed in position, and the top load ram attached with a ball bearing in the top of the soil sample. The cell was filled with de-aired water. Finally, any trapped air inside the cell escaped through a bleed valve in the cell top plate and the bleed valve on the cell top plate was closed, and the test was then ready to proceed.

3.6.6 Measurement of the water and sample volume change.

The water volume change in the soil specimen was measured using the pressure/volume controller. The water draining from the sample flowed along the water back pressure line and then to pressure/volume controller. Due to the high value of pore air pressure inside the soil sample applied, the air could go into the pore water and then diffuse through the high air entry disk. The dissolved air could then come out of result to form air bubbles within the back pressure line. A flushing system, to remove any bubbles of diffused air from beneath the ceramic disk. In order to obtain the correct pore water volume change in the sample, the diffused air volume must be known.

The sample volume change measured as a result of the combined volume changes of the air and water phases. There are two methods for measuring the sample volume change, by the flow of water in and out of the surrounding cell, or measuring the individual lateral and axial strains of the sample. With the double-walled triaxial cell. Sivakumar (1993) and Estabragh (2002) obtained accurate values of overall sample volume change at small and large strains using this method. By the local strain gauges mounted directly on the sample, the second method could be done. With small strains, this method gives an accurate value of deformation. However, it becomes increasingly inaccurate as the sample is sheared towards failure. The main objectives of this project were to investigate the behaviour of unsaturated soil at large strains. As the above reasons the double-walled cell was selected to use in this research.

3.7 Temperature control

All the pressure/volume controllers, Digital Pressure Interface (DPI), other tools must be kept within an ambient temperature as recommended. Furthermore, when measuring the volume change of a sample in the double-wall triaxial cell, it is very important to minimise the variations in temperature. The air conditioning in the research laboratory is on 24/7, thus, there is no variation of ambient temperature, and the tests were carried out at a temperature of 20±1°C. The temperature display was on probation from time to time. This was to ensure that there was no significant variation in the temperature during the tests.

3.8 Soil-water characteristics curve (SWCC) methods

The naming convention is approved for this test as SWCC. The soil water characteristic curve has been chosen as the preferred terminology for this research on geotechnical engineering with unsaturated soils, and because it appears to have the most common term historically used in engineering by (Fredlund 2012). Tests for obtaining soil-water characteristic curve indicates the number of drying and wetting cycles.

In this research, SWCC tests were conducted using two methods, the first one was, modified triaxial (see Figure 3.11), and the second one was, using pre-equalisation procedure. The pre-equalisation method was carried out to determine the SWCC tests for this study. Triaxial apparatus was using for clayey soil, with 5-bar of air entry dick (ceramic dick). Specimens with 0 % of fibre were tested under zero matric suction. The sample was prepared with 13 % of water content and dry density of 1.78 g/cm^3. After the specimen was prepared, it was placed on the pedestal, the cells were assembled and filled

with de-aired water, and a small amount of pressure was applied to the inner and outer cell, to ensure the sample is had a good connection with air entry desk and membrane. Both the cell pressures and the back pressure were increased at the same time, while the mean net stress was kept constant $(\sigma_3 - u_a)$ that to start wetting the sample.

B-value calculating during the wetting path, and once the degree saturation achieved than the drying produce started. The drying path has been done by decreasing the back pressure, while the cells and air pressure were kept constant. By using triaxial apparatus method, it takes long time, and the time can vary from weeks to even months, which affects the course of the research process. With long time processes tests become infeasible and the flushing system was connected under the desk, to remove air from below the air-entry desk, that affected an accurate water volume change measurement. The other problem is that saturated samples need a high pressure of air, which was not possible to provide in the laboratory, the maximum in the laboratory was 400 kPa of air pressure. Besides, a diffused air correction is more challenging. It was recommended by (90 GDS help sheet) to create SWCC by triaxial test system, that should have 1200 kPa of cells pressure, 1160 kPa of air pressure and 1150 of back pressure. It discussed and agreed to use the pre-equalisation method, which has been done successfully by (Sandra 2008).

Sandra (2008) suggested that there was a procedure for the pre-equilibration process that involved preparing the sample to an encoded compaction dry density and 13 % water content. The water content that conforms to the target test suction value was estimated from the as-measured suction versus water content drying curve, and the sample was allowed to dry or be wetted steadily

outside to triaxial cell until the target water level was achieved. In terms of drying, the sample was placed on a base pedestal of a triaxial cell and covered in a membrane. The membrane was only then covering half of the sample for drying for a part of the day, and the weight was always monitored. For the rest of the day the sample was fully covered with the membrane to allow equilibration. The procedure was repeatedly carried out until the required water content that conforms with the target suction value was reached. In the case of wetting, the process was similar but less water was added to the sample, as a result of that it was not possible to monitor the soil suction from the as-measured drying curve because of hysteresis. In this process, to achieve the soil suction, by using this method, the samples must measure directly in the triaxial cell.

Generally, the estimated SWCC seemed to provide the desired water content that corresponded closely to the target suction. The pre-equalisation technique appeared to be practical and saved test time. The pre-equalisation procedure aided in dying and wetting to a target of 50,100 and 200 kPa. the as-measured drying suction versus water content for the compacted test specimen, shown in Figure (3.13).

Figure 3.13 sample during drying path using pre-equalisation method

3.9 Standard of triaxil Test

According to (BS EN 1997-2:2007), the Consolidated-Undrained (CU) triaxial compression test allows pore water pressure measurement. In this test, drainage is not allowed and the pore pressure changes for the duration of the shear, where the undrained shear strength of a sample is subject to initial effective stress. The parameters of shear strength can be copied at failure as c and ∅. The shear strength of the 38 mm diameter soil sample that is subject to lateral pressure and water content is kept constant. Equipment required for the test is described below.

3.9.1 Apparatus

The apparatus for the triaxial test is shown in Figure (3.14).

a. The cell base: this is machined from corrosion resistant metal, and fitted with four channels; each channel can be connected to a tube by a screwed socket in the cell, into which a valve can be fitted. Two of the

channels are connected to the cell pressure and the others are connected on the top surface of the pedestal, where the specimen can be placed, and each valve connected to a suitable pressure line, e.g. all around pressure (cell pressure).

b. Cylindrical cell body and top: the cell body and top consist of a single unit, which is removable for inserting the sample. The top is fitted with an air release valve, where the triaxial cell should be appropriate to take a 38 mm diameter and 76 mm long specimen, and for use with de-aired water to exert internal pressure. Moreover, the sample can be subjected to an all-around pressure, with vertical compression load.

c. A loading piston (ram) is used to apply axial loads to the specimen; the piston is fitted with an adjustable collar, and should be oiled and cleaned.

d. Loading cap; the load from the piston is transmitted to the sample through the top cap.

e. The top cap is perforated with a hole at the top, which can be connected to a gauge to give the back pressure.

f. Some accessories are related significantly to the triaxial cell, such as (a) air bleeds to the plug to de-air the cylinder, (b) membrane to suit the specimen with fitted size, (c) 0-rings for sealing the membrane on the sample, which can be placed on the top cap and base pedestal, (d) two porous discs for placing the top and bottom of the sample, their diameter should be the same as the specimen, (e) tube's length and diameter should be suitable for the pressure to connect them with components of each pressure system.

g. Pressure system, two independent systems should be used; one in the cell and the other at the sample top and bottom. In this test, pressure/volume controllers were used.

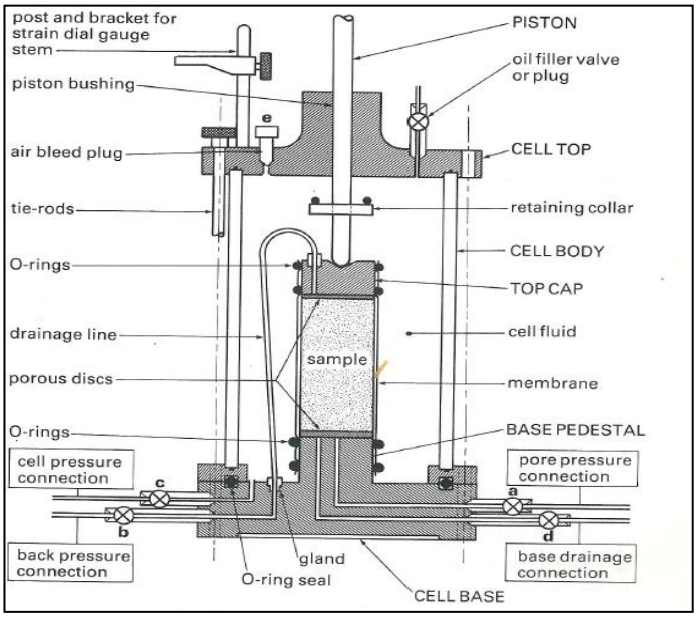

Figure 3.14 apparatus of triaxial test

3.9.2 Test procedure

The test procedure was taken in three stage where sample must be saturation at the first and consolidated it the in the final compression the sample to measure the shear strength as below:

3.9.2.1 Saturated sample

The first stage of the CU test ensures that water fills all the voids between the particles, and that the air has been removed. This method can be done incrementally using the cell pressure and pore pressure (back pressure) system, from that system, the (*B*) coefficient value can be determined for the total stress at each level. According to (BS EN 1997-2:2007), the procedure is as follows:

a. Ensure all the valves are closed at both ends, and apply the first increment of the cell pressure directly.
b. Record the pore pressure when it reaches the equilibrium value of the sample (u_1).
c. Record the cell pressure as (c_1).
d. Increase the cell pressure by 50 KPa.
e. The reading of the pore water pressure is taken at intervals, according to the BS standard, until it becomes steady, and the cell pressure and pore water pressure recorded respectively as (c_1), (u_1). The change in pore pressure and cell pressure is calculated, as coefficient B from the following equation;

$$B=\frac{\Delta\sigma 3}{\Delta u} \qquad 3.3$$

If the *B*-value is greater than 95 %, this means that the sample is saturated, and if more than 97 %, then the sample is fully saturated. The difference between the cell and back pressure should not exceed 20 kPa to avoid water from back pressure goes between sample and membrane, or swelling the specimen due to high pressure, and should not be less than 5 kPa.

3.9.2.2 Consolidated the sample

After full saturation of the specimen, the consolidation stage began immediately. The consolidation stage brings the specimen to effective stress, ready for the compression test. This test measures the triaxial consolidation from the amount of water out of a cylindrical specimen. Once the degree of saturation is successful, the procedure is as follows:

a. Close the back pressure valve and leave the pore water pressure line open until the end of this stage.

b. Increase the cell pressure and adjust the back pressure to equal to the required effective consolidation, σ_3', and record the pore pressure.

$\sigma_3' = \sigma_3 - u$ *3.4*

c. Record the volume change in intervals of time.

d. Continue the consolidation until there is no more important volume change, and then calculate the degree of consolidation using the following equation:

$$U = \frac{ui - u}{ui - ub} \quad 3.5$$

where

U is the degree of consolidation, u is the pore water pressure reading at time *t.* Calculation of the dimensions of the sample were taken as, area, length and volume, and plotted on a root-time or log time curve.

The theory requires the settlement degree to be plotted against the root-time scaled by 1.15, and the 90 percent point is taken where the two curves intersect. Hence, the value of the coefficient of triaxial consolidation may be calculated (Taylor 1948). The log time method presented that the 50 % degree of consolidation, which is at the middle between the 0 % and 100 % degree of consolidation, and the coefficient of consolidation can be computed from the value of *t*50 (Whitlow 2001).

3.9.2.3 Shearing

Once more than 95 % consolidation is achieved, the primary consolidation has been achieved, and is stopped, by closing the back pressure and pore pressure valves, until it is convenient to start the compression stage. While under compression, the change of water content is not allowed, and so the back pressure and pore water pressure valves are closed. The value of time to failure (t_f) calculated from t_{100} related to the time from the start of the compression to failure, (t_f) is obtained with the factor without side drains, which is 0.51 multiplied by t_{100}. The procedure for compression is as follows:

a. Ensure the back pressure and pore water pressure valves are closed. The cell pressure valve is open, and adjust the compression machine for the strain, which can be calculated using:

$$d_r = \frac{\varepsilon_f \times L_c}{t_f} \qquad 3.6$$

where

L_c is the length of the consolidation sample:

t_f is the significant strain interval

ε_f is the significant testing time (in minutes)

b. Set the gauge reading of the axial displacement, load cell, and timer. Record the initial reading of compression stage, date and clock time, deformation, force device, pore pressure and cell pressure.
c. Apply compression to the sample.

d. Calculate the values of deviator stress and effective principal stress ratio, and plot them against axial strain.
e. Keep the test running until the maximum deviator stress, maximum effective principal stress ratio has been identified, and the shear stress, and the pore pressure become constant. If the failure condition is not reached, then leave the test for up to 15 % of axial strain.

In the final stage of measurements, take the weight of the whole sample and calculate the density using volume change, and dry the sample in the oven to determine the moisture content. In this test, the pressure/volume controllers have been used to apply pressure in the cell and back.

3.10 Unsaturated test program and stages

Samples code

- The samples have been named relative to the percentage to fibre and the amount of suction pressure. e.g.
- F1-S200: means that the fibre is 1 % and the tested under matric suction of 200 kPa.
- F0-S50: the fibre is 0 % and matric suction is 50 kPa.
- F5-S100: 5 % of fibre under 100 kPa of matric suction.

Table 3.3 shows the test program of this research, which depends on the matric suction and percentage of fibre, as below:

Table 3.3 tests plan of the investigation

Test code No	Fibre %	Matric suction (kPa)	Test code No	Fibre %	Matric suction (kPa)
F0-S0	0	0	F3-S0	3	0
F0-S50	0	50	F3-S50	3	50
F0-S100	0	100	F3-S100	3	100
F0-S200	0	200	F3-S200	3	200
F1-S0	1	0	F5-S0	5	0
F1-S50	1	50	F5-S50	5	50
F1-S100	1	100	F5-S100	5	100
F1-S200	1	200	F5-S200	5	200

3.10.1 Setting up unsaturated test

After removing the sample from the mould, it was then covered by the membrane and placed direct on the pedestal. The atmosphere during that time effect on the water content of each samples. However, those samples that include 5 % fibre were maintained to be set in less time, as the swelling occurs with a time, due to the high percentage of fibre. The sample was placed and the cell assembled as described early in this chapter. Before that, the dimensions of the sample were measured and weighed. The high air entry disk was saturated and all pressure/volume controllers that were connected to cell, inner cell, the outer, lower chamber, back pressure and air pressure, and drainage line were de-aired. The top ram was lowered and connected to a metal ball bearing on the top cap. The inner and outer cells were connected to the pressure/volume controllers. The spiral groove at the bottom of the ceramic disk was also flushed by closing valve No 1 and opening valve No. 2 (see Figure 3.10). In order to achieve the objectives of this research, a programme of various tests under different suctions and differed percentage of fibre on samples of unsaturated

compacted clayey soil was planned. The procedures stage for performing a test including equalisation, consolidation, and the shearing are to be describe in this section. At all stages, the pressures in the inner and outer cells were the same. The difference between the cell pressure and the air at any time was kept to a minimum of 30 kPa to avoid the membrane being blown up inside the cell. The sample setting up was finished and all the valves of pressure were closed. The test is now ready to start stage by stage.

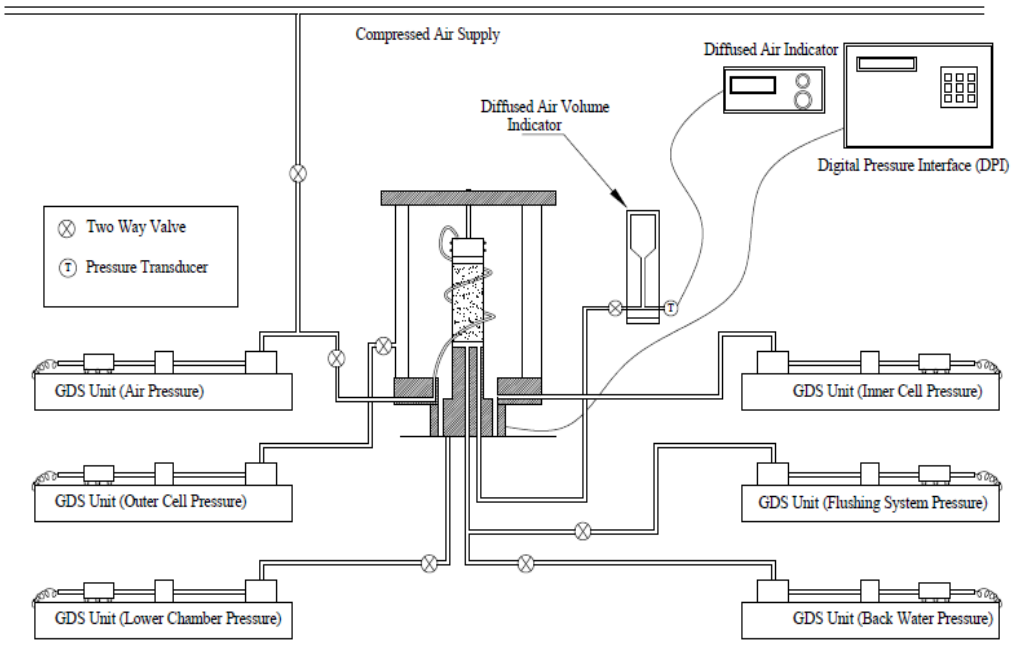

Figure 3.15 . Experimental set-up (not to scale)

3.10.2 Equalisation

The objective of the equalisation stage was to allow the pore water pressure within the sample to equalise to the water back pressure value. The equalisation stage followed directly the application of mean net stress. After the compaction of the sample, the suction within the sample had an unknown value. The suction in the equalisation stage is brought (increased or decreased) to the required value. The valves of the both cells pressure were opened and

manually a 30 kPa was ramped, the air pressure was applied as 15 kPa and small back pressure of 5 kPa was applied, and left for 15-20 minutes to make contact between the sample and ceramic disk. The water inflow into the sample and the volume change in the inner cell pressure were recorded manually during this part of stage, due to the air pressure increase problem. For achieving a desired matric suction in a sample, the target values of cell pressure, back pressure and air pressure were selected. In this research, the suction method was applied as, the cells pressure and the air pressure were increased manually to a target, while the back pressure left to apply a suction in the computer programme. During the ramping procedure, the data was recorded in a definite file. All the related pressure/volume controllers stopped ramping when the target back pressure was achieved, and the control programme was finished. The stage took 5 to 10 days to complete. The equalisation completed when the flow of water decreased less than 0.1 cm^3/day

3.10.3 Consolidation

In the ramped consolidation stage, the suction was kept constant at a required target. While the value of mean net stress p' was increased to a final value target in all tests. This increase of p' was achieved by ramping the cell pressure with pressure/volume controllers of the both cells inner and outer to a new target value. Afterwards, the samples were equalised at a specified suction (0, 50,100 and 200 kPa) and a mean net stress. In order to carry out a consolidation test, the air back pressure and water back pressure were kept constant, while the value of cell pressure was ramped at a given rate to a final target value. In unsaturated soils, the ramp consolidation is preferable to the conventional step loading consolidation since of the generation of high excess

pore water pressure in unsaturated soil sample. Sivakumar (1993) pointed out that for a point within the interior of an unsaturated soil sample subjected to a step increment of total stress, the stress path would be of the form ABC under, shown in Figure. (3.16) Increasing the total stress to the sample, excess pore air and pore water pressures are generated. Due to the high air permeability, the excess of pore air pressure dissipated quickly. However, dissipation of excess pore water pressure requires much more time because of the comparatively low water permeability. Consequently, initially the stress state moves from A to B, as the excess pore water pressure dissipates, to the water back pressure value and the soil sample reaches the final equilibrium point on the yield curve Y_B. At the top face of the sample, excess pore water pressures occur and the soil reaches point C on the yield curve Y_C at the time of loading. Thus the soil is not at a virgin state at the end of consolidation, and additional plastic compression has occurred (compared with the desired stress path direct from A to C). It is therefore very important that consolidation of unsaturated soil samples should be done by ramping, to ensure that the excess pore water pressure remains acceptably small, and the suction is held constant. The ramp consolidation method was selected in this research work. Thomas (1987) proposed an equation for the equilibrium calculation value of excess pore water pressure at the undrained face of a saturated soil sample loaded by ramped consolidation, with the total stress increasing with time at a constant rate A.

$$U_{ex} = \frac{Ah^2}{2c_v} \qquad 3.7$$

where

U_{ex} Excess pore water pressure, c_v is the coefficient of consolidation, *h* was the drainage path length and A is the rate of increase in cell pressure.

The value of c_v was measured as c_v= $8.05 \times 10^{-7}\ m^2/s$ by Sivakumar (1993) from trial step-loading isotropic consolidation tests. *h* = 100 mm into equation [3.7] and the following relationship was obtained:

$$U_{ex} = 1.72A \qquad 3.8$$

By using this rate according to the equation [3.8], the excess pore water pressure will be about 2 kPa at the undrain face in saturated condition. The ramp consolidation took at least 24 hours using this rate, as it corresponded to the final value of *p'* of 100 kPa. With this rate of pressure increase, the ramped consolidation stage took approximately 2 days; the actual time depending on the target value of mean net stress.

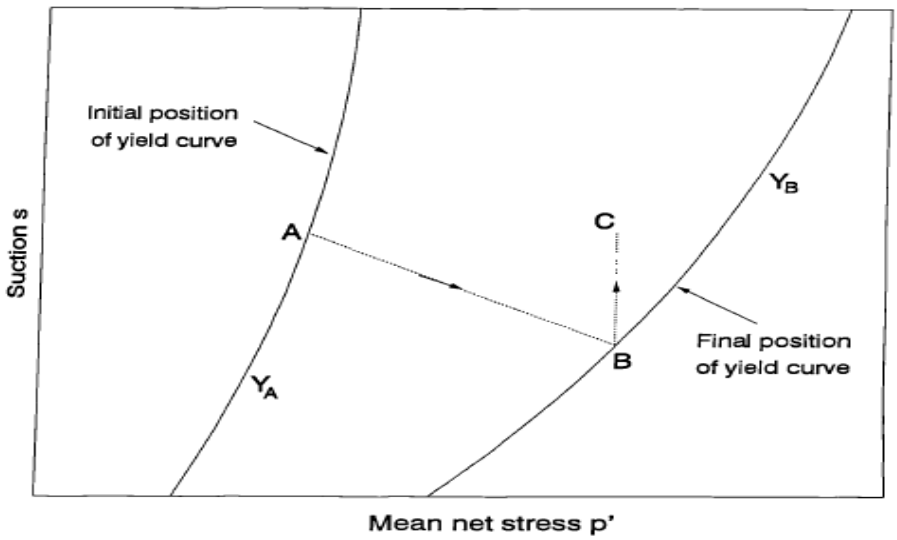

Figure 3.16 Stress path for isotropic consolidation by step-increment of cell pressure (Sivakumar 1993)

In the consolidation stage, the sample is brought to the state of effective stress that is needed for the shearing. That can happen by increasing the cell pressure, whilst at the same time the back pressure is constantly maintained. In this case, the process can be carried on until the volume change is not significant any longer, and at least 95 % of the surplus pore pressure has dissipated. When cohesive samples are sheared, a suitable strain can be estimated using the consolidation response.

3.10.4 Shearing stage

In order to carry out the shearing undrain test, the valves of air pressure and back pressure were closed. The computer programme selected a suitable rate of stress. The method for determination of the required rate of strain in the shearing stage was based on the equation proposed by Bishop and Henkel (1962) for the time for a sample to reach 95 % dissipation of excess pore water pressure. The equation as:

$$t = \frac{20h^2}{\eta c_v} \qquad 3.9$$

where

h is the half-length of sample, η = 0.75 is a factor depending on the drainage condition at the sample boundaries for drainage from only one side c_v is the coefficient of consolidation and t is the time to failure. By setting h = 50 mm, c_v = 8.01*10^{-7} m^2/s the required time was calculated to be about 23 hours for the fully drained condition, the time calculated using equation [3.8] (23 hours) seems to be appropriate for unsaturated clay soil. The aim of the test was to investigate shear strength behaviour of the soil before and after reinforced. The test was ended when the changes in deviator stress and mean net stress were

insignificant with change of axial strain; the rate of an axial displacement rate of 0.1120 mm/hour was selected. The required time was calculated to be about 3 hours.

3.11 Dismantling

When the test was finished, logging was halted and the valves on the water back pressure line and the air back pressure brought to zero, then the lower chamber pressure and finally the inner and outer cell were reduced to zero, respectively. The bleed valves in the cell top plate were opened and water from them was drained into the cylinder. The top ram was released from the top cap and then acrylic cells wall was detached from the cell base of the device. The rubber membrane was carefully removed from the sample and it was stripped from the pedestal. The wet weight of the sample was measured immediately to the nearest 0.01g and the sample dried in an oven for 24 hours before measuring the dry weight. The wet and dry weights were used to calculate the variation of water volume.

3.12 Data logging

Pressure/volume controllers were supported by GDSLab software supplied by the GDS manufacturer (Geotechnical Digital System Instruments Ltd). The software provided computer control of testing with data logging and data presentation. Therefore, during a test, the cell pressure, the volume of water inflow or outflow to the inner cell, the chamber pressure, the volume of water flow to the chamber, the back pressure and flow of water entering, or leaving the sample were logged at time intervals of 10 seconds. After each stage of a test, the data was stored on the computer hard disc. The data could then be

transferred to ASCI format and analysed using a commercial spread sheet such as Excel.

3.13 Calculation of strain and stress parameter

The calculation of axial strain ε_1 was undertaken by means of the volume of water that was sent from the pressure/volume controller in the lower chamber to move the pedestal. The Deviator *q* stress and mean net stress *p'* was calculated as follows:

$$p' = \sigma_3 + \frac{q}{3} - u_a \qquad 3.10$$

$$q = \frac{f}{A} \qquad 3.10$$

where

p' is mean net stress, *q* is the deviator stress, σ_3 is the cell pressure, u_a pore air pressure, *f* is axial force and A was the corrected cross-sectional of area of the sample at any interval of time. The degree of saturation s_r was calculated based on the volume of voids V_v and water volume V_w as follows:

$$S_r = \frac{V_w}{V_v} \qquad 3.11$$

$$V = \frac{\Delta V_s}{V_s} \qquad 3.12$$

$$V_w = \frac{\Delta V_w}{V_{w0}} \qquad 3.13$$

where

V_0 is the initial volume of sample being, V_s is the volume of solid particles, V_{w0} is the volume of sample within a sample at the start of test, ε_v is the volumetric strain that could be calculated by the volume of water which entered or left the inner cell.

CHAPTER 4 SAMLPE PREPARATION DEVELOPMENT AND CALIBRATION PROCEDURE

Summary

This chapter presents the methods and develop of mould, which used to prepare the specimens. In addition, the calibration procedure, including sensors, pressure/volume controller, flushing system devise and double-wall triaxial apparatus that have been used in in this study are described.

4.1 Introduction

Preparing cohesive soil samples at a specific moisture content and dry unit weight for routine soil experiments (i.e. triaxial test, shear box test, Oedometer test, or unconfined compression strength test) is often prepared using static compaction method (Reddy and Jagadish 1993, Head 1998, Oliver and Mesbah 1999, Wang et al., 2011) or dynamic compaction method (Bernhard 1951, Head 1998,). Remoulding of soil samples consists of compacting predetermined amounts of dry soil and water in a known volume mould to create samples with specific target dry unit weight/void ratio and moisture content. In dynamic compaction a known compactive effort is applied to the soil to reach the target dry unit weight. However, in static compaction the soil is continuously and gradually compressed at a constant rate of displacement to reach the target void ratio or dry unit weight.

Several investigations have been conducted to determine the merits of different remoulding methods. Booth (1976) quoting other researches, reported that

static compaction for preparation of soil sample gives the most uniform soil sample compared to dynamic and kneading compaction.

Sivakumar (1993) compared the repeatability of the soil properties of kaolin samples prepared by static compaction against the same kaolin samples prepared by dynamic compaction and reported excellent repeatability of the soil properties of samples prepared by static compaction. Murray and Sivakumar (2010) also reported that static compaction can yield more consistent and uniform samples compared to those prepared by dynamic compaction.

Unlike plain soils, fibre reinforced soils may encounter greater degree of structure non-uniformity if appropriate care in the sample preparation is not considered and undertaken. Mixing fibres with clay soils adds up the difficulty in sample preparation due to the inherent cohesive properties of clay soils and tendency of fibres to become twisted together and create fibre pockets. Therefore, appropriate measures must be sought to inhibit variation in dry unit weight, moisture content and fibre content in such soil samples. It is viably notable that the strength of a soil sample is highly dependent on its structure integrity. Furthermore, samples of the same soil but prepared with different methods may exhibit varying strengths due to variation in density and fibre content across the sample. To the date, investigating the uniformity of fibre reinforced soil samples has not yet been reported in the literature. Therefore, in this study static compaction soil sample preparation method is employed to prepare fibre reinforced soil samples with different layering arrangements to investigate the degree of uniformity of dry unit weight, moisture content and fibre content in different sections of the sample.

Through the undergoing study on fibre reinforcement of clay soils, it was found that increased fibre content may reduce the uniformity of the yielded dry unit weight along the height of the compacted sample by static compaction method. It was observed that static compaction of the soil sample from one end results in the opposite end being less compacted. Therefore, in this study several approaches for sample preparation were examined to maintain the uniformity of dry unit weight and fibre content across height of the fibre reinforced clay soil samples.

4.2 Soil sample preparation

In the first stage, the clay should be completely dry, and to do that, it was kept in the oven 24h, at a temperature for 105°C to 110°C. Wherever possible, procedures are related to this given in BS EN (1997-2:2007), and in some instances, this method made the calculation with and without adding fibres, and the methods that have gained general acceptance are given.

4.2.1 Mixed the soil

The method for forming a triaxial sample is presented. In respect of a uniform mixture of clay and its water content, that has to be prepared many more times. Most of the specimens in this study were 50 mm in diameter and 100 mm long. The components of the specimen were determined based on proportion of fibres, water content, and maximum dry density, these were made in the compaction tests see Figure (4.1). In order to calculate the weight of each component of the sample, such as clay, water, and fibre, the following method was used:

unknown parameters;

M_s is mass of solid (completely dry) (g).

M_w is mass of water (g).

M_f is mass of fibre (g).

Known parameters;

where V_0 , γ_d, WC, W_f are total volume of sample, dry density, water content and percentage of fibre, respectively. The Volume of specimen is

$$V = \frac{\pi\,(D)^2}{4} \times L\ (cm^3) \qquad 4.1$$

where

D and *L* is the diameter and the length of sample respectively

Thus

$$\gamma_d = \frac{M_s}{V_0} \Rightarrow \quad M_s = \gamma_d \times V_0 \qquad 4.2$$

$$\text{WC} = \frac{M_w}{V_0} \Rightarrow M_w = \text{WC} \times M_s \qquad 4.3$$

$$W_f = \frac{M_f}{M_s} \Rightarrow M_f = \frac{W_f}{1+W_f} \times M_s \qquad 4.4$$

Figure 4.1 steps of preparing the specimen

4.2.2 Material

A low plastic clay soil was obtained from the North West region of the UK. For the purpose of repeatability of the results, the clay soil was transformed to a powder-like soil by a series of processes including grinding and sieving. Table (3.1) chapter (3) shows the properties of the clay soil used in the current investigation. The properties of Carpet waste fibres that are used in this investigation were supplied by Carpet Recycling UK and include a mixture of different types of fibre (i.e. nylon, polypropylene, and wool) see chapter 3 section (3.2).

* SBR is a therrmoset material and cannot be melted down to reshape

4.2.3 Equipment

Three sets of moulding equipment were designed and manufactured to prepare samples with a diameter of 50 mm and length of 100 mm. The first mould was a traditional stainless steel tube with a moving rammer to compress the soil to a target void ratio. Another shorter stainless steel mould was manufactured for second and third preparation methods. Three different pairs of mini-rammers were also made to compress the sub-layers of soil in the mould. Figure (4.2) shows the equipment used for soil sample preparation. The surface of the mini-rammers was jagged to increase the interlocking between different soil layers. Figure (4.3) shows the dimensions of the mini-rammers. To relief the generated pore-water pressure in the sample during compression, a 3 mm borehole was manufactured in the mini-rammers.

Component shown in Figure (4.3) (c) was used to create a whole 100 mm (i.e. in length) sample. However, components shown in Figure (4.3) (b) and (a) were used to create sub-layers with length of 67 mm and 34 mm respectively. Using a set of mini-rammers during compaction of the soil in the mould permitted the preparation of different soil samples (i.e. a single 100 mm layer, 3 layers of 16.5 mm, 67 mm and 16.5 mm, or 5 layers of 16.5 mm, 16.5 mm, 34 mm, 16.5 mm and 16.5 mm). All samples in this study were statically compacted using a strain-controlled universal compression loading machine with displacement rate of 2.54 mm/min according to the aforementioned procedure Therefore, the influence of sample preparation method on compression strength of the samples was investigated.

Figure 4.2 Parts of the soil sample preparation equipment

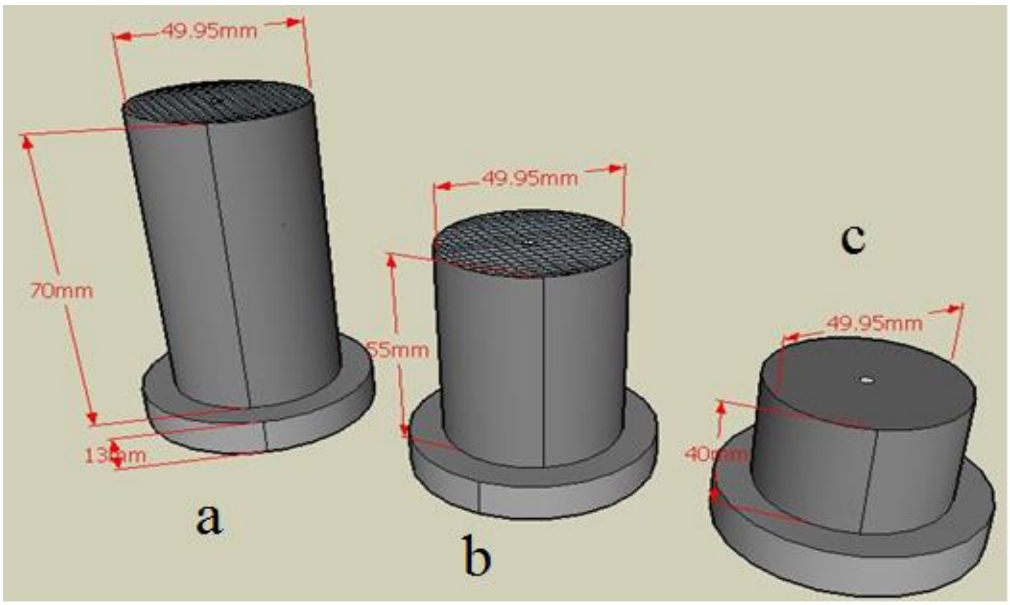

Figure 4.3 Dimension of the mini-rammers

4.3 Uniformity of specimen

Table (4.1) to Table (4.4) show the variation of the fibre content, dry unit weight and moisture content at different sections of the prepared samples. Fibre

content of each section was calculated with regarding to the mass of dry soil in each section.

As it is shown in Table (4.1) to Table (4.4), when the soil was compressed in a single layer (Figure 4.4 (i)), the dry unit weight of the bottom layer was lower than the top sections indicating that it has received less compaction. The effect of reduced dry unit weight at bottom of the sample was reflected in concentrating failure zones in lower end of the sample when it was subjected to axial load (see Figure 4.5 (a)).

In order to rectify this issue, a decision was taken to compress the soil sample from both ends simultaneously. In method (ii) in which the soil was compressed in 3 layers from both sides simultaneously, the arisen low density condition at lower end of the sample was resolved partly. And the density of the lower end of the sample was increased relatively as can be seen in Tables (4.1) to (4.4). However, the middle part of the sample was remained less dense than the other parts. Although the relative change in density across height of the sample was reduced, the results of method (ii) were still considered unsatisfactory. In method (iii), soil was compacted in 5 layers including a central layer and 2 pairs of thin layers around the central layer (see Figure 4.4 (iii)). Therefore, unlike the earlier methods, the density of different parts of the sample remained almost the same. Figure (4.5 (b)) shows the extension of failure zone of such sample across the height of the sample. Comparing the fibre content of the soil samples prepared with different methods, showed that in method (iii), fibres were distributed equally and evenly in different layers. However, in other methods the degree of uniformity of fibre distribution was less compared to that of method (iii).

The change of moisture content in different sections of the samples prepared with different methods was insignificant. And it was concluded that the distribution of moisture content in the prepared sample was independent of the employed preparation method. Therefore, preparation of fibre reinforced clay soil samples in multi-layer fashion reduced the probability of accumulation of fibres in local zones and ensured the uniformity density across the sample. Moreover, compressing the sub-layers from both sides increased the uniformity of dry unit weight in the sample.

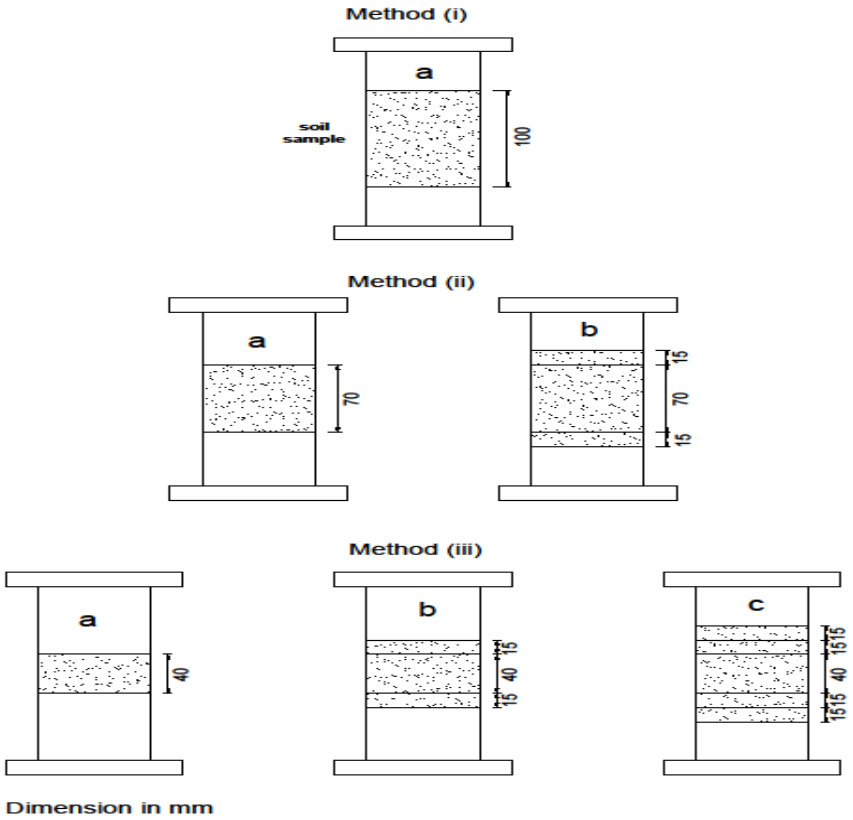

Figure 4.4 Sample preparation procedures

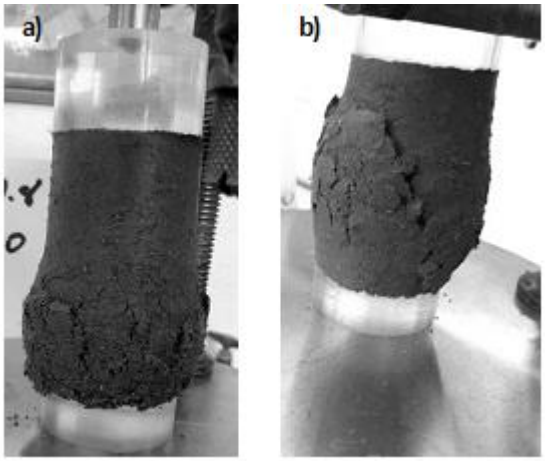

Figure 4.5 Location of failed zones in samples a) with non-uniform density b) with uniform density

Table 4.1 Variation of sample uniformity at different section (non-reinforced soil)

Prep Method	Method (i)			Method (ii)			Method (iii)		
	f (1)	DUW (2)	Wc (3)	f	DUW	Wc	f	DUW	Wc
Top	0	19.4	12.5	0	18.7	12.9	0	18.3	12.9
Mid	0	18.7	12.8	0	17.9	12.4	0	18.2	13.2
Bot	0	16.4	12.4	0	18	13	0	18.4	12.9

1: Fibre Content, %
2: Dry Unit Weight (kN/m^3)
3: Water content %

Table 4.2 Variation of sample uniformity at different section (1 % Fibre reinforced soil)

Prep Method	Method (i)			Method (ii)			Method (iii)		
	f (1)	DUW (2)	Wc (3)	f	DUW	Wc	f	DUW	Wc
Top	0	19.4	12.5	0	18.7	12.9	0	18.3	12.9
Mid	0	18.7	12.8	0	17.9	12.4	0	18.2	13.2
Bot	0	16.4	12.4	0	18	13	0	18.4	12.9

1: Fibre Content, %
2: Dry Unit Weight (kN/m^3)
3: Water content %

Table 4.3 Variation of sample uniformity at different section (3 % Fibre reinforced soil)

Prep Method	Method (i)			Method (ii)			Method (iii)		
	f (1)	DUW (2)	Wc (3)	f	DUW	Wc	f	DUW	Wc
Top	0	19.4	12.5	0	18.7	12.9	0	18.3	12.9
Mid	0	18.7	12.8	0	17.9	12.4	0	18.2	13.2
Bot	0	16.4	12.4	0	18	13	0	18.4	12.9

1: Fibre Content, %
2: Dry Unit Weight (kN/m^3)
3: Water content %

Table 4.4 Variation of sample uniformity at different section (5 % Fibre reinforced soil)

Prep Method	Method (i)			Method (ii)			Method (iii)		
	f (1)	DUW (2)	Wc (3)	f	DUW	Wc	f	DUW	Wc
Top	0	19.4	12.5	0	18.7	12.9	0	18.3	12.9
Mid	0	18.7	12.8	0	17.9	12.4	0	18.2	13.2
Bot	0	16.4	12.4	0	18	13	0	18.4	12.9

1: Fibre Content, %
2: Dry Unit Weight (kN/m^3)
3: Water content %

4.3.1 Uniformity of specimen

In this study three different approaches were examined to prepare the fibre reinforced soil samples by static compaction method. The efficiency of the sample preparation methods was evaluated by quantitatively measuring the dry unit weight, moisture content and fibre content at different sections of the prepared samples. Further evaluation was undertaken by determining the unconfined compression strength of the samples prepared with different methods. It was concluded that the method of sample preparation plays a viable key in achieving homogenous samples.

Uniformity of density across the height of the sample highly influenced the strength of the sample. In fibre reinforced sample, the strengths of the samples are not only dependent on uniformity of density but also on distribution of fibres within the sample. To improve the poor density condition of the bottom section of samples, they were compressed from both directions simultaneously.

The results showed that, increasing the number of soil layers and compressing the soil from both directions aids the uniformity of the sample in terms of density and fiber content. Furthermore, the repeatability of the results improved significantly with increasing the number of layers. The unconfined compression strengths of the samples tested in this study increased by minimum of 45.5 % with increase in the number of layers from a single layer to five thin layers.

4.3.2 Unconfined compression test results

To investigate the influence of sample preparation methods on the stress-strain behaviour and compression strength of fibre reinforced clay soil samples a series of unconfined compression strength tests with axial deformation rate of 1 mm/min were carried out. To evaluate the repeatability of the results, a minimum of two specimens were prepared for each test.

Figure (4.6) to Figure (4.9) show the stress-strain behaviour of samples prepared with method (i), (ii) and (iii) (see Figure 4.4). It can be observed that the compression strengths of the samples were highly sensitive to uniformity of density and fibre content across the sample. Increasing the number of layers in sample preparation method resulted in significant increase in unconfined compression strength. In fibre reinforced soils, due to random distribution and alignment of the fibres in the soil sample, the probability of achieving the same

strength for the same samples is highly dependent on uniformity of the fibre distribution and density at different sections of the prepared samples. In this study at lower fibre contents, all samples prepared with different preparation methods were repeatable however, with increased fibre content to 5 %, the variability in the attained results was widened as the number of layers in sample preparation method was decreased. The results of tests on samples prepared using method (iii) were the most repeatable and reliable results.

Figure (4.9) compares the average of unconfined compression strength of samples prepared with different methods. A suitable sample preparation method yields a homogenous sample with evenly distributed bonding strength between soil particles.

Samples with uniform density and fibre content exhibit higher strength. An intense increase in compression strength was observed for samples prepared with method (iii) compared to those prepared with method (i). For example, with increasing the number of layers from a single 100 mm layer to 5 thin layers, the unconfined compression strength of non-reinforced, 1%, 3% and 5% fibre reinforced samples increased by 58.8 %, 70.5 %, 46.2 % and 45.5 % respectively.

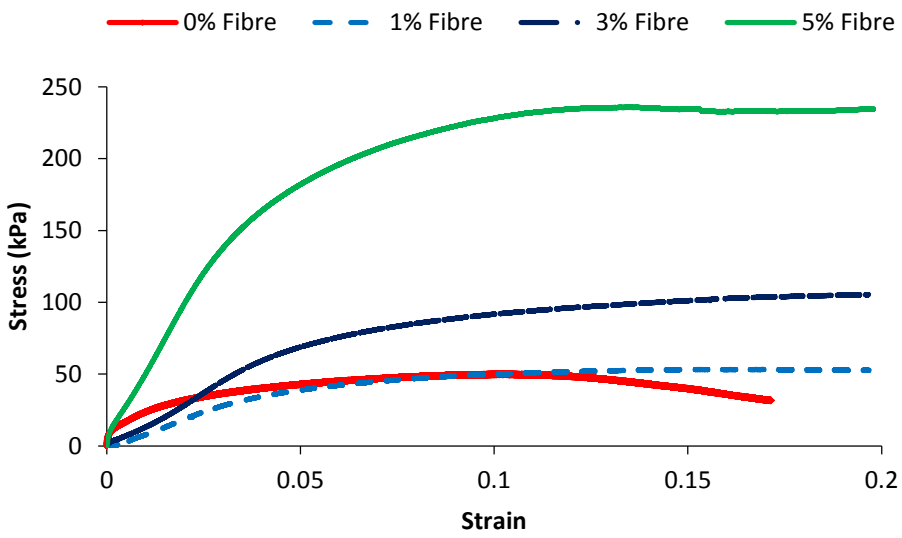

Figure 4.6 Stress strain behaviour of samples prepared by method (i)

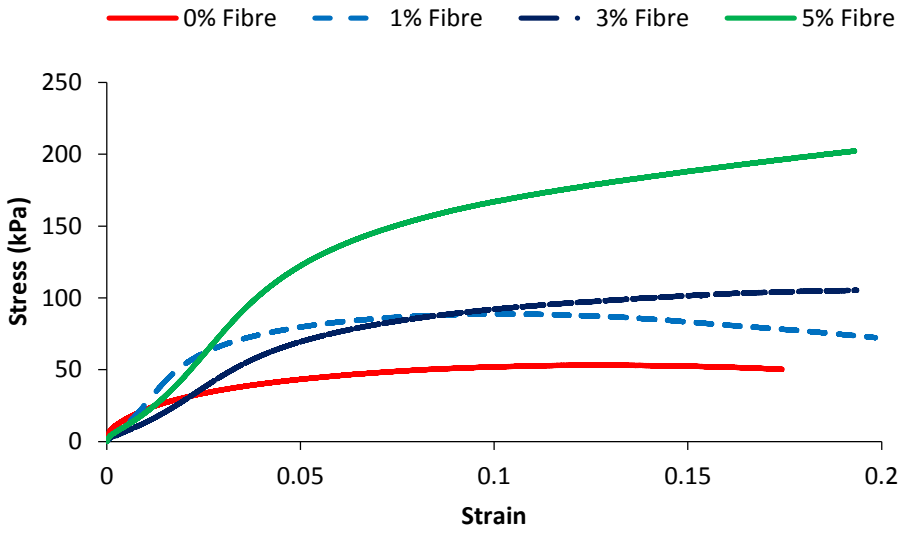

Figure 4.7 Stress strain behaviour of samples prepared by method (ii)

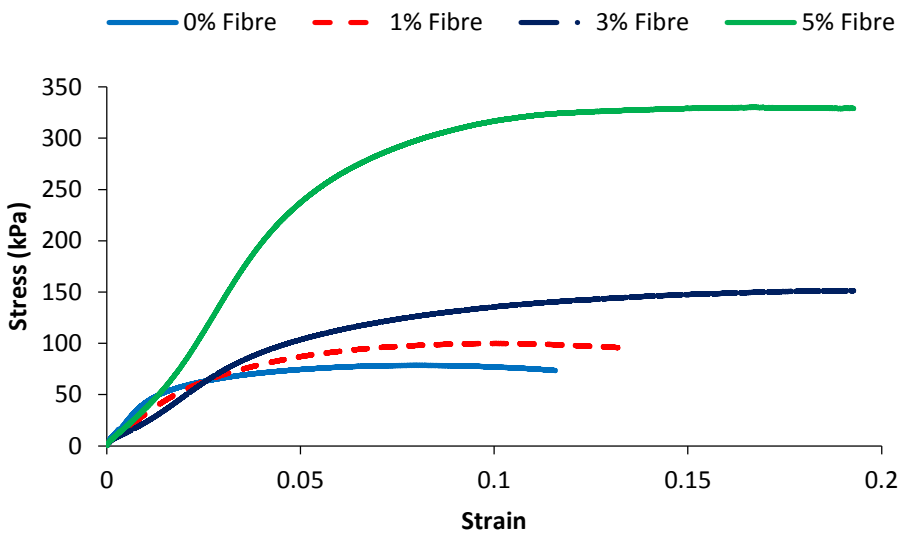

Figure 4.8 Stress strain behaviour of samples prepared by method (iii)

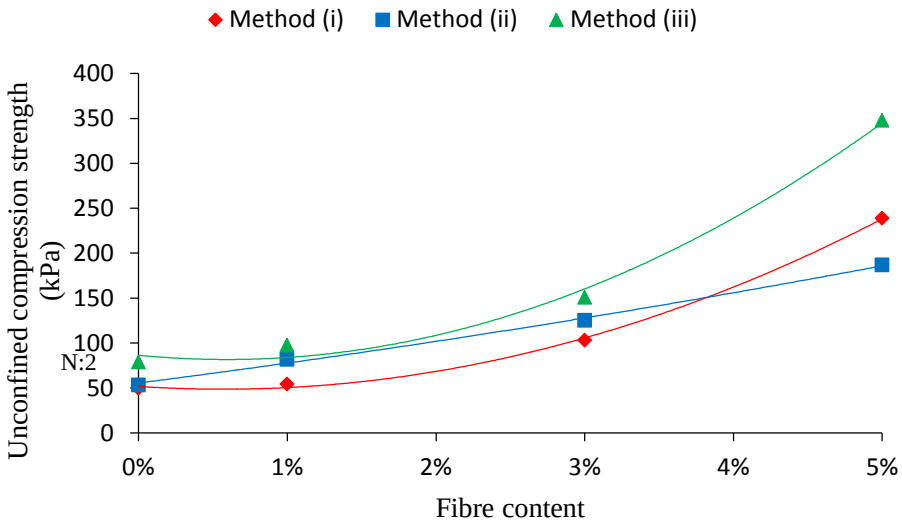

Figure 4.9 Average of unconfined compression strength of sample prepared with different methods

4.4 Uniformity of specimen

In this study three different approaches were examined to prepare the fiber reinforced soil samples by static compaction method. The efficiency of the

sample preparation methods was evaluated by quantitatively measuring the dry unit weight, moisture content and fiber content at different sections of the prepared samples. Further evaluation was undertaken by determining the unconfined compression strength of the samples prepared with different methods. It was concluded that the method of sample preparation plays a viable key in achieving homogenous samples.

Uniformity of density across the height of the sample highly influenced the strength of the sample. In fiber reinforced sample, the strengths of the samples are not only dependent on uniformity of density but also on distribution of fibers within the sample. To improve the poor density condition of the bottom section of samples, they were compressed from both directions simultaneously.

The results showed that, increasing the number of soil layers and compressing the soil from both directions aids the uniformity of the sample in terms of density and fiber content. Furthermore, the repeatability of the results improved significantly with increasing the number of layers. The unconfined compression strengths of the samples tested in this study increased by minimum of 45.5% with increase in the number of layers from a single layer to five thin layers.

4.5 Calibration

Calibration is the tool that establishes the value and quality and the link between them when the measurement and results are uncertain. The calibration is an important method to gain good test results, and to compare the results of the tests. The next sections describe the methods used for calibrating triaxial device, pressure transducer, and pressure/volume controllers, used in the

current research. In this research, the calibrations will be presented in details as below.

4.5.1 Calibration of Cell volume change

The flow of water in or out of the inner cell can be used to measure the volume change of a sample. In order to measure the actual volume change of specimen a number of corrections should be considered. The calibration procedure and the corrections will be described. The calibration of the double-walled triaxial cell must take place before the start of tests and error of the volume change is dependent on some factors such as, the extension of the connections, fittings and taps between the pressure/volume controllers and the cell, A very slight flexure of the top and bottom plates of the cell, compression of the water in the cell, and absorption of water by the wall of the cell. A small amount of water absorption could take place with time in the volume change. More than 250 days is needed to saturate the Perspex wall cell at a known pressure (Wheeler., 1986). This period of time could be reduced by keeping the cells filled with water when no tests are running. The connecting tubes between the pressure/volume controller and the cells should be checked and flushed regularly by applying a low pressure to remove any trapped air from the vents and tubes. The cells were filled with de-aired water and then left for a period of about 48 hours to make sure there is was no leakage from fitting and taps between the pressure/volume controller and the cells. Unfortunately, there was some leakage from the tap connection with the outer cell, therefore, it was decided to replace most of the old taps with new ones to ensure accuracy. Another kind of taps were used that are specially manufactured for air pressure, and were connected with the air pressure lines, as there was leaking there also.

All the fittings were fixed and the checking was carried out again. At this time, a huge problem was observed. Leakage was found underneath the high entry disk and came out of the back water pressure lane.

It was decided that it needed to be refurbished and new top and bottom pedestal were made for the triaxial cell, which spent more than 11 months in the workshop to be finished, and was also sent back to the workshop again and again to fix some other problems. It took more than 1 year for them to be refurbished. (Figures 3.12 in chapter 3 section 3.6.3 and Figure 4.10 and 4.11 in chapter 4 section 4.5.1) show a pedestal with a spiral groove, movement ram, which is connected between the lower chamber and pedestal, and the top cap of the air pressure, which is placed on the top of a sample respectively. It took a long time to design, manufacture and test new pedestals to ensure no leakage was detected. All connections to the cell were flushed again, a dummy sample was enclosed within a rubber membrane (using a membrane stretcher) and was placed in the pedestal. A top cap was placed on the dummy sample and the rubber membrane was sealed at the top and bottom using O-rings. Finally, the cell was assembled. Then the two cells were filled with a water from the storage tank and connected to pressure/volume controller, in order to avoid trapping air within the membrane, any extra rubber membrane at the top and bottom was cut off, then the air valve was closed. The pressure was applied to the cell by the relevant pressure/volume controller. It was an interface (Adlink) between the pressure/volume controllers and the computer. In intervals of 200 kPa the cell pressures to the both cells were increased from 0 to 800 kPa. this was done by selecting the isotropic consolidation test from the software menu. The same procedure was repeated as the pressure was subsequently decreased from 800

to 200 kPa. Each pressure was kept for at least 48 hours and all the data were recorded automatically by the computer. It was concluded from the results shown during increasing pressure in steps in (Figures. 4.12, 4.13, 4.14 and 4.15). Figure 4.16) shows that the immediate volume change of calibration for the cell. that the total volume change can be divided into:

a. Immediate volume changes due to change of the cell pressure,
b. Volume change with time due to water absorption by the Perspex cell wall.
c. volume change due to the slight variation of temperature.

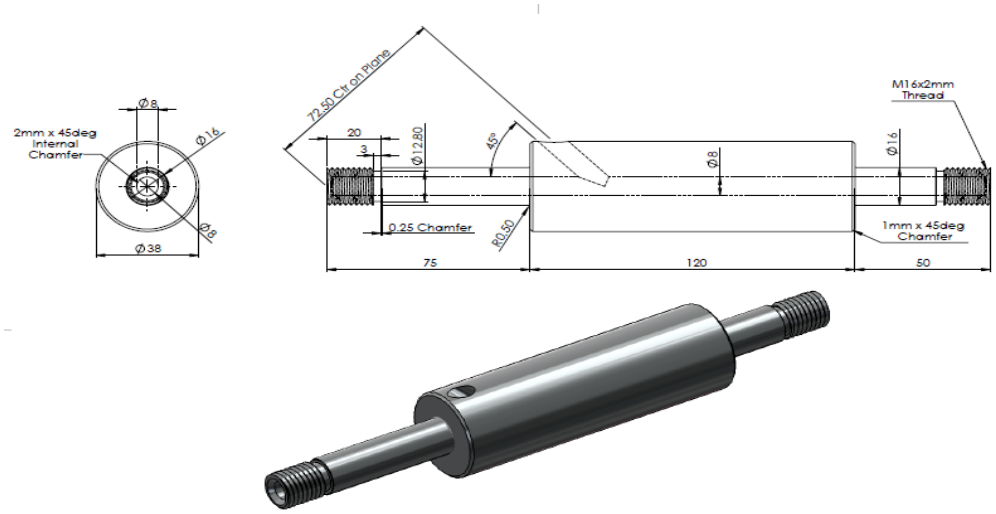

Figure 4.10 Stainless steel movement ram

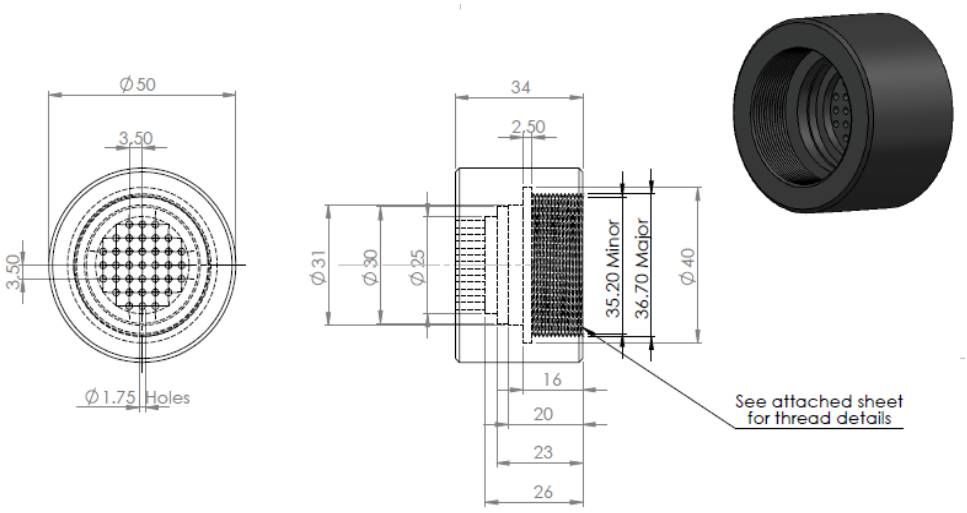

Figure 4.11 Plastic top cap

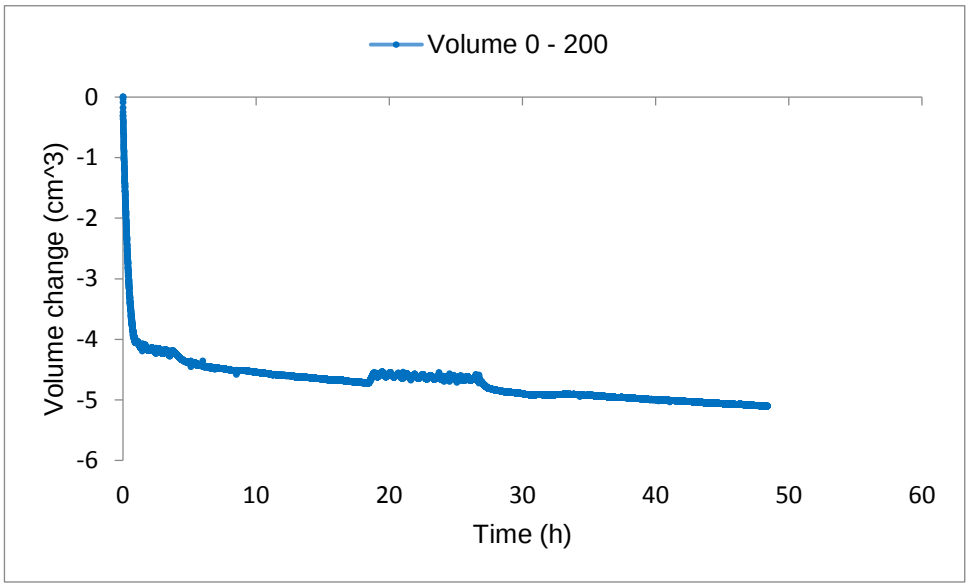

Figure 4.12 cell volume change variation with time due to a pressure increase (0 to 200kPa)

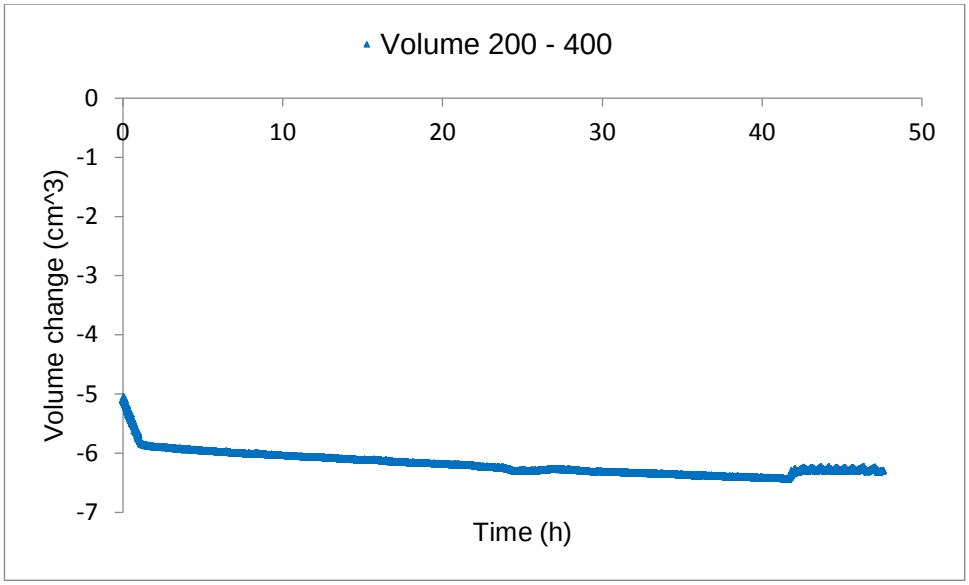

Figure 4.13 cell volume change variation with time due to a pressure increase (200 to 400kPa)

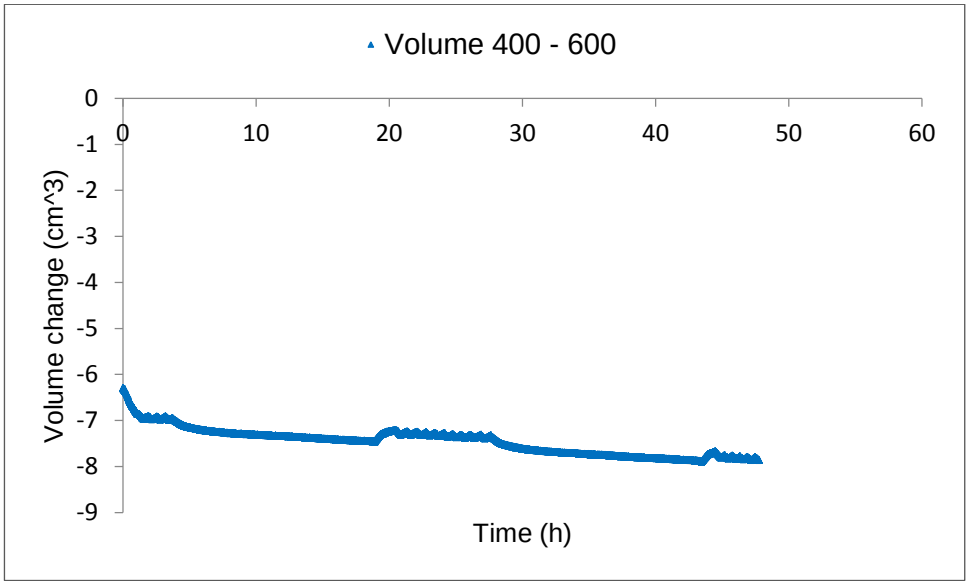

Figure 4.14 cell volume change variation with time due to a pressure increase (400 to 600kPa)

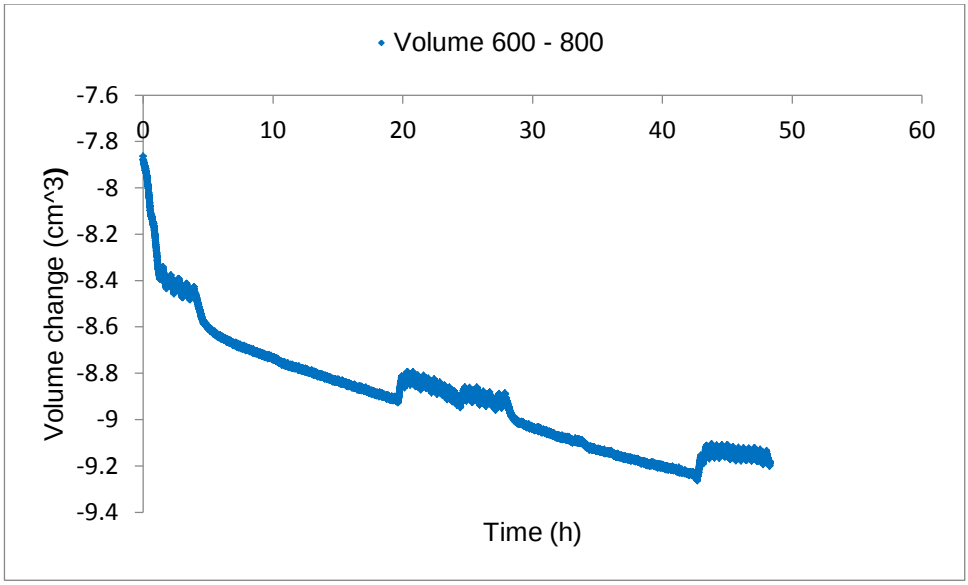

Figure 4.15 cell volume change variation with time due to a pressure increase (600 to 800kPa)

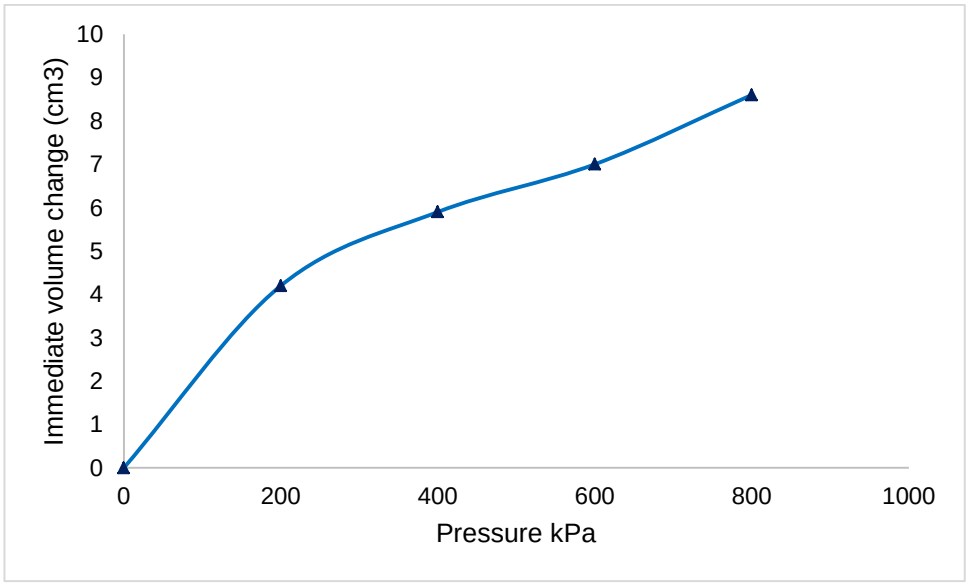

Figure 4.16 the immediate volume change of cell

4.5.2 Calibration of Movement of lower chamber

The pedestal of triaxial cell was connected with external load cell (see Figure 4.17). The pressure/volume controller was connected to the lower chamber. A digital gauge reader (LVDT) also fixed in the linear motion bearing to record the

movement of the pedestal. The volume and pressure of pressure/volume controller set to zero, LVDT, as well as the load cell. The pressure in the lower chamber was applied gradually by pressure/volume controller, from 0 to 800 kPa in intervals of 100 kPa. The volume of water going to the lower chamber was recorded, the load cell and the gauge reading. This procedure was repeated for various pressures. The calibration is calculated by the linear relationship between the volume of the water from the lower chamber (kPa) and the load cell (kN) and also by the linear relationship between the volume of the water from the lower chamber (kPa) and the movement of LVDT (mm). (see Figures. 4.18, 4.19 and 4.20)

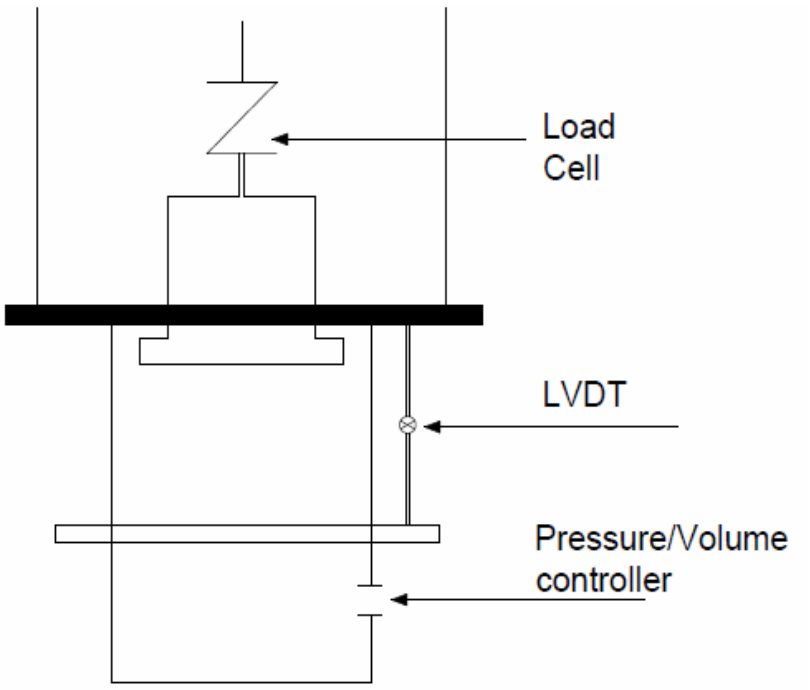

Figure 4.17 sketch of lower chamber with Load cell and LVDT calibration

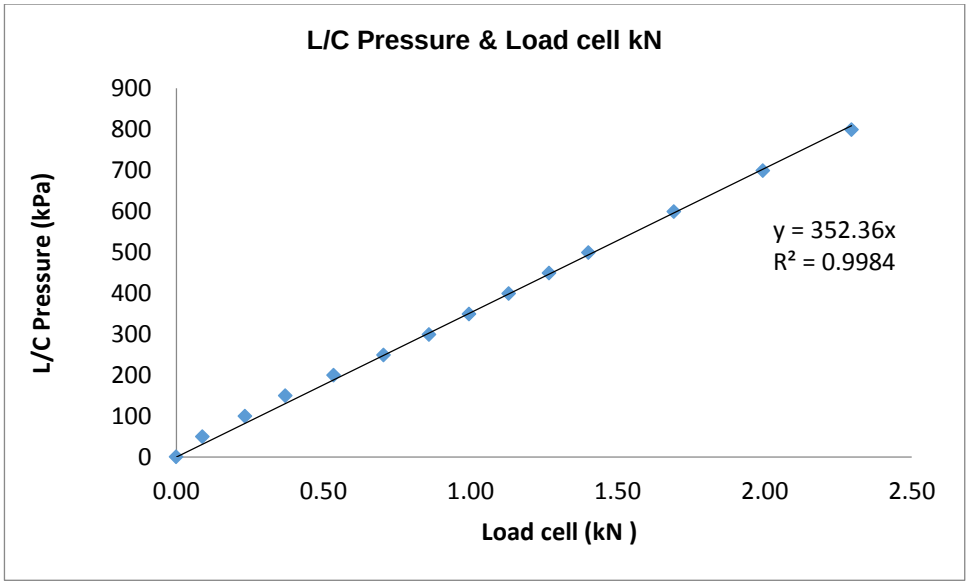

Figure 4.18 Relationship calibration between L/C pressure and Load cell

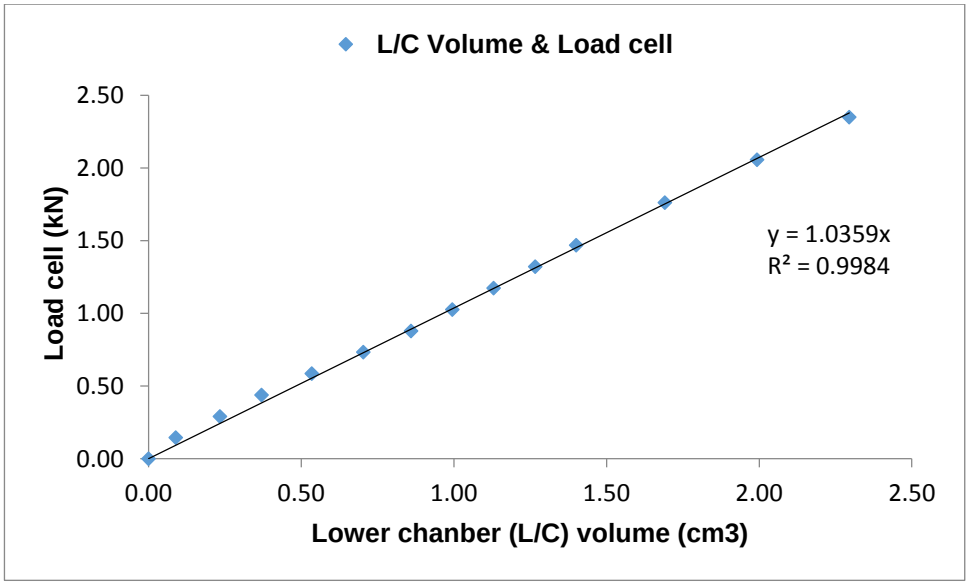

Figure 4.19 Relationship calibration between L/C volume and Load cell

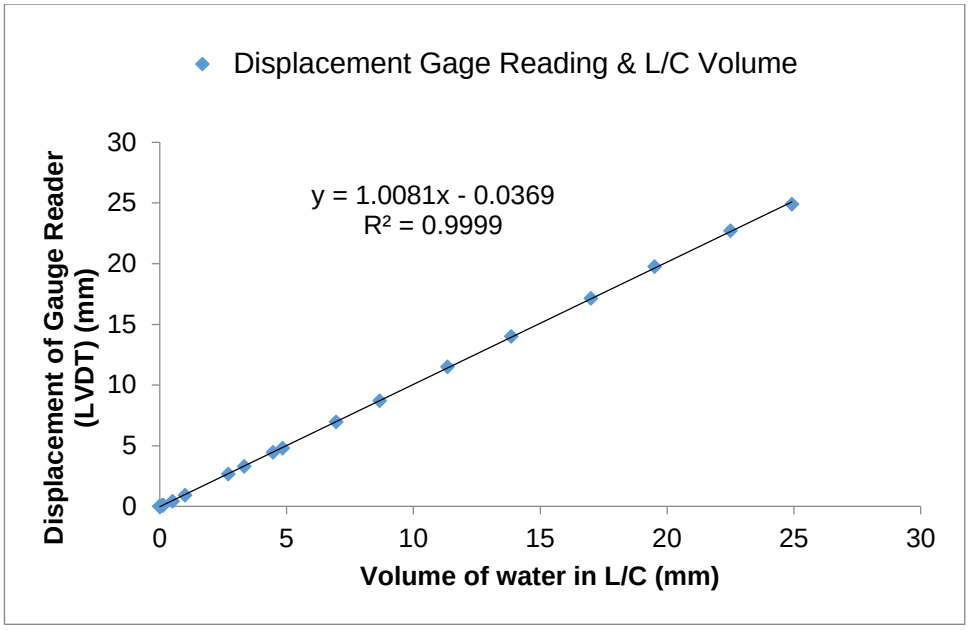

Figure 4.20 Relationship calibration between L/C volume and Gauge reader (LVDT)

4.5.2.1 Axial calibration

A friction between the platform and the lower chamber wall was corrected by a digital gauge reader connected with the ram movement of the lower chamber. A lower chamber pressure was applied on soil sample that was set up in the pedestal. During the test the gauge reading was recorded at 5 minutes' intervals, at the end of the test the axial strain was calculated based on the volume that entered in the lower chamber. Moreover, the axial displacement was recorded by the software, and the average between the axial strain and axial displacement was calculated. This average was subtracted from the gauge reading and then error correction was worked. Table (4.5) show the error correction calculated. The correction was used in each test, and was adding to the axial strain. The development equation was used to calculate the correction axial strain, as follows:

$$\varepsilon_c = \left(\varepsilon_y * 0.0287\right) + \varepsilon_y \qquad 4.5$$

where

ε_c axial strain after correction and ε_y axial normal strain expressed as a percentage.

Table 4.5 correction of axial strain

Axial Strain	Axial Displacement	Gauge Reading	Difference between the Gauge reading and Axial result
%	mm	mm	Error Correction
0.2414	24.1425	24.17	0.0287

4.5.3 Pressure/volume Controllers

All pressure/volume controllers must be calibrated against a master pressure/volume controller or measuring device. To apply pressures, there are five pressure/volume controllers that were used, each pressure/volume will be named as below:

a. Pressure/volume controllers No. 1 for applying pressure to the back pressure which connected at the base of sample and used.
b. Pressure/volume controllers No. 2 was connected to the Air pressure in the top of spacemen.
c. Pressure/volume controllers No. 3 for producing pressure to the Inner cell pressure.
d. Pressure/volume controllers No. 4 was used for applying pressure in the lower chamber.

e. Pressure/volume controllers No. 5 Were used for Outer cell pressure calibration.

Only one pressure/volume controllers were calibrated by the manufacturer and the others were calibrated against it. Each pressure/volume controllers were filled with de-aired water before the calibration (see figure 3.5 in chapter 3).

4.5.3.1 Pressure Calibration

The pressure/volume controller number (1) was selected as a master and calibrated against an accurate pressure gauge. The pressure/volume controller was set to zero while the end of nylon tube was held at the level of mid-height of the cylinder. It was then connected to a gauge and different target pressure was apply from the keypad. The readings from both the gauge and the controller were recoded. The results showed a correlation coefficient of 1 between the gauge reading and pressure/volume controller No. (1). By selecting various target pressure from 0 kPa to 1000 kPa at an increment of 100 kPa in the remaining pressure/volume controller (master). The same procedure was repeated as the pressure was subsequently decreased from 1000 to 100 kPa. Each pressure was kept a period of time to stabilisation. All other pressure/volume controllers (3), (4), (5) and No. (6) were calibrated against the master pressure/volume controller No. (1), by applied pressure in from pressure/volume controller required to calibrate and read it in the master pressure/volume controller. The correlation coefficients in all cases were about 0.999-1 indicating the high accuracy of the pressure/volume controllers.

4.5.3.2 Volume Calibration

The volume of water flowing into or out of the pressure/volume controller is very important for getting accurate results, specifically for estimating the volume

change of samples. In each pressure/volume controllers, the amount of water was collected for 5 minutes in containers and weighed, which was done by pressing the empty button on the keypad. By comparing, the volume was read from the pressure/volume controller display and the weight of water measured. It was found that the accuracy of the pressure/volume controller reading on average was more than 99%. The calibration graph shown as (Figures 4.21 to 4.25) as well as Table (4.6).

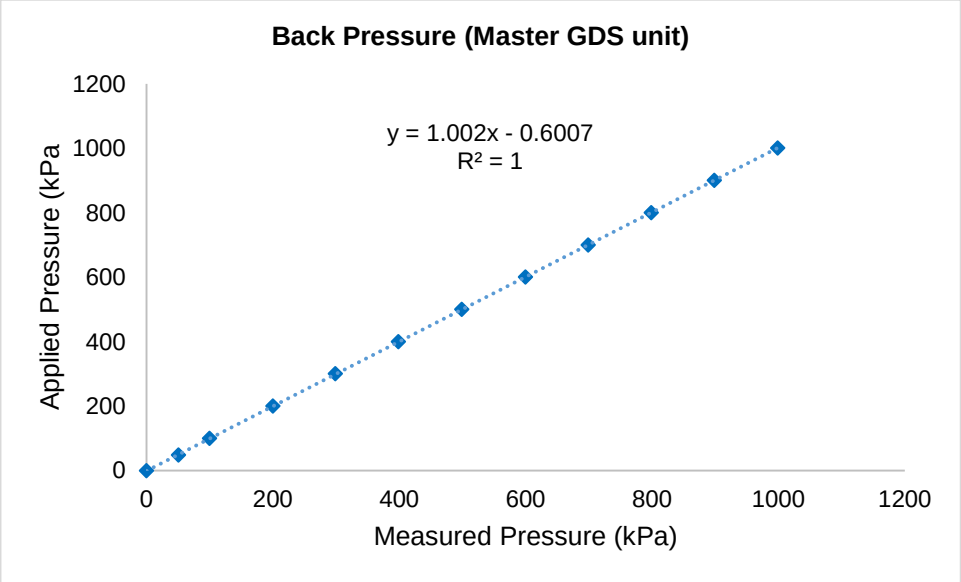

Figure 4.21 pressure/volume controller calibrated against gauge indicator

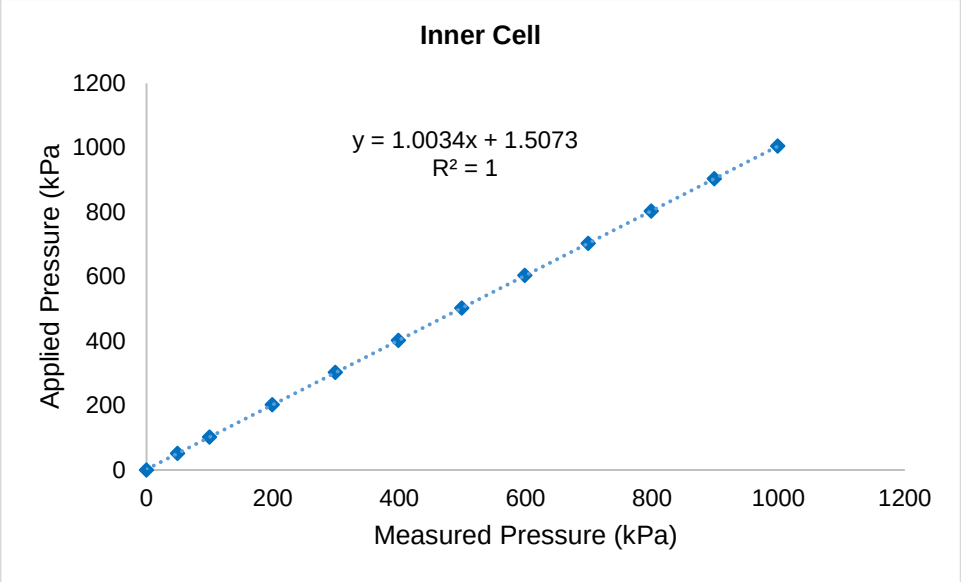

Figure 4.22 Inner pressure/volume controller calibrated against the master pressure/volume controller

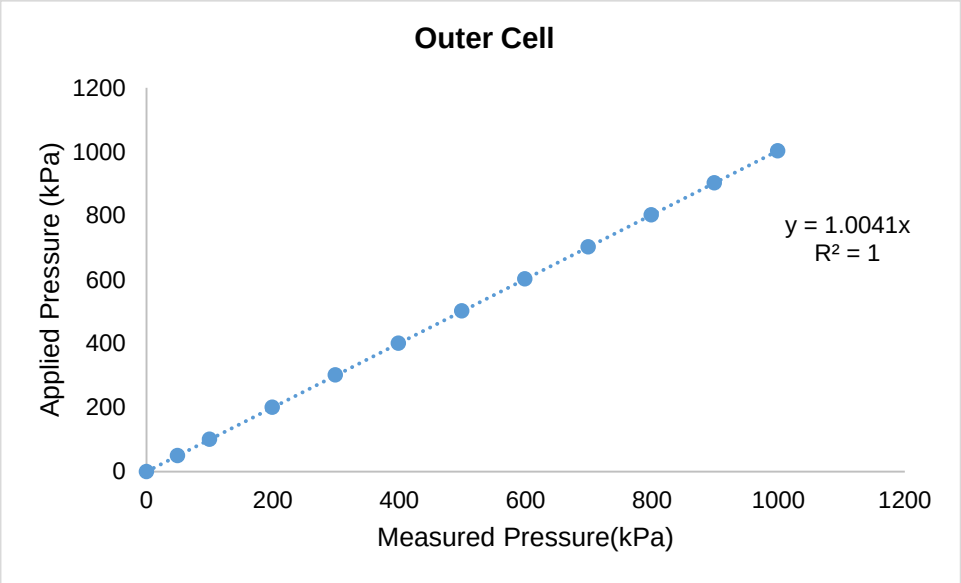

Figure 4.23 Outer pressure/volume controller calibrated against the master pressure/volume controller

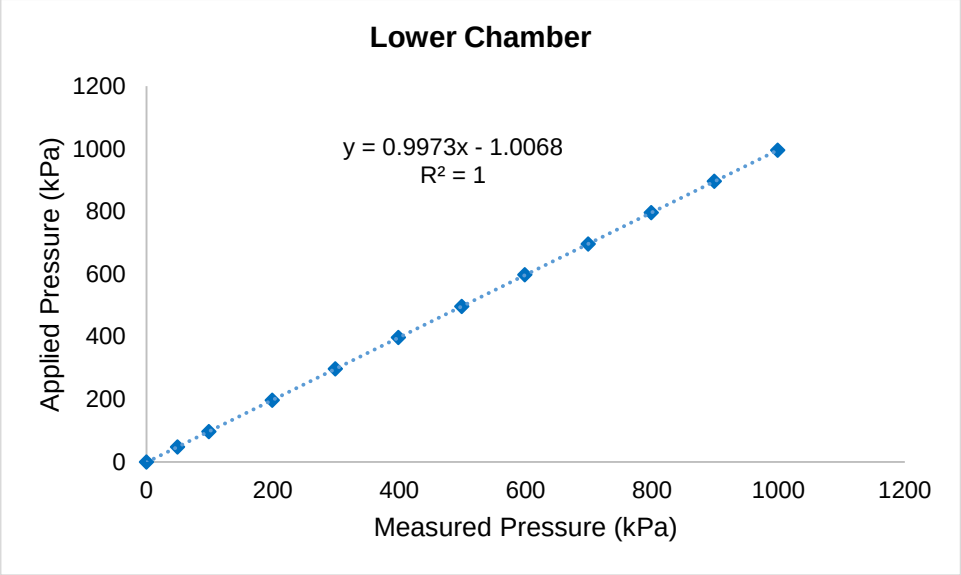

Figure 4.24 Lower chamber pressure/volume controller calibrated against the pressure/volume controller master

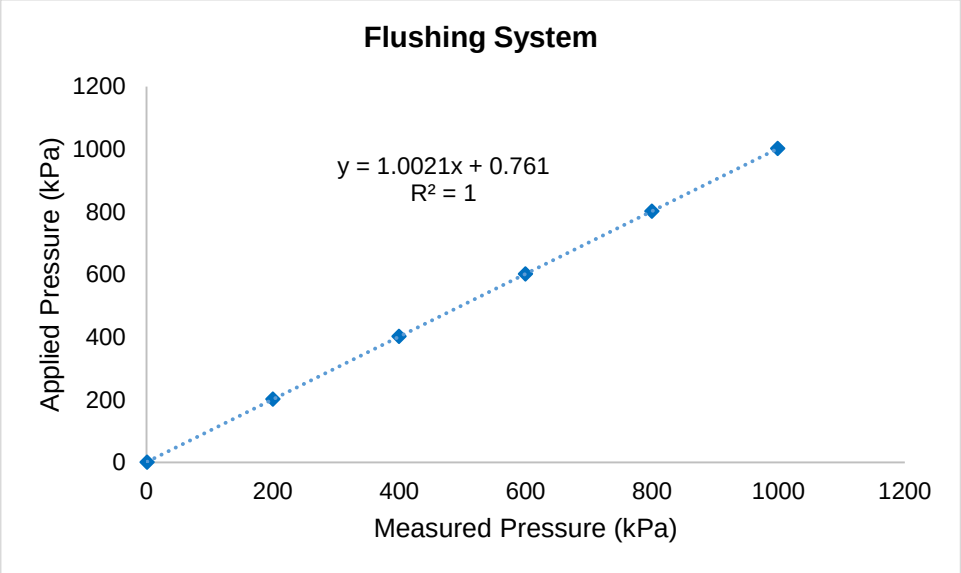

Figure 4.25 flushing device pressure/volume controller calibrated against the master pressure/volume controller

Table 4.6 calibration volume of pressure/volume controllers

GDS controller No	Time (min)	GDS Volume (cm3)	Water collected (g)
GDS controller of the back pressure	5	150.36	149.57
GDS controller of the Inner cell	5	150.768	149.27
GDS controller of the Outer cell	5	150.352	149.46
GDS controller of the Lower chamber	5	150.632	150.642
GDS controller of the flushing system	5	150.43	149.87

4.5.4 Calibration of Pressure Transducer indicator for diffused air flushing device

The pressure transducer indicator E308 shown in Figure (3.8) and Figure (3.9) in chapter (3) section (3.4.3) of the flushing apparatus was calibrated, the procedure was as a follows:

1. The valve controlling flow of water was closed in the base of diffused air flushing device.
2. The differential pressure transducer was connected with transducer indicator E308 and connected to the power.
3. The top cap was opened of the diffused air flushing device and the water was added gradually. For each amount of water added, the pressure transducer indicator was adjusted to read the level of the water in the reservoir.
4. The procedure was continued until the water reservoir was full.

5. The same procedure was repeated as discharge the water from reservoir of diffused air. flushing device. The procedure was repeated five time as shown in (Figures 4.26 and 3.27).

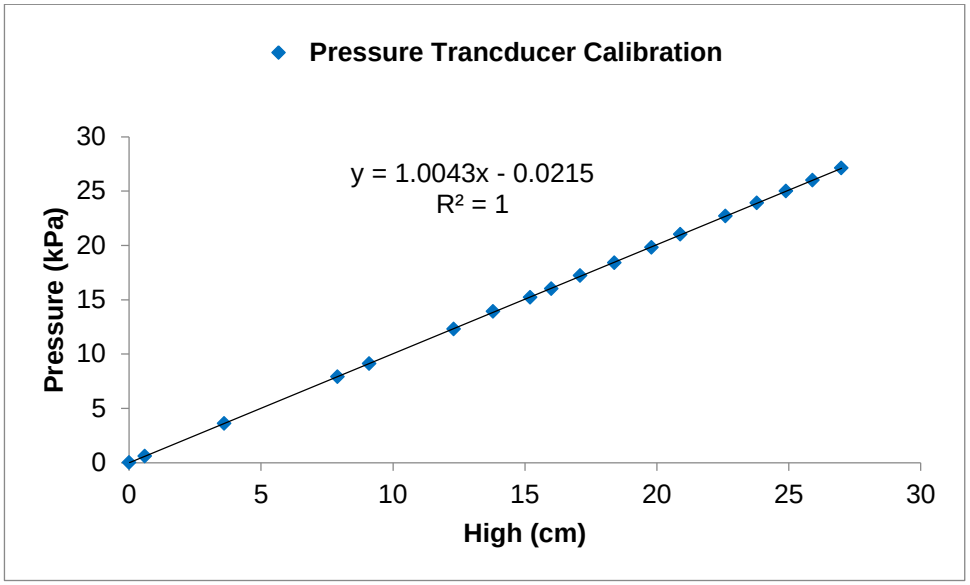

Figure 4.26 The transducer indicator E308 for diffused air flushing device

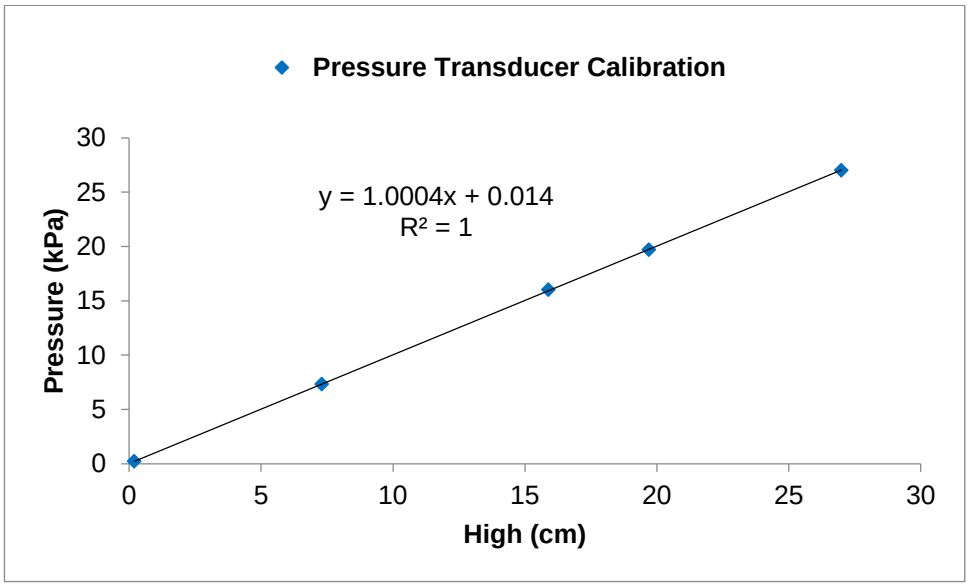

Figure 4.27 The correction of pressure transducer calibration indicator E308

4.6 Calibration of standard triaxial device

Calibration is very significant for obtaining good value experimental results. The calibration of equipment is aimed at eliminating numerous effects of errors, which can take place in laboratory measurement and analysis. Re-calibration of instruments is essential for the triaxial test. Re-calibration of the triaxial apparatus was carried out before the start of the tests, and the result of the loading is shown in Figure (4.28). Furthermore, re-calibration of cell body and transducers was also done.

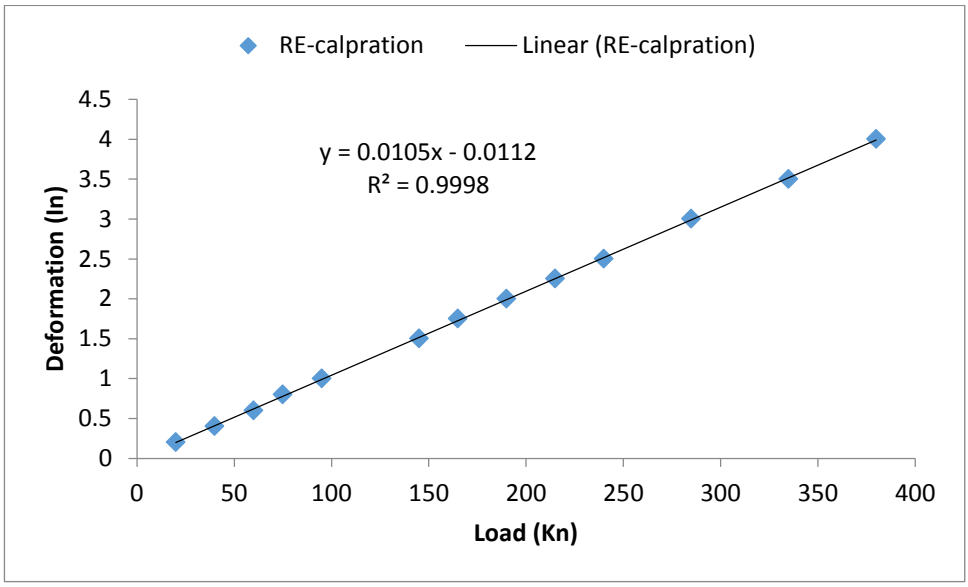

Figure 4.28 calibration of loading ram of triaxial apparatus

4.6.1 Cell calibration

This method for calibration of cell was performed as shown in (Figure 4.29 and Figure 4.30). Initially, the cell was filled with water, connected with volume/pressure controller, pressures (ranging from 100 kPa to 1000 kPa) and was applied over a period of time until there was no net change in the volume. Then once the maximum pressure was reached a gradual decrease in the

pressure occurred (1000 kPa – 100 kPa). Then, the average of the net volume can be calculated by changing in volume (mm^3) over pressure, subtracting the initial volume of the sample after applying different pressure.

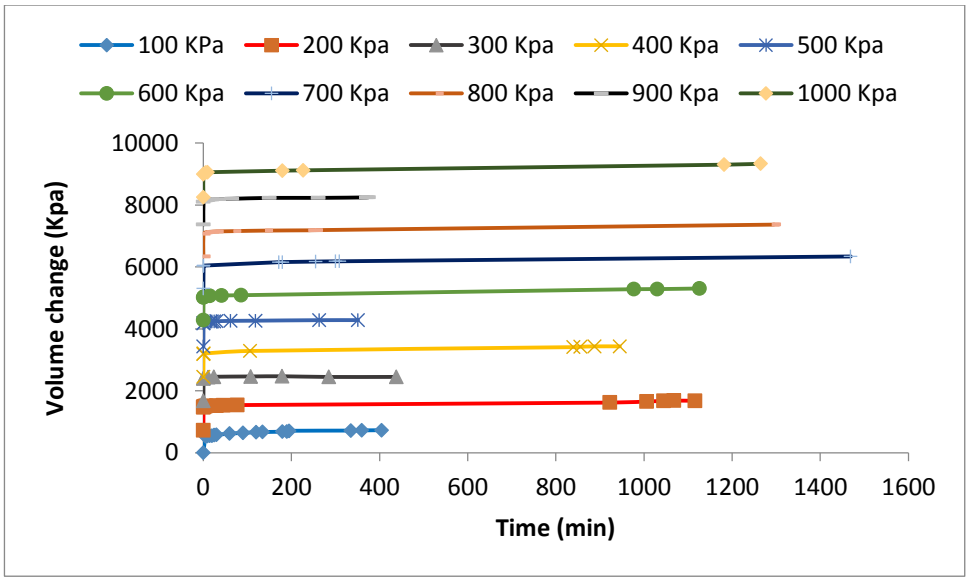

Figure 4.29 Calibration of cell of triaxial apparatus

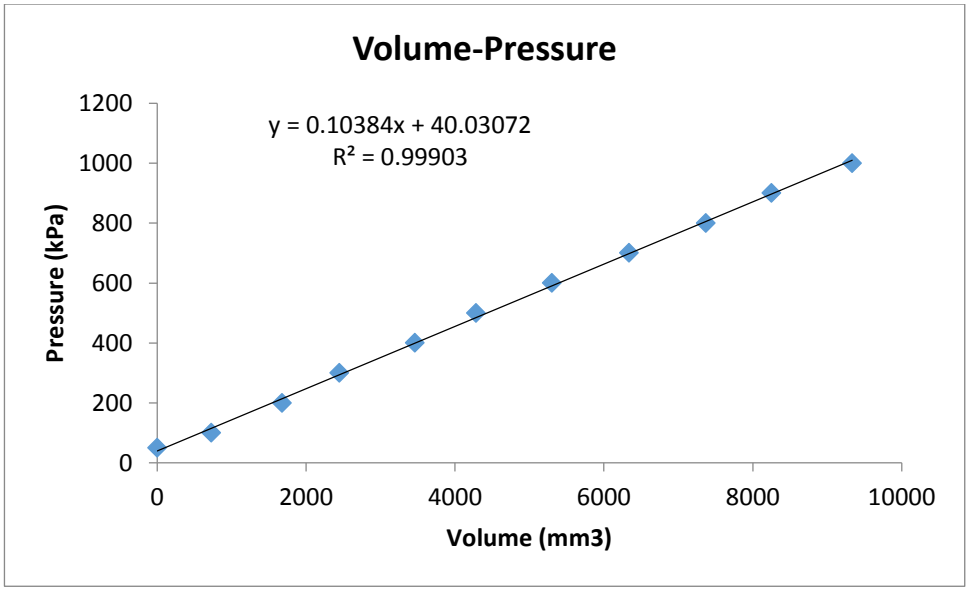

Figure 4.30 Calibration of cell of triaxial apparatus

CHAPTER 5 EXPERIMENTAL RESULTS AND DISCUSSION

Summary

In this chapter the results presented and discussion of influence of waste carpet fibre on the behaviour of unsaturated shear strength parameters, cohesion and volume change. In addition, the results of soil-water characteristic curves of clay-fibre reinforced are also addressed in this chapter.

5.1 Introduction

This chapter presents a summary of the laboratory results attained from

a. Standard consolidated undrained (CU) triaxial compression tests,
b. Soil-water characteristic curves and, and
c. Unsaturated triaxial test as (CU).

The unsaturated triaxial tests are presented per stages, starting with equalisation, consolidation and shearing. In each stage the volume changes and stress-strain behaviour under different percentage of fibre, and different degree of saturation were presented and discussed. The total numbers of tests under standard triaxial test includes 9, and 16 unsaturated triaxial tests. A more detailed discussion will be given in this chapter. A discussion is made on the stress-strain behaviour, excess pore-water pressure generation and stress path of the non-reinforced and fibre reinforced soil specimens. In order to study the unsaturated soil behaviour in different suction and fibre content, the initial conditions of specimen's properties such as water content, dry density etc, should be same for all specimens. In this research, to keep the initial condition of all specimens the same. However, some unavoidable differences were found,

such as the degree of saturation, which had been affected by fibre content and value of suction.

5.2 Standard triaxial test (CU)

The static compaction method was made to prepare the triaxial soil specimens using the method explained in chapter 4 (section 4.2). The specimens were prepared at 13 % of water content and density of 1.84 g/cm^3. After conducting three experiments, each experiment was conducted on three samples, and each test was consolidated under different pressure as 100 kPa, 200 kPa and 300 kPa, each lasting for a period of 5-7 days it was then possible to fully saturate the specimens. Upon starting the standard triaxial test, some problems were encountered with saturating the specimens. A plan was discussed and agreed which included the use of volume/pressure controller to apply constant pressure and to determine the volume of water that is required to fully saturate the samples.

A preliminary investigation was carried out with specimens under different pressures in order to fully saturate them. It was found that a pressure of 600 kPa or more is required to ensure that clay specimens reach the point of full saturation. The pore water pressure measured during the consolidation stage as consolidated undrain (CU). Three CU triaxial compression tests were carried out on ‘remoulded’ samples of clay in order to determine the undrained shear strength. Pore pressures are measured during these tests. Normally, the CU triaxial compression test was performed over several stages, involving the successive saturation, consolidation and shearing of each of three specimens. Saturation is carried out in order to ensure that the pore void in the specimen does not contain free air. Saturation is performed by leaving the specimens to

saturate against an elevated back pressure Table (5.1) shows that the pressure steps against the B-value, and in this test, both cell pressure and back pressure are normally increased in increments of about 50 kPa, until the required degree of saturation is achieved, which is more than 97 %, (see Table (5.2, 5.3 and 5.4).

5.2.1 Saturation stage

Nine specimens with a 38 mm diameter test, which normally have a length of 76 mm, are extruded from the mould and sealed using a rubber membrane, 'O' rings and top and bottom caps. The test specimens have void ratio (e_0) of 0.455, porosity (n_0) of 0.313, and the initial degree of saturation, when prepared was (S_r) 76.44 %. Once a specimen is placed inside the triaxial cell, the cell pressure was increased to a predetermined value. Once the B-value reached 97 % or more than the specimens is fully saturated. The saturation procedure with determined of B-value described in Chapter 3 (Section 3.9.2.1). The degrees of saturation, for the nine samples reached 97% after one week. Table (5.1) shows the B-value at different pressures, which indicated that the specimens are partly saturated, and (Tables 5.2, 5.3 and 5.4) show the achieved B-value with required pressure, were the samples fully saturated. The procedure based on recommendation of EN 1997, Eurocode 7 (2007), which recommends that the value of degree of saturation should be greater than or equal to 90 %, and must be achieved before the consolidation stage is started.

Table 5.1 calculation of B-value during saturation the specimens (test 1a)

Getting B-value			
Test 1			
Effective stress	**Cell pressure**	**Back pressure**	**B-value**
100	401.85	372.14	87.98
200	451.54	424.35	92.24
300	551.05	526.9	94.93

Table 5.2 calculation of B-value at the end of saturation the specimens (test 1b)

Getting B-value			
Test 1			
Effective stress	**Cell pressure**	**Back pressure**	**B-value**
100	654	629	97.32
200	604	579	97.21
300	654	630	98.14

Table 5.3 calculation of B-value at the end of saturation the specimens (test 2)

Getting B-value			
Test 2			
Effective stress	**Cell pressure**	**Back pressure**	**B-value**
100	654	629	97.32
200	604	579	97.21
300	654	630	98.14

Table 5.4 calculation of B-value at the end of saturation the specimens (test 3)

Getting B-value			
Test 3			
Effective stress	**Cell pressure**	**Back pressure**	**B-value**
100	654	629	97.32

200	604	579	97.21
300	654	630	98.14

5.2.2 Consolidation stage

Three effective confining pressures of 100 kPa, 200 kPa and 300 kPa were applied to consolidate the specimens. Consolidation was carried out under different pressures in each test, e.g. Test one has 3 samples that sample 1 consolidated under 100 kPa, sample 2 consolidated under 200 kPa and sample three was consolidated under 300 kPa, as well as test 2 and test 3. As is known, there are two reasons to carried out the consolidation stage of an effective stress triaxial test. First, in order to give samples different strengths, which will produce widely spaced effective stress Mohr-circles, three samples were tested and consolidated at three different effective pressures. Secondly, the results of consolidation were used to determine the minimum time to failure in the shear stage.

The coefficient of consolidation of the clay was determined by plotting the volume change as a function of the square root of time. Figure (5.1) explains the theoretical of considerations, and indicates that the first 50 % of volume loss during consolidation showed a straight line on this plot. This straight line is extended down to the horizontal line representing 100% consolidation, and obtain the time intercept at this point (termed 't_{100}' by Bishop and Henkel). Figure (5.2), 5.3 and 5.4) holds the details of calculation for coefficient of consolidation.

Figures (5.2, 5.3 and 5.4) show that, the consolidation was carried out under different confining pressure at, 100, 200 and 300 kPa. When the experiments were consolidated under 100 kPa, the consolidation stage required a short

period of time for it to be completed with a total volume change of 95 % was achieved. However, the time was longer when other confining pressures were applied. Figures (5.2, 5.3 and 5.4) show that, the volume change of the specimens is no longer significant, and at least 95 % of the excess pore pressure has dissipated. The rate of strain can be calculated to shear the specimens of cohesive clay; the details of the calculation were covered in chapter 3 section (3.9.2.3).

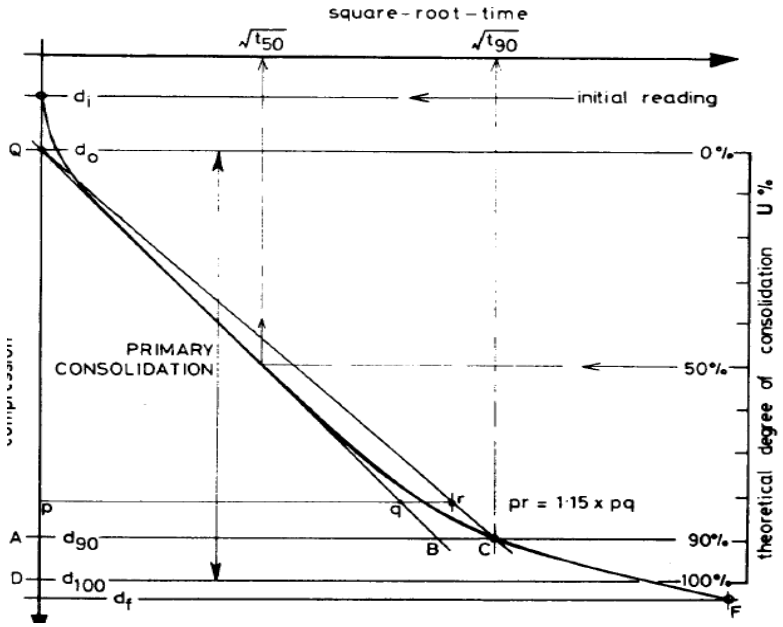

Figure 5.1 analysis of square-root time settlement curve (Head 1994)

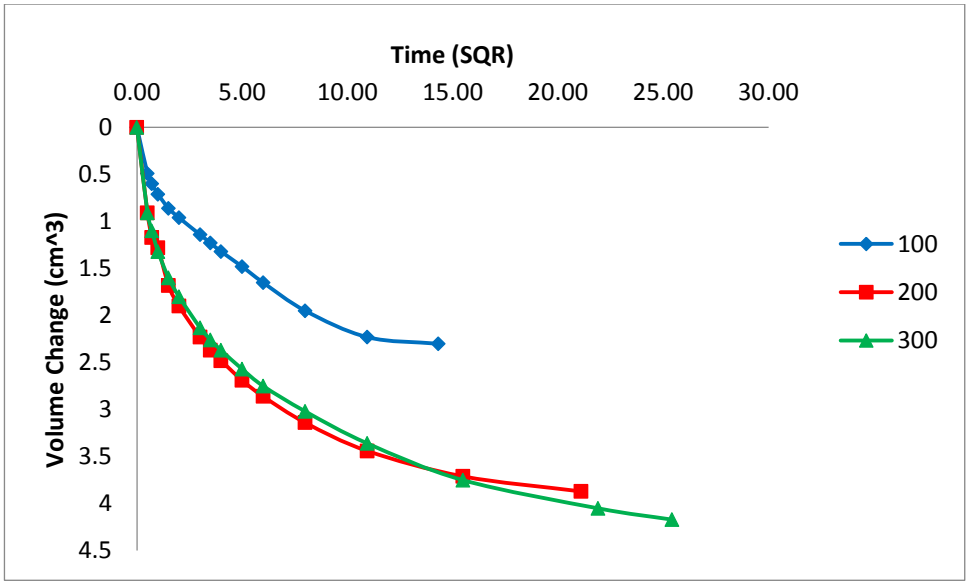

Figure 5.2 volume change curve (test 1)

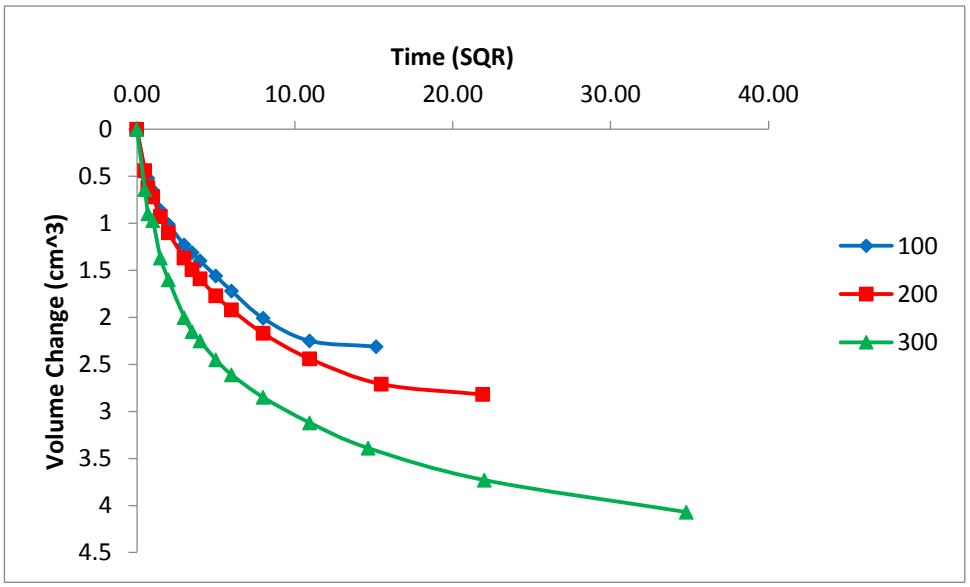

Figure 5.3 volume change curve (test 2)

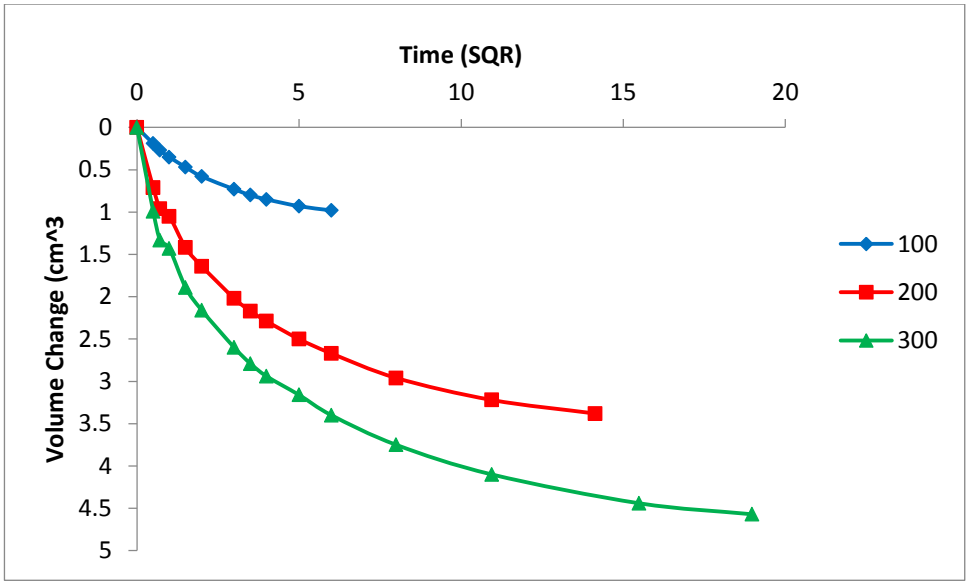

Figure 5.4 volume change curve (test 3)

5.2.3 Shear stage

Shear test was undertaken according to the results of consolidation stage. The calculate procedure for a suitable strain rate to shear a samples were described in chapter 3 section (3.9.2.3). The specimen brought to failure by increasing the vertical stress. During this period, regular readings of the ram load and specimen height decrease are taken, and the effective confining pressures of 100, 200 and 300 kN/m^2 are used. As has been noted, the rate of strain used during the test has been 2 %/mm. This rate is based on the specifications specified in the BS EU 1997-(2:2007) for the maximum strain (20 %). As expected, Figure (5.5) shows an increase in pore water pressure of the soil is observed upon load application. In addition, the results of pore water pressure on samples of test 1, and 3 are consistent. During the shearing stage, the vertical stress is increased, and measurements are taken at regular intervals of deformation of the ram load and pore water pressure. These are converted to graphs of principal stress difference (σ_1 - σ_3) and pore pressure as a function of

strain. After plotting these, their maximum value is used to produce the failure envelope detailed in Figure (5.5).

The results of triaxial compression tests are presented using graphs of deviator stress and excess pore-water pressure against axial strain. Furthermore, to understand the behaviour, stress paths for all specimens are analysed. Figure 5.5 shows the pore-water pressure during the shear stage of consolidated undrained (CU) triaxial tests that were measured from the top of specimens using a fitting pressure sensor, whereas the bottom sensor was used to measure the applied pore water pressure. It can be observed that the soil specimens reached a peak excess pore-water pressure at small strains, and excess pore-water pressure was reduced.

Figures (5.6, 5.7 and 5.8) shows the development of deviator stresses against axial strain at consolidation stresses of 100 kPa, 200 kPa and 300 kPa. In the same graph, soil specimens showed strain behaviour show the failure in 0.02 %, at consolidation stresses of 200 kPa and 300 kPa. However, test of 100 kPa of effective stress shows that the post failure behaviour. Therefore, because of the plastic case, and in this matter once the yield occurs, the stress requirements need to be frequently increased in order to drive the plastic deformation.

Stress path parameters are defined as p' and q, were effective stress and deviator stress respectively. Stress path curve drawn through a series on a plot of stresses, the change that happened in state of the soil specimen under loading or unloading stresses is known as stress path, and stress path parameters are defined as:

$$p' = \frac{\sigma_1' + 2\sigma_3'}{3} \qquad 5.1$$

$$q' = (\sigma_1' - \sigma_3') \qquad 5.2$$

where

σ_1' is major effective principal stress, σ_3' is minor effective principal stress. The stress path was analysed in this study using equation (5.1) and equation (5.2) for all the consolidated undrained triaxial tests that were carried out. Figures (5.9, 5.10 and 5.11) show the stress path diagrams of fully saturated soil specimens. It can be seen that at the different consolidation stress, resulted in an increase in the stress path points. An increase in the slope of stress path of the specimen with increase consolidation stress indicated a combined effect of increase in deviator stress.

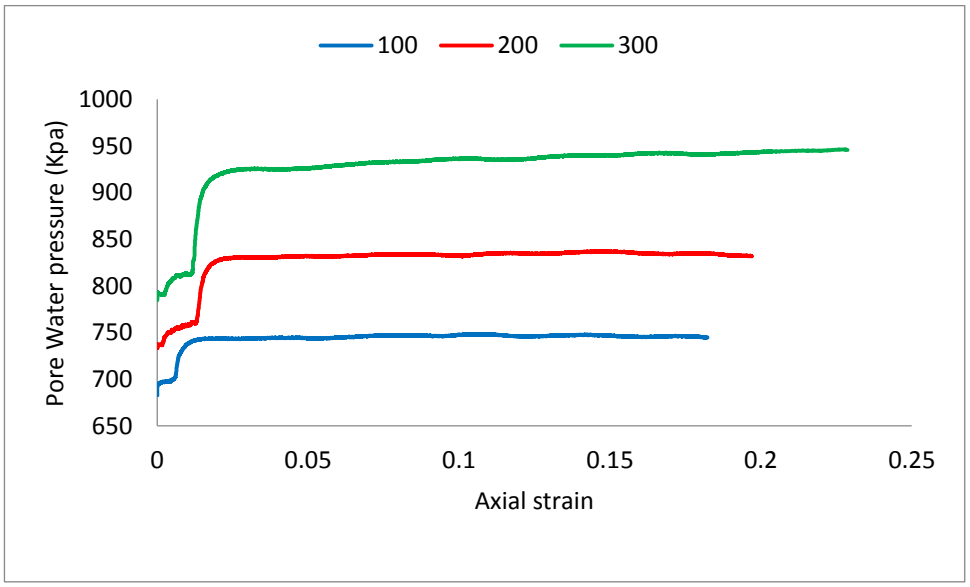

Figure 5.5 pore water pressure

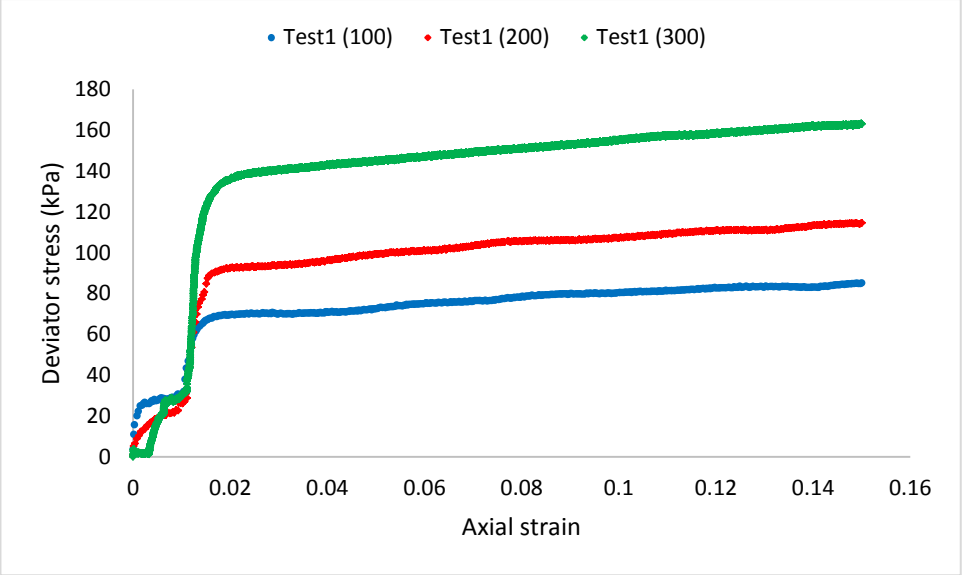

Figure 5.6 stress strain curve (test 1)

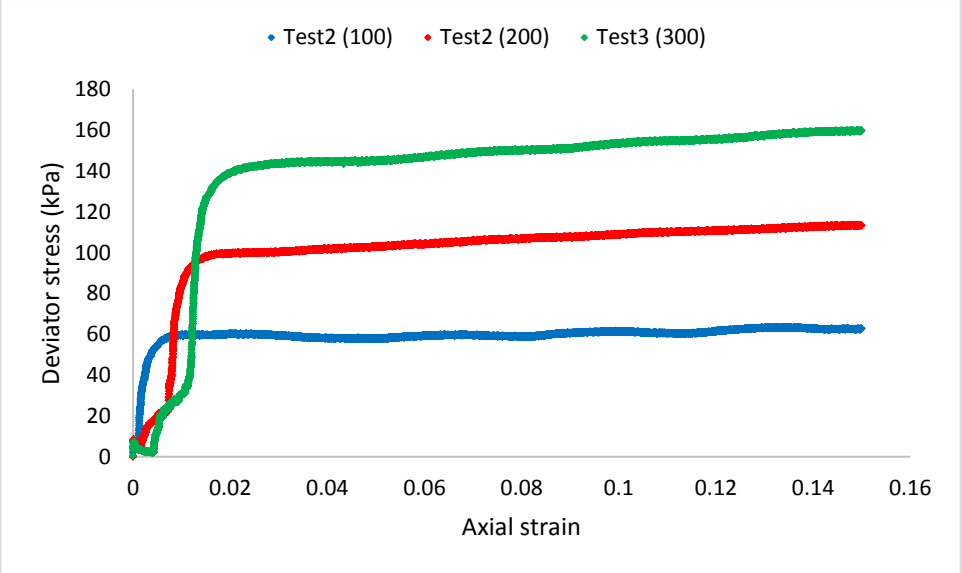

Figure 5.7 stress strain curve (test 2)

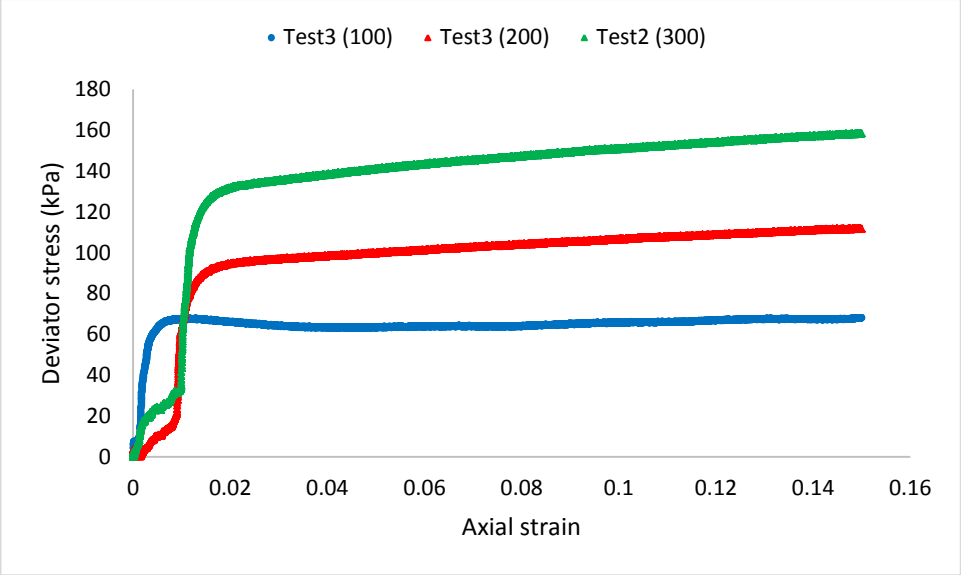

Figure 5.8 stress strain curve (test 3)

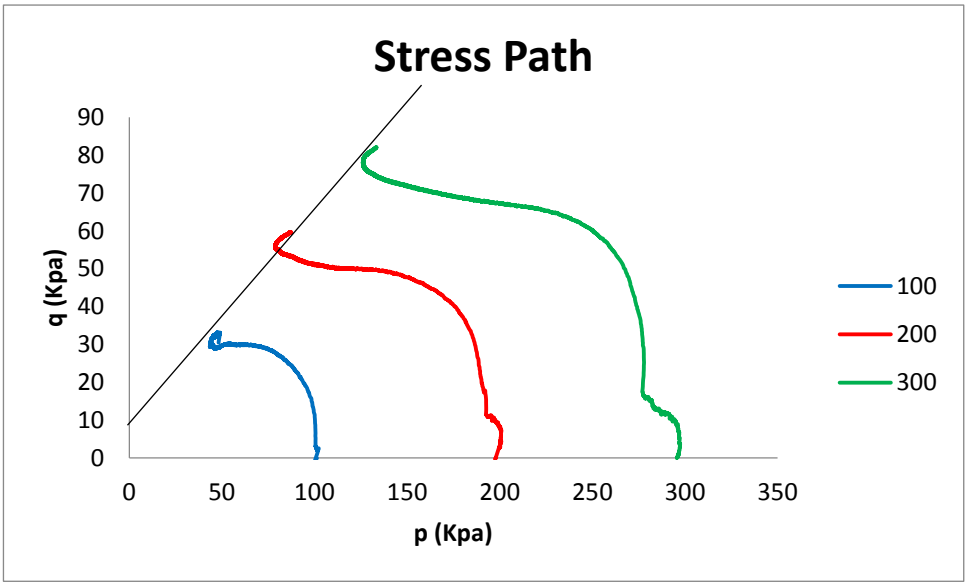

Figure 5.9 stress strain curve (test 1)

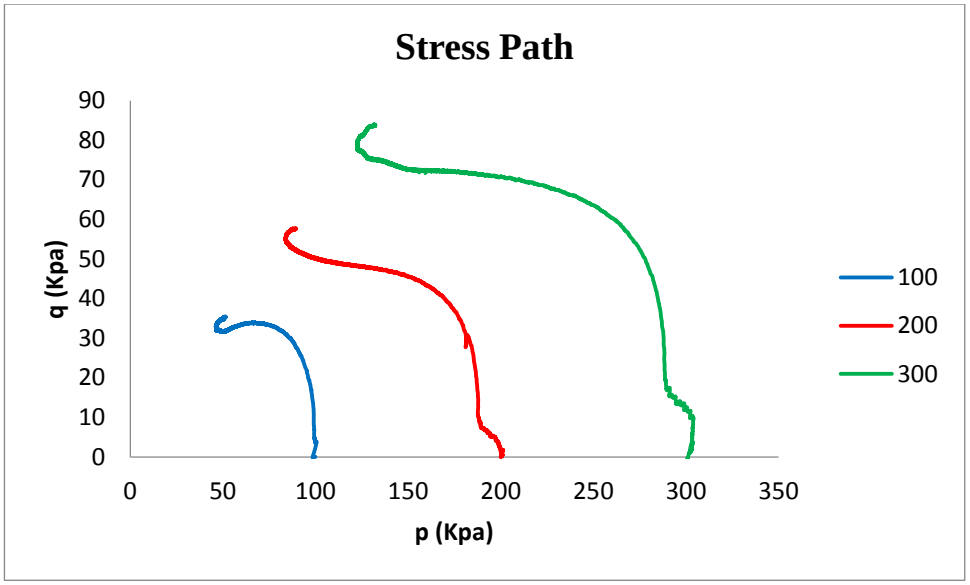

Figure 5.10 stress strain curve (test 2)

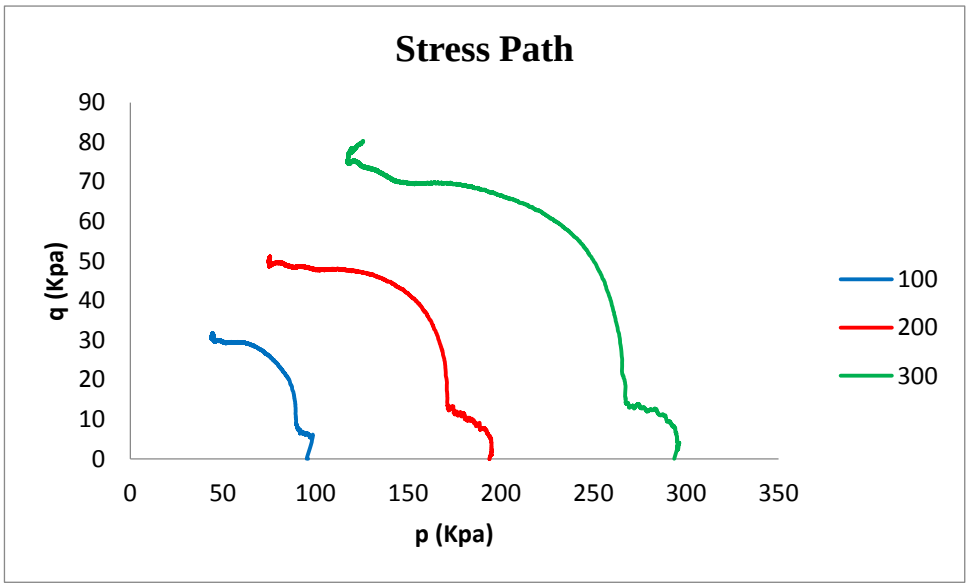

Figure 5.11 stress path curve (test 3)

Figure (5.12, 5.13 and 5.14) show the shear strength parameters including c' and $\emptyset'$, cohesion and effective internal friction angle, respectively. All Mohr circles were drawn based on the effective principal stresses at 15 % axial strain. 15 % is assumed to be the failure strain for plastic soils with strain hardening behaviour based on standard for triaxial or UCS test. Table (5.5) provides a summary of the three tests shear strength parameters.

Table 5.5 Shear strength parameters

Tests No	Cohesion (kPa) c'	friction angle (degree) $\emptyset'$
1	6.9	29.05
2	4.1	30.63
3	4.7	30.43

Comparing the three tests, it indicates that the three tests results have the same value c' and $\emptyset'$ with and slight difference in cohesion. This may be due to the equipment that was used. The same results were obtained from these tests, because the soil sample was compacted and mixed by the same parameters, with water content at 13 % and dry density of 1.84 g/cm^3.

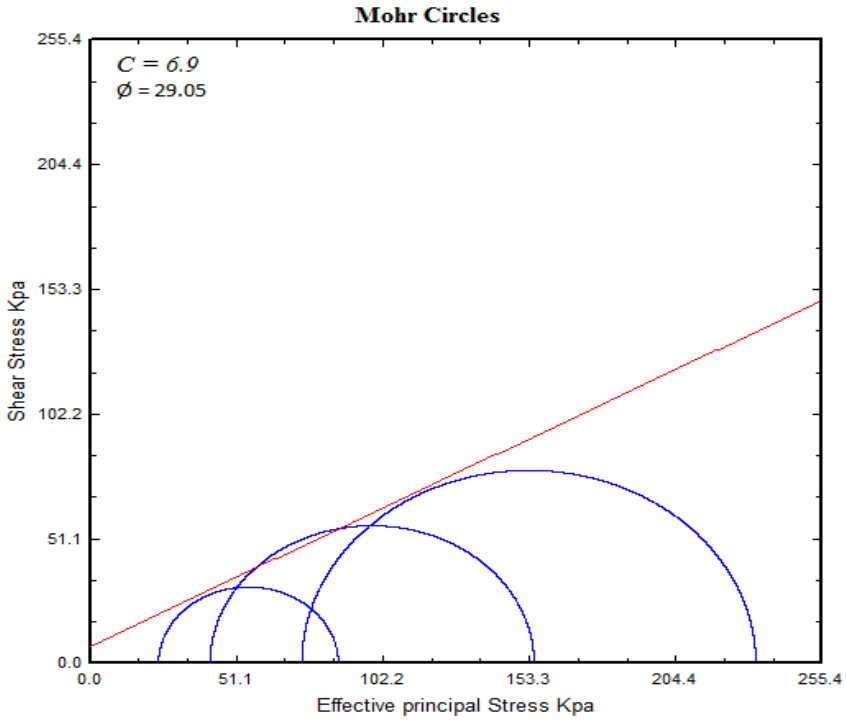

Figure 5.12 Mohr circles at failure for a CU triaxial compression test (1)

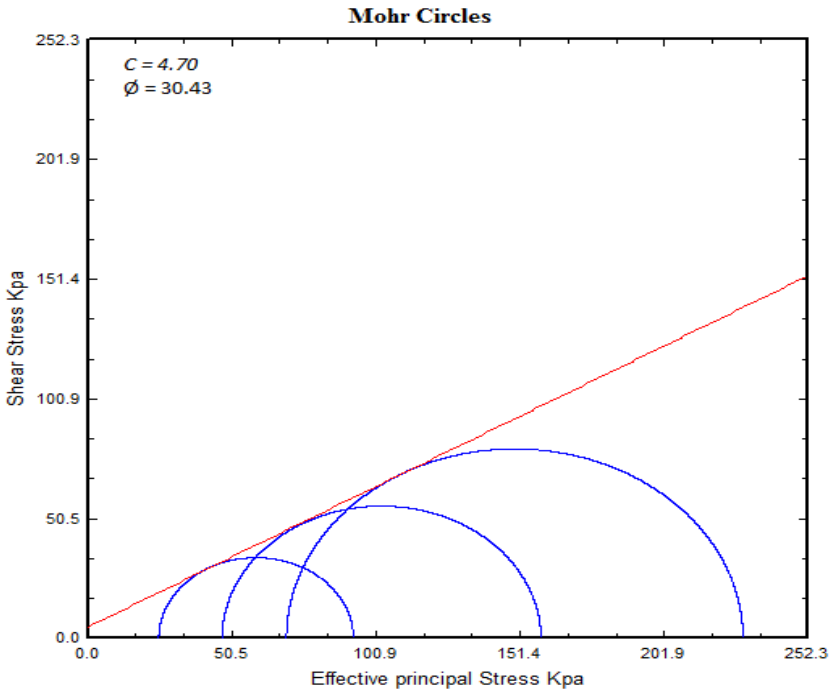

Figure 5.13 Mohr circles at failure for a CU triaxial compression test (2)

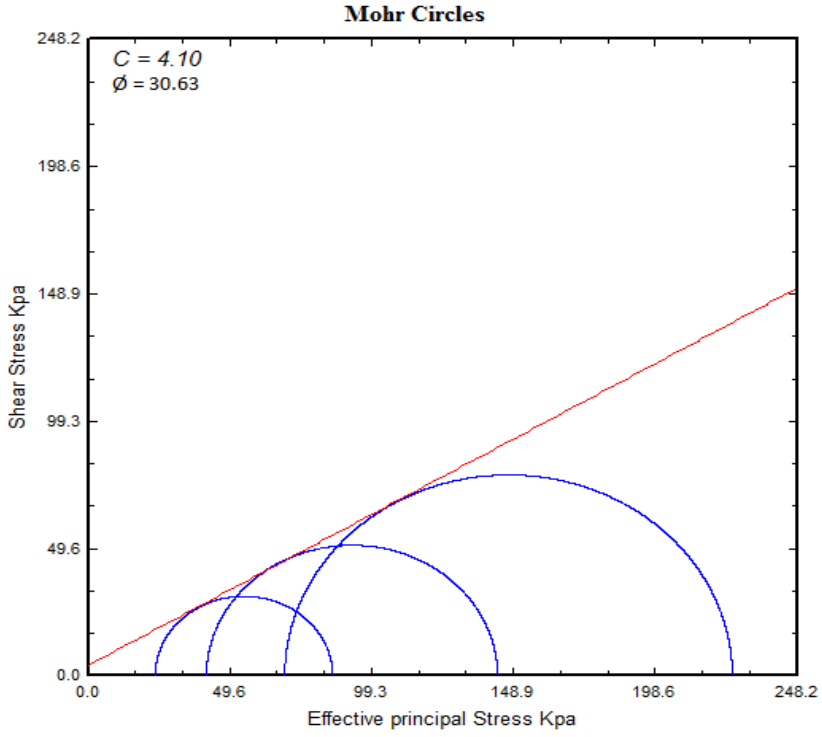

Figure 5.14 Mohr circles at failure for a CU triaxial compression test (3)

5.3 Soil-water characteristic curve (SWCC)

The results of SWCCs were attained by performing a number of cycles of drying and wetting paths, and are presented in this section. All specimens were prepared at water content of 13 % and dry density of 1.78g/m^3. The SWCC could be presented as a function of water content W_C, or degree of saturation S_r. In addition, the results presented in terms of degree of saturation and matric suction. Figure (5.15) is for experiments performed using unsaturated triaxial apparatus at 0 % of fibre. The test specimen was allowed to dry or wet at different suctions, from 0 kPa to 350 kPa, where the maximum pressure existed in the laboratory. Along the first wetting path an increase in water volume was observed in the specimen. When suctions were higher than 100 kPa, soil-water characteristics curve in clayey soil appeared not to be influenced by the mean net stress $(\sigma_3 - u_a)$. However, at suctions of less than 100 kPa, the absorption rate decreased when the mean net increased. This should be attributed to smaller void ratio in a specimen subjected to water flow paths. At the low suction head, the degree of saturation increased further as a specimen was subjected to a higher net mean stress. The volume water change in high suction was controlled by, similar observed in the wetting path. The change of degree of saturation in the soil-water characteristics is related to the change in total volume and water volume. At the end of wetting, the degree of saturation was higher than that when the sample was prepared. The high point of degree of saturation were observed 96.6 %, and the air-entry value was 16.80 kPa, and the fitting parameters a, s, m, and n, were explained in (chapter 2, section 2.6.5) for test under 0 %, are 10.8, 0.0065, 0.0976 and 4.464, respectively. The wetting and drying of soil, with high air entry value of ceramic disc was complex, and took a long time. Then, it was suggested to wet and dry the samples

(SWCCs) outside the triaxial apparatus, using the pre-equalisation procedure proposed by (Sandra 2008), explained in chapter 3 (section 3.8).

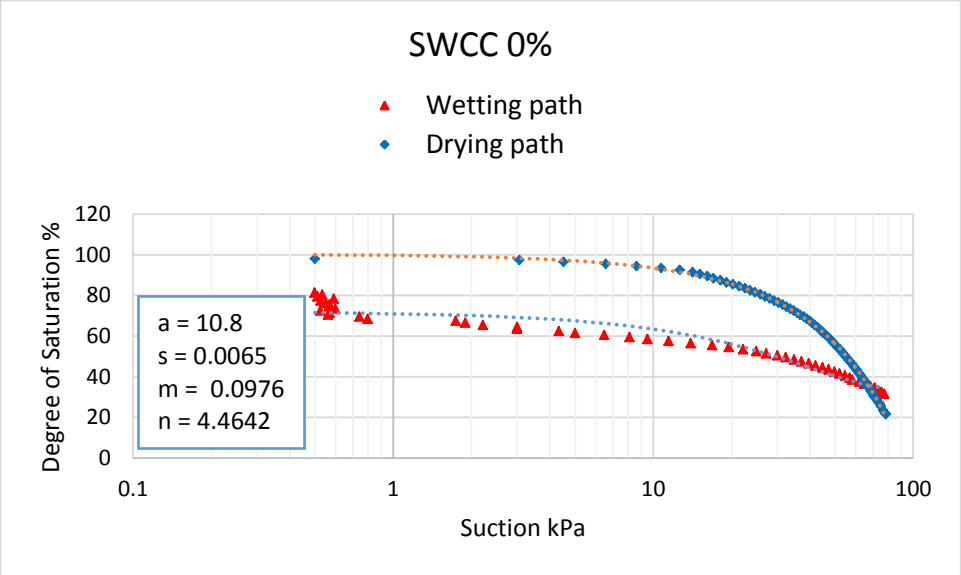

Figure 5.15 Soil-water characteristic curves for 0 % of fibre using triaxial device.

Figure (5.16) illustrates the results of soil-water characteristics curves, which were done by pre-equalisation method, as explained in (chapter 3 section 3.8.). In this study, the equilibrium was developed and done in the triaxial apparatus. All the cycle results of SWCCs were fitted using Fredlund and Xing (1994) equation [2.14] in (chapter 2 section 2.6.5). The fitting parameters of cycle drying (SWCC) of the soil samples, as well as the fitting parameters of wetting cycle are also presented. As a result, the air entry value (AEV) of specimens were mixed with different percentage of fibre 0 %, 1 %, 3 % and 5%, are 17.10 kPa, 18.30 kPa, 18.10 kPa and 18.30 kPa respectively. The fitting parameters $a,\ s,\ m,$ and $n,$ for test under 0 % of fibre 10.7, 0.0066, 0.0692 and 5.0893 respectively. Figures 5.17, 5.18 and 5.19 illustrate the results of 1 %, 3 % and 5 % of fibre under the pre-equalisation method. The fitting parameters are shown in the same figures. It was clear the fibre content reduced the hysteresis.

Comparing the results of 0 % of fibre for test was done in the triaxial apparatus with the other which has been done by pre-equalisation. The results shown in Figures (5.15 and 5.16), reveal there was a slight difference in some parameters as n 4.46 by used triaxial device and 5.08 by used pre-equalisation method. The difference was due to the equipment. However, most of the other parameters were almost the same.

5.3.1 Advantage and disadvantage of pre-equalisation method

There are some advantages of using the pre-equalisation method, such as:

a. Reduced the time from months and even weeks to days,
b. Knowing the degree of saturation of specimen was easier than calculating B-value, as well as the water content.
c. It was very hard to deal with a specimen in the wetting path, epically when the sample placed in the triaxial apparatus that can effective in the volume change, which leads to change the degree of saturation.

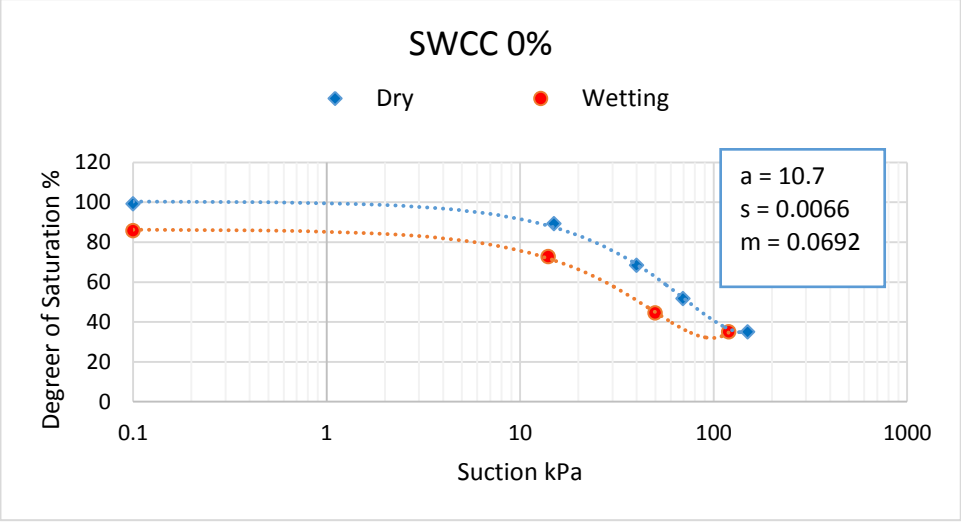

Figure 5.16 Soil-water characteristic curves for 0 % of fibre using pre-equalisation technique (Sandra, 2008)

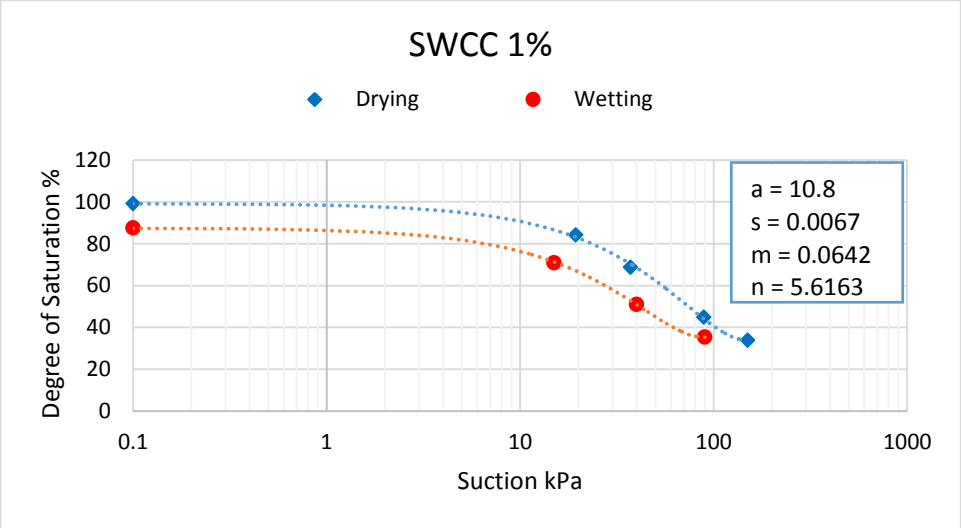

Figure 5.17 Soil-water characteristic curves for 1 % of fibre using pre-equalisation technique (Sandra, 2008)

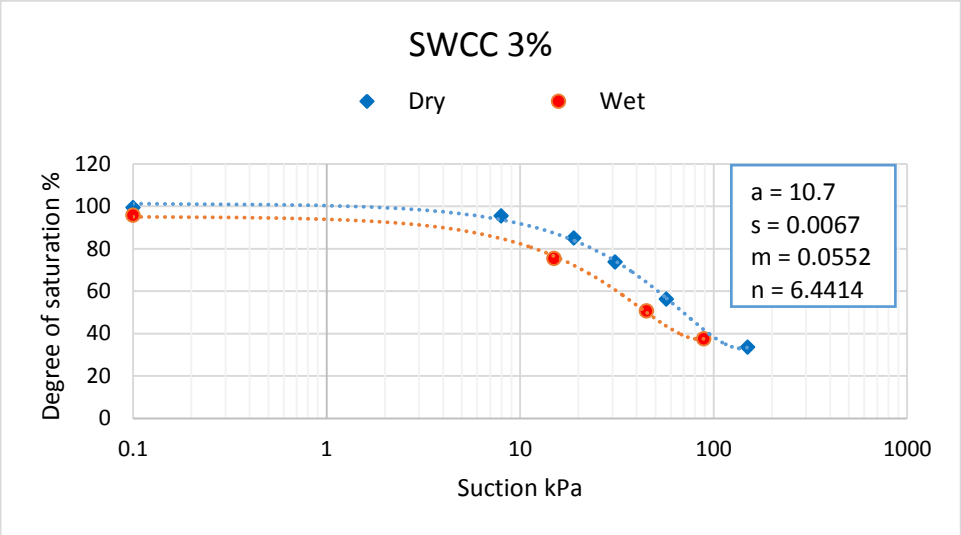

Figure 5.18 Soil-water characteristic curves for 3 % of fibre using pre-equalisation technique (Sandra, 2008)

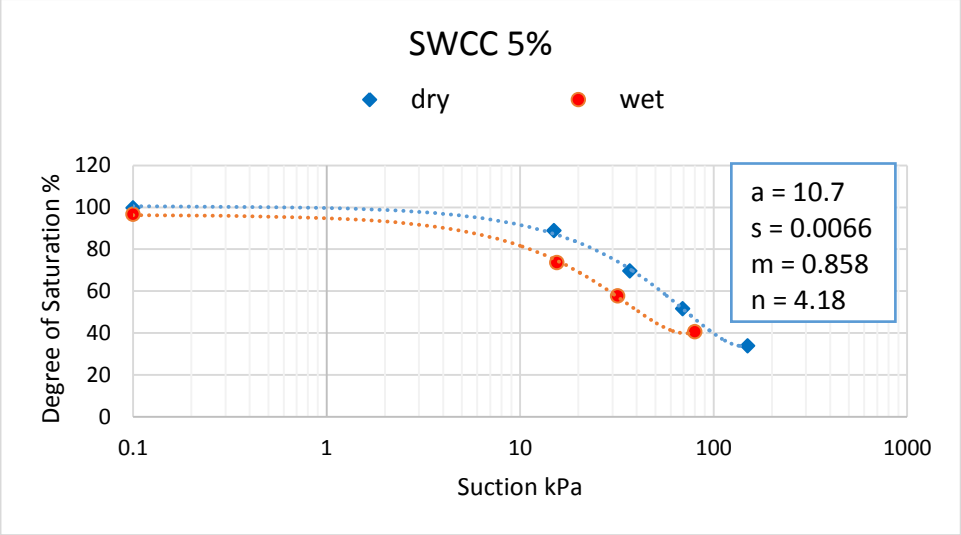

Figure 5.19 Soil-water characteristic curves for 5 % of fibre using pre-equalisation technique (Sandra, 2008)

5.3.2 Effective of fibre on SWCC and hysteresis

As illustrated in the figures presented in chapter 2 of SWCCs tests, it was clear that, the fibre decreased the hysteresis, compared between Figure (5.16) and Figure (5.19). The parameters in hysteresis has been effective such as, the volume of voids is effective on the shape of voids. The pores, neck and the direction of water flow either getting in or out of the pros which acted in the volume, as well as the contact angle. Adding fibre in the soil sample, the shape of voids could be changed. In the other hand the permeability increases because of the addition fibres, so the water can flow more easily. The contact angle of cohesion soil normally high with cohesion soil, it could be less with

adding fibre in soils. Comparing the difference of reduction between 0 % of fibre with 1 %, 3 % and 5 %, in the hysteresis were found 25 %, 62.5 and 81.25 % respectively. Figure (5.20) shows the optical image of soil clay mixture.

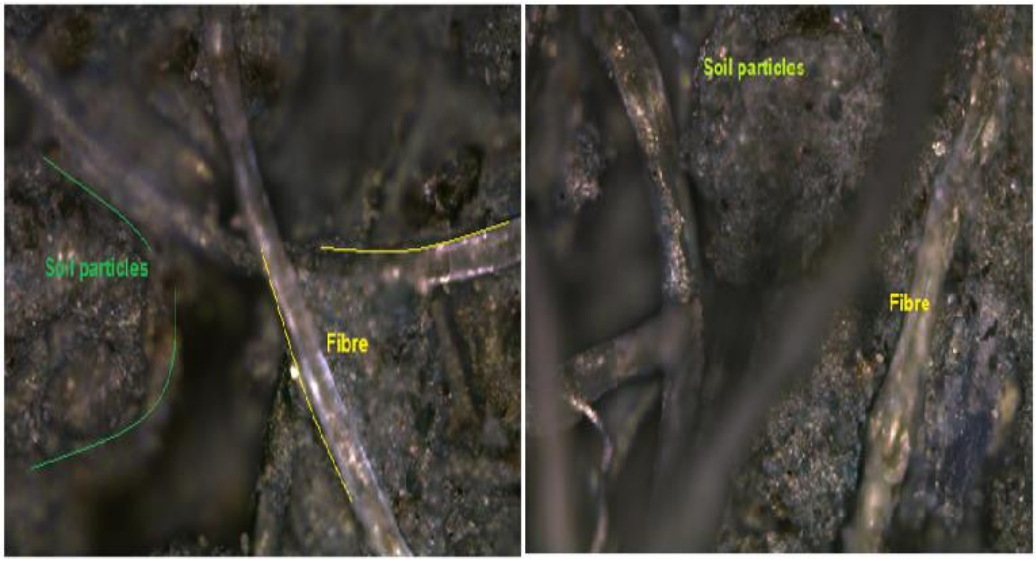

Figure 5.20 microscopic image of clay fibre

5.3.3 Air Entry Value of soil (AEV)

The air entry value of soil is a function of the size of the largest opening between a set of particles. Fredlund et al., (2012). By using the capillary model, the AEV can be estimated. The AEV was calculated as:

$$r = \frac{R}{\cos 45} - R \qquad 5.3$$

where

r= radius of the pore opening size, and

R= radius of the spherical particles.

$$u_a - u_w = \frac{2T_s}{R} \qquad 5.4$$

T_s = surface tension of water (mN/m), at temperature of 20 C^o, T_s = 72,75

D_{50}= 80 µm (r). The air entry value of the soil used in the research is 43.90 kPa.

5.4 Unsaturated triaxial reinforced tests (Consolidated Undrain Test)

The test plan included a number of tests on specimens of clayey soil. All specimens were compacted at the same water content of 13 % and dry density of 1.78 g/cm^3, with different percentages of fibre 0 %, 1 %, 3 % and 5 %. In this research, the samples were prepared under the static compaction method, and the three sets of moulding equipment, developed for this study, were used. The total number of tests on unsaturated samples was 16 tests. Each test comprised a number of stages including equalisation, consolidation and isotropic loading to failure.

5.4.1 Specimens tested at 0 % fibre

At 0 % of fibre the specimens were tested under different matric suctions $(u_a - u_w)$ of 0, 50, 100 and 200 kPa. All tests were carried out in stages including equalisation, consolidation and compression.

5.4.1.1 Water volume change

Since the samples were prepared with different amounts of fibre content, but with same water content, the initial suction would be different and unknown. Therefore, it was important to equalise suction head to a known, predetermined. Thus, in this stage specimens were allowed to equalise at different suctions of 0, 50, 100, and 200 kPa, under constant mean net stress P' which is 20 kPa for all samples. The sample that was tested at 0 kPa of suction were subjected to wetting and drying cycles. Figure (5.21) shows the results of initial equalisation stage for all tests of 0 % fibre, therefore presented together in this graph. This stage took between 5 to 9 days to be complete. The water volume V_w change in the tests of 0 kPa of suction, decreased (water flowed out of the sample) and

degree of saturation S_r were 96.98 %. The Sample was tested under 50 kPa of suction, the volume of water was decreased at 10 hours then increased again up to 2 days, this volume was kept constant in the rest of stage. Figure (5.21) also show the volume of water in tests of 0 % fibre and 100 kPa of suction, and 0 % fibre and 200 kPa value of suction were coded as (F0-S100 and F0-S200) respectively, and was decreased in the first 2 hours then increased until the equalised occurred. The changes (decrease) in specimens F0-S0, F0-S50 are -0.025 % and .015 % respectively. The increase for F0-S100 and S200 are 0.04 % and 0.12 % respectively. The differences in water volume change in samples either decreasing or increasing may be due to variations in initial water content and additional water on the surface of high air entry disk. Furthermore, the initial water content was prepared the same for all specimens, but the water content change due to the evaporation when removed from the mould.

Figure (5.21) shows the results of water volume change during the consolidation stage as well for all specimen tested under 0 % fibre. The ramp consolidation tests were carried out on the samples after the equalisation stages at various constant suctions of 0, 50, 100 and 200 kPa. The mean net stresses were increased from 20 to 100 kPa during the consolidation, whereas the suction was kept constant. The volume of water was continuously calculated from the data recorded by the relevant pressure/volume controller. The variations of volume during consolidation for constant suctions are discussed below.

In sample (F0-S0) zero kPa of suction, that the water volume increase (water flowed in the sample) were the volume decreased in the first stage, and the increase was between -0.02 to 0.008 %. The others (F0-S50, S100 and S200),

slightly increased further following the equalisation stage and seemed to be consistent. Figure (5.21) show the increases, which varied between 0.008 to 0.12 %. Figure (5.21) shows the result of water volume change during the compression stage. In all tests of 0 % fibre the volume change of water remains steady, due to the consolidated undrain test (CU) all the valves of pore air pressure and back water were kept closed during this stage. It was decided that no more result of water volume change would be shown in the other tests including 1, 3 and 5 % of fibre during the shear stage, due to no volume change being observed as the valve of back water pressure was kept close during the shearing stage for all tests.

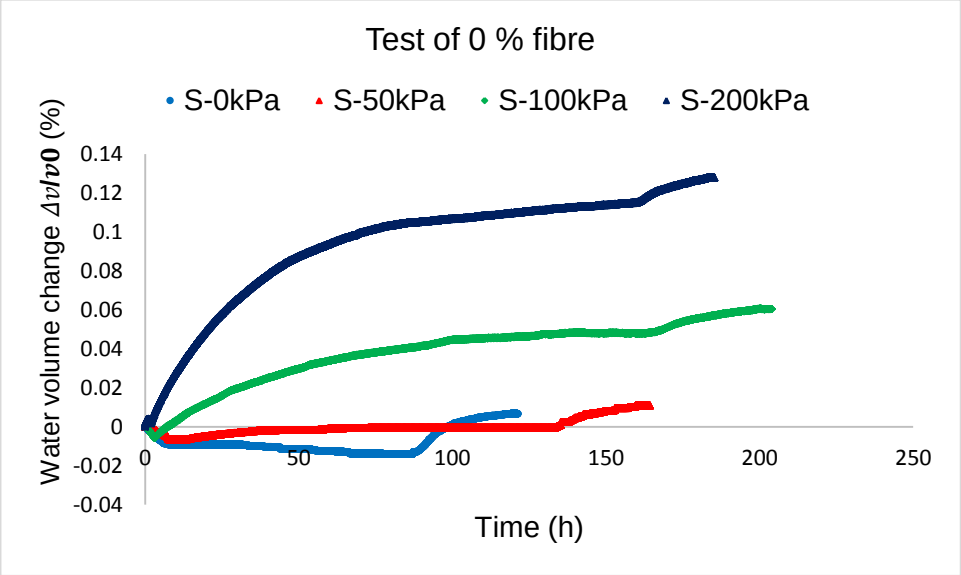

Figure 5.21 water volume change of 0 % fibre tests

5.4.1.2 Specimen volume change

Figure (5.22) illustrates the specimens' volume change during the equalisation stage, at different desired suctions: 0, 50, 100, 200 kPa of 0 % fibre. Figure (5.22) also shows the variation in the volume change of specimens during

equalisation stages. During this stage, the volume of each sample changed as a result of for example, initial water content, applied suction value and temperature room. In the temperature room, there is a test were the controller of the temperature had some problem (stuck), that was effective on the volume of water and sample. Samples with suction 0 and 50 kPa decrease with a time of equalisation, about -0.022 %, this change due to the applied suction method as the only back water pressure increased while the confining pressure and air pressure remain constant (see chapter 3 section 3.5). Testing under 200 kPa suction, the curve shows a decrease and somehow a slight increase and decrease due the temperature of the room. It is clear in the test of 100 kPa of suction how the temperature effort in the sample volume changed. During this stage of the sample tested in 100 kPa suction, the temperature control had some problems for more than week, that effect on the volume of sample appear in the Figure (5.22), which increased and decreased. Al-sharrad et al., (2013) reported a variation of water volume change in the inner cell and temperature fluctuation inside the testing room. According to Figure (5.22), the samples volume change at the consolidation stage with non-reinforced soil specimens, and in all samples the volume decreased during the increment in mean net stress P', when the P' reached the target, the volume remained slightly increased till the value of consolidation achieved.

Shearing stage of each test was performed after the consolidation stages. This stage of the test was conducted on samples under isotropic at constant suction. Figure (5.22) shows the variation of samples volume at different suction for each test specimens, 0, 50, 100 and 200 kPa. The volume changes of samples

decreased due to the increase in the lower chamber pressure to shear the specimen, and the decreased of sample continues until the failure occurs.

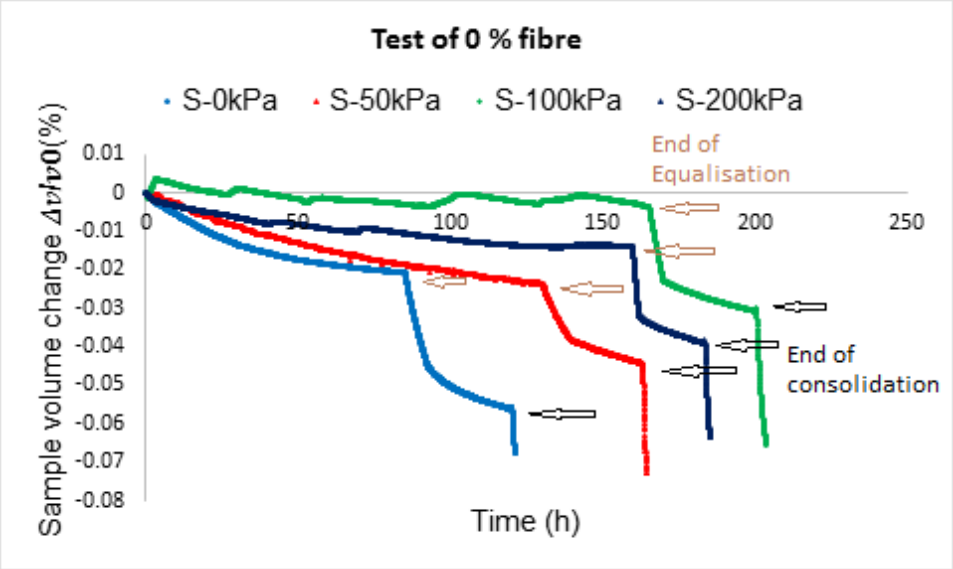

Figure 5.22 specimen volume change of 0% fibre tests

5.4.1.3 Deviator stress

Figure (5.23) illustrates the growth of deviator stresses against axial strain at different suctions of 0, 50, 100 and 200 kPa for non-reinforced specimens prepared at 13 % of water content and 1.78 g/cm^3 dry density. The shearing resistance at 15 % axial strain was used, and continued up to 24 % axial strain to calculate the behaviour of specimens reinforced with fibre. Specimens showed stress-strain hardening behaviour. However, it was clear in sample F0-S200. The hardening occurs due to the plastic case, as soon as the yield occurs, the stress continually increases, in order to achieve the plastic deformation. Specimens showed continuous increase in deviator stress with

increase in suction. According to Figure (5.23), the gradient of the deviator stress-axial strain curve increased with an increase in suction. Moreover, the increment was approximately 119 % between the 0 kPa of suction and 200 kPa of suction.

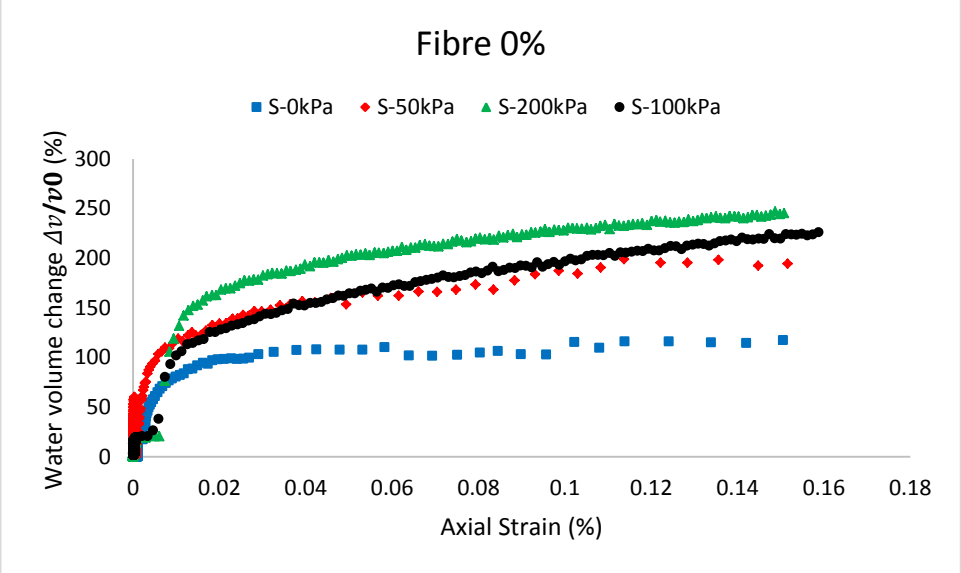

Figure 5.23 deviator stress of 0 % of fibre at different suction

5.4.1.4 Shear strength parameters

Shear strength parameters including cohesion (c') and internal friction angle (ϕ') were calculated for non-reinforced soil specimens using Mohr circle diagrams of shear strength against mean net stress. Figure (5.24) shows an increase in cohesion with increased suction, while the internal friction angle is constant. The extended Mohr diagram failure can be established by testing a soil with saturation condition, and the cohesion can be obtained from a single

Mohr' circle diagram. (Fredlund et al., 2012). The difference between the increase of cohesion for suction at 0 kPa and suction 50, 100 and 200 kPa, were found 26.28, 43.54 and 54.04 kPa, respectively.

Figure (5.25) shows the (ϕ^b) the relationship between the matric suction and cohesion. Table (5.6) shows the parameters of shear strength of the sample prepared at 0 % fibre.

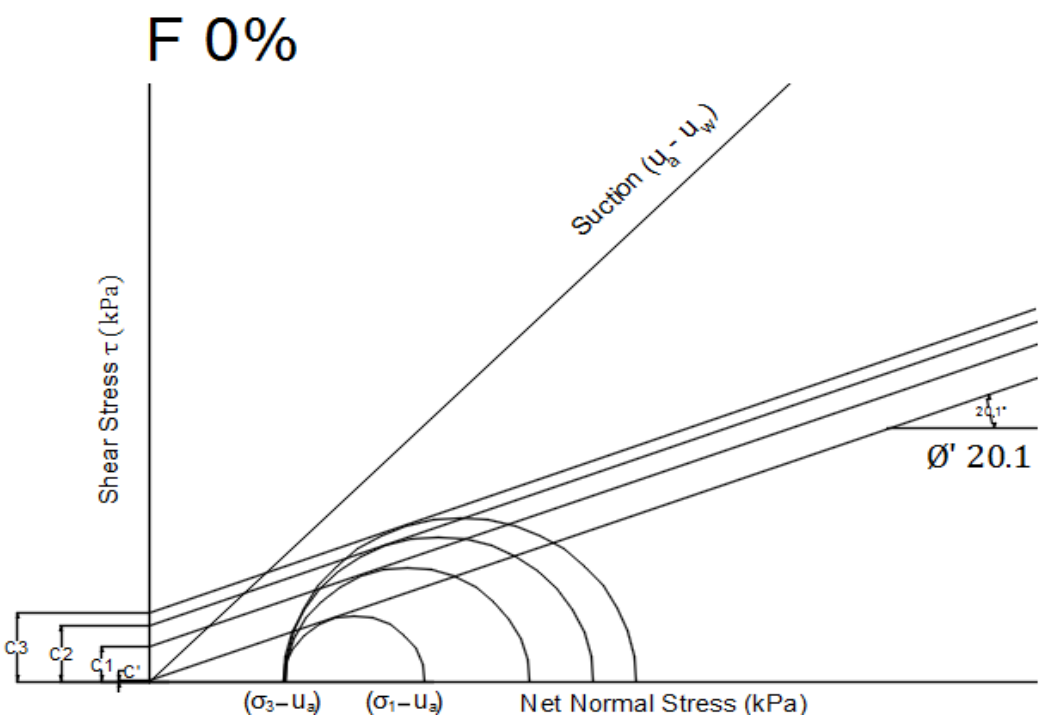

Figure 5.24 Mohr circle diagrams of 0 % fibre

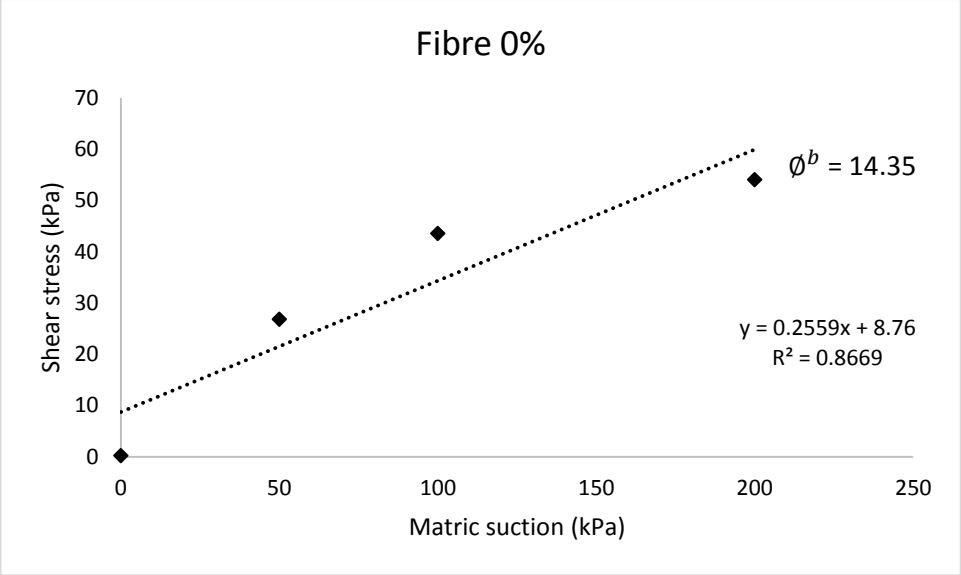

Figure 5.25 shear strength parameters of $\emptyset^b$at 0 % fibre

Table 5.6 shear strength parameters of soil specimen 0% fibre

Specimen	**c' (kPa)**	$\emptyset'$	$\emptyset^b$	**Shear strength τ (kPa)**
F0-S0	0.22	20.1	14.35	48.71
F0- S50	26.28			83.86
F0- S100	43.54			112.56
F0- S200	54.04			120.39

5.4.2 Specimens tested at 1 % of fibre

Specimens with 1 % fibre were tested under different matric suctions $(u_a - u_w)$ of 0, 50, 100 and 200 kPa. All tests were carried out in stages including equalisation, consolidation and shearing.

5.4.2.1 Water volume change

Figure (5.26) illustrates the water volume change in the equalisation stage, at 0, 50, 100 and 200 kPa of suction, and the specimens at 0, 50 and 200 kPa of suction were the volume increased (water flow into the samples), the fibre affected in the flow of water where the water flowed smoothly inside the void between particles. The change in water volume varied between 0.01 and 0.014 %. The sample of 100 kPa of suction appeared to be unstable where the volume decreased and then increased, and the change was large compared to the others. The change was recoded between -0.4 to 0.58 % and this could be due to some leakage were happen during the flushed the air pebbles from underneath the high air entry disk. Therefore, the results of this sample may not be accurate as those of the other tests at this stage. It was noted that if the original suction in the sample is greater than the final at the end of equalisation stages, the water will flow into the specimens. The water inflow into the samples causes the suction to decrease.

The water volume change during the consolidation is presented in Figure (5.26). The results are shown the volume increase of approximately 0.001 % at suction 0, 50 and 200 kPa, while the volume increased further due to the reasons noted in the previous stage. It should be noted that the maximum back water pressure in all tests, either with different suction or fibre, was 30 kPa. It is recommended by GDS not to be more than 50 kPa or 30 kPa, depending on pressure rating the ceramic disk.

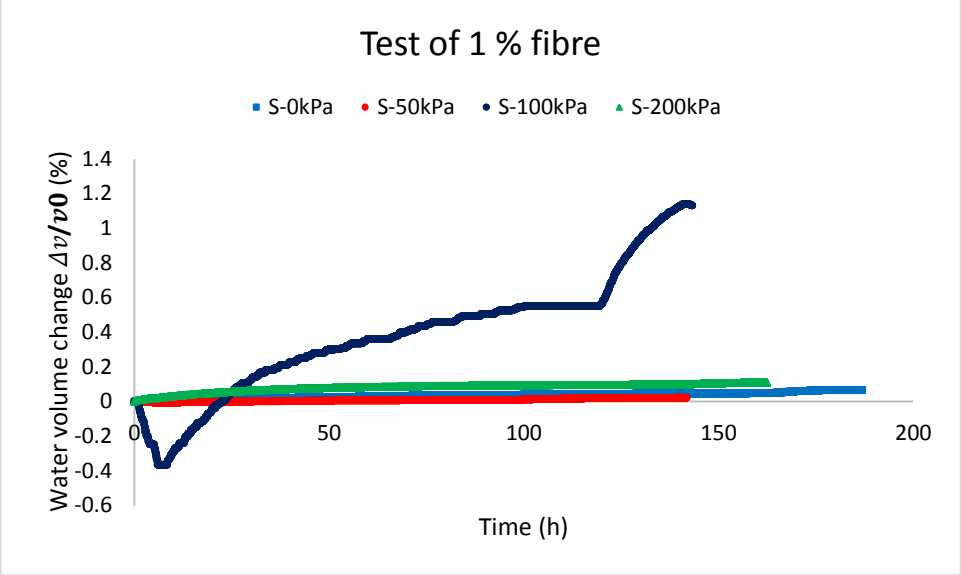

Figure 5.26 water volume change of 1 % fibre tests

5.4.2.2 Specimen volume change

As a result, the stability of the suction changes occurs in soil specimen's volume. Figure (5.27) shows the change in volume as a decrease during the equalisation stage, followed by a more steady decrease on the way to the end of the stabilisation stage. Volume of the sample F1-S100 increased initially then decreased again, and when the suction applied may be the change occurs. The maximum change in samples F1-S50 and F1-S100 were about 0.022 %, in sample F1-S0, it was approximately 0.027 %, and for specimen F1-S200, it was 0.038 %. It has been noted that there was no effective of fibre in volume change compared with non-reinforced specimens during this stage. In the consolidation stage shown in Figure (5.27), the samples volume change continued to decrease gradually to a more or less constant value. The minimum and maximum variations in samples volume, were 0.038 and 0.06 % between samples F1-S100 and F1-S0 respectively. Figure (5.27) shows the volume of samples change through the shearing stage, to shear a samples, the lower

chamber was increased with 0.025 mm/min, while the cell pressure and suction were kept constant, and the valves of pore air pressure and back water pressure closed (CU) tests. At the initial of increasing the lower chamber pressure, the volume of sample resistance, this is due to of the fibre reinforcement compared with the tests under zero percentage of fibre.

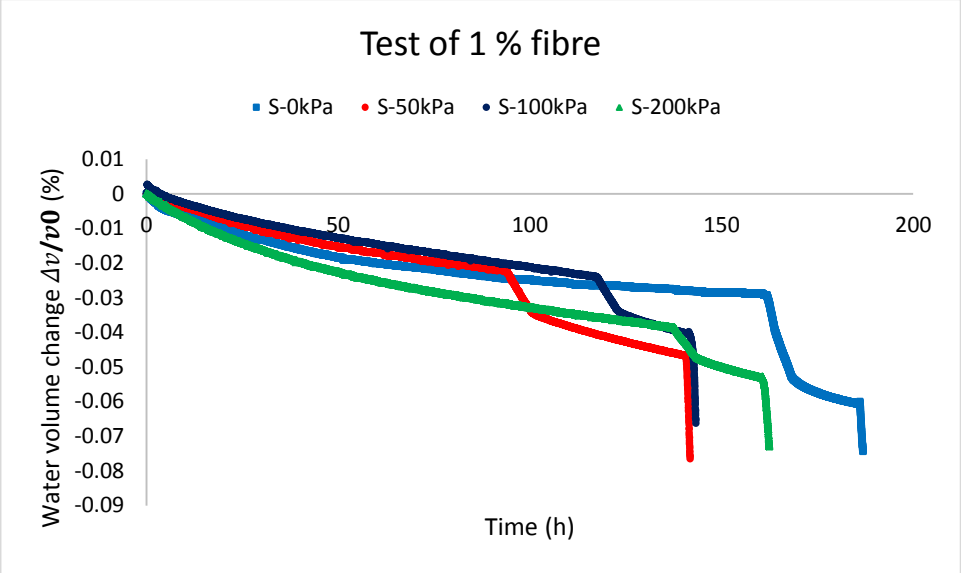

Figure 5.27 specimen volume change of 1 % fibre tests

5.4.2.3 Deviator stress

Together non-reinforced and fibre reinforced samples showed strain hardening behaviour at the initial part of compression stages. Also, both were prepared at the same water content and dry density 13 % and 1.78 g/cm^3 respectively. Figure (5.28) illustrates that the deviator stress increased with increased with suction. However, fibre content case to increase further compared with non-reinforced at the same suction. Tests of 200 kPa of suction increased by 13.55 %, compared to non-reinforced and 1 % of fibre.

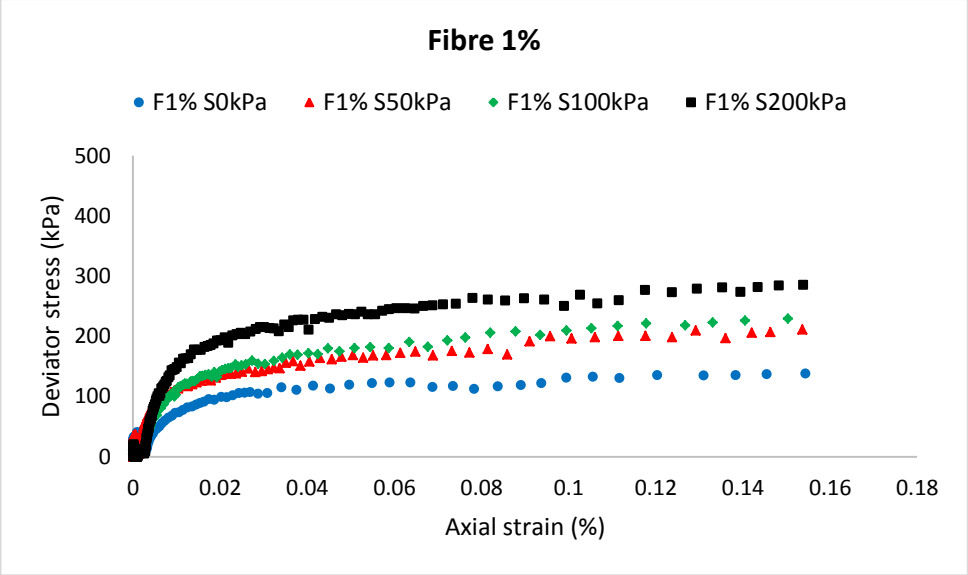

Figure 5.28 deviator stress of 0 % of fibre at different suction

5.4.2.4 Shear strength parameters

As is noted, the internal friction angle (ϕ') is constant for all tests. The cohesion (c') shown in Figure (5.29) increased with an increase in suction and more increase occurred when fibre was added. It was concluded that the (c') of F0-S0 was 0.22 kPa while (c') is 12.6 of 1 % fibre. Figure (5.30) shows (ϕ^b) was 13.48. In general, an increase in fibre content to soil samples, the resultant effective shear strength parameters increased significantly. Table (5.7) summarises the parameters of shear strength of soil specimen prepared with 1 % of fibre.

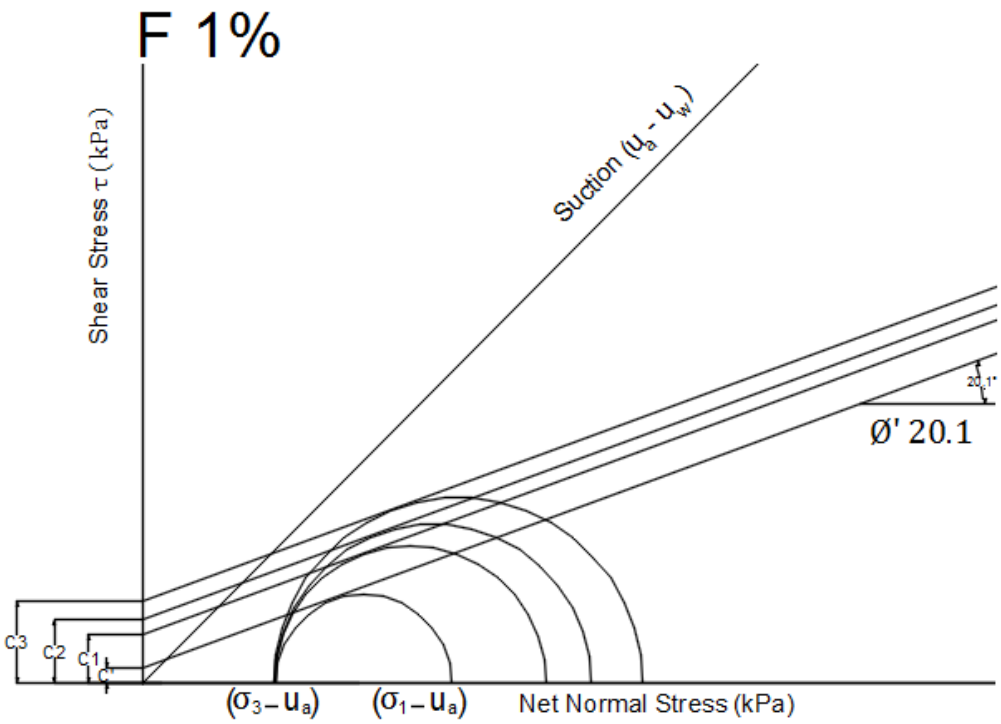

Figure 5.29 Mohr circle diagrams of 1 % fibre

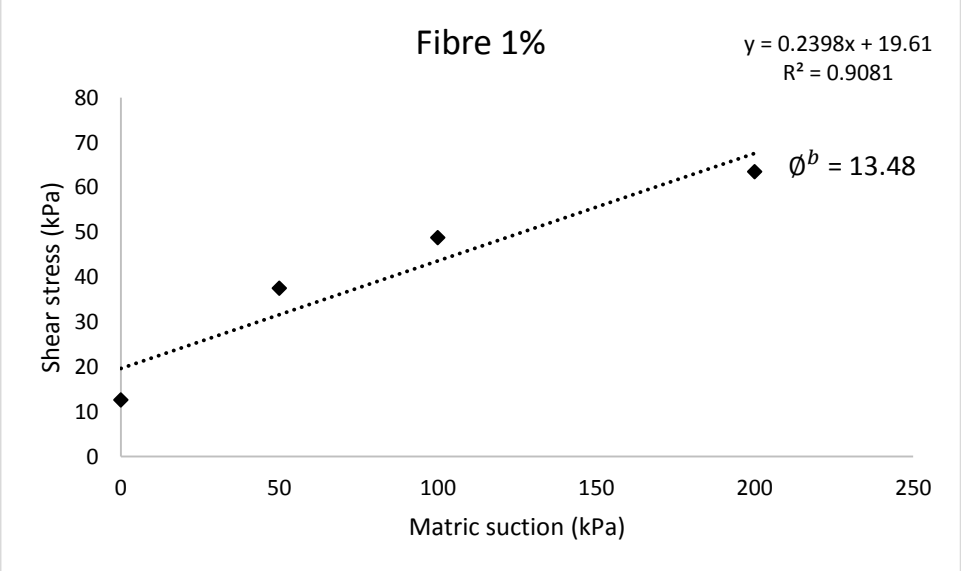

Figure 5.30 shear strength parameters of. $(\emptyset^b)$ ***at 1 % fibre***

Table 5.7 shear strength parameters of soil specimen of 1 % fibre

Specimen	c' **(kPa)**	$\emptyset'$	$\emptyset^b$	**Shear strength** τ **(kPa)**
F1-S0	12.6	20.1	13.48	64.27
F1- S50	37.48			97.04
F1- S100	48.79			105.01
F1- S200	63.50			130.98

5.4.3 Specimens tested at 3 % of fibre

5.4.3.1 Water volume change

The increase in water volume was greater for tests in which the applied suction was highest. Figure (5.31) shows the increase in suction result to increase the volume of water. Sample F3-S200 was clear to show the volume of water during equalisation were the highest value with those have less suction. The increase of water volume was approximately 0.07 % with high suction and around 0.035 % with less suction. During the consolidation stage, in Figure (5.31), the volume of water kept slightly increasing, and in the stages of consolidation the mean net stress increased from 20 kPa to 100 kPa for all the specimen. It might be case to keep the volume of water increase slightly (water flow into samples), as samples sucking a water, due to the fibre content and permeability.

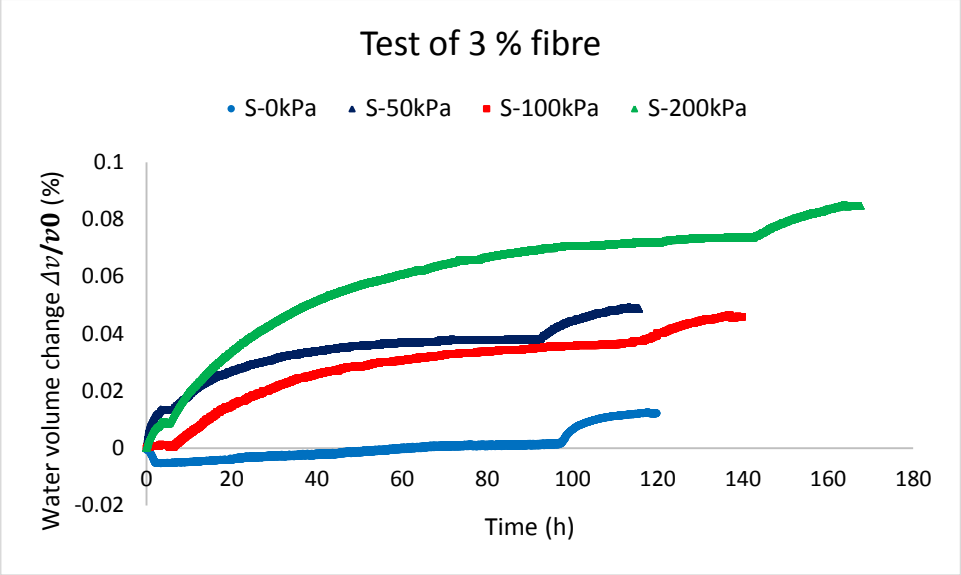

Figure 5.31 water volume change of 3 % fibre tests

5.4.3.2 Specimen volume change

In the equalisation stage, each test started with a reduction in the volume of samples and stayed decreased until the end of this stage, as shown in Figure (5.32). Unusual behaviour in sample F3-S0 were prepared at 13 % of water content and 1.78 g/cm^3 of dry density. In addition, the degree of saturation S_r was increased to 98.08 %, using Sandra's (2008) method. It was observed that the volume of sample immediately decreased by around 0.005 %, then was kept steady with a slight increase until the end of equalisation. This unusual behaviour may be due to some air pebbles trapped in the system which had not been observed, whereas in Figure (5.32), the volume of sample follows normal behaviour, which was decrease when the air dissolved in the water or somewhere else inside the system. Other samples were decreased during both stages around -0.035 % in average. As mentioned before, it has been observed that the fibre content with reduction of soil samples volume. Graph (5.32) shows the volume reduction during the shear stage was approximately of -0.06 for

most of the specimens. In the shearing stage specimen's resistance for about 1 % of strain. And in the rest of strain the volume of samples decreased with an increase in the axial stress.

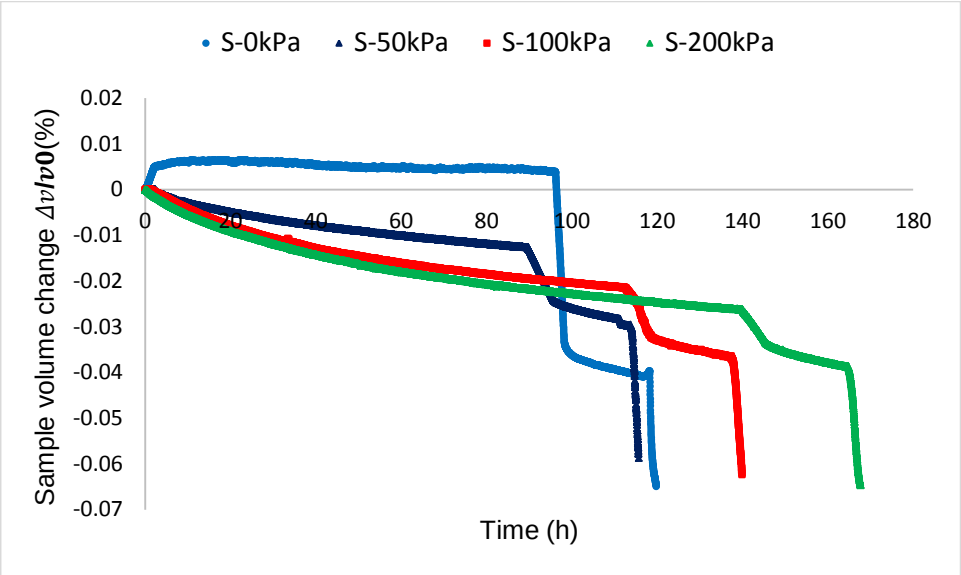

Figure 5.32 specimen volume change of 3 % fibre tests

5.4.3.3 Deviator stress

Figure (5.33) explains the evolution of deviator stresses against axial strain at different suctions: 0, 50, 100 and 200 kPa for 3 % reinforced specimens prepared at 13 % of water content and 1.78 g/cm^3 dry density. Specimens showed the stress-strain hardening behaviour were it strong in sample (F3-S0). Specimens also showed a continuous increase in deviator stress with an increase in suction. However, the increase in fibre significantly increased the deviator stress compared to that of non-reinforced soil specimens.

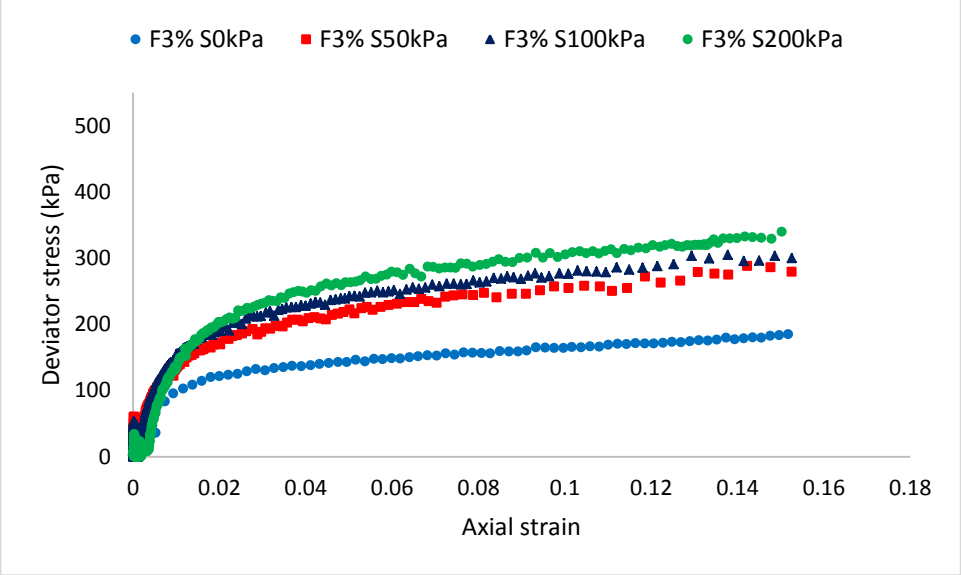

Figure 5.33 deviator stress of 3 % of fibre at different suction

5.4.3.4 Shear strength parameters

Shear strength parameters cohesion (c') and internal friction angle (ϕ') Figure (5.34) showed increase in cohesion with increased suction, as well as the fibre content increase. In Figure (5.34), the 3 % fibre has been tested, and showed improvement in the cohesion, compared to the same value of suction e.g. at 100 kPa with non-reinforced, were 68.86 kPa and 43.54 kPa respectively. Figure (5.35) shows the value of (ϕ^b) which 15.42 degree. Table (5.8) presents the parameters of soil specimen prepared at 3 % of fibre.

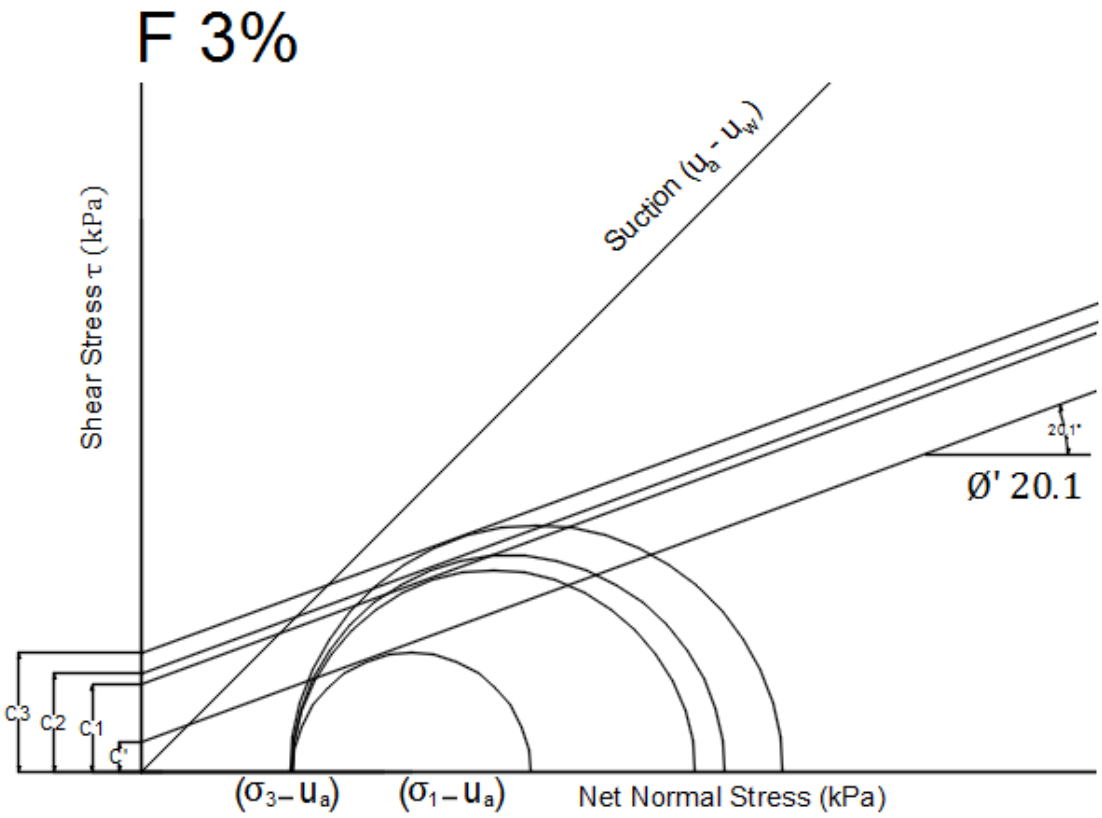

Figure 5.34 Mohr circle diagrams of 3 % fibre

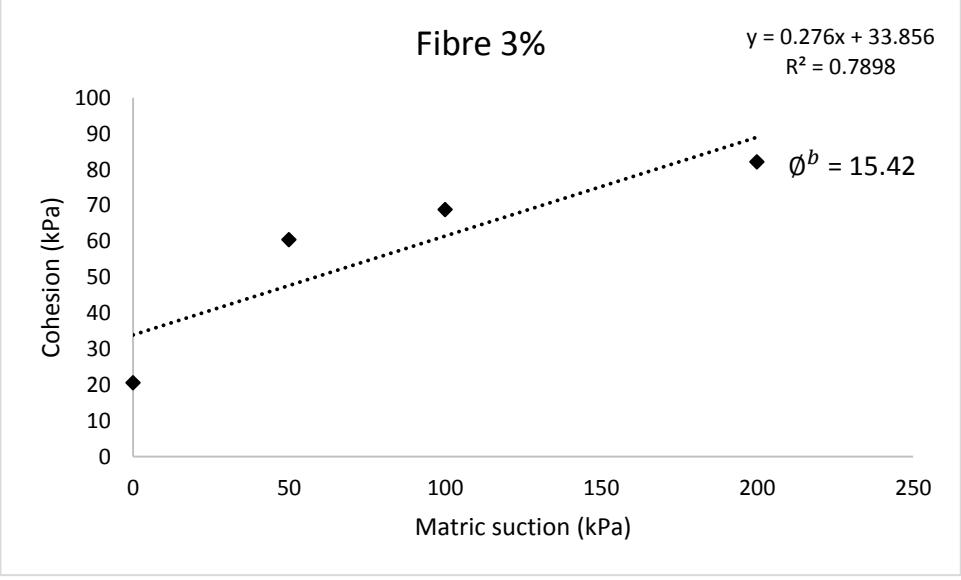

Figure 5.35 shear strength parameters of $(\emptyset^b)$ at 3 % fibre

Table 5.8 shear strength parameters of soil specimen of fibre 3 %

Specimen	c' **(kPa)**	$\emptyset'$	$\emptyset^b$	**Shear strength** τ **(kPa)**
F3-S0	20.55	20.1	15.42	76.09
F3- S50	60.46			127.51
F3- S100	68.86			137.84
F3- S200	82.15			157.78

5.4.4 Specimens tested at 5 % of fibre

5.4.4.1 Water volume change

In most cases the equalisation was completed when the rate of the change in water flow was less than 0.1 cm^3/day. Figure 5.36 shows the volume of water in specimens F5-S0, F5-S50 and F5-S100 decreased at the beginning up to -0.01 % and start increasing again to 0.04 (water flow into the samples), this is due to the high suction in the soil samples. Even though the water increase in sample F5-S0, the water was still getting out from the sample, at sample F5-S200 suction in the sample itself less than 200 kPa. Figure (5.36) shows the water volume change remained slightly increased during the stage of consolidation. The affective of fibre on volume change has not been observed, because of the same result in non-reinforced test with others which have fibre content.

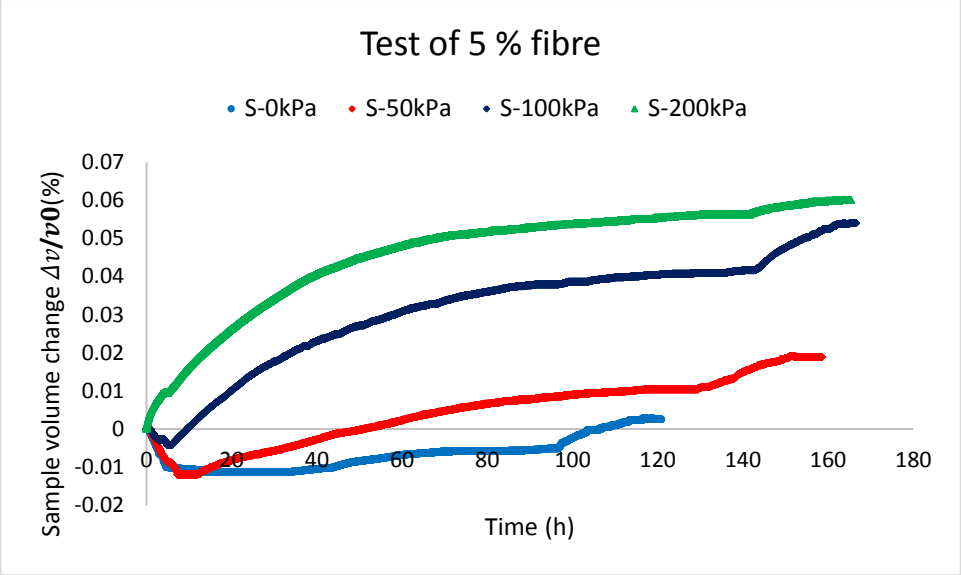

Figure 5.36 water volume change of 5 % fibre tests

5.4.4.2 Specimen volume change

In order to highlight the changes in the volume of samples during the all stages, the difference of volume with time is plotted in Figure (5.37). The results of variation in volume for samples reinforced with 5 % fibre. A review of these figures show that the volume of all specimens decreased sharply during the initial stage, followed by a more gradual decrease towards the end of the other stages. A comparison of the results illustrates that the variation of specimen volume in test F5-S50 was inconsistent with the other tests. The change of volume was about -0.01 % in this sample during the first stage, while the other sample reached around -0.025 %. In general, the observation of samples volume changes, the large change in volume occurring in the specimens have a high degree of saturation, which is almost fully saturated, as well as the suction 0 kPa for those tests.

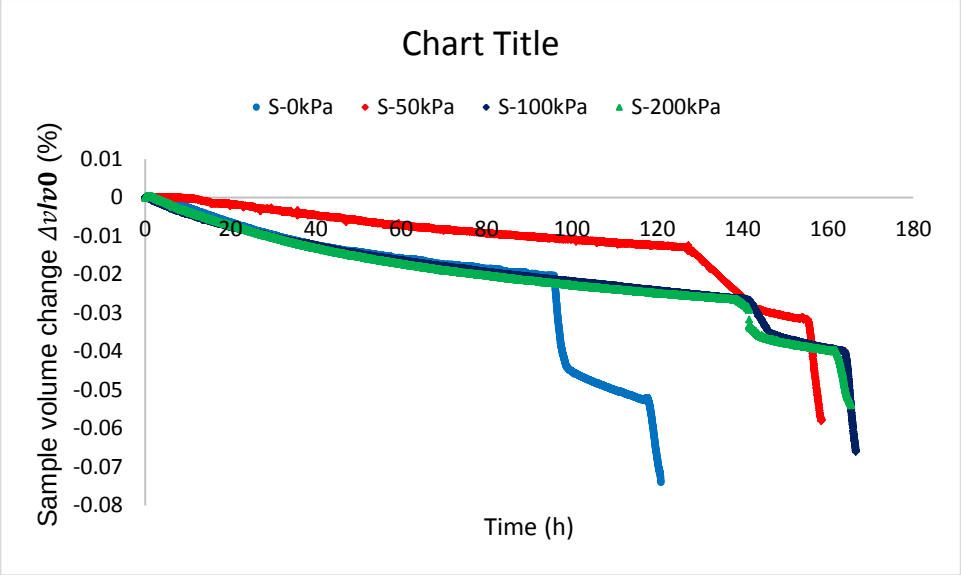

Figure 5.37 specimen volume change of 5 % fibre tests

5.4.4.3 Deviator stress

Figure (5.38) shows the influences of fibres on deviator stresses of soil specimens compacted at dry density of 1.78 g/cm^3 respectively. Non-reinforced soil specimen compacted at the same dry density of 1.78 g/cm^3 showed plastic behaviour. However, there was an increase in fibre content followed by steady change to strain hardening behaviour. Specimens with 5 % fibre content, showed increased deviator stress likened to non-reinforced.

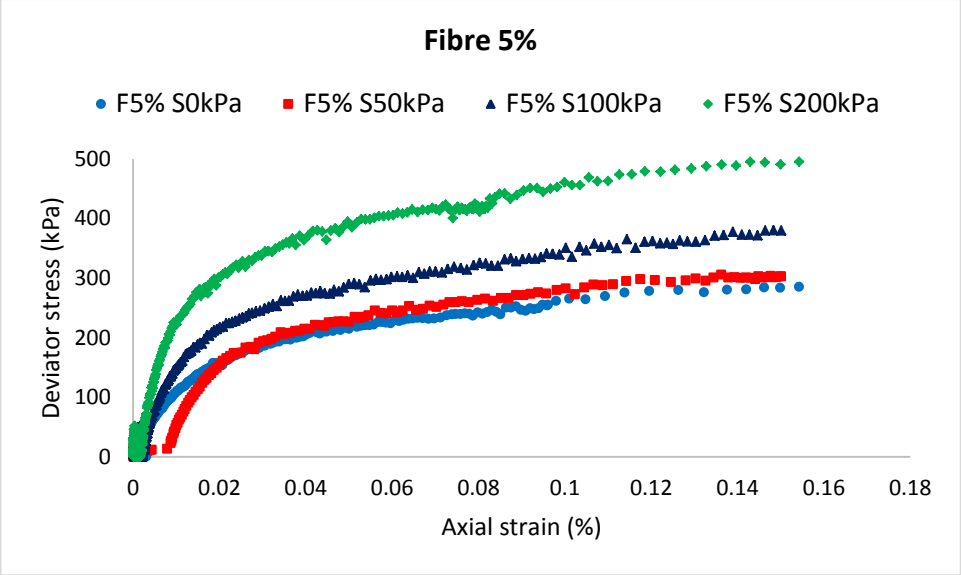

Figure 5.38 deviator stress of 5 % of fibre with different suction

5.4.4.4 Shear strength parameters

Figure (5.39) displays the shear strength parameters as cohesion (c') and internal friction angle (ϕ') shows increase in cohesion with increased of suction. Increment the proportion of fibre case to improve the cohesion. 5 % fibre was added to this test and showed improvement in the cohesion extra, compared to non-reinforced at same value of suction for example at 200 kPa, where 54.04 kPa and 134.39 kPa respectively. Figure (5.40) shows the value of (ϕ^b) which is 20.44 degree and Table 5.9 shows the results of (ϕ^b), the results indicate improved of (ϕ^b), with increased fibre. However, the test of 1 % fibre decreased compared to the others, this might be due to inaccurate results of test F1-S100. Table (5.10) shows the results of soil specimen prepared at 5 % of fibre.

Table 5.9 shear strength parameters of $(\emptyset^b)$ for all tests

Test No	ϕ^b
Non-reinforced	14.35
1 % fibre	13.48
3 % fibre	15.42
5 % fibre	20.44

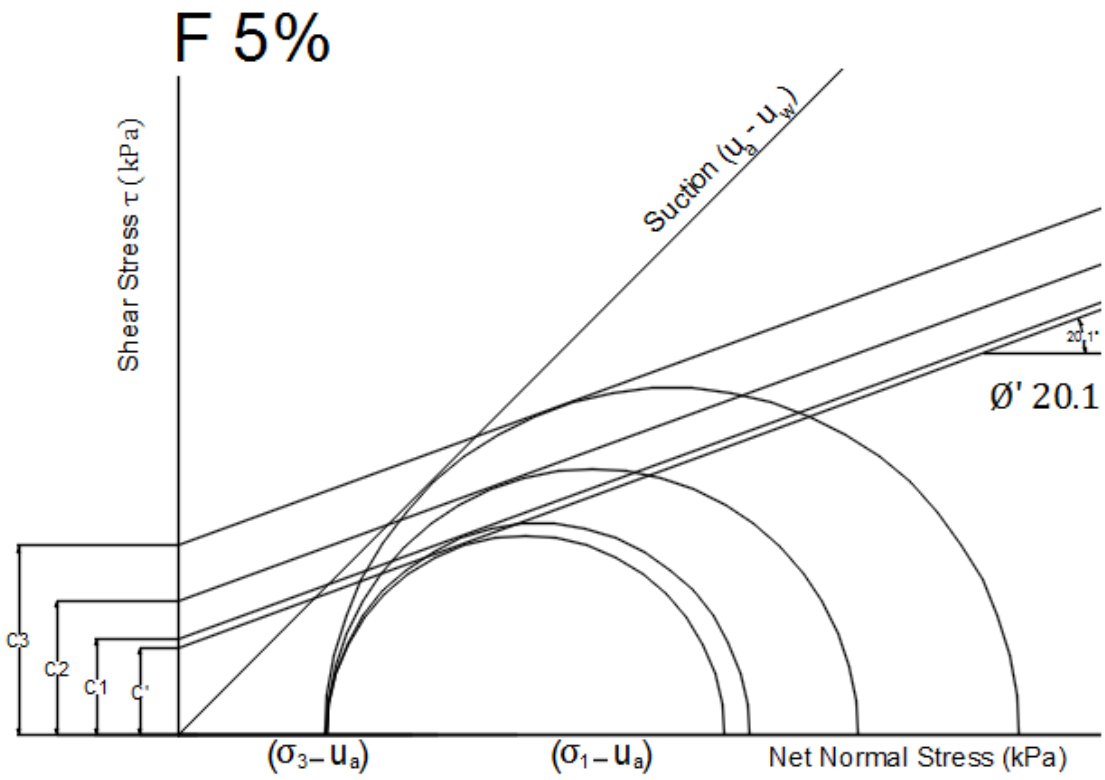

Figure 5.39 Mohr circle diagrams of 5 % fibre

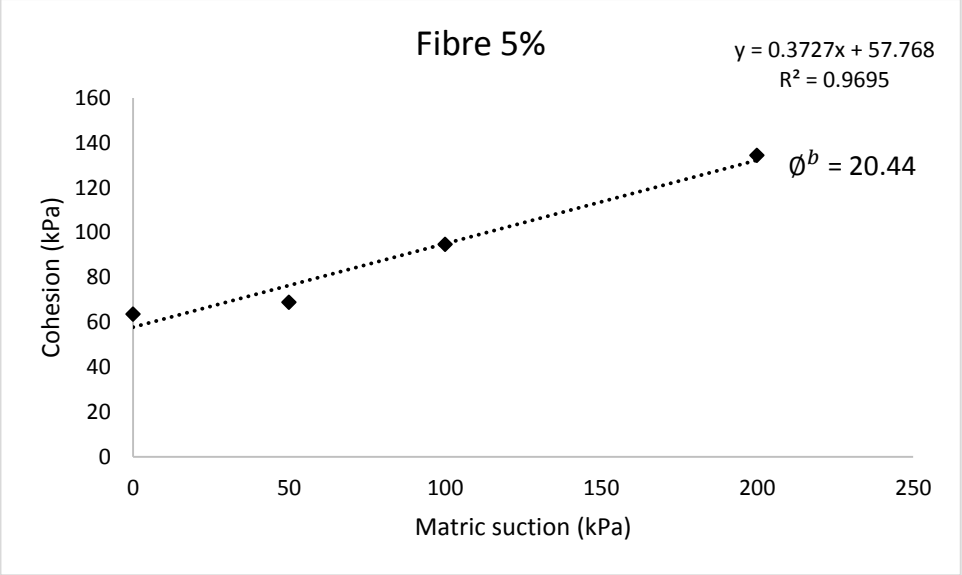

Figure 5.40 shear strength parameters $(\emptyset^b)$ ***at 5 % fibre***

Table 5.10 shear strength parameters of soil specimen of 5 % fibre

Specimen	c' **(kPa)**	$\emptyset'$	$\emptyset^b$	**Shear strength** τ **(kPa)**
F5-S0	63.62	20.1	20.44	131.57
F5- S50	68.84			139.10
F5- S100	94.65			174.73
F5- S200	134.39			227.43

5.5 Evaluating the fibre on mechanical behaviour of unsaturated trixial experimental

For most of the samples the dry density varied by around 3 %. Table (5.11) shows some selected examples from the tests. The insignificant variation in dry density may have been was due to the difference in the soil samples

dimensions, and this variation due to expansion after being released from compaction mould. It is a result of different percentages of fibre content. The water content also had some changed due to the loss of water during sample preparation and compaction.

Table 5.11 dry density affected by percentage of fibre after preparation

Samples code	Samples dimensions (mm)	Dry density $(^{g}/_{cm^3})$
F0-S0	100.1 * 50.02	1.78
F1-S200	100.55 * 50.01	1.77
F3-S50	101.27 * 50.03	1.75
F5-S100	101.45 * 50.04	1.75

5.5.1 Effect of fibre on stress behaviour

Figures (5.41 to 5.44) illustrate the stress-strain behaviour of non-reinforced and fibre reinforced clay soil specimens. Both non-reinforced and reinforced soil specimens were prepared at dry density of 1.78 g/cm^3 and water content of 13 %, compared to the same amount of suction with different percentages of fibre in each graph. Figure (5.41) shows specimens tested under 0 kPa of suction, samples F3S0 with 0.02 strain where hardening behaviour was strong, then deform up to yield point. Stress strain curves of 0 % and 1 % of fibre at small of stress-strain curve (straight part of relationship) is determined. Thus, with increasing inclination, it means that specimens show hardening behaviour. At 5 % fibre content, reinforced specimens showed small strain-hardening behaviour. The detected behaviour was due to the influence of the strength of

fibres at higher strain values. Figure (5.42) shows specimen F5-S200 the strain hardening behaviour, as well as in sample FS-S200 in Figure (5.44). The result shows that the improvement in the deviator stress was result as fibre content increased, while the suction constant.

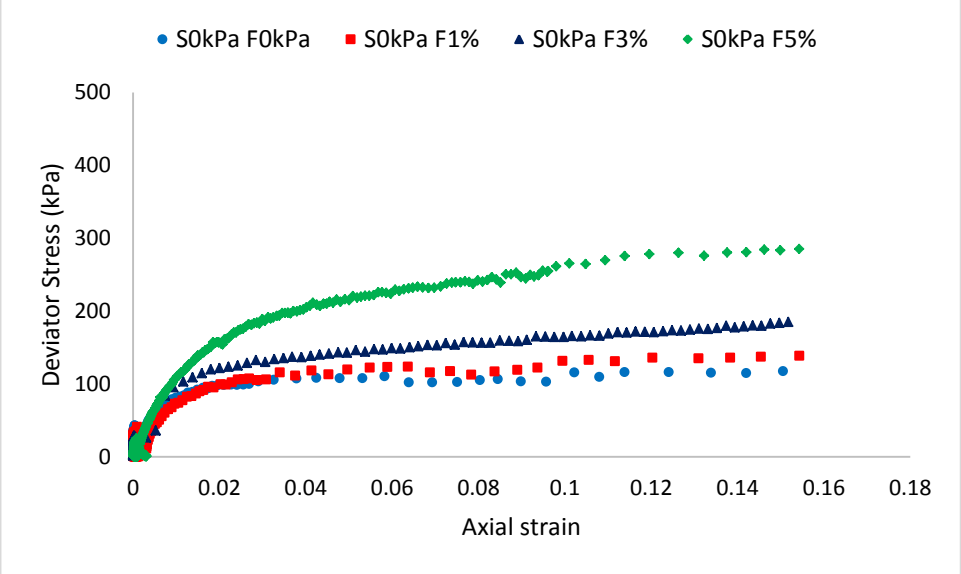

Figure 5.41 stress-strain behaviour of fibre reinforced soil samples at 0 kPa of suction

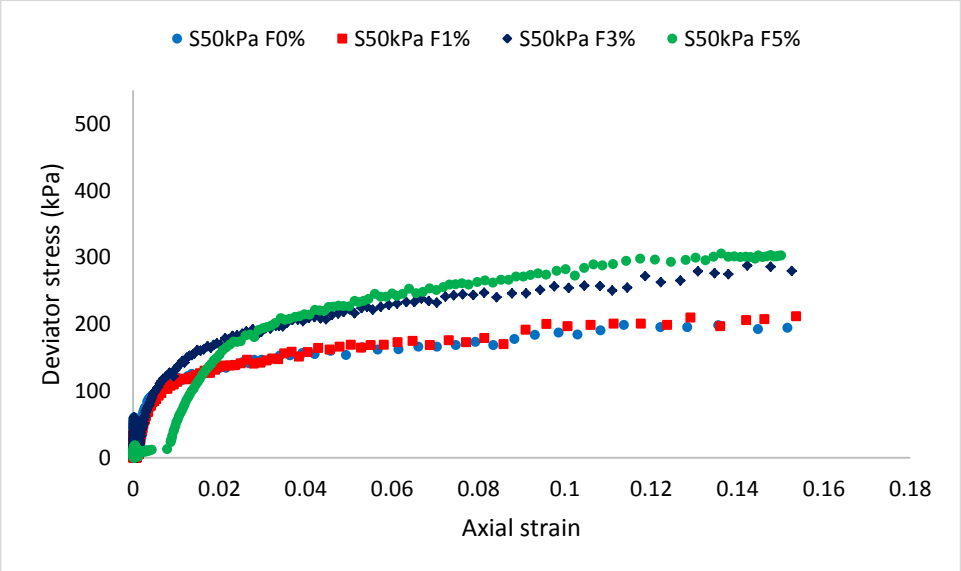

Figure 5.42 stress-strain behaviour of fibre reinforced soil samples at 50 kPa of suction

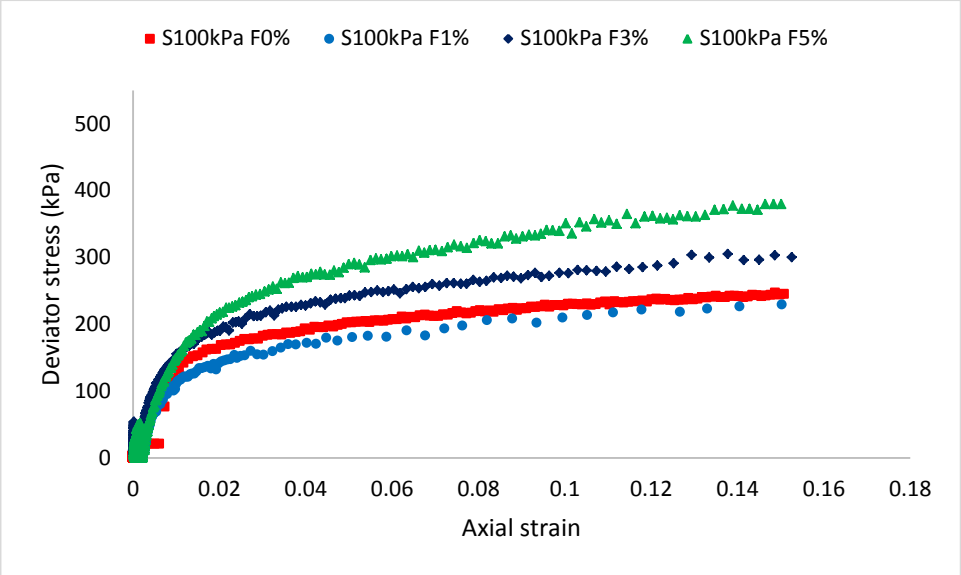

Figure 5.43 stress-strain behaviour of fibre reinforced soil samples at 100 kPa of suction

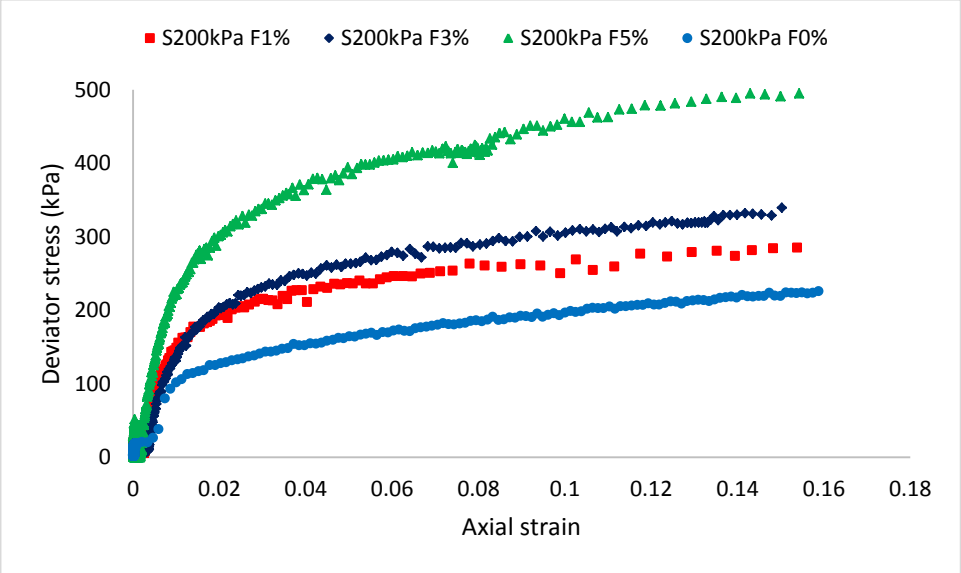

Figure 5.44 stress-strain behaviour of fibre reinforced soil samples at 200 kPa of suction

5.5.2 Effect of fibre on shear strength parameters

Effective shear strength parameters including c' were determined at zero suction and such as 50, 100 and 200 kPa, were calculated for non-reinforced and fibre reinforced soil specimens using Mohr circle diagrams of shear stress versus mean net stresses. Figure (5.45) shows the comparisons of the effective apparent cohesion c', c_1, c_2, and c_3, respectively. With non-reinforced and 5 % fibre reinforced soil specimens, comparing this graphs shows that the increase in fibre content caused a significant increase in cohesion and fibre content. All Mohr circles were drawn based on the mean net stresses at 15 % axial strain (see section 3.10.4 in chapter 3). Table (5.12) shows the summary of the results of both non-reinforced and 5 % of fibre. Effective internal friction angle of fibre reinforced soil specimens are constant in this study due to a single Mohr circle, which can be obtained from saturation condition Fredlund (2012). However, Effective internal friction angle of fibre reinforced soil specimens compacted at the maximum dry unit weight increased significantly with increase in fibre content Mirzababaie (2012).

The affected of fibre content on $\emptyset^b$ (intercepts failure plane on shear stress (τ) versus suction ($u_a - u_w$) plane) improved significantly. However, the sample had 1 % of fibre decrease compared with 0 % of fibre. The effective apparent cohesion of fibre reinforced soil specimens improved significantly.

According to Figure (5.46), the degrees of improvement in cohesion of fibre reinforced specimens corresponding to an increase in fibre content of 1 %, 3 % and 5 % respectively. Therefore, fibres exhibited better contribution to improving cohesion by better interlocking of clay particles.

Figure (5.46) shows the stress path diagrams of 5 % fibre reinforced soil specimens. The specimens were consolidated at the same stress (100 kPa), for non-reinforced and fibre reinforced, which resulted in an increase in the maximum points in the slope of stress path, as all stress in the same line. The increase in the maximum points of stress path with increasing fibre content indicated an increase in deviator stress. Table (5.13) shows the maximum points of p and q, comparing results between non-reinforced and 5 % fibre reinforced soil

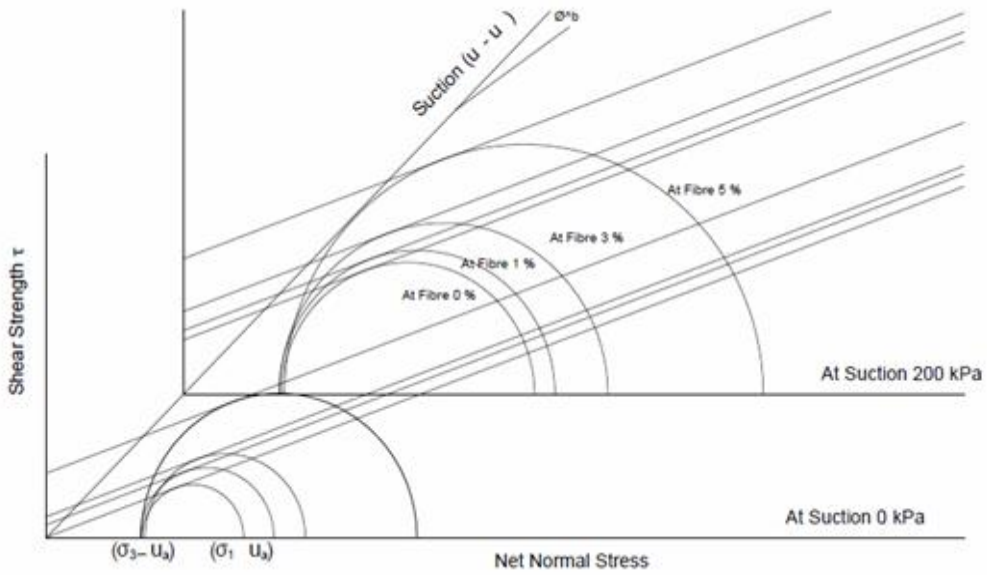

Figure 5.45 Mohr circles at failure for a CU triaxial compression tests 0 and 5 % fibre

Table 5.12 shear strength parameters of 0 and 5 % of fibre

Cohesion (kPa)	0 % fibre	5 % fibre
C'	0.22	63.62
C_1	26.82	68.86
C_2	43.54	94.65

C_3	54.04	134.39

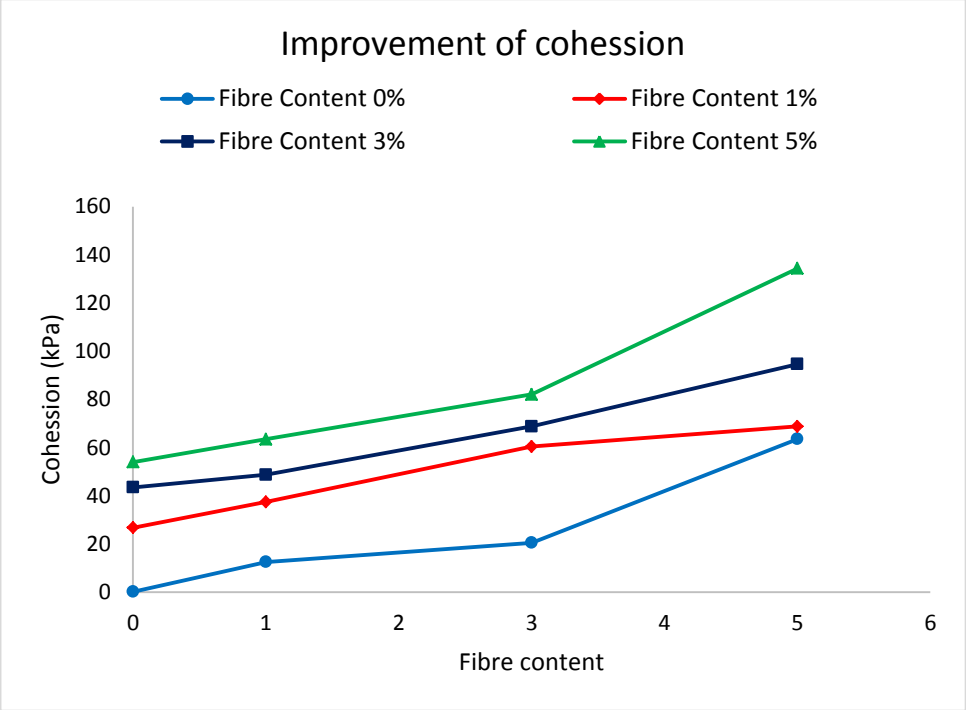

Figure 5.46 improvement of cohesion with increase of fibre content

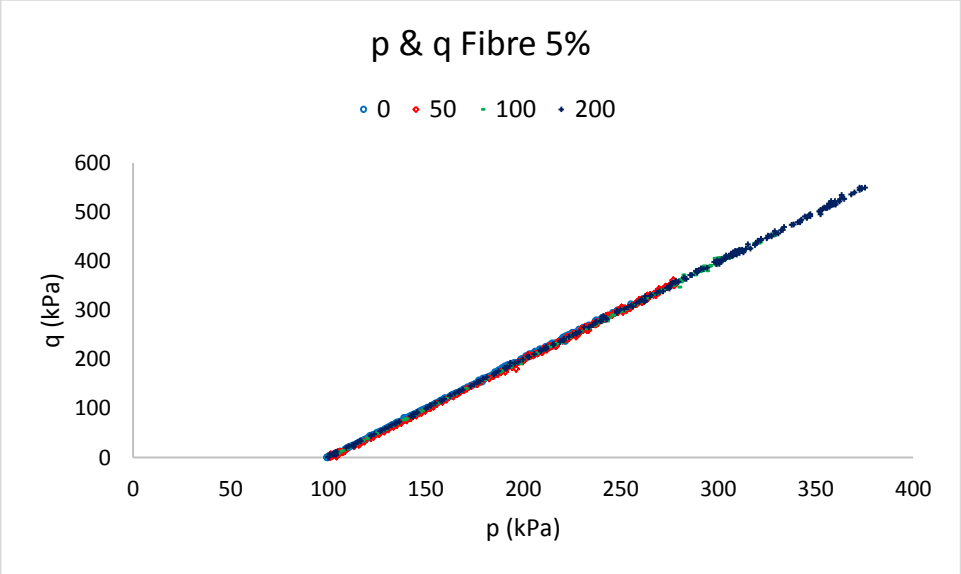

Figure 5.47 stress paths of fibre reinforced soil specimens prepared at 5 % of fibre

Table 5.13 stress paths parameters of test prepared at 5 % of fibre with values of suction

Suction (kPa)	p (kPa)	q (kPa)
0	255.26	312.74
50	272.9	346.01
100	328.19	451.18
200	373.79	548.78

5.5.3 Effect of fibre in the shear strength parameters

In order to study the coupling effect of input parameters, a simple code was written in MATLAB to simulate a wide range of input parameters using the developed regression model and shows the changes in fibre content, suction and cohesion in a 3D graph. Figure (5.48) shows the influence of fibre content and suction on cohesion of mixed specimens. It can be seen in Figure (5.48) that at zero fibre content increase in suction from 0 kPa to 200 kPa resulted in an increase in the reduce of cohesion. At 5 % fibre content increase in suction to 200 kPa was followed by extraordinary exponential growth in cohesion. However, it appears that elsewhere, suction of 200 kPa, the cohesion increased with a fibre content increase. The current regression model effectively supports the cohesion that function of the relationship between fibre content and suction outside the limit of the input parameters. On the other hand, at low suction (i.e. 50 kPa) the cohesion increased nearly linearly with an increase in fibre content. However, an increase in suction turned this relationship into exponential growth. Consequently, it can be concluded that the addition of fibres, as well as

increase in suction, significantly influenced the cohesion fibre reinforced soil specimens. Increases in both fibre content (from 0 % to 5 %) and suction (from 0 kPa to 200 kPa) concurrently resulted in continuous increase in cohesion and deviator stress. The proposed regression model may only be valid for input data within the tested range.

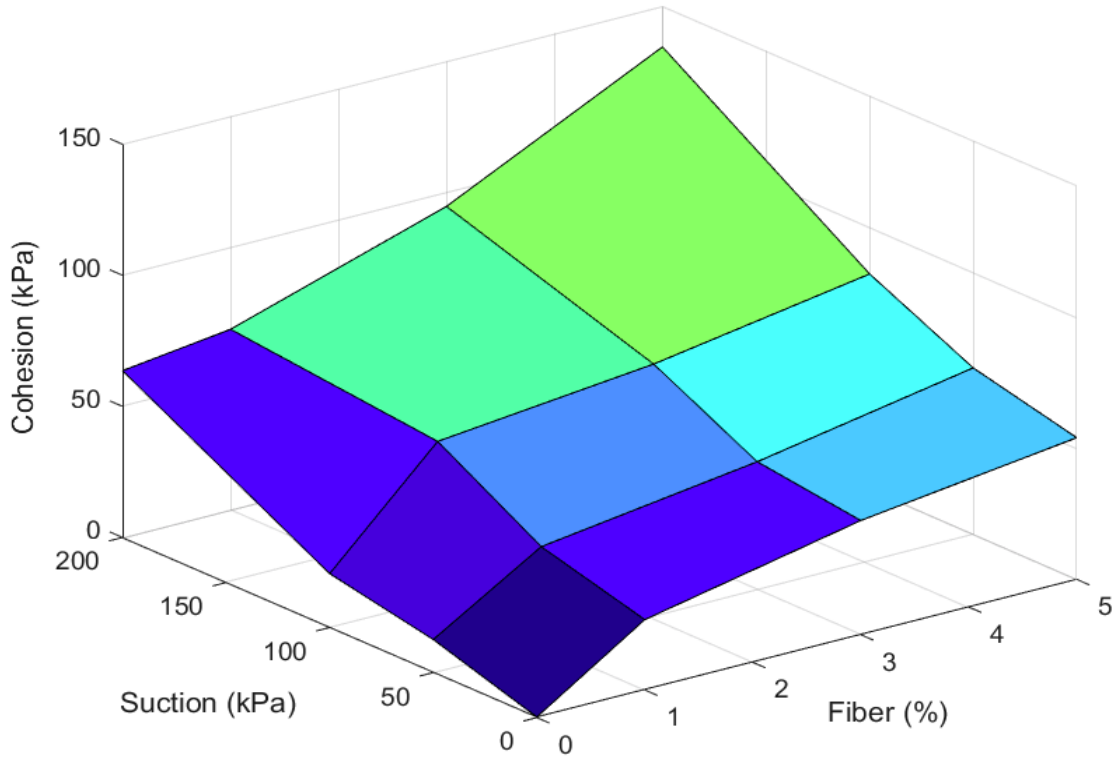

Figure 5.48 intersection effect of fibre content and suction on cohesion of fibre reinforced specimens.

5.6 Results repeatability

The parameters of shear strength behaviour of fibre reinforced soil specimens with random fibres distribution might depend on the uniformity. Hence, the repeatability of the results might possibly be affected. In order to study the repeatability of the results, some random tests on soil specimens were carried out, such as test with 5 % of fibre at 100 kPa of suction (F5-S100) test with fibre

1 % at suction 100 kPa (F1-S100). Figure (5.49) and Figure (5.50) shows the compare results of the main and repeating tests.

Figure (5.49) shows the deviator stress soil specimen prepared at 5 % of fibre. The result of triaxial test consolidated undrained at consolidation stress of 100 kPa showed great degree of repeatability of the test result. Even though the fibre spreading was a key in the repeatability of the results, the effective method of fibre reinforced soil specimen preparation showed great degree of repeatability. Figure (5.50) also shows the deviator stress of 1% fibre reinforced soil specimen. Repeating consolidated undrained triaxial tests were carried out at consolidation stress 100 kPa. The result shows a good degree of repeatability which about 4 % difference. Besides, fibres used in this study contribute better to strengthening the cohesion soil specimens.

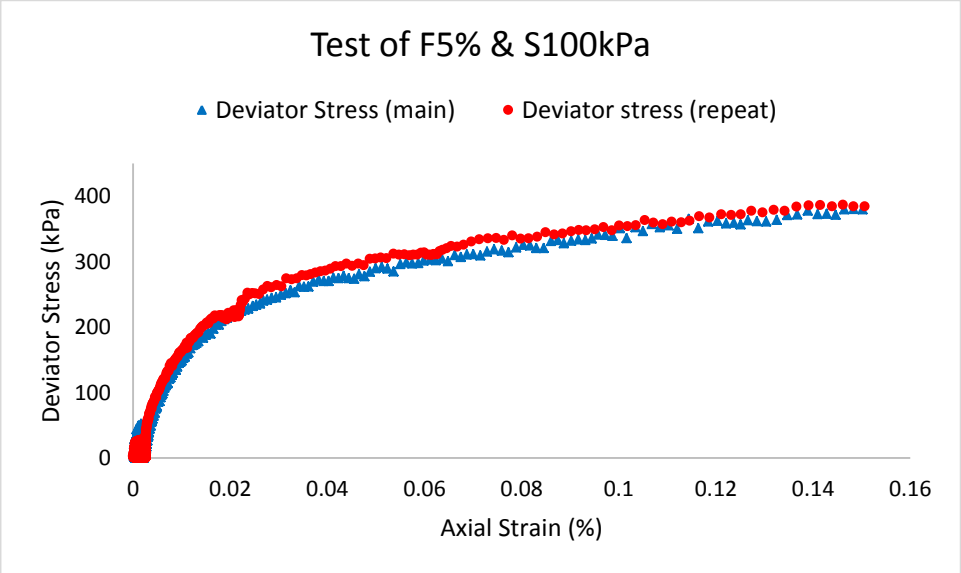

Figure 5.49 results of repeating tests of soil specimen F5S100 of deviator stress

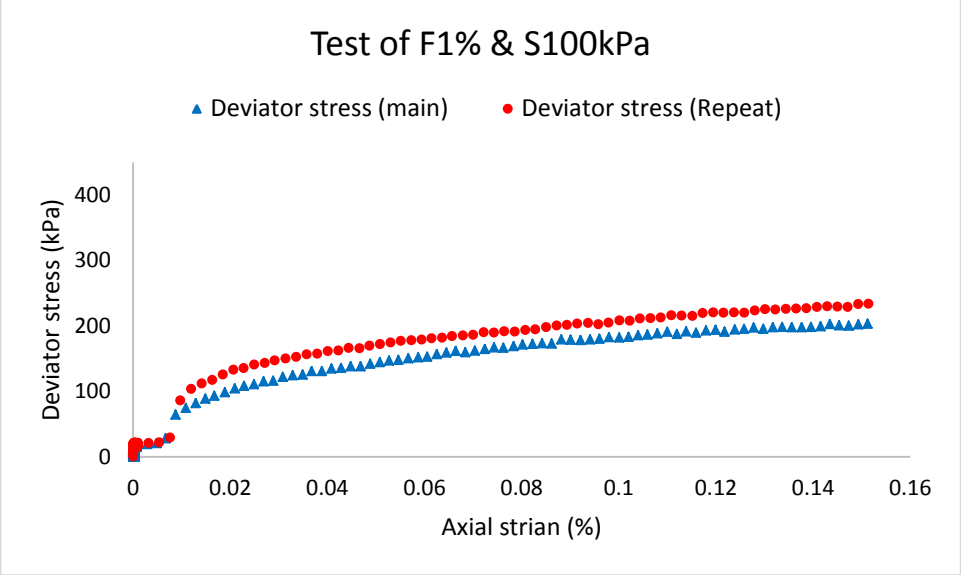

Figure 5.50 results of repeating tests of soil specimen F1S100 of deviator stress

5.7 Conclusion

Tables (5.14 to 5.17) summarised the values parameters of specimens after they were prepared, and at the end of each stages e.g. degree of saturation (S_r), voids ratio (*e*). These tables show that the water content of the samples after compaction varied between 12.44 % and 12.91 %, with a maximum difference of 0.47 %, due to evaporation and room temperature efforts. They also show the volume of samples after compaction varied between 196.39 cm^3 and 199.44 cm^3, about 3.05 cm^3 different. This difference in soil samples volume due to expand some specimens that samples have high percentage of fibre, this caused a variation in the degree of saturation from around 69.22 % to 77.58 %. However, the percentage of fibre caused a variation with degree of saturation as well. As voids filled with a fibre reduce the void ratio, this leads to a reduction the degree of saturation. The samples tested under 0 kPa of suction were almost fully saturated variables between 96.98 % and 99.22 %.

Based on the results of the unsaturated triaxial tests carried out on non-reinforced and fibre reinforced soil specimens prepared at same initial dry density and water content conditions, slight differences occurred on these parameters due to some effects of evaporation in water content. However, increase in fibre content resulted in reduction in the void ratio of fibre reinforced soils, which led to increase the degree of saturation. The shear strength increased with additional fibre content, as well as the increase in value of suction. The cohesion intercept of fibre reinforced soil specimens increased significantly with increased fibre content. The shear strength parameters similarly improvement with increased fibre content.

Table 5.14 Values of state parameter for 0% of fibre after prepared the samples and at the end of each stage.

Test No	At the Strat of test					End of Equalisation				
	S_r%	W_C %	e	V_S (cm^3)	V_W (cm^3)	S_r%	W_C %	e	ΔV_S (cm^3)	ΔV_W (cm^3)
F0-S0	96.98	18.4	0.492	196.86	64.31	97.01	18.14	0.461	-4.09	-0.89
F0-S50	69.22	12.91	0.498	197.53	43.42	72.6	12.12	0.462	-4.72	-0.10
F0-S100	68.71	12.5	0.410	196.43	43.7	70.3	11.89	0.380	-5.31	1.85
F0-S200	70.44	12.62	0.489	196.39	44.13	72.2	11.16	0.468	-5.28	2.49
Test No	End of Consolidation					After shear				
	S_r%	W_C %	e	ΔV_S (cm^3)	ΔV_W (cm^3)	S_r%	W_C %	e	ΔV_S (cm^3)	ΔV_W (cm^3)
F0-S0	98.53	17.95	0.408	-11.05	0.449	99.8	17.54	0.391	-13.34	0.44
F0-S50	79.81	11.84	0.432	-8.723	0.479	87.83	11.81	0.388	-14.38	0.47
F0-S100	75.63	11.74	0.360	-7.96	2.97	79.5	11.7	0.34	-13.87	2.4
F0-S200	75.33	11.01	.43	-7.67	5.65	85.38	10.96	0.394	-12.45	5.65

Table 5.15 Values of state parameter for 1% of fibre after prepared the samples and at the end of each stage.

Test No	At the Strat of test					End of Equalisation				
	S_r%	W_C %	e	V_S (cm^3)	V_W (cm^3)	S_r%	W_C %	e	ΔV_S (cm^3)	ΔV_W (cm^3)
F1-S0	97.60	18.1	0.485	198.43	63.26	97.90	17.87	0.441	-5.79	3.06
F1-S50	68.71	12.61	0.479	197.75	44.07	73.83	12.05	0.446	-4.43	0.37
F1-S100	70.13	12.62	0.489	196.43	44.10	75.85	11.84	0.484	-1.70	2.129
F1-S200	69.81	12.79	0.479	197.66	44.70	79.25	11.78	0.422	-7.64	4.347
Test No	End of Consolidation					After shear				
	S_r%	W_C %	e	ΔV_S (cm^3)	ΔV_W (cm^3)	S_r%	W_C %	e	ΔV_S (cm^3)	ΔV_W (cm^3)
F1-S0	97.54	17.22	0.394	-12.04	4.29	98.01	17.18	0.383	-14.76	4.29
F1-S50	80.24	11.87	0.410	-9.23	0.98	85.09	11.68	0.366	-15.12	0.97
F1-S100	80.23	11.53	0.443	-6.05	2.65	87.44	11.46	0.391	-12.87	2.65
F1-S200	83.46	11.64	0.400	-10.49	4.86	88.87	11.6	0.371	-14.42	4.86

Table 5.16 Values of state parameter for 3% of fibre after prepared the samples and at the end of each stage.

Test No	At the Strat of test					End of Equalisation				
	S_r%	W_C %	e	V_S (cm^3)	V_W (cm^3)	S_r%	W_C %	e	ΔV_S (cm^3)	ΔV_W (cm^3)
F3-S0	98.09	17.19	0.478	198.26	60.11	97.89	17	0.484	0.74	0.08
F3-S50	73.02	12.69	0.443	197.73	44.36	73.24	12.20	0.425	-2.49	1.69
F3-S100	72.60	12.73	0.447	198.30	44.51	77.99	12.18	0.416	-4.26	1.64
F3-S200	71.55	12.44	0.443	197.76	43.48	78.20	11.68	0.405	-5.19	3.21
Test No	End of Consolidation					After shear				
	S_r%	W_C %	e	ΔV_S (cm^3)	ΔV_W (cm^3)	S_r%	W_C %	e	ΔV_S (cm^3)	ΔV_W (cm^3)
F3-S0	98.77	16.98	0.415	-8.04	0.75	99.22	16.98	0.378	-12.86	0.734
F3-S50	76.89	12.06	0.400	-5.89	2.18	85.89	12.07	0.358	-11.64	2.16
F3-S100	82.32	11.83	0.394	-7.25	2.06	89.54	11.54	0.357	-12.37	2.05
F3-S200	81.83	11.33	0.388	-7.66	3.69	86.87	11.22	0.359	-12.80	3.69

Table 5.17 Values of state parameter for 5% of fibre after prepared the samples and at the end of each stage.

Test No	At the Strat of test					End of Equalisation				
	S_r%	W_C %	e	V_S (cm^3)	V_W (cm^3)	S_r%	W_C %	e	ΔV_S (cm^3)	ΔV_W (cm^3)
F5-S0	97.88	16.80	0.414	198.38	58.72	98.01	16.71	0.394	-4.05	-0.30
F5-S50	77.58	12.91	0.414	198.39	45.11	81.14	12.34	0.396	-2.58	0.47
F5-S100	75.01	12.71	0.422	199.44	44.43	78.96	12.18	0.384	-5.32	1.85
F5-S200	74.92	12.64	0.420	199.20	44.19	78.27	11.38	0.383	-5.28	2.49
Test No	End of Consolidation					After shear				
	S_r%	W_C %	e	ΔV_S (cm^3)	ΔV_W (cm^3)	S_r%	W_C %	e	ΔV_S (cm^3)	ΔV_W (cm^3)
F5-S0	98.90	16.21	0.348	-10.52	0.17	98.91	16.15	0.318	-14.79	0.15
F5-S50	86.88	11.87	0.370	-6.18	0.86	92.46	11.71	0.342	-11.48	0.852
F5-S100	81.96	11.74	0.365	-7.96	2.40	88.64	11.59	0.338	-13.19	2.4
F5-S200	84.55	11.34	0.364	-7.94	2.26	89.31	11.32	0.343	-10.76	2.65

CHAPTER 6 DEVELOPMENT OF ANALYTICAL MODEL

Summary

In this chapter a comparison between the measured of the experimental results and predicted shear strength calculated, using approach proposed by Vanapalli et al., (1996). An analysis is carried out on the results of the unsaturated triaxial shear tests of fibre reinforced clay soil. Therefore, a model is developed for predicting the shear strength of fibre reinforced soil samples.

6.1 Introduction

The shear strength envelope becomes nonlinear when soils are unsaturated and soil suction varies over a wide range. The nonlinearity of shear strength envelopes is related to the changes in degree of saturation of soil as soil suction change (Fredlund 2012). This chapter describes the development of a shear strength model for unsaturated soils reinforced with waste carpet fibre. The proposed model for unsaturated soil reinforcement is a modification of the equation developed by Vanapalli et al., (1996) to be used for a soil reinforced. The proposed model combines feature from the SWCC parameters model for unsaturated soils (described in Section 2.6.5).

The mechanical model developed in this chapter requires values of suction and percentage of fibre as a function of shear strength equation. The study is confined to triaxial shear strength. A corresponding degree of saturation is selected to describe soil-water characteristics carve. Then growth of shear stress corresponds to fibre content and another shear stress increment, which is corresponds to suction.

The performance of the model developed by performing simulations of the experimental tests result presented in chapter (5). Sections, and simulations are then compared to the experimental results. The challenge in this chapter that there is no modelling for unsaturated soil reinforced in the literature.

6.2 Applications using experimental results to stimulate models

Models were selected from the literature to stimulate to be used for unsaturated soil reinforced with a fibre, the unsaturated shear strength results are needed for developing the unsaturated shear strength envelope.

6.2.1 Goh et al (2012) model

Goh et al., (2010) obtained SWCC fitting parameter K' by developing Fredlund and Xing's (1994) equation [2.14] in chapter 2. The equation [2.42] in chapter 2 of (Goh et al., 2010) provides good agreement between the predicted and the measured shear strength at the zero suction. However, the predicted curve started to gradually increase at 50, 100 and 200 kPa of suction, which went far away from the measured shear strength. The increase at 50 kPa of suction was 47 %, at 100 kPa was 76 % and at 200 kPa was around 92 %. It can be detected that the proposed equations slightly over-estimate and most of the shear strengths for unsaturated soil reinforced with 5% fibre. This could be attributed to a complex parameter used in this equation.

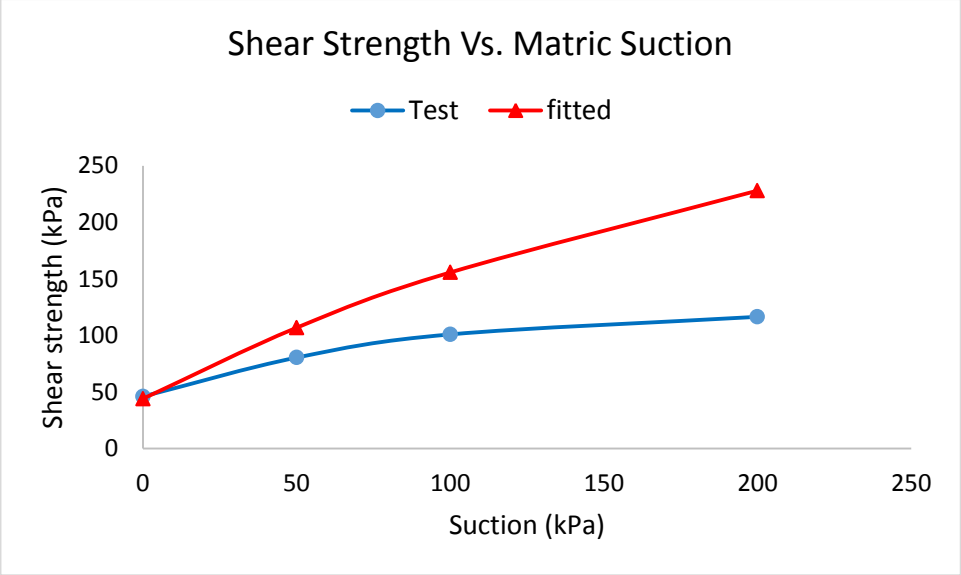

Figure 6.1 result of experimental data versus suction (Goh et al, 2010) model

6.2.2 Khalili and Khabbaz (1998) model

Measured versus predicted shear strength at 5 % of fibre specimens was obtained from this research using the proposed equation [2.35] in chapter 2 of Khalili and Khabbaz (1998). Figure (6.2) shows good agreement at the beginning of the fitted but as the suction increases, the predicted shear strength slightly increased. The increment was observed at 50 kPa of suction with different of 0.58 % between the measurement and prediction. Thereafter, continued gradually increasing at 50 kPa and 200 kPa of suction, by 65 % and 124 % respectively. In this equation no fitted parameters were obtained from soil-water characteristic curve. The approach requires very limited testing of a soil in unsaturated condition, which could be the case for there being no strong agreement between the predicted and the measurement of soil reinforced.

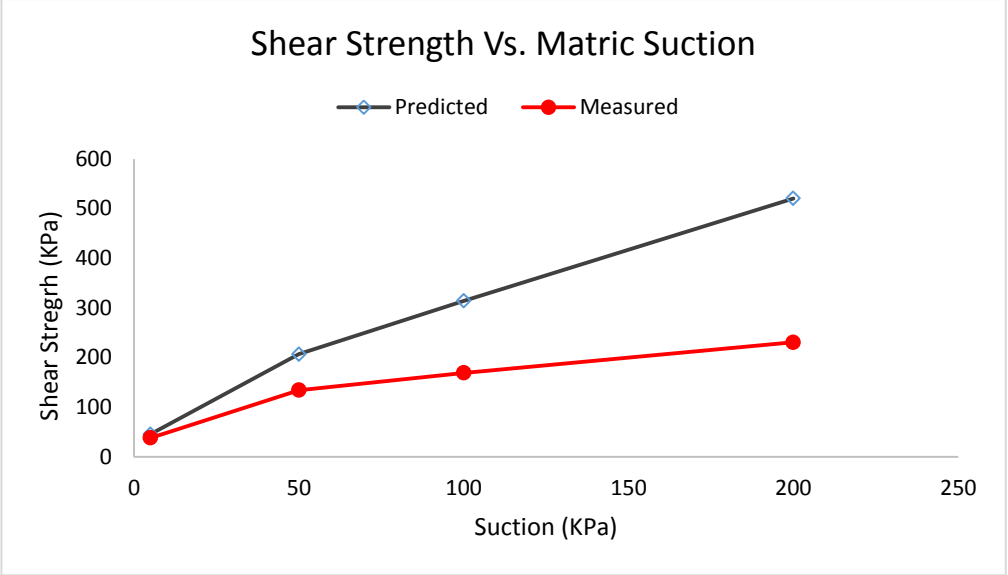

Figure 6.2 result of experimental data versus suction (Khalili and Khabbaz 1998)

6.2.3 Sandra (2008) model

Sandra's (2008) equation [2.43] in chapter 2 is shown in Figure (6.3) that no good agreement between the predicted the measured of shear strength of unsaturated soil reinforced. the predicted curve started to gradually increase between 50 kPa and 100 kPa of suction, where increased by 34 % and 41 % respectively. Also slowly increased between 100 and 200 kPa of suction by 47 %. The approach is used to obtain the secant ϕ^b parameter for a particular value of suction consisted of drawing the Mohr circles in the net normal stress $(\sigma - u_a)$ versus shear strength(τ). The value of ϕ^b is back calculated from total cohesion intercept value, which was explained in chapter 2 equation [2.43]. This model was unsuccessful.

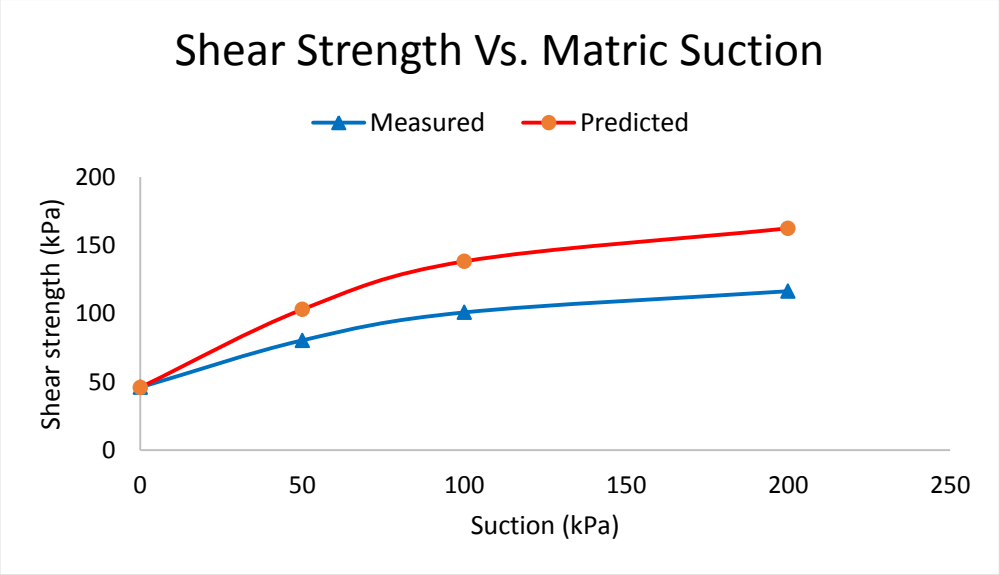

Figure 6.3 result of experimental data versus suction (Sandra 2008)

6.2.4 Vanapalli et al (1996) model

Vanapalli et al., (1996a) equation [2.26] in chapter 2 is used to predict the shear strength of unsaturated soil using the entire SWCC and a fitting parameter, *k* (see chapter 2 section 2.8). The approach was found to be unsuitable to unsaturated soil reinforced. However, it was good agreement at suction of 0 and nearly at 50 kPa which around 11 %. Subsequently, it slightly expands at 100 kPa of suction by 25 % and more at 200 kPa of suction around 44 %.

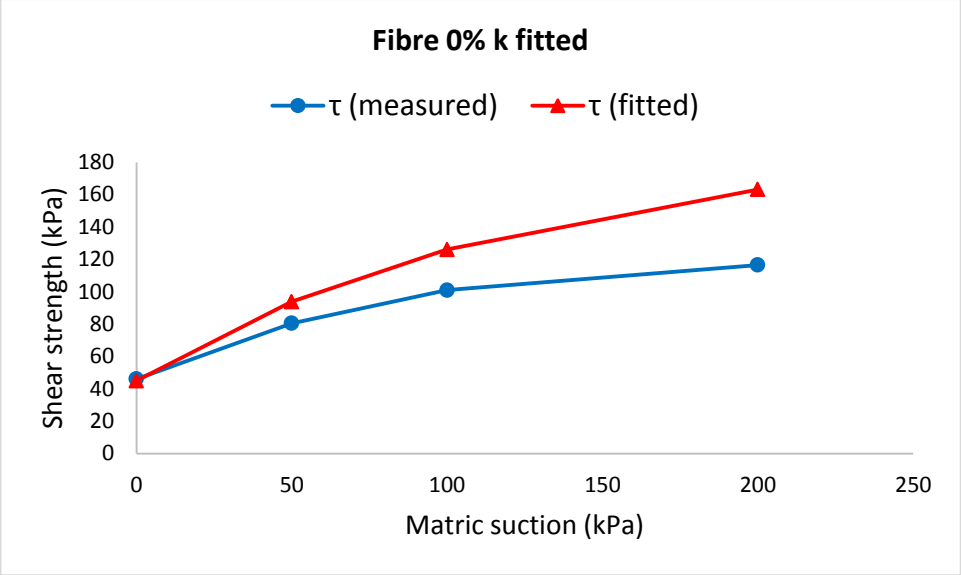

Figure 6.4 suction versus shear stress for test and measured (Vanapalli 1996)

Among all the equations, the predicted shear strengths from the proposed equations generally unsuccessfully measured shear strength experimental, as shown in the Figure (6.5). It can be observed that the proposed equations slightly over-estimate most of the shear strengths for this soils. This could be attributed to the effect of fibre content that is not considered and included in the proposed equations.

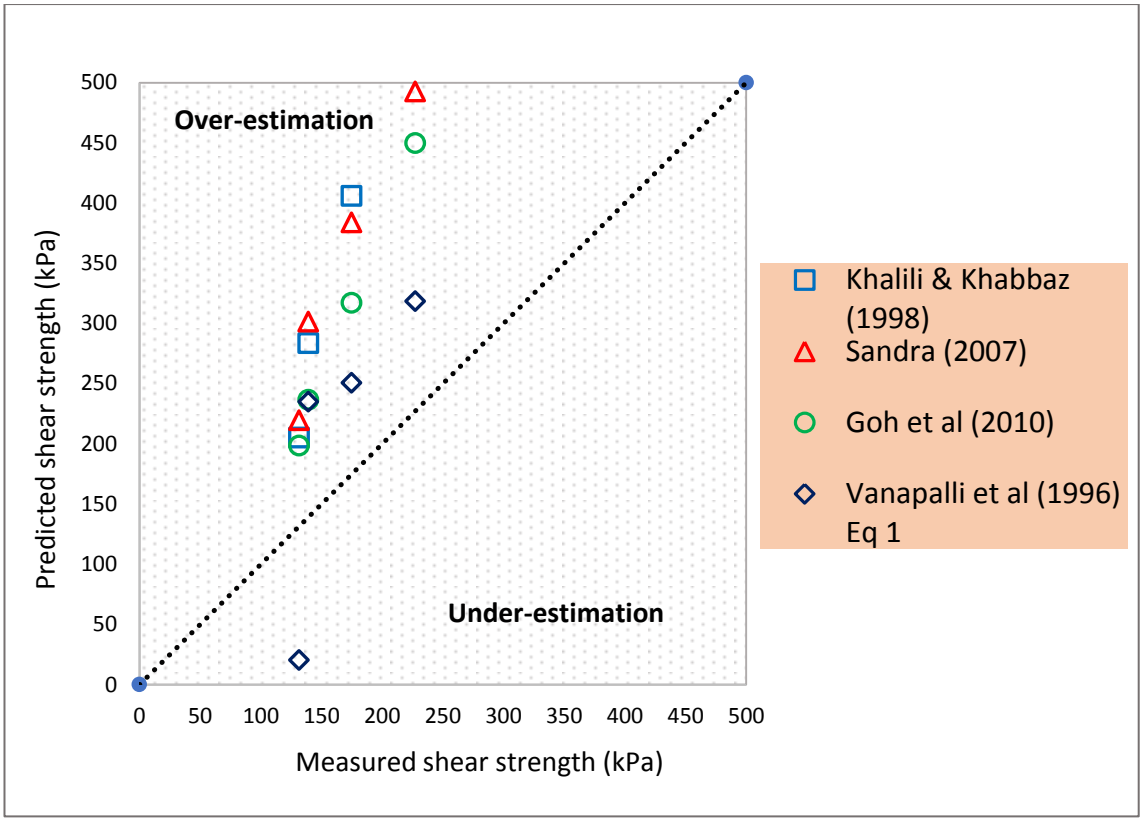

Figure 6.5 Predicted shear strength proposed equations (see graph) versus measured shear strength of specimens has 5% fibre obtained from this research.

6.3 Model Assumptions

6.3.1 Mechanical

- Fibres are randomly distributed sample before compaction – length and embedment angles of fibres are not considered in the study.
- Soil skeleton is composed of (i) solid particles (ii) fibres and (iii) soil suction.
- Soil sample/mixture is taken as homogenous material.

6.3.2 Behaviour Mechanism

- Soil behaves like a composite material.
- Sample reaches optimum fibre content which needs determining (shear strength-fibre % graph).

- Failure deviator stress, effective cohesion and effective angle of friction.

6.3.3 Expected Contribution of fibres

- Improvement in the effective friction angle,
- Impact on the effective cohesion,
- Pull out resistance,
- Possible contribution to the dry density of the sample (higher density due to higher constant at fibre-soil interface.

As expected and confirmed by the results of experiments in chapter 5, the improvement that has occurred in shear strength is through improvement in the cohesion and friction angle. But has been dealing with cohesion to developed the unsaturated soil reinforced model. And due to the friction angle was constant in all results of experiments, because of the applied consolidation stages were constant in the experiments, with a view to know the performance of fiber on shear strength.

6.3.4 Model Development

- The shear strength equation can be split into two parts (i) shear strength parameters $C'$and $\emptyset'$ and (ii) soil properties.
- Soil Water Characteristic Curves (SWCC) can be fitted based on the individual soil properties and the parameters are different.
- The SWCCs account for cohesion (one of the main influences on the shear strength) at different water contents in the soil sample.

6.3.5 Determination of model parameters

Parameters used in the proposed model may be classified into the following: drying and wetting cycle of SWCC, degree of saturation, fibre content and

suction. Figure (6.6) shows how the effect of fibre content on the cohesion as well as the suction increase. The improvement of the degree of cohesion and ($\emptyset^b$) angle is shown in Figure (6.7), it also shows the decrease between 0 and 1 % of fibre, that could be due to the test of 1 % of fibre. Due to the increment in the cohesion, the fibre content and matric suction are assumed to be a function in the equation.

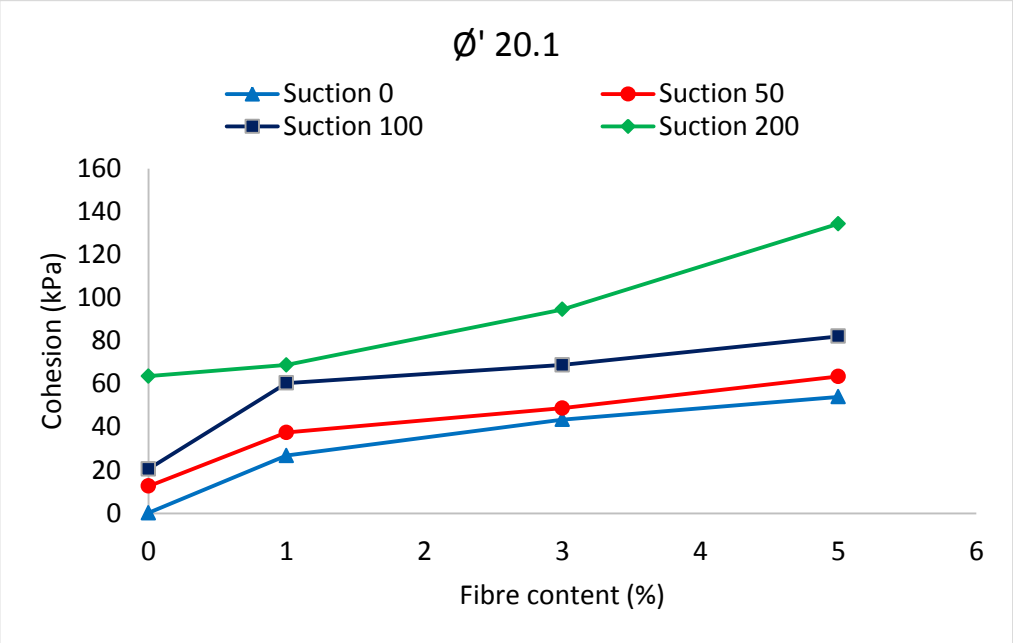

Figure 6.6 Fibre content with development of cohesion

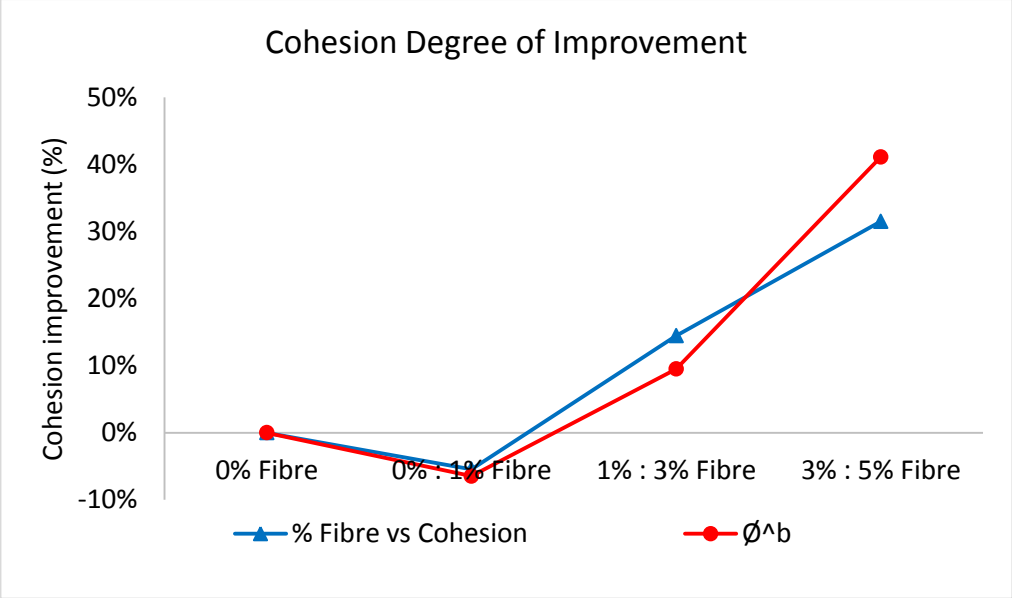

Figure 6.7 improvement of cohesion degree and Ø^b

6.3.6 Experimental study

The purposes of the experimental study were to determine and understand the shear strength behaviour of unsaturated soil reinforced. In addition, the experimental results were also used to examine the validity of the proposed equation presented in this chapter. The soil properties are presented in Table (3.1) chapter (3). The result indicated a maximum dry density of (2.08 g/cm^3) and optimum water content of (9.35). According to BS EN 1997-(2:2007), the soil classified as CL. The parameter of cohesion (c') and friction angle (ø′) were obtained from unsaturated triaxial tests by using Mohr-Coulomb failure envelope using the peak deviator stresses. The clayey specimens used in this study were tested in triaxial apparatus in different fibre contents and different matric suctions, as well as SWCC test in the same percentage of fibre. (See chapter 3 for more details).

6.4 Proposed shear strength equation

The proposed models used the soil-water characteristic curve parameters as $\boldsymbol{a}$, $\boldsymbol{n}$ and $\boldsymbol{m}$ (see chapter 2 equation [2.20]), and the unsaturated shear strength data to predict the variation of shear strength with respect fibre content and matric suction.

The model has a modified equation developed by Vanapalli (1996) equation [2.30] to predict the effect of fibre in the shear strength of unsaturated soil reinforced with carpet waste fibre. In order to evaluate this effect, a regression analysis was performed. To predict the fibre content and soil cohesion for a known suction unsaturated soil specimen. Therefore, the cohesion value could be obtained as a function of fibre content and suction. Table (6.1) shows the value for cohesion in each fibre content and suction. The correlation shows that a good fit of the variation in fibre content was explained by the two independent variables, namely suction and cohesion. However, the overall equals to 0.911, which is a good fit. 91.1 % of the variation in fibre, and this could be due to the results of test of 3 % of fibre.

Table 6.1 show correlation between fibre content and cohesion at each suction

Fibre content (%)	Degree of correlation (%)
0	0.931
1	0.953
3	0.889
5	0.985

6.4.1 The procedure

By using the regression analysis to obtain factors to present the fibre content and matric suction, the following parameters were used as input values.

a) Fibre content (0%, 1%, 3% and 5%).

b) Matric suction (0, 50, 100 and 200 kPa).

c) Cohesion intercept at the shear strength on Mohr diagram (kPa).

It has chosen symbol to present the fibre content as (F_r) and the matric suction (S'), are proportional to the change in fibre content and matric suction in soil at the shear state. The cohesion was correlated with a single output parameter to input parameters of fibre and suction. As a result of the experimental data (chapter 5) that a shear strength increased due to the increase in fibre content as well as matric suction increment. Therefore, from the regression analyses two factors, F_r and S' were selected to be used in the proposed equations. as following:

$$\text{Ϙ} = 13.58 + 11.6 * F_r \qquad 6.1$$

where F_r is the fibre content

$$\text{ß} = 0.094 * S' \qquad 6.2$$

where S' is the matric suction

By applying the shear strength equation [2.30], the effect of fibre content and matric suction on the shear strength were found in the cohesion. Combining equation [6.1] and equation [6.2], therefore the cohesion could be calculated as a function of fibre content and suction, as follows:

$$c' = Ʀ + ß \quad 6.3$$

Or it can be present as follow

$$c' = 13.58 + 11.6 * F_r + 0.094 * S' \quad 6.4$$

The shear strength equation [2.30] in chapter 2, could be modify as follow:

$$\tau = \left[c' + (\sigma_n - u_a) tan\phi'\right] + (u_a - u_w)\left[(tan\phi')\left(\frac{S - S_r}{100 - S_r}\right)\right] \quad 6.5$$

The shear strength of unsaturated prediction depends on the values of residual conditions and the fitting parameter Ʀ and ß. The cohesion has improvement due to fibre content and suction. The results of unsaturated triaxial compression tests which were established in chapter (5) were used to model the shear strength of the fibre reinforced soil specimens.

6.4.2 Comparison between experimental results and model predictions

The proposed model is used to simulate some tests presented in Chapter (5). The simulated tests include wetting-drying and isotropic undrained compression tests. Model predictions are compared with the experimental results to illustrate some capabilities of the proposed model.

Figures (6.8 to 6.11) show the comparison between experimental and predicted, shear strength and suction relationship from the undrain test, suction conducted on clay specimens at different values of matric suction, 0, 50, 100 and 200 kPa, constant net mean stress and fibre content as 0, 1, 3 and 5 %. The model shows reasonably good predictions of clay response under shear strength.

6.4.3 Result and discussion

Figure (6.8) to Figure (6.11) compare the shear stress data from results of the triaxial tests and predicted values by regression model of soil specimens. These figures show that the predicted results using regression model data were fairly acceptable and were highly efficient. It seems that the developed regression model can predict shear strength fibre reinforced specimens precisely compared to that of predicted parameter. However, the predicted data in Figure (6.9) shows some difference of 9 %; this difference may be due to the test results. The introduced model was used to consider the link effect of fibre content and suction on cohesion at failure of soil specimens prepared at the same dry density and water content. The results showed that at the same suction, the rate of increase in cohesion increased exponentially with an increase in fibre content. Coupling increase in fibre content and suction significantly enhanced the cohesion and hence mechanical behaviour of fibre reinforced soil. By using Vanapalli et al., (1996) equation described in section 2.8.3 equation [2.30], the predicted and the result test were fit successfully. As can be detected, a good agreement was obtained between the predicted and measure results, with less than 5% error 8% in average.

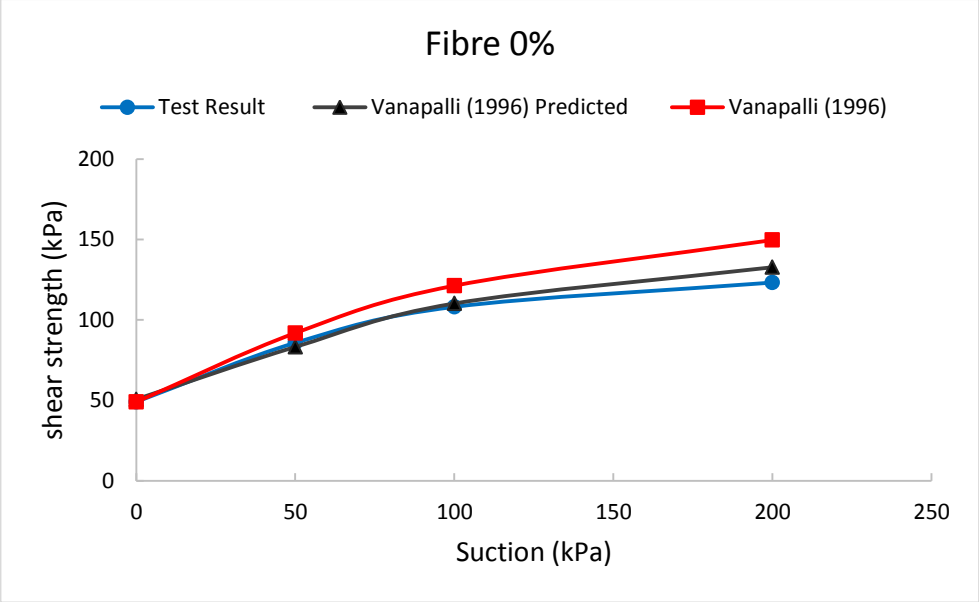

Figure 6.8 test result versus predicted data at 0 % fibre

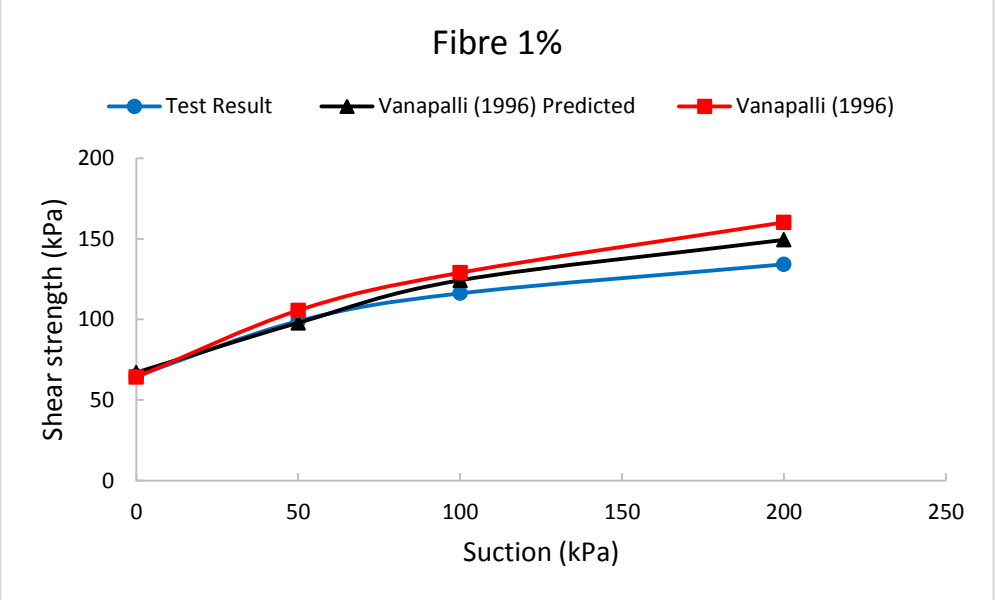

Figure 6.9 test result versus predicted data at 1 % fibre

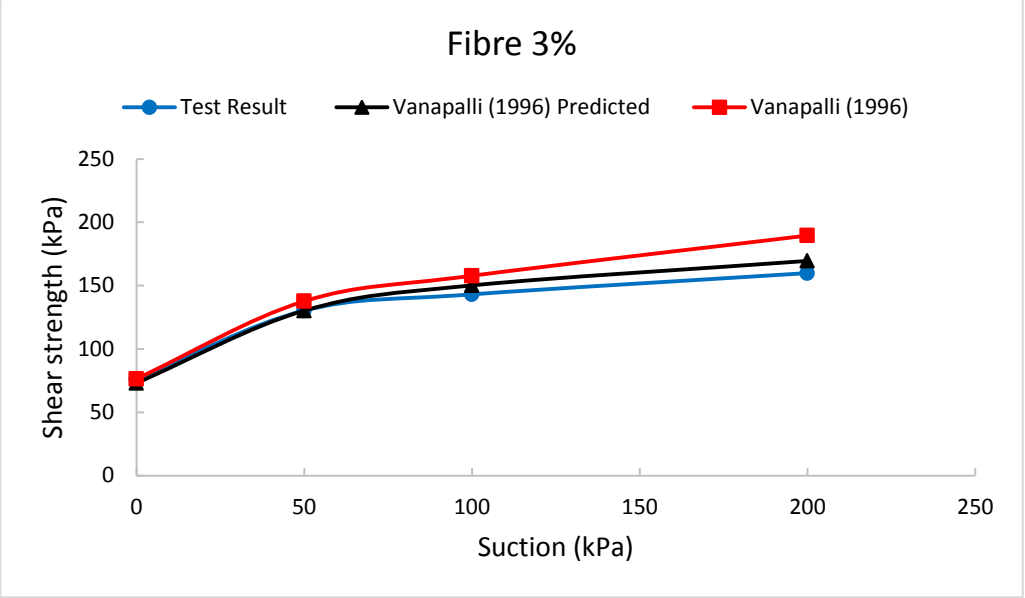

Figure 6.10 test result versus predicted data at 3 % fibre

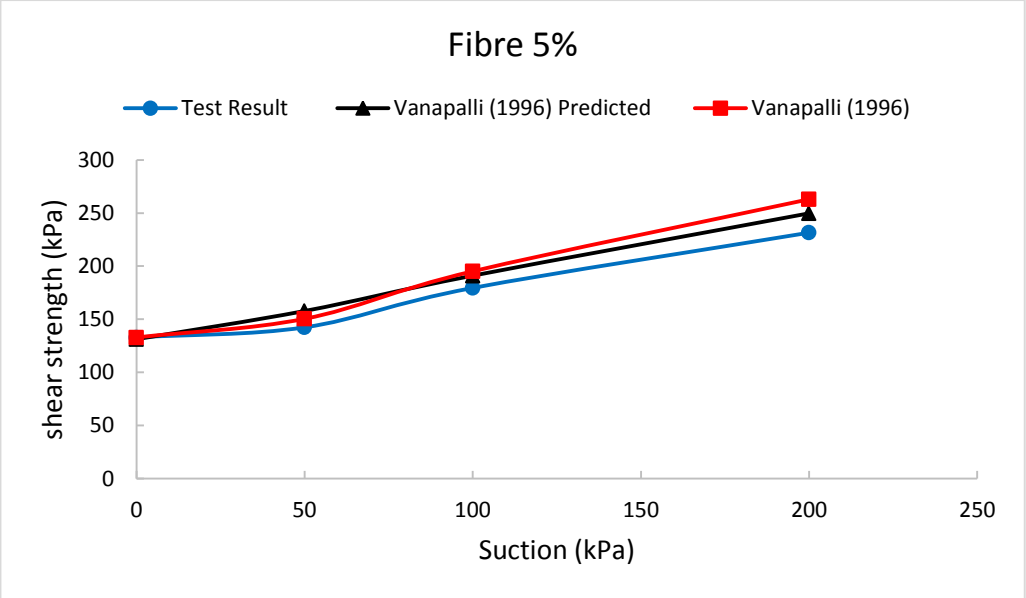

Figure 6.11 test result versus predicted data at 5 % fibre

6.5 Conclusions

In this chapter, the model was intended to improve existing shear strength models for simulating the mechanical behaviour of unsaturated soils reinforced.

This model also was developed and modified from a shear strength models using soil-water characteristic curve (SWCC) parameters, model proposed by Vanapalli et al., (1996). The main improvements were considered, i.e. to simulate cohesion in triaxial tests and reduce the hysteresis in SWCC.

The model was used to predict different fibre contents with different value of suction parameters, including cyclic wetting-drying, isotropic compression and undrained shearing tests. The results of unsaturated reinforced data and the soil-water characteristic curve parameter are sufficient to predict the variation of shear strength respect to fibre content and matric suction using models developed in this chapter.

Closed form solutions were developed using (Vanapalli et al., 1996) equation for predicting the unsaturated reinforced shear strength behaviour of clay. These solutions are estimated but simple. These solutions would be suitable for clayey soil which has low air-entry values. The predicted unsaturated reinforced shear strength is close to the measured experimental value results presented in (chapter 5) under different amount of fibre content and matric suction. However, there is no data available in the literature for unsaturated soil reinforced to be applied in this equation. It is only the test data in this study

CHAPTER 7 CONCLUSIONS AND RECOMMENDATION

In this research, the additions of randomly distributed carpet waste fibres as a reinforcing material, and a clay soils (clayey) were used.

The research was conducted to investigate the mechanical behaviour of unsaturated soil reinforced with waste carpet fibres. The programme tests included a series of proctor compaction tests, unconfined compression tests, soil-water characteristic curve (SWCC) tests, standard consolidated undrained triaxial tests and unsaturated triaxial tests. A model was developed based on the results of the triaxial shear tests to predict the shear strength of fibre reinforced soils.

A number of equipment and tools were designed and developed during the study. These consisted of pedestal, lower and upper Bellofram, stainless steel movement ram, plastic top cap for air pressure and inner and outer cells for triaxial test apparatus. Besides, transducer indicator E308 and flushing apparatus.

7.1 Conclusion

Through the analysis data of the experimental results, the following conclusions were obtained:

- According to the results of liquid limit (21.3 %), plastic limit (10.36 %) and plasticity index (10.94 %), the soil was classifying as CL (low plasticity clay) that used in this study. The specific gravity of the soil is 2.68.

- Fibre contents of 0 %, 1 %, 3% and 5 % were used. The maximum percentage of fibre used in this research was 5 %. Because of the reduced workability and was difficult to mix high percentage of fibre more than 5 % with the soil, the matric suction value was tested in testing program as 0 kPa, 50 kPa, 100 kPa and 200 kPa.
- The strength of unconfined compression test of the clay soils can be well improved by including fibres. The increase in fibre inclusion percentage in the soil presented an increase in optimum water content and a decrease in maximum dry density (compaction test).
- The SWCC experimental results show that the drying and wetting SWCCs of soils were different due to hysteresis. The difference between the drying and wetting SWCCs of non-reinforced were found to be larger than those of the reinforced with fibres. In addition, the fibre was decrease the hysteresis.
- the fibre content effect on the degree of saturation, as increase in fibre content that decrease the degree of saturated.
- it was found that increased matric suction results to increasing the shear strength. However, the effect of fibre was greater than suction.
- The parameters in hysteresis has been effective such as, the volume of voids effective on the shape of voids. The pores, neck and the direction of water flow either getting in or out of the pros which acted in the volume, as well as the contact angle. Adding fibre in soil sample, the shape of voids could be changed. In the other hand the permeability increasing because of addition fibres, so the water can flow more easily. The contact angle of cohesion soil normally high with cohesion soil, it could be less with adding fibre in soils. The parameters of shear strength fibre reinforced soil

increased with addition fibre content, such as cohesion intercept of 5% fibre reinforced increased by 148.69% at 200 kPa of suction and 162.02% at 50 kPa of suction compared to those of non-reinforced soil compacted. The affected of fibre content on $\emptyset^b$ (intercepts failure plane on shear stress (τ) versus suction ($u_a - u_w$) plane) improved significantly. However, sample with 1 % of fibre decrease compared with 0 % of fibre. The effective apparent cohesion of fibre reinforced soil specimens improved significantly.

- Model developed in this study was found to be well predictive of the shear strength of the fibre reinforced soils at failure. The developed model presented that, at the same suction value, the rate of increase in shear strength increased exponentially with increase in fibre content. Besides, it showed that at the same value of suction, increase in strength increased due to increase in fibre content produced from a linear relationship to an exponential one.

Pockets of fibre can be created as a subsequent of mixing fibre and soil, therefore, careful attention is required when mixing the two elements together as their random distributions tend to become twisted together. The strength of the compacted fibre reinforced can be defected due to increased void ratios.

It was found following several methods of mixing clay soils and fibres in this study, that the most suitable results in terms of uniform distribution of fibres in the soil are achieved by mixing dry soil and fibres initially and spraying water on the mixture of soil/fibre. The uniformity of fibre distribution within the soil is reduced slightly by increasing the fibre percentage.

As a result of this experiment regarding the concerning settlement, it is recommended that utilizing the carpet waste fibres in geotechnical engineering and reduce and avoid the effects created from disposal of carpet waste in landfills on environment. Also to reduce disposal pressure in landfills and consequently result in cost cutting.

7.2 Recommendation

The conclusions in this research aid to comprehend the mechanical behaviour of unsaturated reinforced clay soils with waste carpet fibres. The recommended for further study can be as a following:

- Different lengths of carpet waste fibers and on different inclusion methods, for example shear box test, consolidation test and permeability need further investigation to be carried out.
- Further investigation should be carried out of carpet waste fibers reinforcement to unsaturated soil with suction higher than 200 kPa, in order to be able to compare its behavior with suction which was used in this research.
- Soils/fibres reinforcement should be used for further investigation on the soil water characteristic curve (SWCC) in different methods to determine the hysteresis of soil on different cycles of drying and wetting.
- In the current study triaxial unsaturated shear test was not carried out on different value of consolidation and therefore the shear strength parameter friction angle $\emptyset'$ of soil specimen's reinforcement were not available to study the effect of fiber on it. Were it was estimated due to constant consolidation for all tests. Further study is required to determine the friction angle ($\emptyset'$) of soil

reinforcement with different value of consolidation that to determine the friction angle ($\emptyset'$).

- The shear strength equations for predicting the unsaturated shear strength of soil on the fiber reinforced may be further modified by including the effects of fiber on soil. Furthermore, the shear strength equations could be further improved by addition fiber reinforcement.

Reference

Abramento, M. and Carvalho, C.S., 1989. Geotechnical Parameters for the Study of Natural Slopes Instabilization at 'Serra do Mar'Brazil. In *Proc 12th Int Conf Soil Mechanics and Foundations Engineering. Rio de Janeiro* (Vol. 3, pp. 1599-1602).

Al-Moussawi, H.M. and Andersland, O.B., 1988. Discussion of "Behavior of Fabric-versus Fiber-Reinforced Sand" by Donald H. Gray and Talal Al-Refeai (August, 1986, Vol. 112, No. 8). *Journal of Geotechnical Engineering*, *114*(3), pp.383-385.

Alonso, E., 1998. Modelling expansive soil behaviour. *Keynote lecture A*. Proc. 2nd international Conference on Unsatuarted Soil, Beijing, China, Vol. 2: 37-70

Alonso, E.E., Gens, A. and Hight, D.W., 1987, August. Special problem soils. General report. In *Proceedings of the 9th European conference on soil mechanics and foundation engineering, Dublin* (Vol. 3, pp. 1087-1146).

Amir-Faryar, B. and Aggour, M.S., 2015. Effect of fibre inclusion on dynamic properties of clay. *Geomechanics and Geoengineering*, pp.1-10.

Anagnostopoulos, C.A., Tzetzis, D. and Berketis, K., 2014. Shear strength behaviour of polypropylene fibre reinforced cohesive soils. *Geomechanics and Geoengineering*, *9*(3), pp.241-251.

Ayyappan, S., Hemalatha, M.K. and Sundaram, M., 2010. Investigation of Engineering Behaviour of Soil, Polypropylene Fibres and Fly Ash-Mixtures for Road Construction. *International Journal of Environmental Science and Development*, *1*(2), p.171.

Barnes, G.E., 2010. *Soil mechanics: principles and practice*. Palgrave macmillan.

Bear, J., 2012. *Hydraulics of groundwater*. Courier Corporation.

Bernhard, R.K. and Krynine, D.P., 1952. Static and dynamic soil compaction. In *Highway Research Board Proceedings* (Vol. 31).

Bishop, A.W. and Blight, G.E., 1963. Some aspects of effective stress in saturated and partly saturated soils. *Geotechnique*, *13*(3), pp.177-197.

Bishop, A.W. and Donald, I.B., 1961, July. The experimental study of partly saturated soil in the triaxial apparatus. In *Proceedings of the 5th international conference on soil mechanics and foundation engineering, Paris* (Vol. 1, pp. 13-21).

Bishop, A.W. and Henkel, D.J., 1962. The measurement of soil properties in triaxial test. *Edward Arnold, London*.

Bishop, A.W. and Wesley, L.D., 1975. A hydraulic triaxial apparatus for controlled stress path testing. *Geotechnique*, *25*(4), pp.657-670.

Bishop, A.W., 1959. The effective stress principle. *Teknisk Ukeblad*, *39*, pp.859-863.

Booth, A.R., 1976. Compaction and preparation of soil specimens for Oedometer testing. In *Soil Specimen Preparation for Laboratory Testing*. ASTM International, pp.216-228.

Bouma, J., 1989. Using soil survey data for quantitative land evaluation. In *Advances in soil science* (pp. 177-213). Springer US.

British Standards Institution (2007) Eurocode 7: Geotechnical Design-part 2: Ground Investigation and testing *BS EN-2-BSI,* London.

British Standards, *BS1377-2:1990*, Classification tests.

British Standards, *BS1377-4:1990,* Compaction tests.

British Standards*, BS1377-6:1990,* Consolidation and permeability tests in hydraulic cells and with pore pressure measurement.

British Standards, *BS1377-7:1990*, Determination of unconfined compression strength.

British Standards, *BS1377-8:1990*, Shear strength tests effective stress.

Brooks, R.H. and Corey, A.T., 1964. Hydraulic properties of porous media and their relation to drainage design. *Transactions of the ASAE*, *7*(1), pp.26-0028.

Bulut, R., Lytton, R.L. and Wray, W.K., 2001. Soil suction measurements by filter paper. In *Expansive clay soils and vegetative influence on shallow foundations* (pp. 243-261). ASCE.

Cairns, H. and Minshull, R., Fisons Ltd Felixstowe, 1975. *Compositions and methods for the prevention of asthmatic symptoms*. U.S. Patent 3,864,493.

Chen, C.W. and Loehr, J.E., 2008. Undrained and drained triaxial tests of fiber-reinforced sand. In *Geosynthetics in Civil and Environmental Engineering* (pp. 114-120). Springer Berlin Heidelberg.

Chen, F.H., 1988. Foundation on Expansive Soils, Amsterdam. *Elseveier Scientific Publication Company, New York, USA*, p.463.

Chen, F.H., 2012. *Foundations on expansive soils* (Vol. 12). Elsevier. 1988

Consoli, N.C., Casagrande, M.D., Prietto, P.D. and Thomé, A., 2003. Plate load test on fiber-reinforced soil. *Journal of Geotechnical and Geoenvironmental Engineering*, *129*(10), pp.951-955.

Craig, R.F., 2004. *Craig's soil mechanics*. CRC Press.

Croney, D., Coleman, J.D. and Black, W.P.M., 1958. Movement and distribution of water in soil in relation to highway design and performance. *Water and Its Conduction in Soils, Highway Res Board, Special Report, Washington, DC*, (40), pp.226-252.

Cuccovillo, T. and Cabarkapa, Z., 2005. Automated Triaxial Apparatus for Testing Unsaturated Soils, Geotechnical Testing Journal, 21-29.

Cui, Y.J. and Delage, P., 1996. Yielding and plastic behaviour of an unsaturated compacted silt. *Géotechnique*, *46*(2), pp.291-311.

Delage, P., Howat, M.D. and Cui, Y.J., 1998. The relationship between suction and swelling properties in a heavily compacted unsaturated clay. *Engineering geology*, *50*(1), pp.31-48.

Donaghe, R.T., Chaney, R.C. and Silver, M.L., 1988, December. Advanced triaxial testing of soil and rock. ASTM.

Escario, V. and Saez, J., 1986. The shear strength of partly saturated soils. *Geotechnique*, *36*(3), 453-456.

Escario, V., Juca, J.F.T. and Coppe, M.S., 1989. Strength and deformation of partly saturated soils. *Proc. 12th ICSMFE, Rio de Janeiro*, *1*, pp.43-46.

Estabragh, A.R., 2002. *Yielding and critical state of unsaturate silty soils* (Doctoral dissertation, The University of Bradford).

Estabragh, A.R., Bordbar, A.T. and Javadi, A.A., 2011. Mechanical behavior of a clay soil reinforced with nylon fibers. *Geotechnical and Geological Engineering*, *29*(5), pp.899-908.

Fredlund, D.G. and Morgenstern, N.R., 1977. Stress state variables for unsaturated soils. *Journal of Geotechnical and Geoenvironmental Engineering*, *103*(ASCE 12919), 447-466.

Fredlund, D.G. and Rahardjo, H., 1993, March. The role of unsaturated soil behaviour in geotechnical engineering practice. In *Proceedings of the 11th Southeast Asian Geotechnical Conference, Singapore* (pp. 37-49).

Fredlund, D.G. and Rahardjo, H., 1993. An overview of unsaturated soil behaviour. *Geotechnical special publication*, pp.1-1.

Fredlund, D.G. and Rahardjo, H., 1993. *Soil mechanics for unsaturated soils*. John Wiley & Sons.

Fredlund, D.G. and Xing, A., 1994. Equations for the soil-water characteristic curve. *Canadian geotechnical journal*, *31*(4), pp.521-532.

Fredlund, D.G., 2000. The Implementation of Unsaturated Soil Mechanics into Geotechnical Engineering Practice. *National Research Council of Canada*. 37, 963-986.

Fredlund, D.G., 2002, March. Use of soil-water characteristic curves in the implementation of unsaturated soil mechanics. In *Proceedings of the 3rd International Conference on Unsaturated Soils, Recife, Brazil* (pp. 20-23). Vol. 3, pp. 887-902.

Fredlund, D.G., 2006. Unsaturated soil mechanics in engineering practice. *Journal of geotechnical and geoenvironmental engineering*, *132*(3), pp.286-321.

Fredlund, D.G., Morgenstern, N.R. and Widger, R.A., 1978. The shear strength of unsaturated soils. *Canadian geotechnical journal*, *15*(3), pp.313-321.

Fredlund, D.G., Rahardjo, H. and Fredlund, M.D., 2012. *Unsaturated soil mechanics in engineering practice*. John Wiley & Sons.

Fredlund, D.G., Rahardjo, H. and Fredlund, M.D., 2012. *Unsaturated soil mechanics in engineering practice*. John Wiley & Sons.

Fredlund, D.G., Stone, J., Stianson, J. and Sedgwick, A., 2011, November. Determination of water storage and permeability functions for oil sands tailings. In *Proceedings of the Tailings and Mine Waste Conference, Vancouver, BC*.

Fredlund, D.G., Xing, A., Fredlund, M.D. and Barbour, S.L., 1996. The relationship of the unsaturated soil shear to the soil-water characteristic curve. *Canadian Geotechnical Journal*, *33*(3), pp.440-448.

Freilich, B.J., Li, C. and Zornberg, J.G., 2010, May. Effective shear strength of fiber-reinforced clays. In *9th International Conference on Geosynthetics, Brazil* (pp. 1997-2000).

Fung, Y.C., 1977. A first course in continuum mechanics. *Englewood Cliffs, NJ, Prentice-Hall, Inc., 1977. 351 p.*

Gallage, C.P.K. and Uchimura, T., 2010. Effects of dry density and grain size distribution on soil-water characteristic curves of sandy soils. *Soils and Foundations*, *50*(1), pp.161-172.

Gan, J.K.M., Fredlund, D.G. and Rahardjo, H., 1988. Determination of the shear strength parameters of an unsaturated soil using the direct shear test. *Canadian Geotechnical Journal*, *25*(3), pp.500-510.

Gao, L., Hu, G., Xu, N., Fu, J., Xiang, C. and Yang, C., 2015. Experimental Study on Unconfined Compressive Strength of Basalt Fiber Reinforced Clay Soil. *Advances in Materials Science and Engineering*, *2015*.

Gardner, W.R., 1958. Some steady-state solutions of the unsaturated moisture flow equation with application to evaporation from a water table. *Soil science*, *85*(4), pp.228-232.

Gart, K.J. and Fredlund, D.G., Multistage Direct Shear Testing of Unsaturated Soils. Geotechnical Testing Journal, ASTM, 11 (2): 132-138.

Garven, E.A. and Vanapalli, S.K., 2006. Evaluation of empirical procedures for predicting the shear strength of unsaturated soils. In *Unsaturated Soils 2006* (pp. 2570-2592). ASCE.

Gens, A., 1996. Constitutive modelling: application to compacted soils. In *Proceedings of the first international conference on unsaturated soils, Unsat'95, Paris, France 6-8 September 1995. Vol 3.*

Gray, D.H. and Al-Refeai, T., 1986. Behavior of fabric-versus fiber-reinforced sand. *Journal of Geotechnical Engineering*, *112*(8), pp.804-820.

Gray, D.H. and Ohashi, H., 1983. Mechanics of fiber reinforcement in sand. *Journal of Geotechnical Engineering*, *109*(3), pp.335-353.

Guan, G.S., Rahardjo, H. and Choon, L.E., 2009. Shear strength equations for unsaturated soil under drying and wetting. *Journal of geotechnical and geoenvironmental engineering*, *136*(4), pp.594-606.

Habibagahi, K. and Mostaghel, N., 1974. Methods of Improving Low-Cost Construction Materials Against Earthquake. In *New Horizons in Construction Materials, Envo Publishing Co., Inc., Library of Congress* (Vol. 76, p. 27387).

Haines, W.B., 1930. Studies in the physical properties of soil. V. The hysteresis effect in capillary properties, and the modes of moisture distribution associated therewith. *The Journal of Agricultural Science*, *20*(01), pp.97-116.

Head, K.H., 1998. *Vol. 3: Effective stress tests*. London [etc.]: Wiley.

Hilf, J.W., 1956. An investigation of pore water pressure in compacted cohesive soils.

Hillel, D. and Mottes, J., 1966. Effect of plate impedance, wetting method, and aging on soil moisture retention. *Soil Science*, *102*(2), pp.135-139.

Hillel, D., 1971. *Physical Principles and Processes*. New York: Academic Press, Inc.

Hillel, D., 1998. *Environmental soil physics: Fundamentals, applications, and environmental considerations*. Academic press, Vol. 9, pp. 177-213.

Ho, D.Y. and Fredlund, D.G., 1982, March. A Multistage Triaxial Test for Unsaturated Soil. American Society for Testing and Materials.

Hoare, D.J., 1979. Laboratory study of granular soils reinforced with randomly oriented discrete fibers. In *Proceedings of the International Conference on Soil Reinforcement* (Vol. 1, pp. 47-52).

Houston, S.L., Perez-Garcia, N. and Houston, W.N., 2008. Shear strength and shear-induced volume change behavior of unsaturated soils from a triaxial

test program. *Journal of geotechnical and geoenvironmental engineering*, *134*(11), pp.1619-1632.

Huat, B.B.K., Ali, F.H. and Maail, S., 2005. The effect of natural fiber on the shear strength of soil. *American Journal of Applied Sciences*, pp.9-13.

Ismail, M.A., Joer, H.A., Sim, W.H. and Randolph, M.F., 2002. Effect of cement type on shear behavior of cemented calcareous soil. *Journal of Geotechnical and Geoenvironmental Engineering*, *128*(6), pp.520-529.

Jiesheng, L., Juan, Z. and Lin, X., (2014) Deformation and Strength Characteristics of Sisal Fibrous Soil. EJGE Vol. 9 Bund. H.

Kayadelen, C., Tekinsoy, M.A. and Taşkıran, T., 2007. Influence of matric suction on shear strength behavior of a residual clayey soil. *Environmental geology*, *53*(4), pp.891-901.

Khabbaz, M.H. and Khalili, N., 2002. A unique relationship for chi for the determination of the shear strength of unsaturated soils. *Geotechnique*, *52*(1), pp.76-77.

Khalili, N., Geiser, F. and Blight, G.E., 2004. Effective stress in unsaturated soils: review with new evidence. *International Journal of Geomechanics*, *4*(2), pp.115-126.

Krahn, J. and Fredlund, D.G., 1972. On total, matric and osmotic suction. *The Emergence of Unsaturated Soil Mechanics*, p.35.

Krishna, T.M. and Beebi, S.S., 2015. Soil Stabilization by Groundnut Shell Ash and Waste Fiber Material. *International Journal of Innovations in Engineering and Technology (IJIET)*, *5*(3), pp.52-57.

Kumar, A., Walia, B.S. and Mohan, J., 2006. Compressive strength of fiber reinforced highly compressible clay. *Construction and building materials*, *20*(10), pp.1063-1068.

Kumar, D., Nigam, S., Nangia, A. and Tiwari, S., (2015). Improvement in CBR Values of Soil Reinforced with Jute Fibre. *International Journal of Engineering and Technical Research (IJETR)* ISSN: 2321-0869, Volume-3, Issue-5, May 2015

Lee, I.M., Sung, S.G. and Cho, G.C., 2005. Effect of stress state on the unsaturated shear strength of a weathered granite. *Canadian Geotechnical Journal*, *42*(2), pp.624-631.

Leong, E.C. and Rahardjo, H., 1997. Permeability functions for unsaturated soils. *Journal of Geotechnical and Geoenvironmental Engineering*, *123*(12), pp.1118-1126.

Leong, E.C. and Rahardjo, H., 1997. Review of soil-water characteristic curve equations. *Journal of geotechnical and geoenvironmental engineering*, *123*(12), pp.1106-1117.

Loehr, J.E., Axtell, P.J. and Bowders, J.J., 2000, November. Reduction of soil swell potential with fiber reinforcement. In *ISRM International Symposium*. International Society for Rock Mechanics.

Logeshwari, J. and Premalatha, K., (2014) Stress Strain Behavior of Clayey Sand. *PARAMETERS*, *1*(2), p.3.

Lu, N. and Likos, W.J., 2004. *Unsaturated soil mechanics*. Wiley.

Malekzadeh, M. and Bilsel, H. (2012), Swell and compressibility of fibre reinforced expansive soils, International journal of advanced Technology in civil engineering, 1(2),42-45.

Marandi, S.M., Bagheripour, M.H., Rahgozar, R. and Zare, H., 2008. Strength and ductility of randomly distributed palm fibers reinforced silty-sand soils. *American Journal of Applied Sciences*, *5*(3), pp.209-220.

Matyas, E.L. and Radhakrishna, H.S., 1968. Volume change characteristics of partially saturated soils. *Géotechnique*, *18*(4), pp.432-448.

McKee, C.R. and Bumb, A.C., 1987. Flow-testing coalbed methane production wells in the presence of water and gas. *SPE formation Evaluation*, *2*(04), pp.599-608.

Menzies, B.K., 1988. A computer controlled hydraulic triaxial testing system. In *Advanced triaxial testing of soil and rock*. ASTM International.

Mercer, F.B., Andrawes, K.Z., McGown, A. and Hytiris, N., 1984. A new method of soil stabilization. *Polymer Grid Reinforcement*, pp.244-249.

Mesbah, A., Morel, J.C. and Olivier, M., 1999. Clayey soil behaviour under static compaction test. *Materials and structures*, *32*(223), pp.687-694.

Miller, D.J., 1997. *Expansive soils: problems and practice in foundation and pavement engineering*. John Wiley & Sons.

Minshull, R.M. and Minshull, R., 1975. *An introduction to models in geography*. London: Longman.

Miraftab, M. and Lickfold, A., 2008. Utilization of carpet waste in reinforcement of substandard soils. *Journal of industrial textiles*, *38*(2), pp.167-174.

Mirzababaei, M., Miraftab, M., McMahon, P. and Mohamed, M., 2009, May. Undrained behaviour of clay reinforced with surplus carpet fibres. In *Second International Symposium on Fiber Recycling, Atlanta, Georgia, USA*.

Mirzababaei, M., Miraftab, M., Mohamed, M. and McMahon, P., 2013. Impact of carpet waste fibre addition on swelling properties of compacted clays. *Geotechnical and Geological Engineering*, *31*(1), pp.173-182.

Mukherjee, K and Mishra, K, A (2014), Performance enhancement of sand bentonite mixture due to addition of fibre and geo-synthetic clay liner, IGC-2014, Kakinada, 321-329.

Murray, E.J. and Sivakumar, V., 2010. *Unsaturated soils: a fundamental interpretation of soil behaviour*. John Wiley & Sons.

Nelson, J.D. and Miller, D.J., 1992. Expansive soils. Problems and practice in foundation and pavement engineering. *Willy, New York*.

Ng, C.W., Zhan, L.T. and Cui, Y.J., 2002. A new simple system for measuring volume changes in unsaturated soils. *Canadian geotechnical journal*, *39*(3), pp.757-764.

Padilla, J.M., Houston, W.N., Lawrence, C.A., Fredlund, D.G., Houston, S.L. and Perez, N.P., 2006. An automated triaxial testing device for unsaturated soils. *Geotechnical Special Publication*, *147*(2), p.1775-1786.

Park, S.S., 2009. Effect of fiber reinforcement and distribution on unconfined compressive strength of fiber-reinforced cemented sand. *Geotextiles and Geomembranes*, *27*(2), pp.162-166.

Qu, J.and Z. Sun (2016). “Strength Behavior of Shanghai Clayey Soil Reinforced with Wheat Straw Fibers. *Geotechnical and Geological Engineering* 34(2): pp 515-527.

Ramasamy, S. and Arumairaj, P.D., 2013. The Effect of Polypropylene Fiber On Index Properties and Compaction Characteristics of Clay Soil. *Turkish Journal of Engineering*, *2*, pp.35-38.

Raveendiraraj, A., 2009. *Coupling of mechanical behaviour and water retention behaviour in unsaturated soils* (Doctoral dissertation, University of Glasgow).

Shahnazari, H.A.B.I.B., Ghiassian, H., Noorzad, A., Shafiee, A., Tabarsa, A.R. and Jamshidi, R., 2009. Shear modulus of silty sand reinforced by carpet waste strips. *Journal of Seismology and Earthquake Engineering*, *11*(3), p.133.

Sharma, R.S., 1998. *Mechanical behaviour of unsaturated highly expansive clays* (Doctoral dissertation, University of Oxford).

Shbib, R. and Okumura, T., 2002, June. Quantitative analysis of fiber reinforced cement deep mixing soil composite (FR-CDM). In *The 15th Engineering Mechanics Conference, Columbia University* (pp. 2-5).

Sheng, D., Gens, A., Fredlund, D.G. and Sloan, S.W., 2008. Unsaturated soils: from constitutive modelling to numerical algorithms. *Computers and Geotechnics*, *35*(6), pp.810-824.

Sillers, W.S., Fredlund, D.G. and Zakerzadeh, N., 2001. Mathematical attributes of some soil—water characteristic curve models. In *Unsaturated soil concepts and their application in geotechnical practice* (pp. 243-283). Springer Netherlands.

Sivakumar, R., Sivakumar, V., Blatz, J. and Vimalan, J., 2006. Twin-cell stress path apparatus for testing unsaturated soils. *Geotechnical Testing Journal*, *29*(2), p.175-197.

Sivakumar, V., 1993. *A critical state framework for unsaturated soil* (Doctoral dissertation, University of Sheffield).

Smith, I., 2007. *Smith's elements of soil mechanics*. John Wiley & Sons.

Tang, C., Shi, B., Gao, W., Chen, F. and Cai, Y., 2007. Strength and mechanical behavior of short polypropylene fiber reinforced and cement stabilized clayey soil. *Geotextiles and Geomembranes*, *25*(3), pp.194-202.

Thomas, H.R. and He, Y., 1998. Modelling the behaviour of unsaturated soil using an elastoplastic constitutive model. *Géotechnique*, *48*(5), pp.589-603.

Toll, D.G., 1990. A framework for unsaturated soil behaviour. *Géotechnique*, *40*(1), pp.31-44.

Van Genuchten, M.T., 1980. A closed-form equation for predicting the hydraulic conductivity of unsaturated soils. *Soil science society of America journal*, *44*(5), pp.892-898.

Vanapafli, S.K., Fredlund, D.G. and Pufahl, D.E., 1999. The influence of soil structure and stress history on the soil-water characteristics of a compacted till, Geotechnique Vol. 49, No. 2: 143–159.

Vanapalli, S.K., 1994, Simple test procedures and their interpretation in evaluating the shear strength of an unsaturated soil. PhD thesis, University of Saskatchewan, Canada.

Vanapalli, S.K., Fredlund, D.G., Pufahl, D.E. and Clifton, A.W., 1996. Model for the prediction of shear strength with respect to soil suction. *Canadian Geotechnical Journal*, *33*(3), pp.379-392.

Venkatarama-Reddy, B.V. and Jagadish, K.S., 1993. The static compaction of soils. *Geotechnique*, *43*(2), pp.337-341.

Vidal, H., 1969. The principle of reinforced earth. *Highway research record*, (282).

Waldron, L.J., 1977. The shear resistance of root-permeated homogeneous and stratified soil. *Soil Science Society of America Journal*, *41*(5), pp.843-849.

Wheeler, S.J. and Sivakumar, V., 1995. An elasto-plastic critical state framework for unsaturated soil. *Géotechnique*, *45*(1), pp.35-53.

Wheeler, S.J., 1986. *The stress-strain behaviour of soils containing gas bubbles* (Doctoral dissertation, University of Oxford).

Wheeler, S.J., 1988. The undrained shear strength of soils containing large gas bubbles. *Géotechnique*, *38*(3), pp.399-413.

White, N.F., Duke, H.R., Sunada, D.K. and Corey, A.T., 1970. Physics of desaturation in porous materials. *Journal of the Irrigation and Drainage Division*, *96*(2), pp.165-191.

Xie, X., Yao, Y., Liu, J., Li, P. and Yang, G., 2015. Mechanical Behavior of Unsaturated Soils Subjected to Impact Loading. *Shock and Vibration*, *2016*.

Yang, H., Rahardjo, H., Leong, E.C. and Fredlund, D.G., 2004. Factors affecting drying and wetting soil-water characteristic curves of sandy soils. *Canadian Geotechnical Journal*, *41*(5), pp.908-920.

Yin, J.H., 2003. A double cell triaxial system for continuous measurement of volume changes of an unsaturated or saturated soil specimen in triaxial testing. *Geotechnical Testing Journal*, *26*(3), pp.353-358.

Zhou, A. and Sheng, D., 2009. Yield stress, volume change, and shear strength behaviour of unsaturated soils: validation of the SFG model. *Canadian Geotechnical Journal*, *46*(9), pp.1034-1045.